OPTIMAL DESIGN OF A MICRO VERTICAL AXIS WIND TURBINE FOR SUSTAINABLE URBAN ENVIRONMENT

Kyooseon Park

PhD

2013

University of Huddersfield

School of Computing and Engineering

ABSTRACT

The need for sustainable energy sources becomes greater each year due to the continued depletion of fossil fuels and the resulting energy crisis. Solutions to this problem are potentially in the form of wind turbines, for sustainable urban environment, that have been receiving increased support. At present, a number of wind turbines have been developed that show significant increase in performance compared to existing technologies. From an extensive literature review, a number of key issues have been highlighted which are concerned with the design, optimisation and diagnostics of Vertical Axis Wind Turbines (VAWTs) that have been used to formulate the scope of this research.

A design procedure for a vertical axis wind turbine, that features both multi-blade rotor and fixed outer stator guide vanes, has been derived, in which both rotor and stator blade profiles have been generated for a low wind speed application. In the presented work, numerical investigations have been carried out extensively to determine the optimised design of the VAWT. Sliding mesh technique has been used for the rotation of rotor blades. This new technique captures the transient flow phenomena that occur when the rotor and the stator blades interact with each other. Hence, the results predicted by CFD using this technique are much superior in accuracy. Furthermore, a detailed flow field analysis of the VAWT has highlighted large asymmetries in both pressure and flow velocity about the central axis of the VAWT in both the stationary and the rotating frames of references.

Various geometric parameters associated with the design of the VAWT have been investigated over a wide range in order to analyse the effect of these parameters on the performance output of the VAWT. These geometric parameters are the blade angles, the number of blades in the VAWT and the size of the rotor/stator sections of the VAWT. It has been shown that all these parameters considerably affect the performance output of the VAWT and hence have been optimised in the present study for maximum performance output of the VAWT. One of the key elements of this study is the development of a performance prediction model of the VAWT that takes into account the effects of the aforementioned geometric parameters of the VAWT. This novel prediction model is both robust, user-friendly and has shown to predict the performance output of the VAWT with reasonable accuracy. Hence, the prediction model can be used by the designers of the VAWT.

Nowadays, condition based health monitoring of mechanical systems is topic of vast research. Most of the studies in this field use experimental facilities and conventional toolboxes to handle the output data from the sensors. With the advent of advanced CFD tools, it has now become possible to use CFD as an effective tool for fault detection in VAWTs. An attempt has been presented in this study regarding condition monitoring of VAWTs for sustainable urban environment. Various faults like missing blade and slits in blade have been investigated and analysed. It has been shown that CFD can detect these faults and show the effects of these faults on local flow parameters such as pressure and velocity.

Optimal Design of a Micro Vertical Axis Wind Turbine for Sustainable Urban Environment
By Kyooseon Park, School of Computing and Engineering, University of Huddersfield, UK (2013)

ii

DECLARATION

- The author of this thesis (including any appendices and/or schedules to this thesis) owns any copyright in it (the "Copyright") and he has given The University of Huddersfield the right to use such Copyright for any administrative, promotional, educational and/or teaching purposes.

- Copies of this thesis, either in full or in extracts, may be made only in accordance with the regulations of the University Library. Details of these regulations may be obtained from the Librarian. This page must form part of any such copies made.

- The ownership of any patents, designs, trademarks and any and all other intellectual property rights except for the Copyright (the "Intellectual Property Rights") and any reproductions of copyright works, for example graphs and tables ("Reproductions"), which may be described in this thesis, may not be owned by the author and may be owned by third parties. Such Intellectual Property Rights and Reproductions cannot and must not be made available for use without the prior written permission of the owner(s) of the relevant Intellectual Property Rights and/or Reproductions.

Optimal Design of a Micro Vertical Axis Wind Turbine for Sustainable Urban Environment
By Kyooseon Park, School of Computing and Engineering, University of Huddersfield, UK (2013)

iii

ACKNOWLEDGEMENTS

Optimal Design of a Micro Vertical Axis Wind Turbine for Sustainable Urban Environment
By Kyooseon Park, School of Computing and Engineering, University of Huddersfield, UK (2013)

iv

CONTENTS

Optimal Design of a Micro Vertical Axis Wind Turbine for Sustainable Urban Environment
By Kyooseon Park, School of Computing and Engineering, University of Huddersfield, UK (2013)

v

Optimal Design of a Micro Vertical Axis Wind Turbine for Sustainable Urban Environment
By Kyooseon Park, School of Computing and Engineering, University of Huddersfield, UK (2013)

vi

Optimal Design of a Micro Vertical Axis Wind Turbine for Sustainable Urban Environment
By Kyooseon Park, School of Computing and Engineering, University of Huddersfield, UK (2013)

vii

Optimal Design of a Micro Vertical Axis Wind Turbine for Sustainable Urban Environment
By Kyooseon Park, School of Computing and Engineering, University of Huddersfield, UK (2013)

viii

LIST OF FIGURES

Optimal Design of a Micro Vertical Axis Wind Turbine for Sustainable Urban Environment
By Kyooseon Park, School of Computing and Engineering, University of Huddersfield, UK (2013)

ix

Optimal Design of a Micro Vertical Axis Wind Turbine for Sustainable Urban Environment
By Kyooseon Park, School of Computing and Engineering, University of Huddersfield, UK (2013)

x

Optimal Design of a Micro Vertical Axis Wind Turbine for Sustainable Urban Environment
By Kyooseon Park, School of Computing and Engineering, University of Huddersfield, UK (2013)

xi

Optimal Design of a Micro Vertical Axis Wind Turbine for Sustainable Urban Environment
By Kyooseon Park, School of Computing and Engineering, University of Huddersfield, UK (2013)

xii

Optimal Design of a Micro Vertical Axis Wind Turbine for Sustainable Urban Environment
By Kyooseon Park, School of Computing and Engineering, University of Huddersfield, UK (2013)

xiii

Optimal Design of a Micro Vertical Axis Wind Turbine for Sustainable Urban Environment
By Kyooseon Park, School of Computing and Engineering, University of Huddersfield, UK (2013)

xiv

Optimal Design of a Micro Vertical Axis Wind Turbine for Sustainable Urban Environment
By Kyooseon Park, School of Computing and Engineering, University of Huddersfield, UK (2013)

xv

Optimal Design of a Micro Vertical Axis Wind Turbine for Sustainable Urban Environment
By Kyooseon Park, School of Computing and Engineering, University of Huddersfield, UK (2013)

xvi

LIST OF TABLES

Optimal Design of a Micro Vertical Axis Wind Turbine for Sustainable Urban Environment
By Kyooseon Park, School of Computing and Engineering, University of Huddersfield, UK (2013)

xvii

Optimal Design of a Micro Vertical Axis Wind Turbine for Sustainable Urban Environment
By Kyooseon Park, School of Computing and Engineering, University of Huddersfield, UK (2013)

xviii

NOMENCLATURE

T	Torque Output of VAWT (N-m)
P	Power Output of VAWT (W)
r	Radius (m)
v	Linear Flow Velocity (m/sec)
ω	Angular Velocity (rad/sec)
λ	Tip Speed Ratio (-)
α	Outlet Angle of Stator blades ($^{\circ}$)
β	Inlet Angle of Stator blades ($^{\circ}$)
δ	Inlet Angle of Rotor blades ($^{\circ}$)
γ	Outlet Angle of Rotor blades ($^{\circ}$)
rbr	Radius of Rotor Blades (m)
sbr	Radius of Stator Blades (m)
h	Height of Vertical Axis Wind Turbine (m)
ρ	Density (Kg/m^3)
A	Frontal Area of the VAWT (m^2)
C_T	Torque Coefficient (-)
NSB	Number of Stator Blades (-)
NRB	Number of Rotor Blades (-)
u	Flow Velocity in x direction (m/sec)
w	Flow Velocity in z direction (m/sec)
g	Acceleration due to Gravity (m/sec^2)
τ	Shear Stress (Pa)
σ	Normal Stress (Pa)
i	Specific Internal Energy (J/Kg)
C_p	Coefficient of Pressure
P_c	Power Coefficient
Re	Reynolds Number
K	Frictional Coefficient

Optimal Design of a Micro Vertical Axis Wind Turbine for Sustainable Urban Environment
By Kyooseon Park, School of Computing and Engineering, University of Huddersfield, UK (2013)

xix

SUBSCRIPTS

min   Minimum

max   Maximum

avg   Average

i   Inlet

o   Outlet

r   Rotor

c   Core

s   Stator

t   Total

∞   Free Stream

Optimal Design of a Micro Vertical Axis Wind Turbine for Sustainable Urban Environment
By Kyooseon Park, School of Computing and Engineering, University of Huddersfield, UK (2013)

xx

CHAPTER 1
INTRODUCTION

This chapter provides an overview of current wind power technologies and their associated benefits. From this review a number of key questions are raised which correspond to recent trends observed in the micro wind energy community and in particular the suitability of current technologies to operate effectively within this environment. The latter part of this chapter discusses the need for wind turbine diagnostics and how current state of the art techniques can be implemented onto wind turbine systems to determine specific fault conditions. Equations for the design of rotor and stator blades have been derived. Motivation to carry out this research and the main aims of this study are the highlight of this chapter.

Optimal Design of a Micro Vertical Axis Wind Turbine for Sustainable Urban Environment
By Kyooseon Park, School of Computing and Engineering, University of Huddersfield, UK (2013)

1

1.1.   Wind as a source of Energy

In recent years, the number of wind turbines that have been deployed all over the world has increased considerably. According to the Global Wind Energy Council [1], more than 38GW of new wind power capacity was installed worldwide in the year 2009, bringing the total installed capacity, by the end of 2009, to 160GW. The development and deployment of devices that generate useful energy from the kinetic energy contained in the wind are motivated largely by two objectives. Firstly, there is a perceived need to reduce emissions of carbon dioxide and other pollutants by replacing fossil fuel-fired power plants with renewable energy technologies. Secondly, there is a perceived demand to establish an alternative to fossil fuels in the light of the finite nature and unequal global distribution of the known coal, oil and gas resources.

The energy company BP plc [2] estimates that the generation of electricity by wind turbines in 2009 was over 260TWh which corresponds to merely 1.3% of the amount of electricity generated globally, but the share of wind energy in the electricity that is generated worldwide is expected to increase substantially in the coming decades. The contribution of wind power to the future electric energy supply will be highly dependent on governmental policies, however. Indeed, the International Energy Agency [3] predicts, in a baseline scenario which assumes that governments introduce no new energy and climate policies, that the share of wind energy in the global electricity generation will be only 5% in the year 2050. In contrast, the most ambitious scheme, the so-called BLUE Map scenario that includes the target of halving global energy-related emissions of carbon dioxide by the year 2050 compared to the levels in the year 2005, projects up to 22% of the worldwide electricity demand to be provided by wind energy in the year 2050. The target setting of the BLUE Map scenario is motivated by the findings of the studies that were carried out by the Intergovernmental Panel on Climate Change [4-7]. According to these investigations, substantial changes in structure and function of the worldwide ecosystems are very likely to occur when global warming, associated with increased atmospheric concentration of carbon dioxide, exceeds 2°C compared to the pre-industrial level. Furthermore, it is concluded that the reduction of the emissions of carbon dioxide by 50% by the year 2050 compared to the levels in the year 2005 is necessary if global warming is to be confined to 2°C.

The current generation of wind turbines that are being deployed around the world features, almost exclusively, a three-bladed rotor with a horizontal-axis configuration. In recent years, however, there has been a resurgence of interest in both large-scale and small-scale vertical-axis wind turbines. The development of large-scale vertical-axis wind turbines is a response to the apparent exhaustion of the potential for significant improvement of horizontal-axis turbine configurations in the near future. For instance, the UK Energy Technologies Institute is conducting the Novel Offshore Vertical Axis (NOVA) project [8] with the aim of installing a prototype large offshore vertical-axis wind turbine by the year 2020. The study hopes to demonstrate that such devices have improved stability and simpler maintenance access compared to horizontal-axis designs. The proposed configuration is depicted in figure 1.1.

In contrast to current plans for providing electricity at the scale of the national grid by concentrating large-scale wind turbines in on- and offshore wind farms, another potentially effective strategy for harvesting wind energy, particularly in the urban environment, relies on using small-scale wind turbines, with rotor diameters of only several metres. These devices can be distributed within cities and thus contribute to a decentralised energy supply in which the urban energy requirement is provided by on-site energy production equipment. The design of a wind turbine that operates efficiently within an urban area poses a significant challenge, however, since the wind in the built environment is characterised by frequent and often rapid changes in direction and speed, as

Optimal Design of a Micro Vertical Axis Wind Turbine for Sustainable Urban Environment
By Kyooseon Park, School of Computing and Engineering, University of Huddersfield, UK (2013)

2

described by McIntosh [9] amongst others. In these wind conditions, vertical-axis wind turbines might offer several advantages over horizontal-axis wind turbines. This is because vertical-axis turbines do not require a yaw control system, whereas horizontal-axis wind turbines have to be rotated in order to track changes in wind direction. In addition, the gearbox and the generator of a vertical-axis turbine can be situated at the base of the turbine, thereby reducing the loads on the tower under unsteady wind conditions, and facilitating the maintenance of the system. The principal advantage of these features of a vertical-axis configuration is to enable a somewhat more compact design that alleviates the material stress on the tower and requires fewer mechanical components compared to a horizontal-axis turbine.

Figure 1.1 NOVA Offshore Aero-generator concept developed by Wind Power Limited [8]

1.2. Advancements in Wind Power Technologies

The mankind has been using wind power for more than thousand years for different purposes. The earliest record showing usage of wind power for mechanical purposes is from tenth century in Persia. The Persian windmill [10] was drag-based and was in extensive use in Arab countries (figure 1.2). In early middle age, horizontal axis windmill appeared, and its large-scale production began predominantly in England and Holland. The horizontal axis wind energy convertor usage was wide spread. These wheels were built with around 20 blades, and in 1930s, some 8 million wheel units were built and installed.

Optimal Design of a Micro Vertical Axis Wind Turbine for Sustainable Urban Environment
By Kyooseon Park, School of Computing and Engineering, University of Huddersfield, UK (2013)

3

Figure 1.2 Persian Windmill [10]

Half a century ago, the first wind energy convertor appeared for electricity generation purpose. However, the first wind power plants for mass production were installed in early 1950s by a German constructor. The project delivered the electricity far from the public grid. The blades used in these turbines were 10m in diameter and were aerodynamically designed. Also, these blades could be pitched about the longitudinal axis to regulate the power capture from the wind. Some of these turbines are still fully functional after more than 50 years in services. During 1960 onwards, because of the cheap availability of fossil fuel power, wind turbine technology was largely ignored. However, in 1970 as fossil fuel price rose, the wind turbine development again gathered momentum. This development led to mass production of wind turbines [11]. However, because of the new power sources like nuclear power, wind energy conversion system development got slower. The other available energy conversion systems were producing much larger amount of electricity but those energy sources were also producing highly radiated wastes and harmful gases. These harmful gases resulted in greenhouse effect. Therefore, many countries signed on Climate Change agreement (treaty) at Rio 1992: since then the use of the renewable energy resources has accelerated. UK is committed to reducing greenhouse gases considerably by the year 2020. Due to this commitment, Renewable energy development program has been launched. Still, renewable energy, including wind energy, is more expensive than other energy sources. Therefore, reduction in carbon dioxide cannot be achieved in short term through market mechanism. To promote this, non-market mechanism needs to be implemented for the development of the renewable energy.

Wind energy is however growing rapidly. In 2006 wind turbine installation increased by 25% across the world. UK has planned to install wind turbines to generate 2GW of electric power by 2020. In addition, wind energy industries cooperate with public sector to improve the technology and reliability. In Denmark more than 20% of electrical power is generated by wind energy and the wind energy industry in Denmark has extensive research ties with universities. The main targets of these programs are to reduce power generation costs when using wind turbine and increasing the reliability and predictability of energy sources [12-14].

Therefore, with the support of the government, and other stakeholders, the wind energy development is taking place at a faster rate, and the wind power capacity is increasing in the world. The annual report published by EWEA shows that wind energy capacity is increasing every year throughout the world. Figure 1.3 shows the installed wind power capacity of the world [15].

Optimal Design of a Micro Vertical Axis Wind Turbine for Sustainable Urban Environment
By Kyooseon Park, School of Computing and Engineering, University of Huddersfield, UK (2013)

4

		End 2009	New 2010	End 2010
AFRICA & MIDDLE EAST	Egypt	430	120	550
	Morocco	253	33	286
	Tunisia	54	60	114
	Iran	92	0	92
	Other [1]	37	0	37
	Total	866	213	1,079
ASIA	China	25,805	18,928	44,733
	India	10,926	2,139	13,065
	Japan	2,085	221	2,304
	Taiwan	436	83	519
	South Korea	348	31	379
	Philippines	33	0	33
	Other [2]	6	48	54
	Total	39,639	21,450	61,087
EUROPE	Germany	25,777	1,493	27,214
	Spain	19,160	1,516	20,676
	Italy	4,849	948	5,797
	France	4,574	1,086	5,660
	UK	4,245	962	5,204
	Denmark*	3,465	327	3,752
	Portugal	3,535	363	3,898
	Netherlands	2,215	32	2,237
	Sweden	1,560	604	2,163
	Ireland	1,310	118	1,428
	Turkey*	801	528	1,329
	Greece	1,087	123	1,208
	Poland	725	382	1,107
	Austria	995	16	1,011
	Belgium	563	350	911
	Rest of Europe [3]	1,610	1,070	2,684
	Total	76,471	9,918	86,279
	of which EU-27 [4]	75,090	9,295	84,278
LATIN AMERICA & CARIBBEAN	Brazil	606	326	931
	Mexico	202	316	519
	Chile	168	4	172
	Costa Rica	123	0	123
	Caribbean	91	8	99
	Argentina	34	27	60
	Others [5]	83	23	106
	Total	1,306	703	2,008
NORTH AMERICA	USA	35,086	5,115	40,180
	Canada	3,319	690	4,009
	Total	38,405	5,805	44,189
PACIFIC REGION	Australia	1,712	167	1,880
	New Zealand	497	9	506
	Pacific Islands	12	0	12
	Total	2,221	176	2,397
	World total	158,908	38,265	197,039

Figure 1.3 Installed wind power capacity of the world

Figures 1.4 shows installed capacity of top 10 countries in the world in January 2011 and December 2010.

Optimal Design of a Micro Vertical Axis Wind Turbine for Sustainable Urban Environment
By Kyooseon Park, School of Computing and Engineering, University of Huddersfield, UK (2013)

5

Country	MW	%
China	18,928	49.5
USA	5,115	13.4
India	2,139	5.6
Spain	1,516	4.0
Germany	1,493	3.9
France	1,086	2.8
UK	962	2.5
Italy	948	2.5
Canada	690	1.8
Sweden	604	1.6
Rest of the world	4,785	12.5
Total TOP 10	33,480	87.5
World Total	38,265	100.0

Country	MW	%
China	44,733	22.7
USA	40,180	20.4
Germany	27,214	13.8
Spain	20,676	10.5
India	13,065	6.6
Italy	5,797	2.9
France	5,660	2.9
UK	5,204	2.6
Canada	4,009	2.0
Denmark	3,752	1.9
Rest of the world	26,749	13.6
Total TOP 10	170,290	86.4
World Total	197,039	100

(a)   (b)

Figure 1.4 Installed capacity of top 10 countries in the world in (a) December 2010 (b) January 2011

Figures 1.5 and 1.6 show cumulative installed wind capacity between 1996 and 2010. The cumulative wind power capacities increased every year, but after 2009 annual wind capacities decreased.
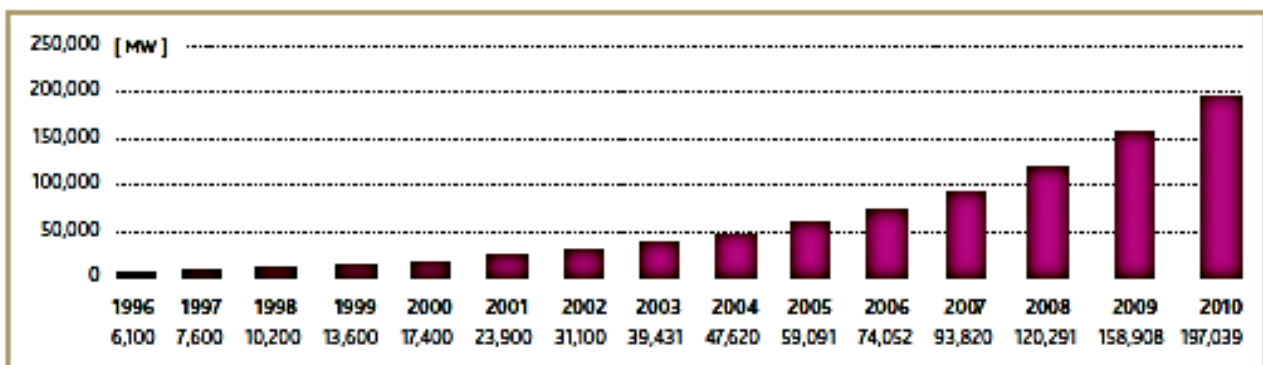
Figure 1.5 Global Cumulative Installed Wind Capacity 1996-2010
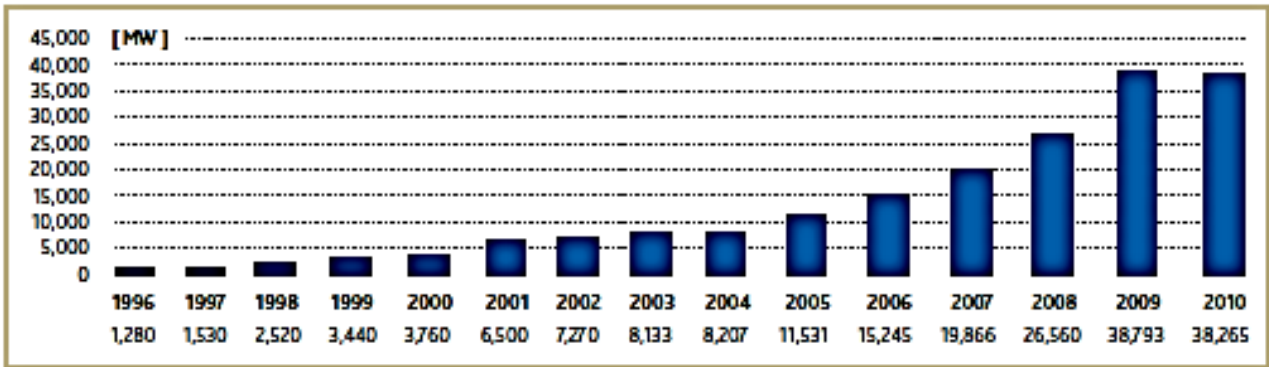
Figure 1.6 Global Annual Installed Wind Capacity 1996-2010

The global wind turbine manufacturing industry is dominated by a small number of original equipment manufacturers (OEMs). The top five OEMs, Vestas, GE, Gamesa, Enercon, and Suzlon, had a combined 62% of the global market in 2008. GE is the leading USA based supplier and was second in the world in market share in 2008. Most other companies are European and Asian OEMs. Many European OEMs are among the most mature and competitive global companies. Manufacturing capacity in Asia is growing rapidly and five Asian companies are now among the 13 largest OEMs.
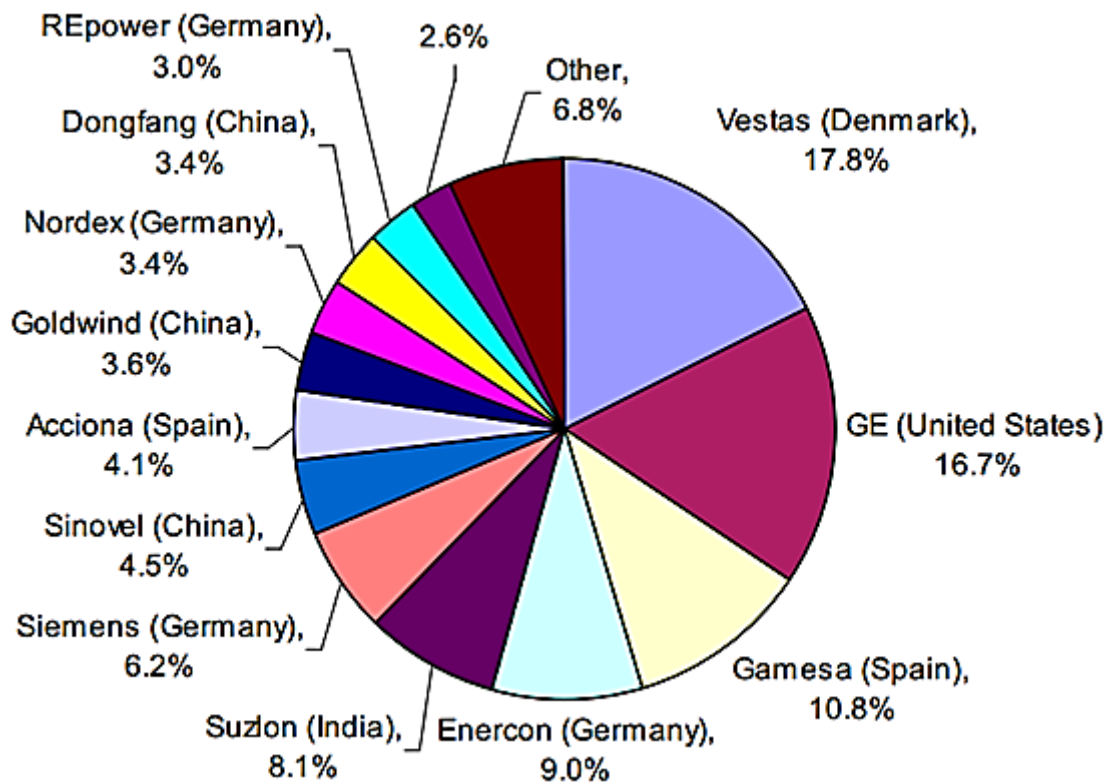
Figure 1.7 Global wind turbine market share, by OEM (2008)

Optimal Design of a Micro Vertical Axis Wind Turbine for Sustainable Urban Environment
By Kyooseon Park, School of Computing and Engineering, University of Huddersfield, UK (2013)

7

1.3. Wind Turbines

At present a number of wind turbines exist for sustainable urban environment with some considerably more advanced than others. Such technologies fall into two main categories depending on their rotational axis relative to the ground. The first type of wind turbine is the Horizontal Axis Wind Turbine (HAWT) which during normal operation has its axis of rotation parallel to the ground. These wind turbines are now considered industry standard particularly for large wind farms located both on and off shore. An example of a typical horizontal axis machine is provided in figure 1.8(a) where a domestic three-bladed rotor and nacelle are depicted:

| (a) | (b) | (c) |
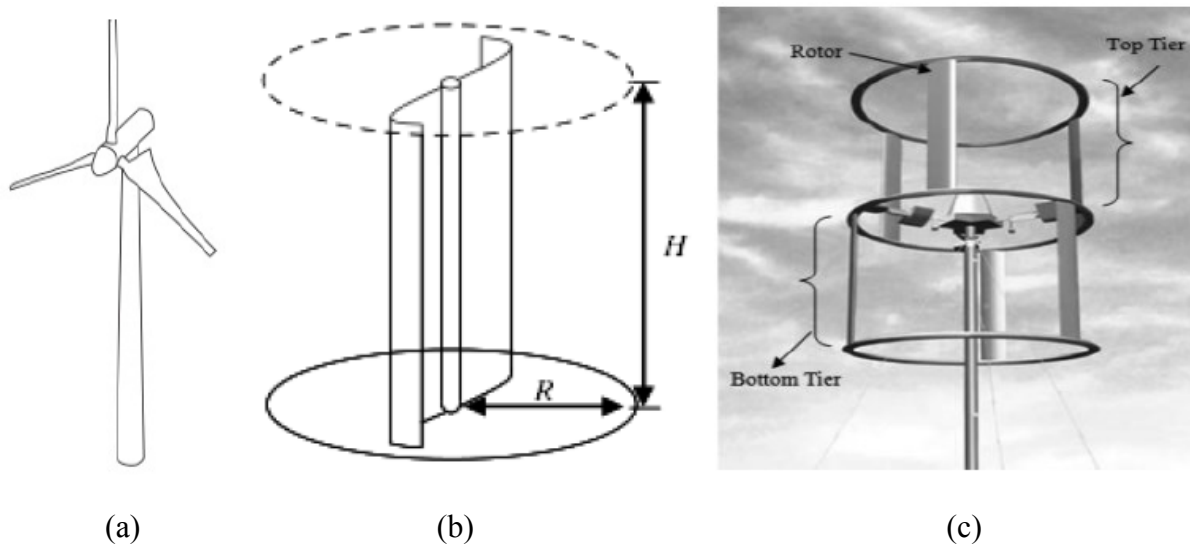
Figure 1.8 (a) Horizontal Axis Wind Turbine (HAWT) (b) Savonius Vertical Axis Wind Turbine (VAWT) (c) Darrieus Vertical Axis Wind Turbine (VAWT)

Current HAWTs have encountered a number of problems since their birth such as their effectiveness to generate power in winds that constantly change direction [16]. On large scale projects many systems are fitted with yawing mechanisms such that the machine can be directed into the wind upon a change in direction. Although this control mechanism is well proven its response times during varied wind conditions are relatively high. Further, due to large component inertias a considerable amount of power is used in directing the rotor into the primary wind direction and hence results in further inefficiencies. Similar systems are employed in the micro wind field in which small scale HAWTs are fitted with a basic yawing device which consists of a sail like paddle. Using the energy contained in the prevailing wind this paddle is yawed such that it sits in line with the dominant stream wise flow component resulting in the rotor being subjected to the full force of the wind. It is seen that the most recent generation of micro HAWTs have proven to be widely inefficient due to this system [17-18]. Additionally, it is observed that when using this passive paddle system further problems are experienced during highly turbulent conditions which result in large power fluctuations giving rise to structural and electrical instabilities. Reducing this variation in power can therefore help prolong machine life and reduce the need for regular maintenance [19]. Such problems have led to the development of the Vertical Axis Wind Turbine (VAWT) as a potential successor to the horizontal axis turbine [20].

A VAWT uses similar principals as a traditional horizontal axis turbine to extract energy from the wind using both a combination of aerodynamic lift and drag but has its axis of rotation normal to

Optimal Design of a Micro Vertical Axis Wind Turbine for Sustainable Urban Environment
By Kyooseon Park, School of Computing and Engineering, University of Huddersfield, UK (2013)

8

the ground. Vertical axis technologies have the advantage of being uni-directional in design and hence can accept and respond to changes in local wind direction [21-23]. This has resulted in many micro VAWTs outperforming equivalent horizontal axis technologies in environments where wind direction is constantly changing. Further, vertical axis technologies have major differences in structural dynamics, control systems and maintenance which make these machines less complex and cheaper to install. Figure 1.8(b) provides an example of a typical Savonius type VAWT which utilises the principle of aerodynamic drag as its primary torque generating mechanism. Although clear advantages of using this technology are documented below, they have not been investigated in sufficient detail and hence existing designs suffer from lower efficiencies when compared to more mainstream horizontal axis machines.

- Silent running
- Low start up speed
- Only one moving part, there is no gearbox
- Design allows a turbine to be mounted nearer to the ground. Also suitable for commercial roof mounting
- Giving easier access for maintenance / service
- Blends better into the environment
- Safe at high wind speeds
- Rotating diameter smaller than that of HAWT
- Safer to wildlife and birds

At this point it is important to observe two subtle differences between the Darrieus and Savonius vertical axis rotors. The Darrieus turbine, as depicted in figure 1.8(c), operates using some degree of aerodynamic drag but primarily relies on aerodynamic lift for torque generation. The opposite applies to the Savonius rotor in that its reaction type operation utilizes the principal of aerodynamic drag and the exchange of momentum from the air to the rotor surface. This report will focus on the Savonius rotor due to its suitability for low speed environments and the similarities with the wind turbine described in this thesis.

The basic configuration of the Savonius drag rotor has two semi-circular blades with a central gap defined as overlap [24]. Previous studies were mostly conducted on the optimization of design parameters such as blade number, blade shape and overlap distances. Experimental studies carried out by Sheldahl et al [25], Sivasegaram [26], Clayton [27] and Fujisawa et al [28] all report varying power coefficients for Savonius rotors ranging from 0.14 to 0.33 within a Tip Speed Ratio (λ) range of 0.8 to 1.0. Given the high solidity of this type of rotor significant torque output was observed during static and rotational modes of operation making start-ability consistent at low wind speeds. Due to this high solidity/low speed design the acoustic emission from this machine during normal operation is considerably less than the traditional HAWT described previously. With current UK planning legislation in mind this type of machine lends itself to installation in the built urban environment where noise restrictions are of primary concern [29].

One problem that was present in some machines was the large variation in rotor torque output due to the fixed two blade design. Upon detailed investigations into the flow fields across the machine it was found that blade interaction effects were present on the non-torque generating blade. It was identified that unfavourable pressure gradients were the primary cause which resulted in a counter-rotating torque which significantly reduced the efficiency of the rotor. These blade interaction effects have become one of the major limitations of this type of turbine given torque generation is only provided by one bucket each rotor cycle. Such limitations provide strong justification for

exploring alternative reaction type devices which maintain similar high levels of starting torque and provide a more consistent power delivery.

1.4.   Design considerations for Vertical Axis Wind Turbines

In the following section an overview of the wind turbine design specification and a step by step design methodology is provided. The VAWT geometry considered in the present study has the same overall geometrical dimensions as that of Colley [30]. It has been chosen so that the validation of the current study can be conducted against Colley's results. The VAWT consists of three distinct zones, as depicted in figure 1.9. These zones correspond to the core, rotor and stator regions having radii r_c, r_r and r_s respectively. Furthermore, the VAWT consists of 12 equally spaced rotor and stator blades. The inlet angle of the stator blades is a constant throughout this study i.e. $\beta=90^\circ$, such that the blade is in-line with the incident flow.
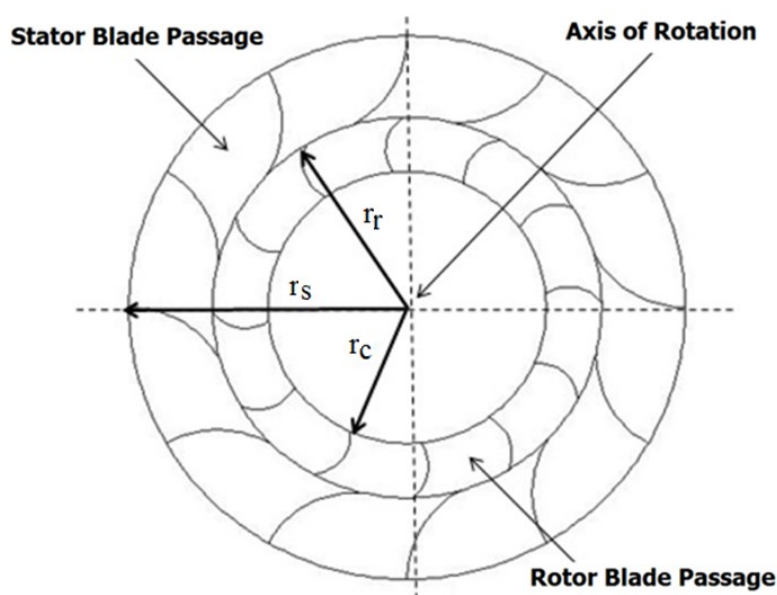
Figure 1.9 Plan view of wind turbine stator/rotor blade configuration

In the following, the design methodology used for both rotor and stator blade profile computation is described. The design equations presented are one-dimensional and correspond to an ideal flow theory [31]. The inlet and outlet velocity triangles derived for a typical radial cross-flow rotor blade are provided in figure 1.10. Using this nomenclature, a set of design equations are derived to allow for computation of primary blade geometric features namely the stator blade outlet angle (α), rotor blade inlet angle (δ) and rotor blade outlet angle (γ) along with rotor blade radius (rbr, shown in figure 1.11). V_{Ri} is the radial flow velocity vector at the inlet of the blade while V_{Ro} is the radial flow velocity vector at the outlet of the blade. Vi and Vo are the incident flow velocities and outlet flow velocities. Furthermore, V_F and V_W are the orthogonal components of the flow velocity vectors.

Optimal Design of a Micro Vertical Axis Wind Turbine for Sustainable Urban Environment
By Kyooseon Park, School of Computing and Engineering, University of Huddersfield, UK (2013)

10
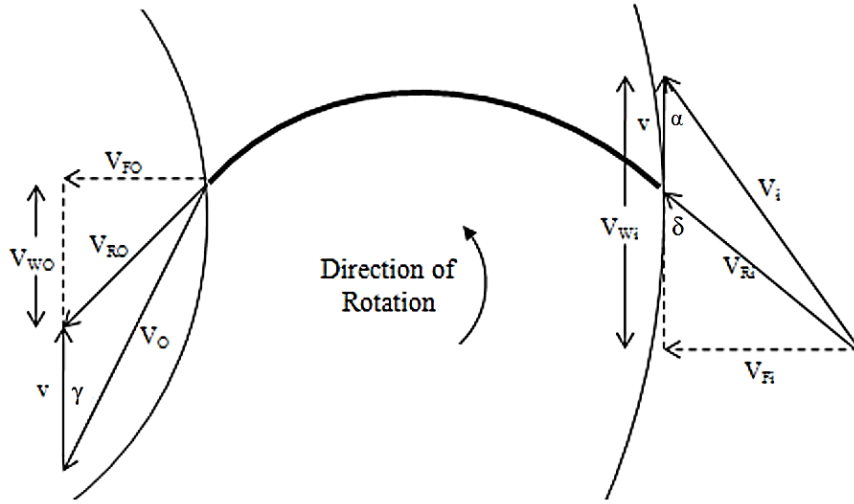
Figure 1.10 Wind turbine rotor blade velocity triangle

In the above figure the direction of rotor blade rotation is taken in the anti-clockwise direction with the main flow direction from right to left or radially inwards. The first stage of the rotor blade design is to derive a relation for rotor blade inlet angle (δ) with respect to the flow, whirl and blade tip velocities. This rotor blade inlet angle is subtended between the tangent of the blade and the direction of motion. This angle can be represented by the following expression:

$$\text{Tan}\delta = \frac{V_{Fi}}{V_{Wi}-v} \tag{1.1}$$

This equation can be expressed in alternative form where sine and cosine functions are used on the parameter V_i as per equation (1.2).

$$\text{Tan}\delta = \frac{V_i \sin\alpha}{V_{i\,\cos\alpha}-v} \tag{1.2}$$

Here v is defined as the blade tip velocity and allows for calculation of rotor angular velocity. Using this relation the rotor blade Tip Speed Ratio (λ) can be computed which is the ratio of blade angular velocity relative to the free-stream velocity or wind speed given by:

$$\lambda = \frac{\omega r}{V_i} \tag{1.3}$$

Modification of equation (1.2) using this relationship of V_i and gives the following:

$$\text{Tan}\delta = \frac{V_i \sin\alpha}{V_{i\,\cos\alpha}-v_i\lambda} \tag{1.4}$$

This equation can be simplified for a given operating condition where rotor blade inlet angle can be computed for a design stator outlet angle and expected tip speed ratio as per equation (1.5).

$$\text{Tan}\delta = \frac{\sin\alpha}{\cos\alpha-\lambda} \tag{1.5}$$

Optimal Design of a Micro Vertical Axis Wind Turbine for Sustainable Urban Environment
By Kyooseon Park, School of Computing and Engineering, University of Huddersfield, UK (2013)

11

Using the principal of conservation of mass the following expression can be given for the volumetric flow rate through the blade passage from inlet to outlet:

$$V_{Fi} * (2 * r_r) * h = (V_{F0} * 2 * r_c) * h \qquad (1.6)$$

Simplifying equation (1.6) by removing constants yields:

$$\frac{V_{Fi}}{V_{Fo}} = \frac{r_c}{r_r} \qquad (1.7)$$

The following expression gives V_{Fi} in the form of $V_{Ri} \sin(\delta)$ along with a frictional constant K. Here this constant allows for frictional losses over the surface of the blade and an initial value of 0.99 has been used for conceptual design of the rotor blade.

$$\frac{V_{Ri} \sin\delta}{K V_{Ro} \sin\delta} \qquad (1.8)$$

Simplification gives:

$$\sin\gamma = \left(\frac{1}{k}\right)\left(\frac{r_r}{r_c}\right)\sin\delta \qquad (1.9)$$

In the above, relations for both rotor blade inlet and outlet angles have been derived which can be used during the design phase. These relations assume the inner and outer extremes of the rotor blade tip radii are known along with the stator blade outlet angle which has been assumed on the basis of existing cross-flow turbines. The remaining rotor blade design parameter corresponds to the blade radius. A relation for this parameter is defined in the following section to complete the rotor blade profile design procedure.

1.4.1. Rotor Blade derivation

This section describes the derivation of the primary rotor blade design equation which allows for computation of the full rotor blade profile. This assumes both inlet and outlet blade angles have been computed using previous equations provided and allows for calculation of the blade profile radius. Here two triangles namely OAC and OCB are constructed from key blade features and are used to formulate the design equation. In order to obtain this relation two triangles are constructed about the blade profile as shown below. Using previously described nomenclature key elements of each triangle can be related to critical rotor blade design parameters:

Triangle OAC: AC=rbr, OA=r_c and Angle OAC=180 - γ
Triangle OBC: BC=rbr, OB=r_r and Angle OBC=δ

Optimal Design of a Micro Vertical Axis Wind Turbine for Sustainable Urban Environment
By Kyooseon Park, School of Computing and Engineering, University of Huddersfield, UK (2013)

12
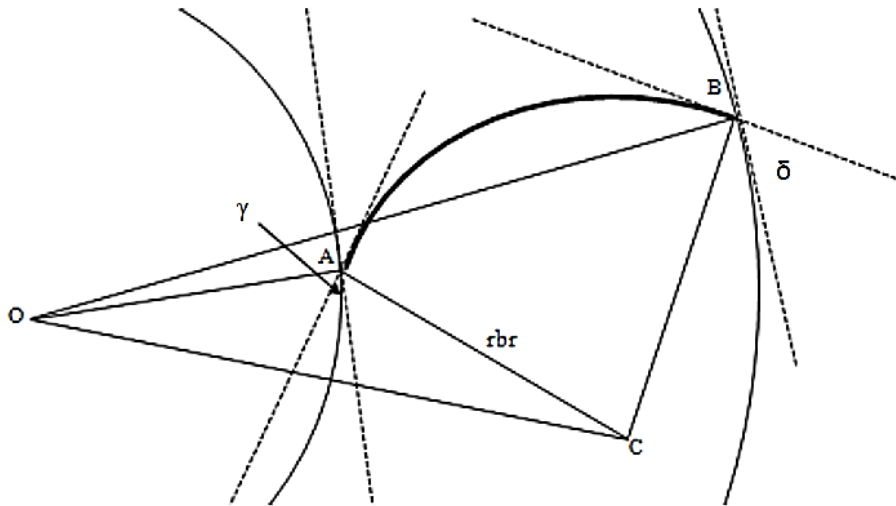
Figure 1.11 Wind turbine rotor blade design

Using the cosine relation to compute side OC gives the following two expressions from triangles OAC and OBC.

$$OC^2 = OA^2 + AC^2 - 2OA \; AC\cos(180 - \gamma) \tag{1.10}$$

$$OC^2 = OB^2 + BC^2 - 2OB \; BC\cos(180 - \delta) \tag{1.11}$$

Solving (1.10) and (1.11) simultaneously gives an expression to compute rbr using both inlet and outlet angles along with r_c and r_r:

$$rbr = r_c^2 - \frac{r_r^2}{(2(r_c\cos\delta + r_r\cos\gamma))} \tag{1.12}$$

or,

$$rbr = 0.5 * \frac{r_c^2 - r_r^2}{r_c\cos\delta + r_r\cos\gamma} \tag{1.13}$$

1.4.2. Stator Blade derivation

The key feature of this cross-flow wind turbine is the use of a fixed stator guide vane to condition the flow into the rotating rotor blade passages and enhance power generation capabilities. As already described the stator blade outlet angle has been used to compute the rotor blade inlet angle such that energy losses are minimized assuming a no-shock inlet condition. The following section describes the design procedure for the stator blade profile when used in conjunction with the rotor blade described previously. The stator blade used in this design is of fixed radius and has its inlet blade tip tangentially constrained such that it is parallel to the main flow direction. Again two triangles are constructed about the blade profile in order to derive a relation between the key blade design parameters. Here the rotor blade inlet tip (r_r) is of a modified form (r_{rc}) and allows for a

Optimal Design of a Micro Vertical Axis Wind Turbine for Sustainable Urban Environment
By Kyooseon Park, School of Computing and Engineering, University of Huddersfield, UK (2013)

13

small clearance to be maintained between the two blades given variations in manufacturing tolerances and the nature of the fabricated prototype design. This stator blade outlet radius (r_{rc}) is taken as 0.71m from the central axis of the rotor assembly as depicted in the following figure.
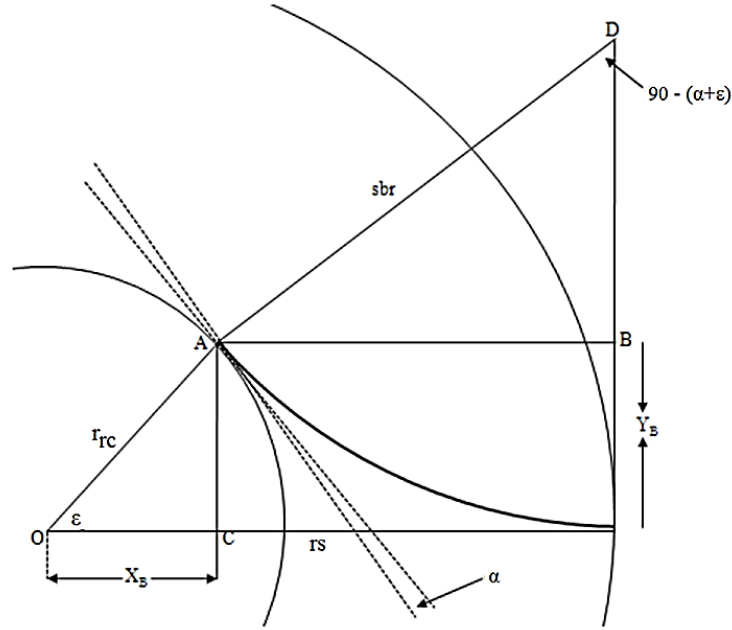
Figure 1.12 Wind turbine stator blade design

Triangle OAC: OC=XB, OA=r_{rc} and Angle AOC=ε
Triangle DAB: DA=sbr and Angle ADB=90 - (α+ε)

When considering XB which relates the x coordinate of position A and YB which defines the y coordinate relative to origin O the following relation can be derived using the stator blade outlet angle given by:

$$\text{Tan}\varepsilon = \frac{Y_B}{X_B} \tag{1.14}$$

Also relations for YB and XB can be derived using stator blade radius (sbr), stator blade inlet radius (r_s), stator blade outlet angle (α) and the angle subtended between tangent of blade inlet tip and point A:

$$Y_B = \text{sbr}\bigl(-s(\alpha + \varepsilon)\bigr) \tag{1.15}$$

$$X_B = r_s - \text{sbr}\cos(\alpha + \varepsilon) \tag{1.16}$$

Or in alternative form:

$$Y_B = r_{rc}\sin(\varepsilon) \tag{1.17}$$

$$X_B = r_{rc}\cos(\varepsilon) \tag{1.18}$$

Solving the above two equations yields: the following expressions for r_{rc}:

$$r_{rc} \sin\varepsilon = (sr)(1 - \sin(\alpha + \varepsilon)) \tag{1.19}$$

$$r_{rc} \cos\varepsilon = r_s - sbri \cos(\alpha + \varepsilon) \tag{1.20}$$

Also,

$$sbr = r_s - r_{rc} \cos\varepsilon / \cos(\alpha + \varepsilon) \tag{1.21}$$

Combining equations (1.19) and (1.21) provides a relation that allows for calculation of ε which governs the location of point A and hence the stator blade outlet tip. Hence, for a given r_{rc}, r_s and α, could be computed from the following equation:

$$r_{rc} \sin\varepsilon = (r_s - \frac{r_{rc} \cos\varepsilon}{\cos(\alpha+\varepsilon)}(1 - \sin(\alpha + \varepsilon)) \tag{1.22}$$

In alternative form:

$$\sin\varepsilon = \frac{\left(\frac{r_s}{r_{rc}} - 1\right)(1 - \sin(\alpha+\varepsilon))}{\cos(\alpha+\varepsilon)} \tag{1.23}$$

Once ε has been computed the stator blade radius (sbr) can be calculated from equation (1.21) and hence the stator profile is fully defined for use with a rotating rotor blade. Using the design equations derived for the rotor and stator blade profiles the wind turbine presented in this thesis has been designed.

1.5.   Wind Turbine Diagnostics

Renewable energy sources such as wind energy are available without any limitations. Harnessing this energy using wind power technologies allows for the potential extraction of millions of megawatts worldwide. In order to extract this energy effectively, the reliability of such technologies is critical if pay back periods and power generation requirements are to be met.

Wind power technologies have experienced rapid technological advancement over the past 20 years in aerodynamics, structural dynamics and power electronics. The integration of each of these technologies to enhance energy extraction is paramount in the success of wind turbine design and performance. It is reported that the annual power output of wind turbines can be increased by the establishment of more wind monitoring stations, improved maintenance procedures and condition monitoring [32]. The benefits of diagnostic systems that allow for characterisation of wind turbine health are documented in [33-34] in which tools that allow for identification of component wear and failure can be used to minimize wind turbine downtime. Research has therefore been focussed on developing new Condition Monitoring Systems (CMS) and Fault Detection Systems (FDS) for use on wind turbines to maintain system reliability. CMS with integrated fault detection algorithms allow for early warnings of mechanical and electrical defects to prevent major component failures along with reducing side effects on other components. The need for such a system is clear and has been shown by the Scientific Measurements and Evaluation Program in which field tests showed that 25% of a total number of 5500 repair actions were caused by loose components, wear and failure. Providing this early detection of component fault can be achieved, repair actions can be

Optimal Design of a Micro Vertical Axis Wind Turbine for Sustainable Urban Environment
By Kyooseon Park, School of Computing and Engineering, University of Huddersfield, UK (2013)

15

planned thus eliminating the need for reactive type maintenance. Using this strategy, machine downtime can be minimized considerably which is seen to have huge cost implications particularly on off-shore applications [35].

CMS are now widely used for analysis of component condition and can be used for predictive fault detection and preventive maintenance. Such practices are documented in the recent EN 13306:2010 Maintenance Terminology standard which can be used to determine remaining useful life [36]. The nature of wind turbine faults is seen to vary considerably between different machines which are due to the differences in design and system complexity. When considering the fundamental components that make up a wind turbine system, namely rotor assembly, transmission and electronics it is clear that such components are common to any wind power technology. Hence, regardless of the design and scale of the machine each is prone to component failures corresponding to the above subsystems. Figure 1.13 depicts the percentage of failure number distribution on Swedish wind turbines as reported in [37]. It highlights the large failure rate of blades/pitch components which is in the order of 13.4% between 2000 and 2004. Further studies described in [38] are concerned with types of wind turbine failure along with overall severity from a cost perspective. In this study Kahrobaee et al report a total Cost Priority Number (CPN) of \$25.5k over the period of the study which highlights the significant costs of wind turbine faults and gives further justification for developing improved maintenance strategies.
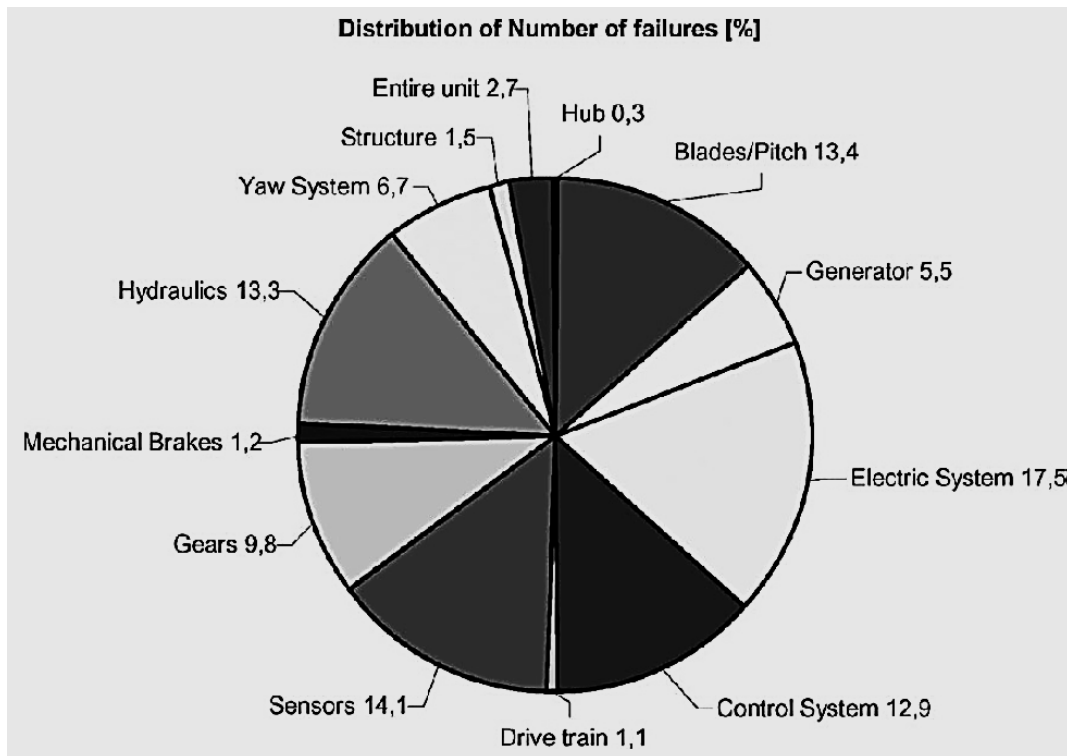
Figure 1.13 Failure number distribution [%] for Swedish wind power plants

It is however well accepted that at present, particularly for large scale machines, that drive-train problems are most common [39] given the lack of understanding of the flow conditions at the installation site and standard gearbox design practice not being sufficient for turbulent wind spectra. Such problems as documented from leading gear manufactures have resulted in a requirement for more sophisticated condition monitoring systems that allow for prediction of specific types of failure. At present the use of simulation based condition monitoring is at an early stage and hence requires considerable development particularly when considering aerodynamic, structural and

Optimal Design of a Micro Vertical Axis Wind Turbine for Sustainable Urban Environment
By Kyooseon Park, School of Computing and Engineering, University of Huddersfield, UK (2013)

16

mechanical aspects which are required for accurate prediction of wind turbine operational signatures. In addition and in relation to the machine described in this thesis, the use of multi-blade technology for micro scale cross-flow machines significantly increases the probability of rotor faults and hence any future developments in simulation based condition monitoring should have the ability to predict micro variations in wind turbine outputs. This general research problem is addressed in the following chapter where a detailed review of literature in this area is conducted and a more application based review is provided.

1.6. Motivation

From the general review carried out in this chapter a number of key areas have been identified for further investigation in this thesis. These key areas are concerned with the design and diagnostics of Vertical Axis Wind Turbines (VAWTs). VAWT provides uni-directionality and hence is well suited to turbulent flow conditions and variations in flow direction. Hence, a modelling technique is required to analyse the VAWT which can take into account these transient effects. Sliding mesh technique in CFD has the ability to consider the unsteady blade interactions of the VAWT and hence has been used throughout this study. Furthermore, it has been shown that CFD can be used as an effective tool to predict the performance output of a VAWT with reasonable accuracy.

Optimal designing of vertical axis wind turbines is very important as far as commercial viability of such machines is concerned. The optimal design of a VAWT, considered in the present study, is based on the blade angles. This includes the inlet and the outlet angles of the rotor blades plus the outlet angle of the stator blades. The inlet angles of the stator blades are always aligned with the incoming flow and hence their angle cannot be changed (i.e. $\beta=90^{\circ}$). It is hence valuable to optimise the angle of the blades in a VAWT based on the performance output. This study also provides data for the misalignment of the blades and hence will help in providing insight into condition monitoring of wind turbines. Another important aspect of the optimal designing of a VAWT is the number of blades and the size of the rotor/stator sections. It has been seen that these parameters affect the performance output of a VAWT considerably and hence a detailed and systematic investigation is required to understand and establish the effect of these parameters of VAWT's geometry on the overall performance output. Numerical studies have been conducted in the present study to analyse these effects in great detail.

A final problem identified from the general review is the requirement for wind turbine diagnostic tools that allow for fault detection and condition monitoring. Given that new wind technologies feature increased numbers of blades the probability of blade faults increases considerably. Hence, a study is required to understand the effects associated to blade loss etc on the resultant torque generating capabilities of the machine. This thesis investigates a novel area of research aimed at simulation based fault detection whereby performance signatures can be predicted and used for a range of applications.

1.7. Research Aims

The specific research aims formulated for this research study are described in this section whereas the objectives for this study will be discussed after carrying out an extensive literature review in the next chapter. Based on the motivation of this study, the research aims have been broken down into the following:

Optimal Design of a Micro Vertical Axis Wind Turbine for Sustainable Urban Environment
By Kyooseon Park, School of Computing and Engineering, University of Huddersfield, UK (2013)

17

1. Optimal Design of Vertical Axis Wind Turbines based on the Blade Angles

2. Optimal Design of Vertical Axis Wind Turbines based on Number of Rotor/Stator Blades and Size of Rotor/Stator

3. CFD Based Condition Monitoring of Vertical Axis Wind Turbines

The aforementioned research aims cover a wide range of operation of the VAWTs and hence can be considered satisfactory for this study. Detailed literature review is presented in the next chapter which focuses on the aforementioned research aims in order to find knowledge gaps in the existing literature.

1.8. Organisation of Thesis

Based on the discussions presented in the previous sections, this thesis presents the body of work, which has been carried out for the current research study.

Chapter 1 provides an overview of Vertical Axis Wind Turbines. The expressions for the design of rotor and stator blades have been presented. A condition based health monitoring perspective for VAWTs is also presented. From this overview, the motivation for carrying out this research is described, which identifies key areas to be reviewed in Chapter 2.

Chapter 2 consists of a detailed review of the research that has been carried out in the area of optimisation of VAWTs. It includes the review of published literature regarding the effect of the blade angles, number of blades and size of rotor/stator sections, on the performance output of VAWTs. Furthermore, a review of the literature available for the condition monitoring and fault detection of VAWTs has also been presented. Details of the scope of research are provided in the form of specific research objectives.

Chapter 3 documents the fundamental principles of Computational Fluid Dynamics. It includes the CFD modelling of the VAWTs; including the solver settings and the appropriate boundary conditions that have been specified to solve the flow domain. The meshing technique that has been used for the flow domain has been discussed. Furthermore, a detailed discussion on the sliding mesh technique used for the rotation of the rotor blades is the highlight of the chapter.

Chapter 4 sheds light on the flow structure in VAWTs having different blade angles. The pressure and the velocity fields have been analysed in detail to formulate the effects of the blade angles on the performance output of the VAWT. An optimal combination of the blade angles has been identified which corresponds to the maximum power output of the VAWT. Furthermore, a torque prediction model has been developed that takes into account these geometric parameters and link them to the design process of the VAWT.

Chapter 5 consists of detailed studies on the effect of the size of the VAWT and the number of blade sin the VAWT, on its performance output. The optimal VAWT design obtained from Chapter 4 has been numerically simulated for various rotor and stator sizes and blade numbers of the VAWT.

Optimal Design of a Micro Vertical Axis Wind Turbine for Sustainable Urban Environment
By Kyooseon Park, School of Computing and Engineering, University of Huddersfield, UK (2013)

18

In combination with the results from Chapter 4, an optimal design of the VAWT has been presented. Furthermore, a torque prediction model has been developed that takes into account these geometric parameters and link them to the design process of the VAWT.

Chapter 6 deals with the condition based health monitoring of the VAWTs based on missing rotor/stator blade and slits in the rotor blade of the VAWT. The detailed investigation reveals the changes in the flow field within and in the vicinity of the VAWT as a blade goes missing from either the stator or the rotor of the VAWT or if there is a fault within a rotor blade. The degradation in the performance output of the VAWT helps in the detection of these faults carrying distinct signatures.

Chapter 7 concludes the findings of this study, clearly mentioning the goals achieved and additions to the existing knowledge about VAWTs in terms of both the optimal design and the condition monitoring of VAWTs. Recommendations for future work have also been included.

CHAPTER 2
LITERATURE REVIEW

<div style="font-size:200%">T</div>he following chapter provides a detailed review of the available literature in the field of wind engineering with emphasis given to the vertical axis wind turbines. The main areas addressed in this chapter are associated to wind turbine design and diagnostics which form the basis of this thesis. Within each of these areas, specific limitations have been identified which have been used to define the scope of the research. From the scope, specific research objectives of this thesis are provided such that efforts are made to provide novel contributions in each of the areas investigated.

Optimal Design of a Micro Vertical Axis Wind Turbine for Sustainable Urban Environment
By Kyooseon Park, School of Computing and Engineering, University of Huddersfield, UK (2013)

20

2.1. Introduction

In recent years the majority of wind turbine research has been focussed on the development of existing technologies using both experimental and numerical techniques. From the late 1970's a considerable amount of research has been communicated which documents the design and development of the Vertical Axis Wind Turbine (VAWT). From a general review of literature it is noticed that each technology produces a wide range of operating characteristics depending on both the geometric configuration and fluid flow condition. This chapter aims to provide a clear and concise review of the major works conducted in this area with reference made to Darrieus, Savonius and cross-flow wind turbines. Additionally, the need for simulation based diagnostics as described in Chapter 1 is also considered in which a review of relevant literature in this area is documented. Throughout this chapter emphasis will be given to reaction type wind turbines given the similarities to the machine presented in this thesis.

2.2. Wind Turbine Optimisation

Baird et al [40] conducted a series of wind tunnel experiments on the performance output of a small scale vertical axis wind turbine. Various blade shapes, with and without deflectors, have been analysed for power generation from the VAWT. Pressure and power coefficients for S shaped blades have been drawn. It has been reported that the use of deflectors decrease the power output of the VAWT instead of increasing it (figure 2.1).
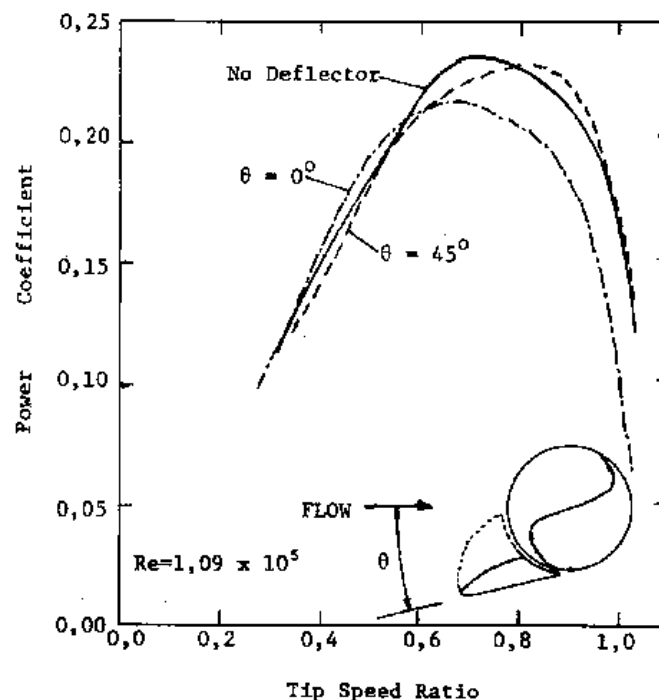
Figure 2.1 Experimental power curves comparing the results for the S rotor with no deflector and a small deflector at 0° and 45° [40]

Travis [41] conducted numerical studies on the aerodynamic shape optimisation of conventional VAWT designs. Differential evolution algorithms have been used with Computational fluid dynamics tools in order to minimise an objective function based on constraints that are represented

Optimal Design of a Micro Vertical Axis Wind Turbine for Sustainable Urban Environment
By Kyooseon Park, School of Computing and Engineering, University of Huddersfield, UK (2013)

21

by floating point values rather than binary strings. It has been shown that optimised VAWT design shows a slight increase (1 - 2%) in the performance output of the VAWT.

Yonghai et al [42] have proposed a new design of the VAWT that increases its performance output. The design of the new VAWT is based on a windshield attached to the end of the rotor blades. Computational fluid dynamics based analysis has been used to analyse the performance output of this new VAWT design. It has been shown that the new VAWT design increases the torque output of the VAWT (figure 2.2).
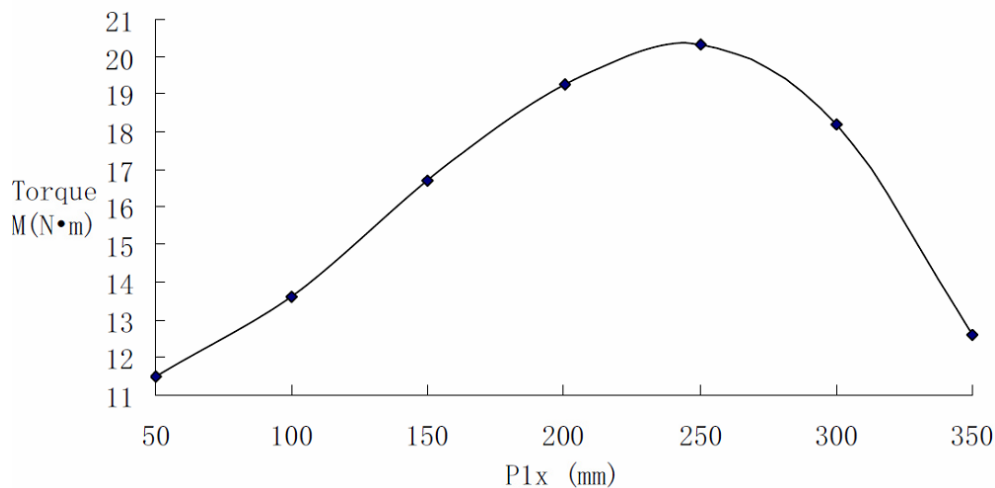
Figure 2.2 Torque output of the new VAWT design [42]

Aron [43] has conducted field test to optimise the shape of a VAWT based on the shape of the blades. Three various shapes of a VAWT i.e. conventional, ridged and window type, have been analysed (figure 2.3) for the torque output and it has been shown that the conventional design of the VAWT performs better than the other two designs. It has also been shown that at lower wind speeds, window type VAWT provides higher torque than ridged type VAWT whereas at higher wind speeds the trend is opposite.

Figure 2.3 Conventional, Ridged and Window type Rotors [43]

Leal [44] presents a methodology for an automated optimization of the rotor of a vertical axis wind turbine based on genetic algorithms. Rotor profile shape, diameter and tip speed ratio of the wind turbine have been optimised to yield maximum power using CFD. Several blade shapes have been proposed with different twist angles and profiles.

Samuel [45] has conducted studies on the optimisation of VAWTs and presents a concept that utilises each blade's entire rotational cycle for power generation by having adjustable blade angles. The study uses both CFD techniques and lab based tests. It has been shown that static torque and

Optimal Design of a Micro Vertical Axis Wind Turbine for Sustainable Urban Environment
By Kyooseon Park, School of Computing and Engineering, University of Huddersfield, UK (2013)

22

optimal tip speed ratio are both greater than those with fixed blade angle design of the VAWT (figure 2.4).
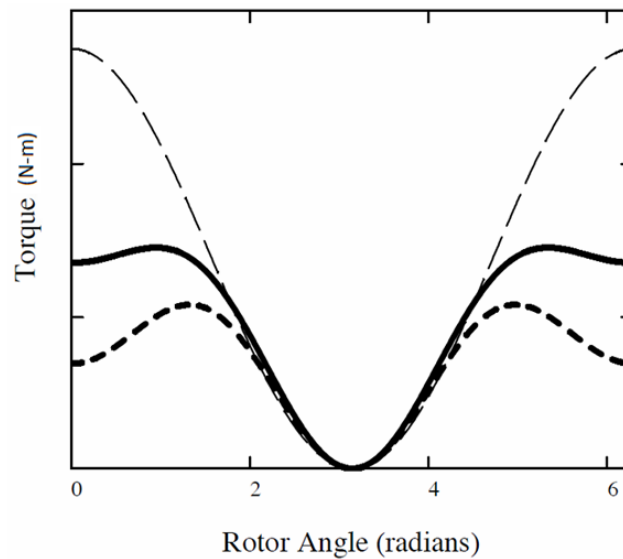
Figure 2.4 Static Torque on the blades having different blade angles [45]

Paul [46] carried on experimental studies on curved blade Darrieus type VAWTs to analyse the effects of blade pre-set pitch on its aerodynamic performance. A VAWT has been mounted such that its symmetrical cross-section blades intersect with the blade chord at points between -180⁰ and 77⁰ of the chord. It has been shown that small variations in blade pre-set pitch/offset lead to large variations in the aerodynamic performance of the VAWT. Efficiency and power output of the VAWT has been shown to increase by 50%.

Colley et al [47] conducted numerical studies to analyse the effects of rotor blade position on the performance output of a VAWT. Multiple Reference Frame approach has been used to rotate the rotor blades of the VAWT. It has been shown that torque output of the turbine decreases with an increase in rotor tip speed ratio for all rotor blade positions. Furthermore, it has been concluded that the VAWT power curve characteristics vary with relative rotor blade position (figure 2.5).
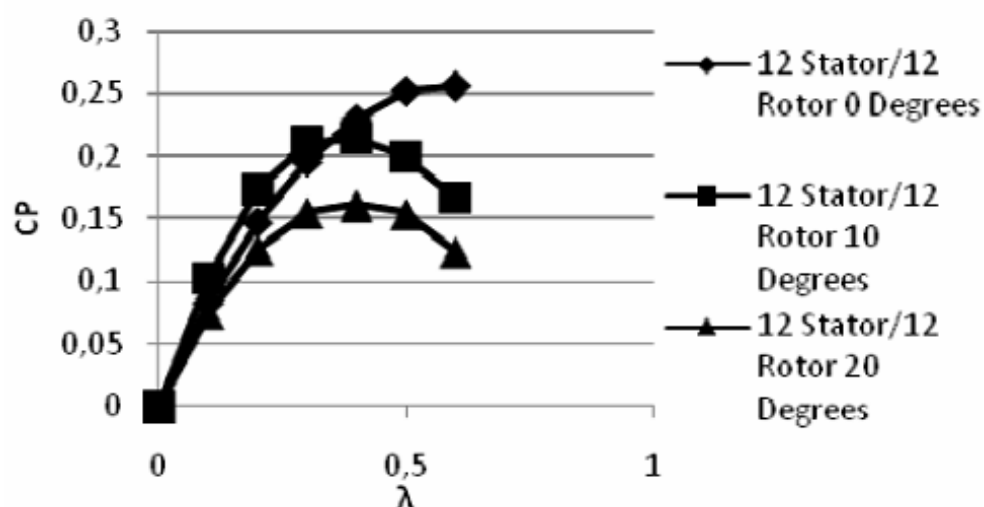
Figure 2.5 Variations in Power output w.r.t. Tip Speed Ratio [47]

Wirachai [48] conducted a series of laboratory and field tests on various blade designs of Darrieus type VAWT. It has been reported that CFD is unable to accurately predict the performance output of a VAWT and hence stress has been made on performing field tests. However, the modelling techniques incorporated within the CFD domain are not accurate enough. Only a highly simplified model with very basic boundary conditions (not accurately capturing the transient phenomena) have been used that have resulted in a very crude agreement between the published and CFD results.

Manabu et al [49] have conducted experimental studies to analyse the effects of directed guide vanes on the performance output of a VAWT. The effects of setting angle and gap between rotor blade and guide vane on power coefficient and starting characteristic have been investigated in detail. It has been shown that use of directed guide vanes increases the peak coefficient of the VAWT considerably. Furthermore, increase in the setting angle increase the performance output of the VAWT (figure 2.6).

(a) Power coefficient

(b) Torque coefficient
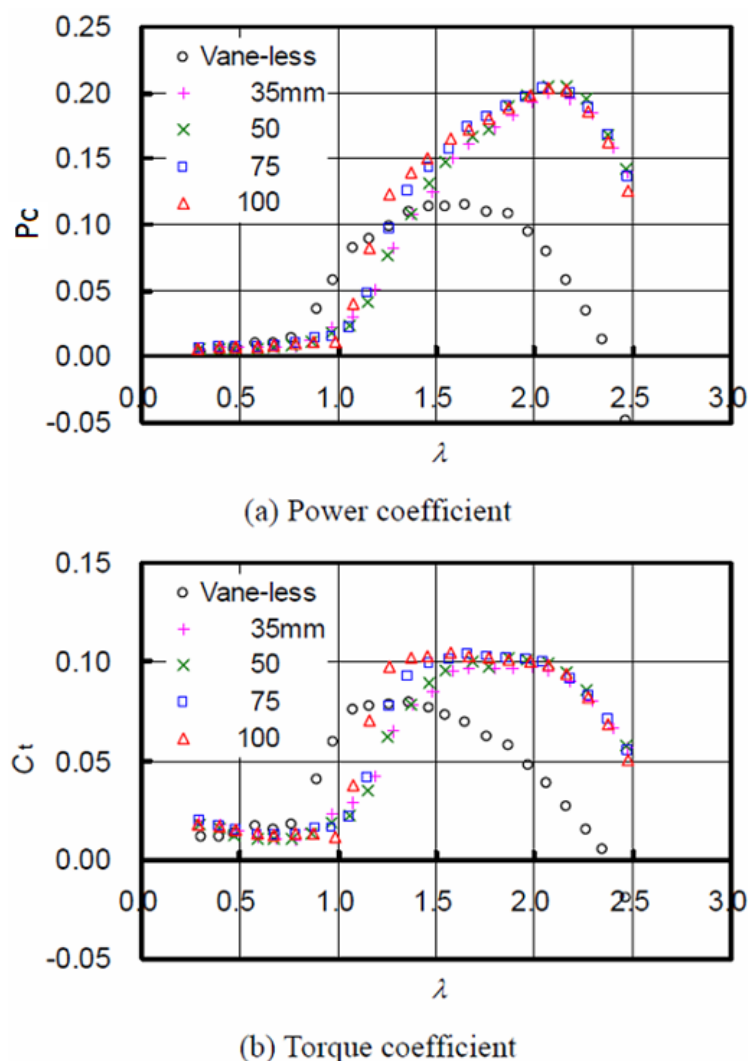
Figure 2.6 Effect of Guide Vanes on the performance output of a VAWT [49]

Marco et al [50] conducted CFD based studies on a two dimensional model of the VAWT, having straight blades, in order to reduce the torque variations during the revolution by increasing blade number. It has been shown that increase in the number of blades increases the torque output but at the same time decreases the efficiency of the VAWT. Furthermore, it has observed that increase in the number of blades reduces the variations in the cyclic torque output of the VAWT.

Optimal Design of a Micro Vertical Axis Wind Turbine for Sustainable Urban Environment
By Kyooseon Park, School of Computing and Engineering, University of Huddersfield, UK (2013)

24

Chein-Chang et al [51] carried out numerical studies to analyse the effects of pitch angle and blade camber on flow characteristics and performance of a small sized Darrieus VAWT. Three different blade profiles with various pitch angles have been investigated in this study. It has been shown that the initial acceleration of the VAWT decreases as the pitch angle increases. Furthermore, increase in the camber of the blades increases VAWT's ability of self-starting. Hence, it has been observed that blades of proper camber are helpful to enhance the moment coefficient at a fixed inflow wind speed (table 2.1).

Table 2.1 The coefficient variations of RMS Moment and Time Averaged Reacting Moment [51]

θ	$-10°$	$-5°$	$0°$	$5°$	$10°$
NACA0012					
$C_{Mr.m.s}$	0.07696	0.07056	0.09774	0.11543	0.09056
C_{Ms}	0.09363	0.13984	0.16402	0.19564	0.27441
NACA2412					
$C_{Mr.m.s}$	0.09073	0.09941	0.102	0.17339	0.13726
C_{Ms}	0.19357	0.20102	0.20063	0.22406	0.23361
NACA4412					
$C_{Mr.m.s}$	0.10338	0.09699	0.09468	0.09617	0.06906
C_{Ms}	0.1755	0.18811	0.18356	0.204	0.22712

Soraghan et al [52] conducted numerical studies using double multiple streamtube method to optimise the aerodynamic performance of a VAWT having straight blades. The study introduces a method of calculating effective lift to drag ratio based on averaged torque per cycle. It has been shown that solidity and conning angle of a VAWT has huge impact on its optimal tip speed ratio and power generation. Furthermore, it has been demonstrated that an H-rotor with the same solidity as a V-rotor will operate optimally at a much lower rotational speed and attain a higher power coefficient (figure 2.7).
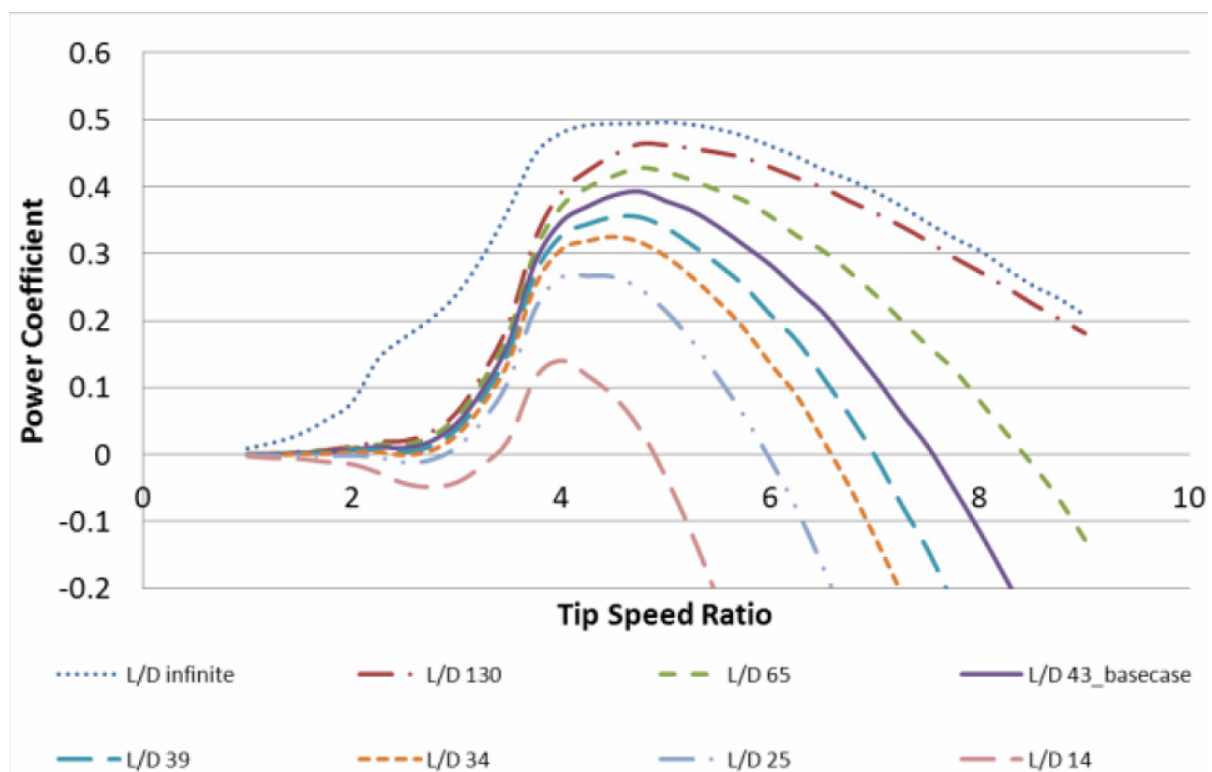
Figure 2.7 Effect of L/D on Power Coefficient of a VAWT [52]

Optimal Design of a Micro Vertical Axis Wind Turbine for Sustainable Urban Environment
By Kyooseon Park, School of Computing and Engineering, University of Huddersfield, UK (2013)

Pope [53] conducted experimental investigations on a Zephyr type VAWT and validated the results with numerical simulations using CFD tools. k-ε turbulence model has been used to perform the transient simulations. The 3-D numerical predictions are based on the time averaged Spalart-Allmaras equations. Prototype Zephyr VAWT model consists of 9 stator and 5 rotor blades, however a modified model, having stator blade guide vanes, has also been investigated. It has been shown that both numerical formulations provide correct trends for the changes of flow dynamics and power coefficients for changes in the VAWT geometry. The constant speed model predicts the optimal TSR at lower wind speeds that are more likely to be found where the Zephyr turbine would be located. The simulations also exhibit a high degree of scalability for both configurations.

Howell [54] carried out a combined experimental and computational study into the aerodynamics and performance of a small scale vertical axis wind turbine (VAWT). Wind tunnel tests were carried out to ascertain overall performance of the turbine and two- and three-dimensional unsteady computational fluid dynamics (CFD) models were generated to help understand the aerodynamics of this performance. Wind tunnel performance results are presented for cases of different wind velocity, tip-speed ratio and solidity as well as rotor blade surface finish. It is shown experimentally that the surface roughness on the turbine rotor blades has a significant effect on performance. Below a critical wind speed (Reynolds number of 30,000) the performance of the turbine is degraded by a smooth rotor surface finish but above it, the turbine performance is enhanced by a smooth surface finish. Both two bladed and three bladed rotors were tested and a significant increase in performance coefficient is observed for the higher solidity rotors (three bladed rotors) over most of the operating range. Dynamic stalling behaviour and the resulting large and rapid changes in force coefficients and the rotor torque are shown to be the likely cause of changes to rotor pitch angle that occurred during early testing. This small change in pitch angle caused significant decreases in performance (figure 2.8).
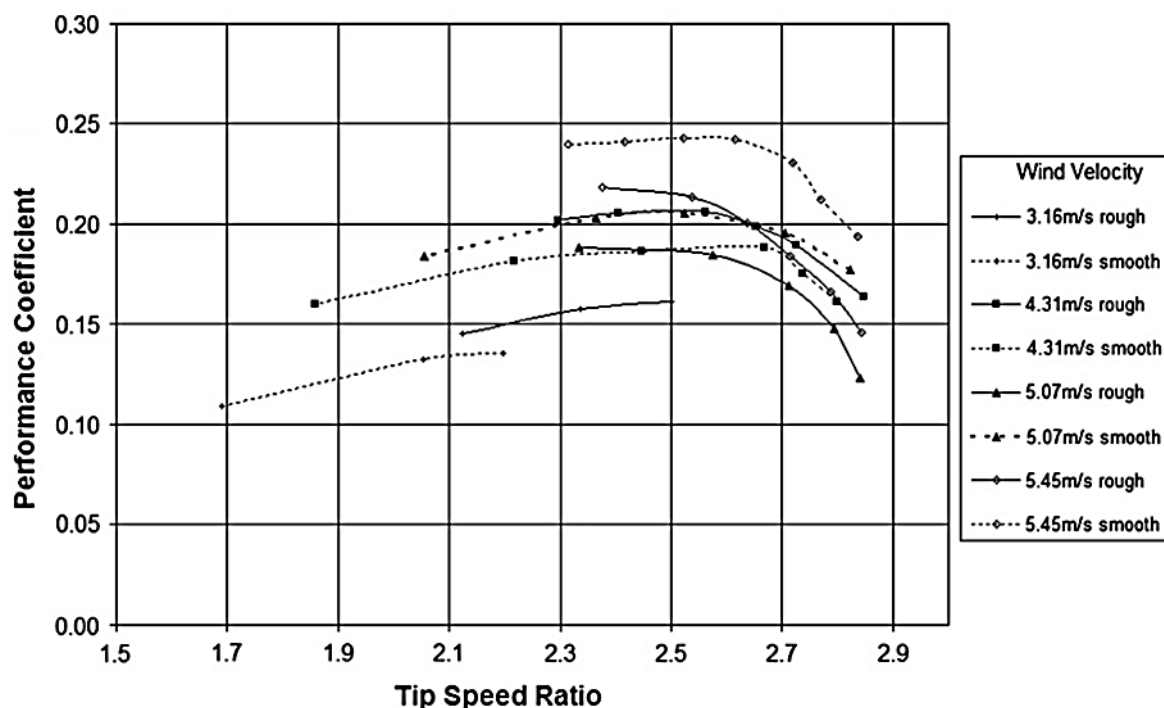
Figure 2.8 Performance Coefficient variation with rotational velocity for turbine model with two blades, for smooth and rough blade surfaces [54]

Optimal Design of a Micro Vertical Axis Wind Turbine for Sustainable Urban Environment
By Kyooseon Park, School of Computing and Engineering, University of Huddersfield, UK (2013)

26

2.3.   Wind Turbines Diagnostics

Due to recent developments in the field of wind energy and in particular the expansion of installed capacity around the world, the need for reliable and intelligent diagnostic tools is of greater importance. As the rated capacity of wind turbines increases so does the overall system cost along with the need to have online diagnostic capabilities. The following section describes briefly some of the tools available not only in the field of wind engineering but also from the field of rotating machinery given the similarities between the two. It assumes the reader is familiar with traditional well established measurement techniques such as vibration, acoustic and current signal analysis and focuses on application issues and scope for future development in this field.

Condition monitoring and fault detection techniques have been used to predict and determine machine faults in a diverse range of industries and are particularly common for rotating machinery. Hameed et al [33-34] provides a general review of existing techniques used to determine wind turbine system and component faults. The authors discuss the limitations of such technologies and make general remarks regarding future advancements in this area. The major techniques described are associated to vibration, acoustic, current signal analysis and oil spectrum analysis which have been widely used in industry for the last 60 years. It is shown that by carrying out spectral analysis on vibration, acoustic and current signals [55-61] the nature of machine faults can be characterized and used for predictive maintenance strategies and on-line fault detection.

Andrzej et al [62] conducted a series of experimental studies on a high solidity small scale VAWT with different blade shapes. Wind tunnel experiments have been conducted to investigate the effects of pre-set toe-in and toe-out turbine blade pitch. The effect of blade mount-point offset was also investigated. The results from these tests are presented for a range of tip speed ratios, and compared with an extensive data base. Results show measured performance decreases of up to 47% for toe-in, and increases of up to 29% for toe-out blade pitch angles, relative to the zero pre-set pitch case. Also, blade mount-point offset tests indicate decreases in performance as the mount location is moved from mid-chord towards the leading edge, as a result of an inherent toe-in condition (figure 2.9).
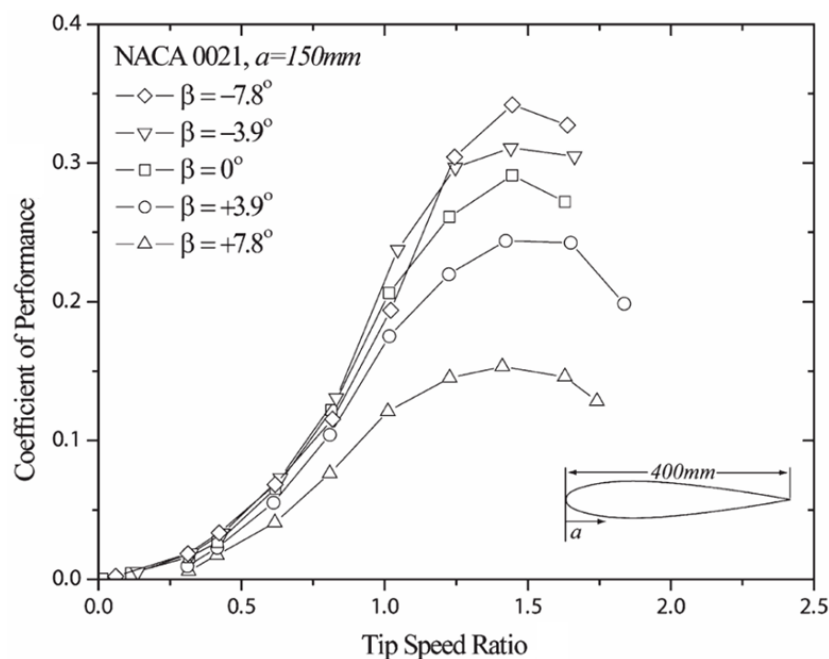
Figure 2.9 Effect of Preset Pitch on Performance Coefficient [62]

Optimal Design of a Micro Vertical Axis Wind Turbine for Sustainable Urban Environment
By Kyooseon Park, School of Computing and Engineering, University of Huddersfield, UK (2013)

27

Colley [63] conducted numerical and experimental studies on stator blade diagnostics. The configurations of the two dimensional VAWT considered in the study comprises of 3, 6 and 12 stator blades respectively. Multiple Reference Frame (MRF) approach has been used to mimic the rotation of the rotor blades. The tip speed ratio has been varied from 0 to 0.6 in increments of 0.1. The results show that in the VAWT having 12 stator blades, torque output reduces as rotational speed increased. Maximum power output of the VAWT has been noted to occur at TSR=0.4. When stator blades are reduced to 6, power output is reduced by 50%, whereas in VAWT having 3 stator blades, power output reduces a further 30%.

Gahatage et al [64] conducted both experimental and numerical studies to yield maximum power from a VAWT which in-turn can be used to stir a tank. Efficiency of a basic wind turbine's design has been shown to be a function of the shape and the number of blades. The results depict that a provision in blade twist enhances the efficiency of the VAWT. Furthermore, it has been concluded that a VAWT with two blades yield more power than a VAWT with three blades.

Preen et al [65] have used artificial neural networks to optimise the shape of the VAWTs. It has been shown that surrogate models are more efficient, less time consuming and computationally inexpensive as compared to traditional CFD tools regarding the optimisation of VAWTs. However, the designs proposed by these models are unrealistic as far as manufacturing techniques available are concerned (figure 2.10).
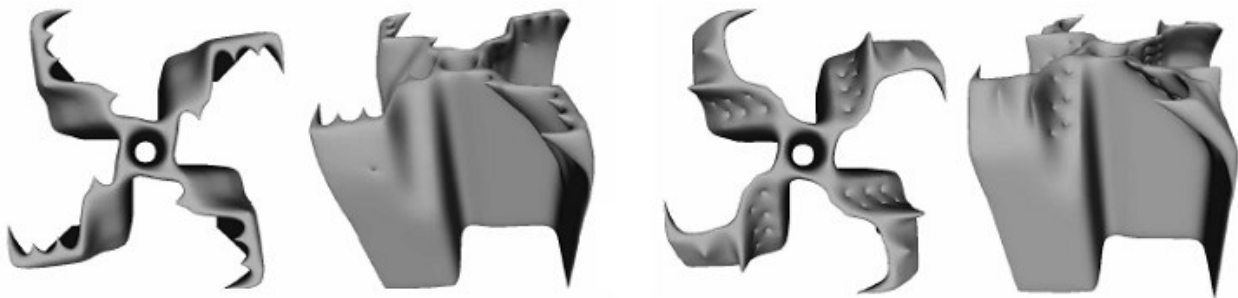
Figure 2.10 Proposed Designs [65]

Castillo [66] conducted numerical studies on the performance output of a VAWT. The aerodynamic analysis of the VAWT has been performed using double-multiple streamtube method with variable interference (DMSV) which is based on conservation of momentum and was developed by Paraschivoiu [67]. It has been shown that this model performs quite well for VAWTs and can be used as an alternative tool for aerodynamic analysis of VAWTs.

Ramkissoon et al [68] conducted a series of field test on a modified design of VAWT having NACA 0018 airfoil type blades. The modification to the design was carried out by using strut modifiers to decrease the aerodynamic drag on the blades and hence increase the power output of the VAWT (figure 2.11). It has been shown that using this method, the power output of the VAWT increases up to 25% (in some cases).

Optimal Design of a Micro Vertical Axis Wind Turbine for Sustainable Urban Environment
By Kyooseon Park, School of Computing and Engineering, University of Huddersfield, UK (2013)

28

(a)   (b)
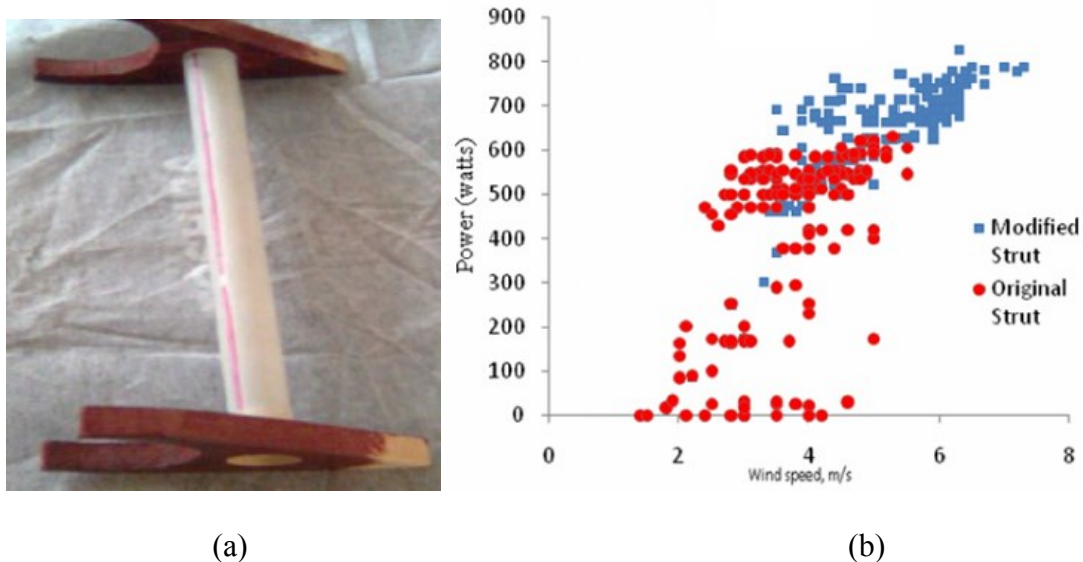
Figure 2.11 (a) Modified Strut Design (b) Comparison of Power Outputs [68]

Beri et al [69] have conducted extensive CFD based studies to analyse the effects of camber airfoil on self-startup of two dimensional VAWTs at low Reynolds's numbers. Hydrodynamic forces acting on cambered airfoil section have been computed from different angles of attack with fixed pitch. It has been shown that camber airfoils have the potential to self-start at reduced coefficient of power.

Zhang et al [70] carried out a series of CFD based studies to analyse the effect of numerical schemes on the predicted aerodynamic performance of the VAWT. It has been shown that although k-e model predicts the performance output of the VAWT with reasonable accuracy, however, the predicted turbulent viscosity coefficient is very high. Hargreaves [71] has indicated the same problem with k-e turbulence model and has shown that the turbulent kinetic energy shows a spike in the near wall region (figure 2.12). Hence, other models have been suggested to be used for better prediction of performance output in VAWTs.
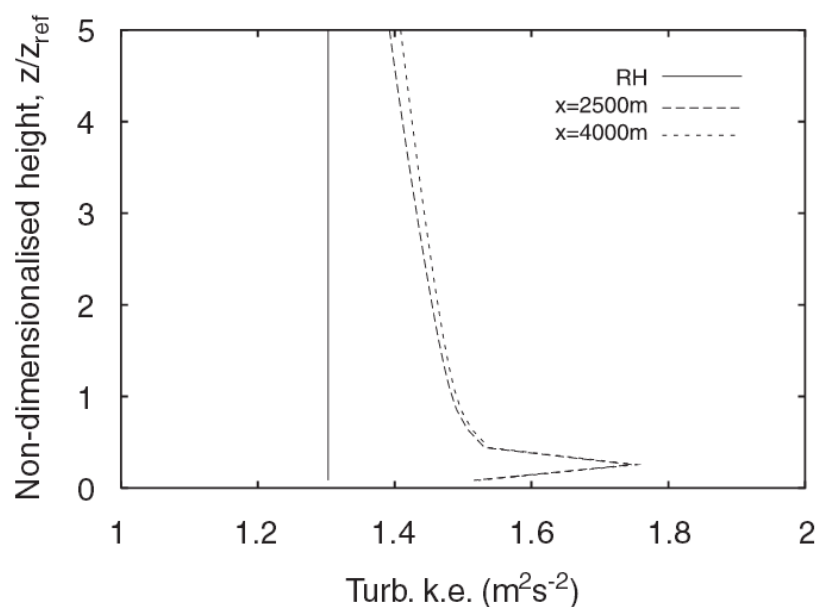
Figure 2.12 Turbulent Kinetic Energy in the Near-Wall Region [71]

Li et al [72] conducted numerical studies to analyse the effect of solidity on the straight-bladed vertical axis wind turbine. Two dimensional models of VAWTs have been analysed for steady flow of air through them. It has been shown that increase in solidity increases average torque output of the VAWT. Furthermore, increase in solidity first increases the power output of the VAWT, however, at higher tip speed ratios, the power output decreases.

Sabaeifard et al [73] conducted both experimental and CFD based numerical studies to analyse the performance output of a small scale VAWT and hence to optimise the design of the VAWT. Multiple Reference Frame technique has been used to rotate the blades of a two dimensional model of the VAWT. It has been reported that increase in number of blades increases the power output of the VAWT (figure 2.13). Furthermore, the results regarding the effect of the solidity on the power output of VAWT match with that of Shenmao et al [72] i.e. increase in solidity increases power output at lower tip speed ratios only.
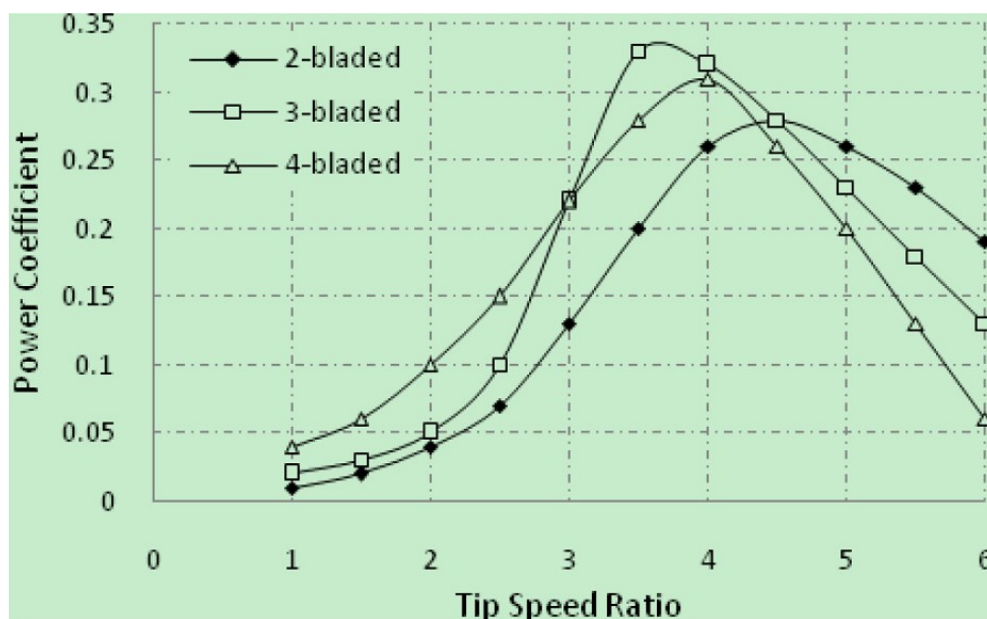
Figure 2.13 Effect of number of blades on Power Coefficient [73]

Colley [74] conducted numerical and experimental studies on rotor diagnostics. A two dimensional model of the VAWT has been analysed using multiple reference frame approach to rotate the rotor blades. It has been shown that as a rotor blade gets detached from the VAWT, the average torque output increases. However, the experimental results show the opposite trend. It has therefore been recommended to use a full three dimensional model for better accuracy of the results.

Atif et al [75] conducted CFD based studies on the effects of cracks in the rotor blades of a vertical axis wind turbine. Three dimensional VAWT models with various sized cracks have been analysed using sliding mesh technique. It has been shown that as the size of the crack increases, the amplitude of torque variations increases considerably even though the average torque output of the VAWT remains almost constant (figure 2.14).

Optimal Design of a Micro Vertical Axis Wind Turbine for Sustainable Urban Environment
By Kyooseon Park, School of Computing and Engineering, University of Huddersfield, UK (2013)

30
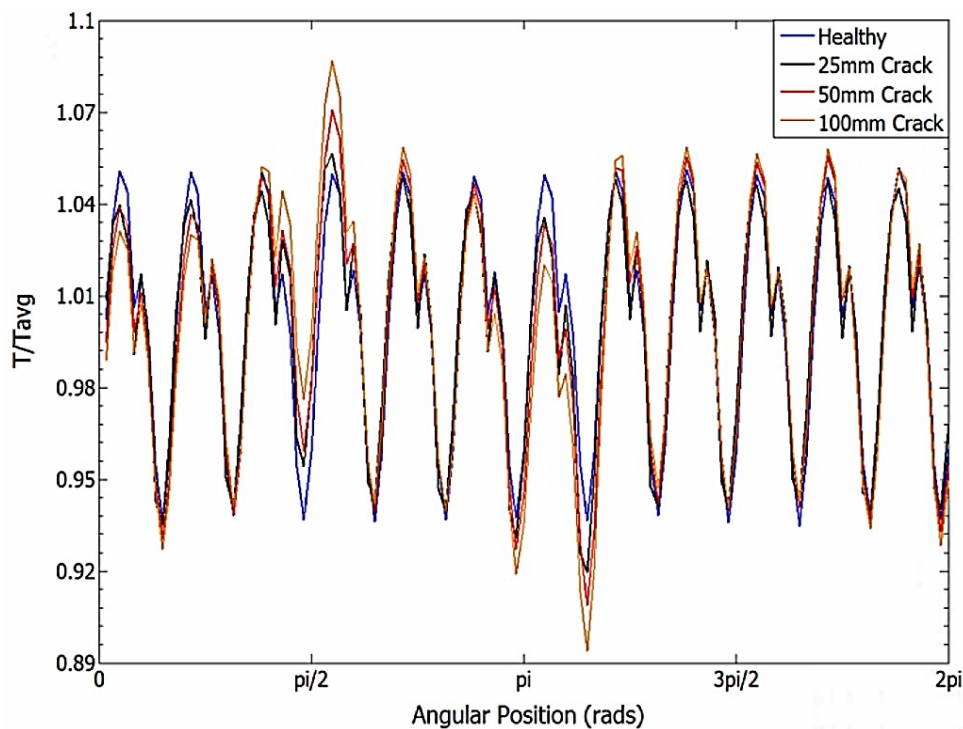
Figure 2.14 Effect of Cracks on Torque Output [75]

Park et al [76] conducted numerical studies on the effects of missing rotor blades in a vertical axis wind turbine. Two dimensional VAWT models have been analysed using sliding mesh technique. It has been shown that as the number of missing rotor blade increases, the torque and power outputs of the VAWT decreases, decreasing its performance output (figure 2.15).
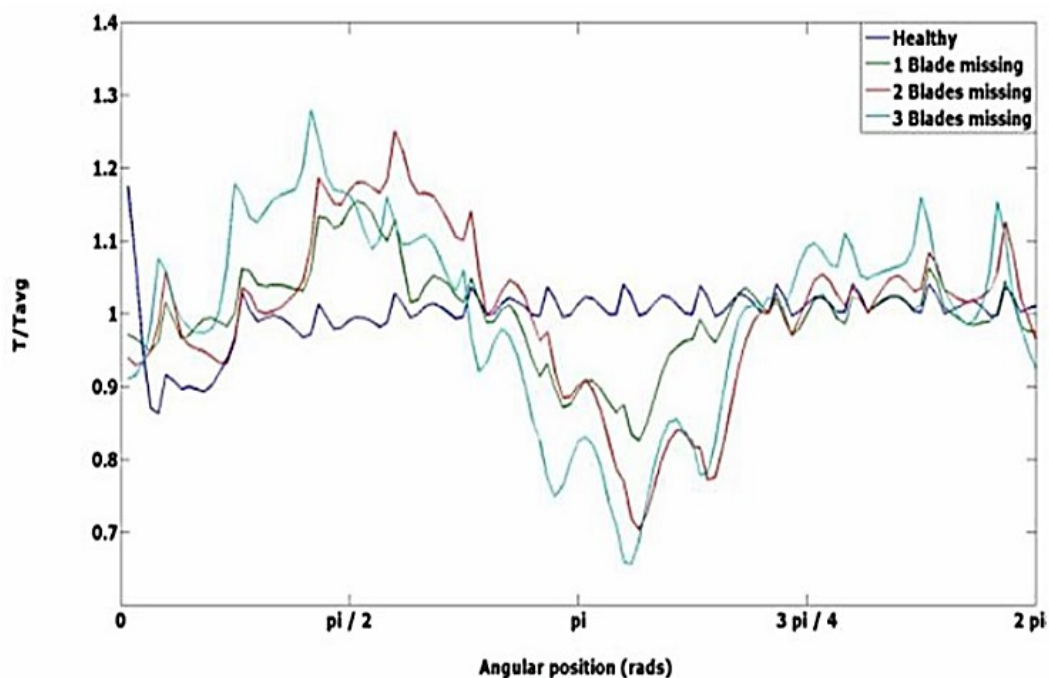
Figure 2.15 Effects of missing blade/s on Torque Output of VAWT [76]

Optimal Design of a Micro Vertical Axis Wind Turbine for Sustainable Urban Environment
By Kyooseon Park, School of Computing and Engineering, University of Huddersfield, UK (2013)

31

2.4.   Scope of Research

The literature review presented in this chapter has shown that there are various geometric variables within a VAWT that significantly affects its performance output. These geometrical features include the blade angles, the number of blades, the size of rotor/stator sections, the height of the VAWT etc. There is a need for a study, carried out in a systematic way that quantifies these effects and link them to the design process of a VAWT. For this purpose, a specific range of blade angles have been chosen in the present study (α from 1.689° to 21.689°, δ from 22.357° to 42.357° and γ from 18.2° to 38.2°) while β has been kept constant to 90°. β has been kept constant because of the design requirement that the incident flow and the stator blade's inlet should be in-line with each other. The range of other blade angles (α, δ and γ) has been chosen keeping in mind the difficulties in the manufacturing of such blades and integration of these blades with the in-house built VAWT shown in the next chapter (under experimental setup section). Hence, a range of -10° to original VAWT to +10° has been chosen for analysis in the present study and all the results are valid in this range of angles only. Furthermore, the number of blades has been varied between 4, 8 and 12 as the original design contains 12 blades. Size of the VAWT has also been varied such that both the diameter and the height of the VAWT should not exceed 1m (based on the original design of the VAWT).

At present Vertical Axis Wind Turbines (VAWTs) are in the initial stages of development. The key design and diagnostic characteristics of these machines are not well understood and hence primary areas have been identified from the literature review for investigation. These areas are used to define the general scope of this research along with specific research objectives which are described in the following section. In general, the scope of this thesis is concerned with the design and diagnostics of a VAWT. The first major area of this research is aimed at the investigations into the effect of the blade angles on the performance output of the VAWT under transient operation using sliding mesh technique. These investigations have been conducted at both micro and macro levels. Micro level analysis is concerned with the flow field characteristics across the machine at transient modes of operation. In general, this investigation considers the development of both pressure and velocity fields within the stationary and rotating frames of reference namely stator and rotor blade passages. Furthermore, the unique distribution of flow around the machine is evaluated and where possible its relation with torque generating mechanisms within the rotor described. Macro level analysis is aimed at understanding the machines performance characteristics by the quantification of both the torque and power outputs of the rotor. Rigorous statistical tools have been employed to analyse the variations in the torque signals from the VAWT.

From reviewed literature, the torque generation capabilities of the VAWT are not well documented particularly when considering the angle of the blades and the angular position of the blades within the VAWT under transient operation. Understanding such characteristics is critical if the unique behaviour of this format is to be determined and design characteristics are to be highlighted. The performance study is extended to consider effects related to the number of blades and the size of the rotor/stator sections. The highlight of these investigations is the development of the torque prediction model that is both robust and user friendly. Author is not aware of any published literature where such a model has been developed for diverse geometric variables such as blade angles, number of blades and size of rotor/stator sections. This novel prediction model can be directly used by VAWT designers while designing the blades etc. of the VAWT.

The final area investigated in this thesis is focussed on the development of a CFD based fault detection model which can be used to predict blade faults. Although wind turbine condition

Optimal Design of a Micro Vertical Axis Wind Turbine for Sustainable Urban Environment
By Kyooseon Park, School of Computing and Engineering, University of Huddersfield, UK (2013)

32

monitoring is well documented in the form of vibration and acoustic techniques much of this research is focussed on non-blade faults. Given the recent emphasis on multi-blade rotor designs the probability of failure is significantly increased. A detailed investigation into these faults and their associated effects on the performance output of the VAWT have been analysed in detail. It is noteworthy here that the author is not aware of any published literature where CFD has been used for flow diagnostics in VAWTs under transient conditions. The use of sliding mesh technique captures the unsteady complex flow phenomena which is not possible to capture using conventional CFD tools.

2.5. Research Objectives

Based on the research aims presented in the previous chapter, and after conducting a detailed literature review, the following objectives have been formulated which will aid the research aims and address the issues in the existing knowledge:

1. To analyse the effect of the rotor blade angles on the performance output of a VAWT

2. To evaluate the effect of the stator blade exit angle on the performance output of a VAWT

3. To investigate the effect of the rotor size on the performance output of a VAWT

4. To formulate the effect of the stator size on the performance output of a VAWT

5. To evaluate the effect of number of rotor blades on the performance of a VAWT

6. To investigate the effect of number of stator blades on the performance of a VAWT

7. To analyse the effect of a VAWT's height on its performance output

8. To analyse the effect of missing rotor blade on the performance output of a VAWT

9. To investigate the effect of missing stator blade on the performance output of a VAWT

10. To formulate the effect of rotor blade slits on the performance output of a VAWT

In order to satisfactorily achieve the aforementioned research objectives, this study uses Computational Fluid Dynamic tools to numerically simulate the flow within and in the vicinity of a VAWT. The next chapter presents the numerical modelling techniques being incorporated in this study.

Optimal Design of a Micro Vertical Axis Wind Turbine for Sustainable Urban Environment
By Kyooseon Park, School of Computing and Engineering, University of Huddersfield, UK (2013)

33

CHAPTER 3
NUMERICAL MODELLING OF VERTICAL AXIS WIND TURBINES

I n order to investigate the research objectives of this study that have been identified in the previous chapter, advanced CFD techniques have been used to computationally simulate the transient flow of air in the vicinity of a VAWT. The use of CFD, along-with a novel methodology for the rotation of the rotor blades that captures the unsteady complex flow phenomena, enables to predict the performance output of the VAWT. For this purpose, appropriate solver settings and boundary conditions needs to be specified, that are discussed in this chapter. The sliding mesh technique, used for the rotation of the rotor blades, is the highlight of this chapter.

3.1. Introduction to Computational Fluid Dynamics

Computational Fluid Dynamics or CFD is the analysis of systems involving fluid flow, heat transfer and associated phenomena such as chemical reactions by means of computer-based simulation. The technique is very powerful and spans a wide range of industrial and non – industrial application areas. From the 1960s onwards, the aerospace industry has integrated CFD techniques into the design, R&D and manufacture of aircraft and jet engines. More recently, the method has been applied to the design of internal combustion engines, combustion chambers of gas turbines and furnaces. Furthermore, motor vehicle manufacturers now routinely predict drag forces, under – bonnet air flows and the in – car environment with CFD. CFD is becoming a vital component in the design of industrial products and processes.

The variable cost of an experiment, in terms of facility hire and/or person – hour costs, is proportional to the number of data points and the number of configurations tested. In contrast, CFD codes can produce extremely large volumes of results at no added expense, and it is very cheap to perform parametric studies, for instance, to optimise equipment performance.

3.1.1. Working of CFD Codes

There are three distinct streams of numerical solution techniques. They are finite difference, finite element and spectral methods. Finite volume method, a special finite difference formulation, is central to the most well established CFD codes. The numerical algorithms include integration of the governing equations of fluid flow over all the control volumes of the domain, discretisation or conversion of the resulting integral equations into a system of algebraic equations and the solution of these equations by an iterative method.

CFD codes are structured around the numerical algorithms that can tackle fluid flow problems. In order to provide easy access to their solving power, all commercial CFD packages include sophisticated user interfaces to input problem parameters and to examine the results. Hence, all codes contain three main elements. These are:

- Pre – Processor

- Solver Execution

- Post – Processor

Pre – processing consists of the input of the flow problem to a CFD programme by means of an operator – friendly interface and the subsequent transformation of this input into a form suitable for use by the solver. The user activities at the pre – processing stage includes definition of the geometry of the region of interest. It is called the computational domain. Grid generation is the sub – division of the domain into a number of smaller, non – overlapping sub – domains. It is also called Mesh. Selection of the physical or chemical phenomena that needs to be modelled, definition of fluid properties and the specification of appropriate boundary conditions at cells, which coincide with or touch the domain boundary, are also included in pre – processing [77].

The solver primarily consists of setting up the numerical model and the computation/monitoring of the solution. The setting up of the numerical model includes the following:

- Selection of appropriate physical models. These included turbulence, combustion, multiphase etc.
- Defining material properties like the fluid, solid, mixture etc.
- Prescribing operating conditions
- Prescribing boundary conditions
- Prescribing solver settings
- Prescribing initial solution
- Setting up convergence monitors

The computation of the solution includes:

- The discretised conservation equations are solved iteratively. A number of iterations are required to reach a converged solution.
- Convergence is reached when change in solution variables from one iteration to the next is negligible. Residuals provide a mechanism to help monitor this trend.
- The accuracy of the converged solution is dependent upon problem setup, grid resolution, grid independence, appropriateness and accuracy of the physical model.

Figure 3.1 describes the working of the solver.

Post processing comprises the examination of the results obtained and revision of the model based on these results. These can be further elaborated into:

- Examine the results to view solution and extract useful data.
- Visualization tools can be used to extract the overall flow pattern, separation, shocks, shear layers etc.
- Numerical reporting tools are used to calculate quantitative results like forces, moments, and average heat transfer co-efficient, flux balances, surface and volume integrated quantities.
- Are physical models appropriate?
- Are boundary conditions correct?
- Is the grid adequate?
- Can grid be adapted to improve results?
- Does boundary resolution need to be improved?
- Is the computational domain large enough?
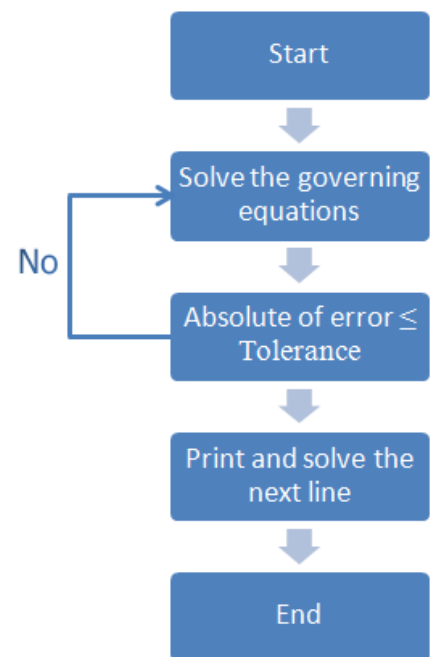
Figure 3.1 CFD Solver

Due to the increased popularity of engineering workstations, many of which have outstanding graphic capabilities, the leading CFD packages are now equipped with versatile data visualisation tools. These include domain geometry, grid display, vector plots, line and shaded contour plots, 2D and 3D surface plots, particle tracking, view manipulations, colour post – script output etc. more recently these facilities may also include animation for dynamic result display, and in addition to graphics, all codes produce trusty alphanumeric output and have data export facilities for further manipulation external to the codes. As in many other branches of CAE, the graphics output capabilities of CFD codes have revolutionised the communication of ideas to the non – specialists. An overview of CFD modelling is presented in figure 3.2.

Optimal Design of a Micro Vertical Axis Wind Turbine for Sustainable Urban Environment
By Kyooseon Park, School of Computing and Engineering, University of Huddersfield, UK (2013)

36
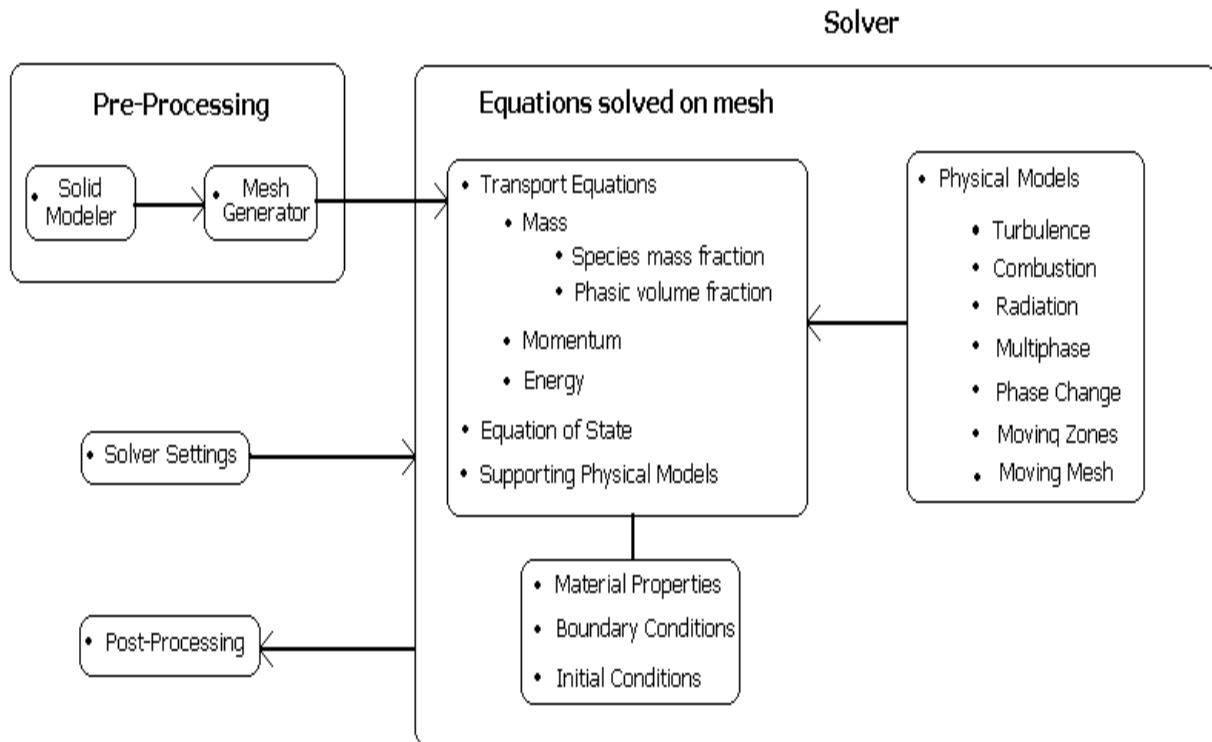
Figure 3.2. Overview of CFD Modelling [78]

3.1.2. Numerical Formulation of Fluid Flow

The governing equation of fluid flow represents mathematical statements of the conservation laws of Physics:

- The mass of a fluid is conserved.

- The rate of change of momentum equals the sum of the forces on a fluid particle. (Newton's second law)

- The rate of change of energy is equal to the sum of the rate of heat addition to and the rate of work done on a fluid particle. (First law of thermodynamics)

The fluid is regarded as a continuum. For the flow diagnostics at macroscopic length scales, the molecular structure of matter and molecular motions may be ignored. The behaviour of the fluid is described in terms of macroscopic properties such as velocity, pressure, density and temperature etc. These are averages over suitably large numbers of molecules. A fluid particle or point in a fluid is then the smallest possible element of fluid whose macroscopic properties are not influenced by individual molecules.

3.1.3. Conservation of Mass

The mass balance equation for the fluid element can be written as [79]:

$$
\begin{gathered}
Rate\ of\ increase\ of\ mass\ in = Net\ rate\ of\ flow\ of\ mass\ into \\
fluid\ element \qquad\qquad\quad fluid\ element
\end{gathered}
\tag{3.1}
$$

For liquids, as the density is constant, the mass conservation equation is:

$$
Div\ V = 0
\tag{3.2}
$$

This equation describes the net flow of mass out of the element across its boundaries. The above equation in longhand notation can be written as:

$$
\frac{\partial u}{\partial x} + \frac{\partial v}{\partial y} + \frac{\partial w}{\partial z} = 0
\tag{3.3}
$$

This equation represents the steady, three dimensional mass conservation of the fluid or continuity at a point in an incompressible fluid.

3.1.4. Conservation of Momentum

Newton's second law states that the rate of change of momentum of a fluid particle equals the sum of the forces on the particle [80]:

$$
\begin{gathered}
Rate\ of\ increase\ of\ Momentum\ of = Sum\ of\ forces\ acting\ on\ the \\
the\ fluid\ particle \qquad\qquad\quad fluid\ particle
\end{gathered}
\tag{3.4}
$$

There are two types of forces on fluid particles. These are surface forces and the body forces. Surface forces include pressure, viscous and gravity forces while body forces include centrifugal, coriolis and electromagnetic forces. It is a common practice to highlight the contributions due to the surface forces as separate terms in the momentum equations and to include the effects of body forces as source terms.

The x – component of the momentum equation is found by setting the rate of change of x – momentum of the fluid particle equal to the total force in the x – direction on the element due to surface stresses, plus the rate of increase of x – momentum due to sources. The equation is as follows:

$$
\rho g_x + \frac{\partial \sigma_{xx}}{\partial x} + \frac{\partial \tau_{yx}}{\partial y} + \frac{\partial \tau_{zx}}{\partial z} = \rho \left(\frac{\partial u}{\partial t} + u\frac{\partial u}{\partial x} + v\frac{\partial u}{\partial y} + w\frac{\partial u}{\partial z} \right)
\tag{3.5}
$$

The y and z – component of momentum equation are given by:

$$
\rho g_y + \frac{\partial \tau_{xy}}{\partial x} + \frac{\partial \sigma_{yy}}{\partial y} + \frac{\partial \tau_{zy}}{\partial z} = \rho \left(\frac{\partial v}{\partial t} + u\frac{\partial v}{\partial x} + v\frac{\partial v}{\partial y} + w\frac{\partial v}{\partial z} \right)
\tag{3.6}
$$

Optimal Design of a Micro Vertical Axis Wind Turbine for Sustainable Urban Environment
By Kyooseon Park, School of Computing and Engineering, University of Huddersfield, UK (2013)

38

$$\rho g_z + \frac{\partial \tau_{xz}}{\partial x} + \frac{\partial \tau_{yz}}{\partial y} + \frac{\partial \sigma_{zz}}{\partial z} = \rho \left(\frac{\partial w}{\partial t} + u \frac{\partial w}{\partial x} + v \frac{\partial w}{\partial y} + w \frac{\partial w}{\partial z} \right) \tag{3.7}$$

3.1.5. Energy Equation

The energy equation is derived from the first law of thermodynamics which stated that the rate of change of energy of a fluid particle is equal to the rate of heat addition to the fluid particle plus the rate of work done on the particle:

$$
\begin{aligned}
&\textit{Rate of increase of energy of fluid particle} = \\
&\textit{Net rate of heat added to the fluid particle} + \\
&\textit{Net rate of work done on the fluid particle}
\end{aligned}
\tag{3.8}
$$

Conservation of energy of the fluid particle is ensured by equating the rate of change of energy of the fluid particle to the sum of the net rate of work done on the fluid particle, the net rate of heat addition to the fluid and the rate of increase of energy due to sources. The energy equation is [81]:

$$\rho \frac{DE}{Dt} = -div(pu) + \begin{bmatrix} \frac{\partial(u\tau_{xx})}{\partial_x} + \frac{\partial(u\tau_{yx})}{\partial y} + \frac{\partial(u\tau_{zx})}{\partial_z} + \frac{\partial(v\tau_{xy})}{\partial x} + \frac{\partial(v\tau_{yy})}{\partial y} + \\ \frac{\partial(v\tau_{zy})}{\partial z} + \frac{\partial(w\tau_{xz})}{\partial x} \frac{\partial(w\tau_{yz})}{\partial y} + \frac{\partial(w\tau_{zz})}{\partial z} \end{bmatrix} + div(k\, grad\, T) + S_E \tag{3.9}$$

3.1.6. Equations of State

The motion of a fluid in three dimensions is described by a system of five partial differential equations, i.e. mass conservation, x, y and z momentum equations and energy equation. Among the unknowns are four thermodynamic variables, i.e. density, pressure, temperature and internal energy. Relationships between the thermodynamic variables can be obtained through the assumption of thermodynamic equilibrium.

The fluid velocities may be large, but they are usually small enough that, even though properties of a fluid particle change rapidly from place to place, the fluid can thermodynamically adjust itself to new conditions so quickly that the changes are effectively instantaneous. Thus, the fluid always remains in thermodynamic equilibrium. The only exceptions are certain flows with strong shockwaves, but even some of those are often well enough approximated by equilibrium assumptions. The state of a substance in thermodynamic equilibrium can be described by means of just two state variables. Equations of state relate the other variables to the two state variables, i.e. density and temperature. The equations of state are [82]:

$$p = p\,(\rho, T) \tag{3.10}$$

$$i = i\,(\rho, T) \tag{3.11}$$

Liquids and gases flowing at low speeds behave as incompressible fluids. Without density variations, there is no linkage between the energy equation, mass conservation equation and

Optimal Design of a Micro Vertical Axis Wind Turbine for Sustainable Urban Environment
By Kyooseon Park, School of Computing and Engineering, University of Huddersfield, UK (2013)

39

momentum equations. The flow field can often be solved by considering mass conservation and momentum conservation equations only. The energy equation only needs to be solved alongside the others if the problem involves heat transfer.

3.1.7. Navier – Stokes equations

In a Newtonian fluid, the viscous stresses are proportional to the rates of deformation. Liquids are incompressible; the viscous stresses are twice the local rate of linear deformation times the dynamic viscosity. The Navier – Stokes equations are [83]:

$$\rho g_x - \frac{\partial p}{\partial x} + \mu \left(\frac{\partial^2 u}{\partial x^2} + \frac{\partial^2 u}{\partial y^2} + \frac{\partial^2 u}{\partial z^2} \right) = \rho \left(\frac{\partial u}{\partial t} + u \frac{\partial u}{\partial x} + v \frac{\partial u}{\partial y} + w \frac{\partial u}{\partial z} \right) \qquad (3.12)$$

$$\rho g_y - \frac{\partial p}{\partial y} + \mu \left(\frac{\partial^2 v}{\partial x^2} + \frac{\partial^2 v}{\partial y^2} + \frac{\partial^2 v}{\partial z^2} \right) = \rho \left(\frac{\partial v}{\partial t} + u \frac{\partial v}{\partial x} + v \frac{\partial v}{\partial y} + w \frac{\partial v}{\partial z} \right) \qquad (3.13)$$

$$\rho g_z - \frac{\partial p}{\partial z} + \mu \left(\frac{\partial^2 w}{\partial x^2} + \frac{\partial^2 w}{\partial y^2} + \frac{\partial^2 w}{\partial z^2} \right) = \rho \left(\frac{\partial w}{\partial t} + u \frac{\partial w}{\partial x} + v \frac{\partial w}{\partial y} + w \frac{\partial w}{\partial z} \right) \qquad (3.14)$$

3.2. Pre-Processing

Further details about computational fluid dynamics and difference turbulence models can be found in any good CFD book. For reader's interest, some books regarding CFD are recommended here [84-88]. The following sections provide details of the numerical modelling that has been used in the present study. The CFD package that has been used to achieve this is known as Ansys [89]. At the time when this study was carried out, version 13.0.0 was the latest version of this package and hence has been used for simulations/analysis in this thesis. The pre-processing in CFD is subdivided into two main categories, i.e. creation of the geometry and the meshing of the flow domain. This section provides details of the geometric modelling and the meshing of the hydraulic capsule pipelines.

3.2.1. Geometry of VAWT

A three dimensional vertical axis wind turbine model, similar to Colley [30], has been numerically created as shown in figure 3.3. The model has 12 rotor blades and 12 stator blades where the blade angles are variable in order to formulate the optimal VAWT design (discussed in the next chapter). The radius of the core region r_c=0.5m whereas the radii of the stator and the rotor regions i.e. r_r and r_s are 0.7m and 1m respectively. The height of the VAWT, h=1m.
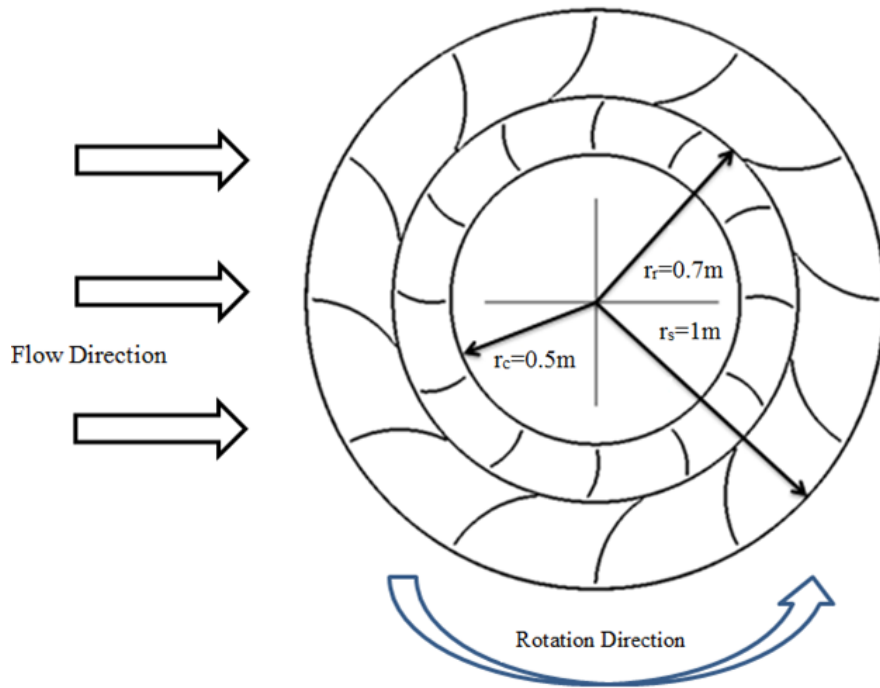
Figure 3.3 Geometry of the VAWT

Figure 3.4 shows the flow domain of the VAWT. The length, width and the height of the flow domain are 13m, 9m and 3m respectively. These dimensions have been taken from Colley [30] and have been used here because the validation of the CFD results, presented in this study, will be carried out against the published results of Colley in the next chapter.
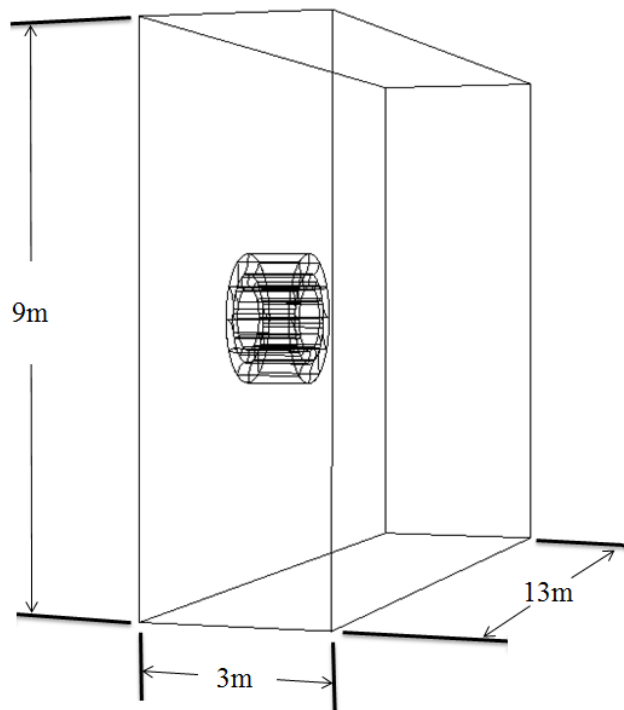
Figure 3.4 Flow Domain of the VAWT

Optimal Design of a Micro Vertical Axis Wind Turbine for Sustainable Urban Environment
By Kyooseon Park, School of Computing and Engineering, University of Huddersfield, UK (2013)

41

Although the blade angles have already been defined in Chapter 1, figure 3.5(a &b) shows the blade angles here again. Figure 3.5(a) shows the angles related to stator blades while figure 3.5(b) shows the angles related to the rotor blades.

(a)

(b)
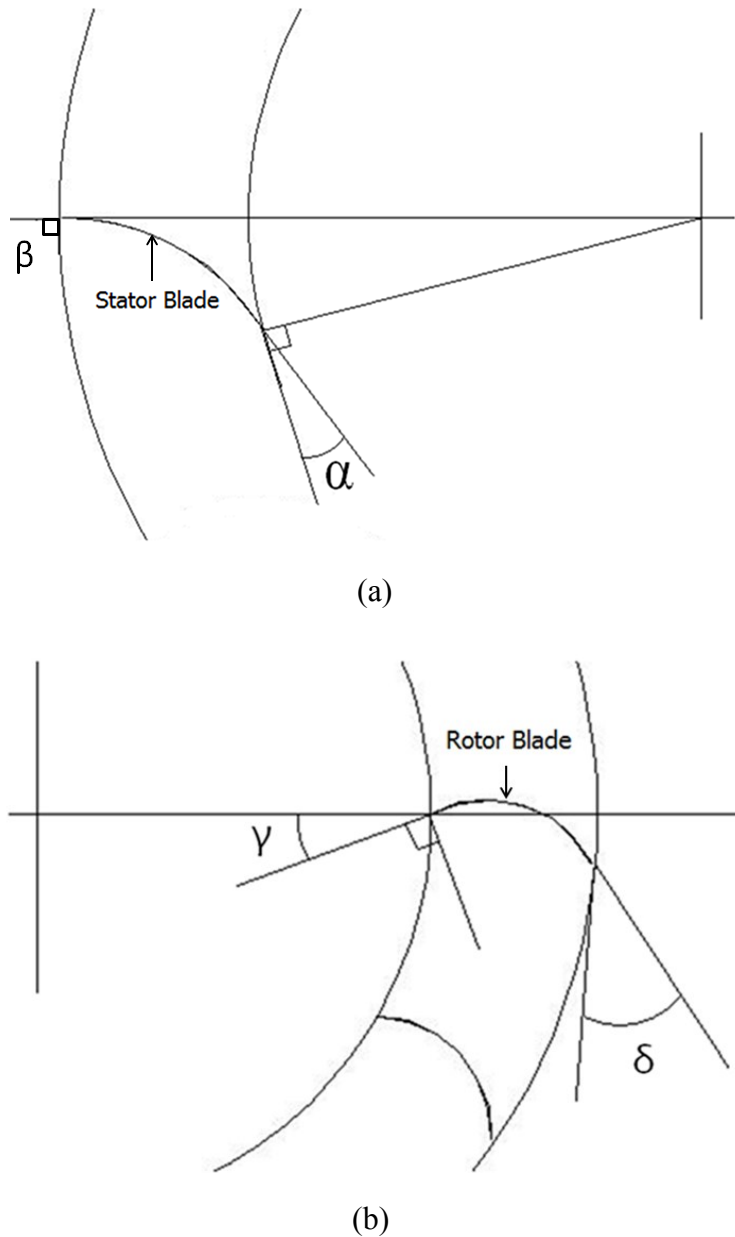
Figure 3.5 Angles related to (a) Stator Blades (b) Rotor Blades

3.2.2. Meshing of the Flow Domain

The mesh has been created in five different steps. Domain mesh has been controlled by global sizing function i.e. maximum size of 100mm and minimum size of 0.1mm. Stator, rotor and the core zones have been meshed for 20mm mesh sizing. The blade edges have been meshed with 0.1mm sizing. The details of the mesh sizing being used are summarized in the table 3.1.

Optimal Design of a Micro Vertical Axis Wind Turbine for Sustainable Urban Environment
By Kyooseon Park, School of Computing and Engineering, University of Huddersfield, UK (2013)

42

Table 3.1 Details of the Mesh Sizing used

Zone	Maximum Size (mm)	Minimum Size (mm)	Number of Mesh Elements
Domain	100	0.1	24097
Stator	20	0.1	34075
Rotor	20	0.1	28167
Core	20	0.1	4061
Blade Edges	0.1	0.1	

Figures 3.6(a & b) show mesh in the VAWT and in the flow domain respectively.
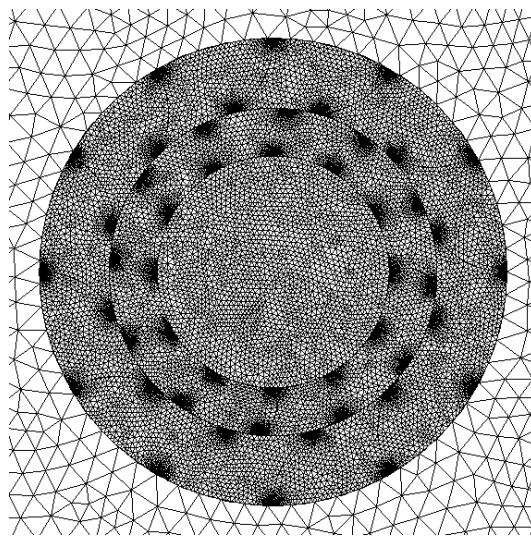
(a)
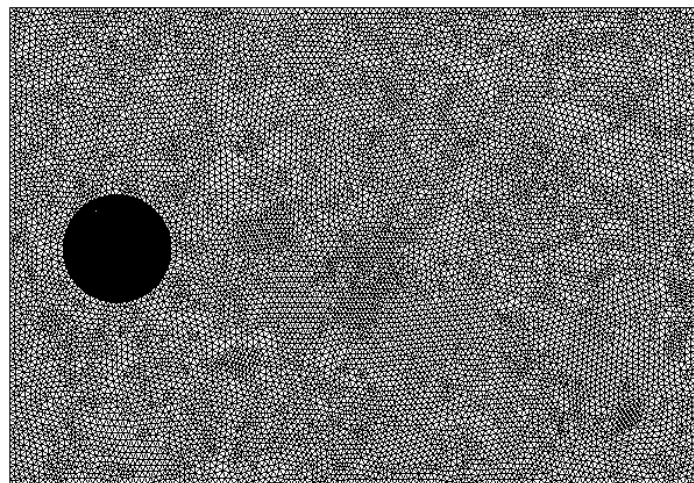
(b)

Figure 3.6 Mesh in the (a) VAWT (b) Flow Domain

Optimal Design of a Micro Vertical Axis Wind Turbine for Sustainable Urban Environment
By Kyooseon Park, School of Computing and Engineering, University of Huddersfield, UK (2013)

43

3.3.   Solver Execution

As the flow of air in the present study is at low speeds (4m/sec), pressure based solver has been chosen for the flow diagnostics of VAWT. In this solver, the density of the fluid remains constant and the primary fluid flow parameter, that is being solved iteratively, is the pressure within the flow domain.

As the interaction between the stationary (stator) and rotating (rotor) frames of references is highly transient, an unsteady solver has been designed to simulate the flow of air in the vicinity of the VAWT. In addition to the aforementioned solver settings, there is a need to model the turbulence in the flow as well. This is because the investigations carried out in the present study focuses on the turbulent flow of air. The criteria for external flows (such as VAWT) to be turbulent is that the Reynolds number of the flow should be higher than 500,000. Furthermore, in practical applications of VAWTs, the velocity of the flow normally ranges from 2m/sec to 6m/sec. These velocities correspond to Reynolds number of 136,917 to 410,752 for the VAWT under consideration. Hence, the flow is turbulent and a turbulence model is required to predict the parameters of turbulence in the vicinity of the VAWT with reasonable accuracy.

There are many turbulence models available in the commercial CFD package that has been used in this study. Each one of these turbulence models has got their own advantages and disadvantages, which can be found out in any CFD text book. As far as VAWTs are concerned, due to the formation of a wake region downstream the VAWT, k-ω model has been chosen for the modelling of turbulence. The primary reason behind choosing k-ω model is its superiority in accurately modelling the wake regions and extreme pressure gradients. Most recent studies also show that k-ω turbulence model predicts the changes in the flow parameters in VAWTs with reasonable accuracy.

The k-ω is a two equation model that is further divided into two types. The first type is called Standard k-ω model whereas the second type is called Shear-Stress Transport (SST) k-ω model. In the present study, SST k-ω model has been chosen because it includes the following refinements:

- The standard k-ω model and the transformed k-ε model are both multiplied by a blending function, and both models are added together. The blending function is designed to be one in the near-wall region, which activates the standard k-ω model, and zero away from the surface, which activates the transformed k-ε model.

- The definition of the turbulent viscosity is modified to account for the transport of the turbulent shear stress.

These features make the SST k-ω model more accurate and reliable for a wider class of flows (e.g., adverse pressure gradient flows, aerofoils, transonic shock waves) than the standard k-ω model. Other modifications include the addition of a cross-diffusion term in the ω equation and a blending function to ensure that the model equations behave appropriately in both the near-wall and far-field zones. Further details of SST k-ω model can be found in any turbulence modelling text book and hence have not been included here.

3.3.1. Boundary Conditions

The boundary types that have been specified are listed in the table 3.2. The incident flow velocity remains constant as 4m/sec throughout this study as it is a practical wind speed value in urban environments. Tip Speed Ratio (λ) is also kept constant at 0.2 because it represents the most common operating condition in real world practice (Colley [30]). Atmospheric conditions at pressure outlet boundary means that zero gauge static pressure has been prescribed, which again is expected in real world conditions. Furthermore, all the walls in the flow domain have been modelled as no-slip boundaries which mean that the flow does not slip on the surface of the walls. This is because, in real world, zero velocity gradient is observed between the walls and the flow layer adjacent to the wall.

Table 3.2 Boundary Types and Conditions

Boundary Name	Boundary Type	Boundary Condition
Inlet	Velocity Inlet	4m/sec
Outlet	Pressure Outlet	Atmospheric Conditions
Surrounding Sides	Stationary Walls	No-Slip
Rotor Blades	Rotating Walls	No-Slip
Stator Blades	Stationary Walls	No-Slip
Core & Passages	Interior	Interior

As the interactions between the rotor and the stator blades are highly transient, a novel technique has been used to rotate the rotor blades corresponding to stationary stator blades. The details of this technique are presented in the next section.

3.3.2. Sliding Mesh

When a time-accurate solution for rotor-stator interaction (rather than a time-averaged solution) is desired, sliding mesh model should be used to compute the unsteady flow field. The sliding mesh model is the most accurate method for simulating flows in multiple moving reference frames, but also the most computationally demanding. In the sliding mesh technique two or more cell zones are used. Each cell zone is bounded by at least one interface zone where it meets the opposing cell zone, as shown in figure 3.7 for VAWTs. The interface zones of adjacent cell zones are associated with one another to form a mesh interface. The two cell zones will move relative to each other along the mesh interface. During the calculation, the cell zones slide (i.e. rotate) relative to one another along the mesh interface in discrete steps. As the rotation takes place, node alignment along the mesh interface is not required. Since the flow is inherently unsteady, a time-dependent solution procedure is required. The sliding mesh model allows adjacent meshes to slide relative to one another. In doing so, the mesh faces do not need to be aligned on the mesh interface. This situation requires a means of computing the flux across the two non-conformal interface zones of each mesh interface.
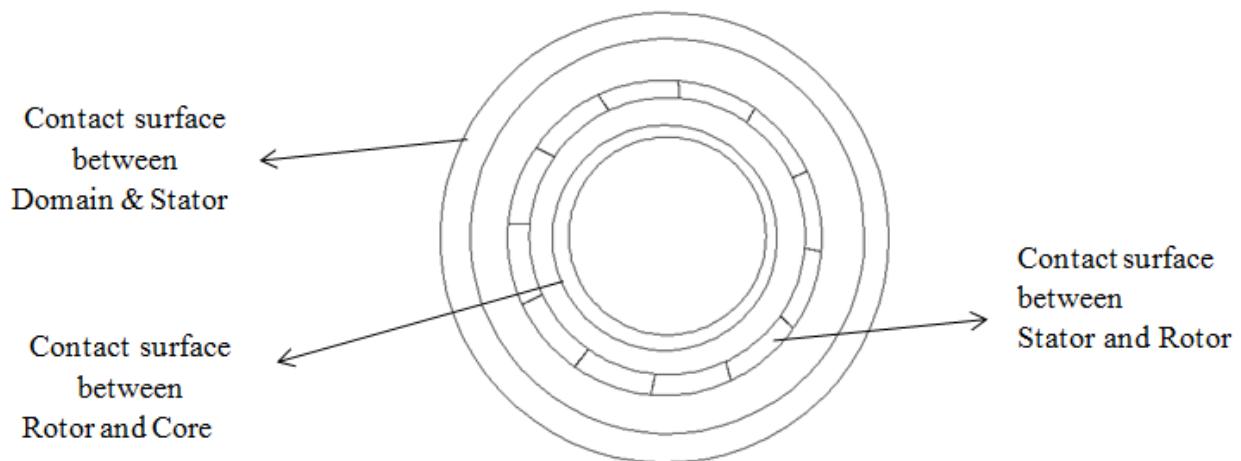
Figure 3.7 Interfaces between different zones

The flow domain is divided into sub-domains, each of which may be rotating and/or translating with respect to the inertial frame. The governing equations in each sub-domain are written with respect to that sub-domain's reference frame. At the boundary between two sub-domains, the diffusion and other terms in the governing equations in one sub-domain require values for the velocities in the adjacent sub-domain. The solver used in the present study enforces the continuity of the absolute velocity to provide the correct neighbour values of velocity for the sub-domain under consideration. When the relative velocity formulation is used, velocities in each sub-domain are computed relative to the motion of the sub-domain.

3.3.3. Solver Settings

Application based solver settings are required to accurately predict the fluid flow behaviour in the flow domain. These settings comprise:

- Pressure – Velocity Coupling
- Gradient
- Spatial Discretisation

The Navier-Stokes equations are solved in discretised form. This refers to the linear dependency of velocity on pressure and vice versa. Hence, a pressure – velocity is required to predict the pressure distribution in the flow domain with reasonable accuracy. In the present study, SIMPLE algorithm for pressure – velocity coupling has been incorporated because it converges the solution faster and is often quite accurate for flows in and around simple geometries such as spheres, cylinders etc. In SIMPLE algorithm, an approximation of the velocity field is obtained by solving the momentum equation. The pressure gradient term is calculated using the pressure distribution from the previous iteration or an initial guess. The pressure equation is formulated and solved in order to obtain the new pressure distribution. Velocities are corrected and a new set of conservative fluxes is calculated.

Gradients are needed for constructing values of a scalar at the cell faces, for computing secondary diffusion terms and velocity derivatives. Green – Gauss Node – based gradient evaluation has been used in the present study. This scheme reconstructs exact values of a linear function at a node from

Optimal Design of a Micro Vertical Axis Wind Turbine for Sustainable Urban Environment
By Kyooseon Park, School of Computing and Engineering, University of Huddersfield, UK (2013)

46

surrounding cell – centred values on arbitrary unstructured meshes by solving a constrained minimization problem, preserving a second-order spatial accuracy.

The CFD solver stores discrete values of the scalars at the cell centres. However, face values are required for the convection terms and must be interpolated from the cell centre values. This is accomplished using an upwind spatial discretisation scheme. Upwinding means that the face value is derived from quantities in the cell upstream, or upwind relative to the direction of the normal velocity. In the present study, 2nd order upwind schemes have been chosen for pressure, momentum, turbulent kinetic energy and turbulent dissipation rate. The use of 2nd order upwind scheme results in increased accuracy of the results obtained.

3.3.4. Convergence Criteria

Getting to a converged solution is often necessary. A converged solution indicates that the solution has reached a stable state and the variations in the flow parameters, w.r.t. the iterative process of the solver, have died out. Hence, only a converged solution can be treated as one which predicts the solution of the flow problem with reasonable accuracy.

The default convergence criterion for the continuity, velocities in three dimensions and the turbulence parameters in Ansys 13.0.0 is 0.001. This means that when the change in the continuity, velocities and turbulence parameters drops down to the fourth place after decimal, the solution is treated as a converged solution. However, in many practical applications, the default criterion does not necessarily indicate that the changes in the solution parameters have died out. Hence, it is often better to monitor the convergence rather than relying on the default convergence criteria.

In the present study, torque output of the blades of the VAWT has been monitored throughout the iterative process. The solution has been considered converged once it has become statistically steady i.e. the variations in the torque output become negligibly small between two consecutive rotations of the VAWT.

After numerically simulating the flow of air in the vicinity of VAWT, various results have been gathered from CFD. Detailed discussions on these results are presented in the proceeding chapters, where the next chapter deals with the optimisation of VAWT based on blade angles.

3.4. Experimental Setup of VAWT

A full scale prototype machine has been fabricated for development testing. The wind turbine uses the same rotor/stator configuration and has a design envelope with outer diameter of 2.0m and 1.0m in height. Within this space the machine features two distinct zones namely the stator and rotor rings. Each of these rings contains 12 blades fabricated from 1mm thick sheet aluminium cold rolled to create a fixed radius profile which corresponds to that computed using the design equations. The blades are installed such that a 30° angular spacing is maintained and hence blades are equally spaced relative to the central axis of rotation which is concentric to the transmission shaft. The material used is aluminium due to its lightweight and relatively stiff characteristics once formed. Both stator and rotor blades are located between two support rings, both above and below the blade end sections. In order to fix the blade in place a tab is created on the bottom of each blade which mates to a slot in each of the rings, hence during operation the blades are held in shear. Both

Optimal Design of a Micro Vertical Axis Wind Turbine for Sustainable Urban Environment
By Kyooseon Park, School of Computing and Engineering, University of Huddersfield, UK (2013)

47

stator and rotor assemblies are located by two cradle like structures on the upper and lower sides of the machine. At the centre of each cradle is a bearing housing which is welded to each of the support arms which connects to the blade support rings. The vertical and radial position of the rotor is maintained using two taper roller bearings which provides a fixed tip clearance of 10mm between the rotor and stator assemblies. For reference the stator and rotor support rings are laser cut to ensure high accuracy and reduce material distortions. Figure 3.8 shows the full scale wind turbine prototype.

(a)   (b)

(c)
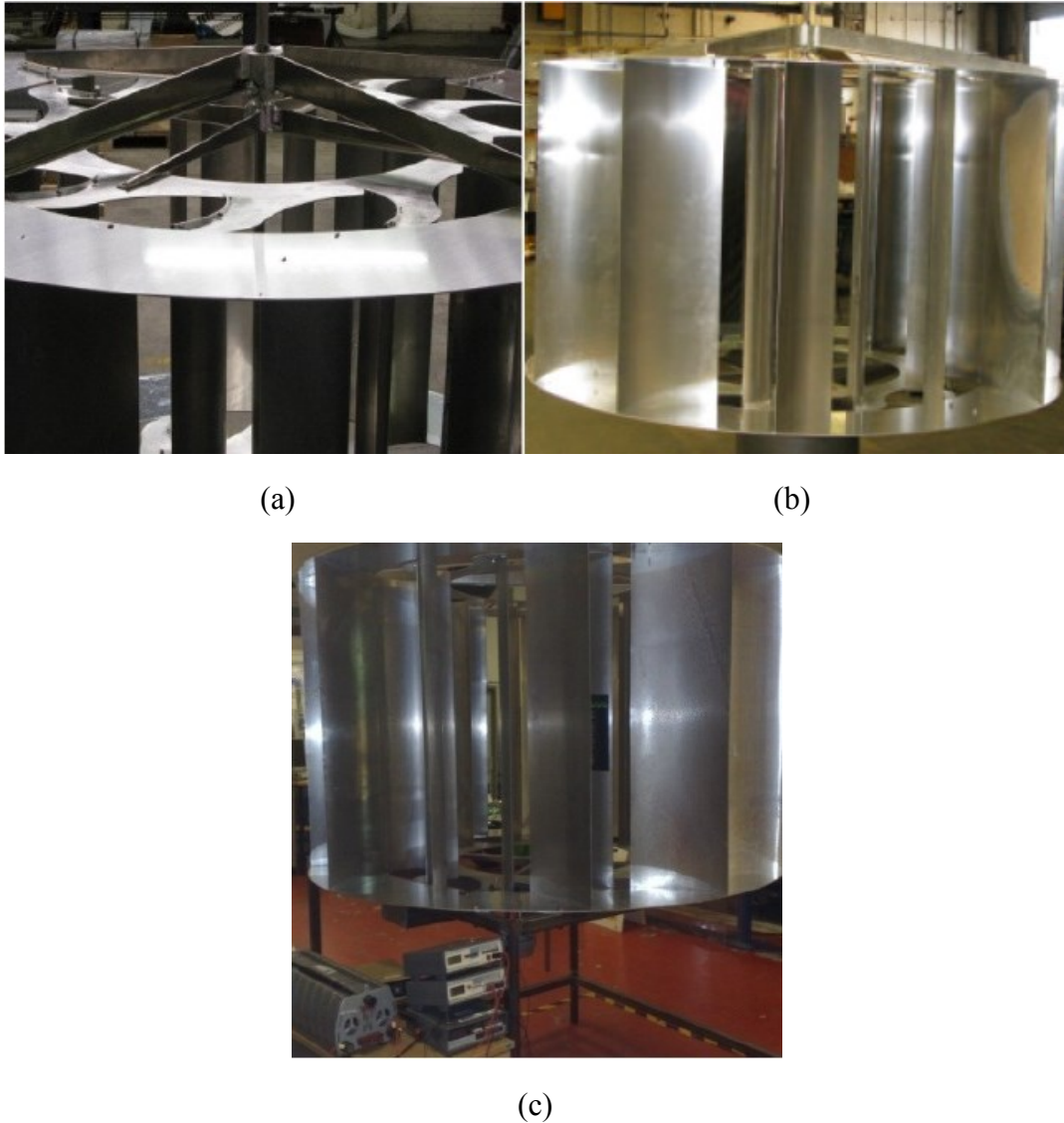
Figure 3.8 Experimental Setup of the VAWT (a) Top View (b) Side View (c) Control System

The wind turbine test rig consists of a low speed wind tunnel with a 0.6m x 0.6m square test chamber and a full-scale prototype wind turbine as per the baseline geometry presented in Chapter 1. This arrangement has the wind turbine positioned downstream of the wind tunnel test chamber exit and hence is studied under jet flow conditions. The turbine has been instrumented such that operational and performance related data can be obtained via a data acquisition card. An overview of the wind turbine system used is provided in figure 3.9.
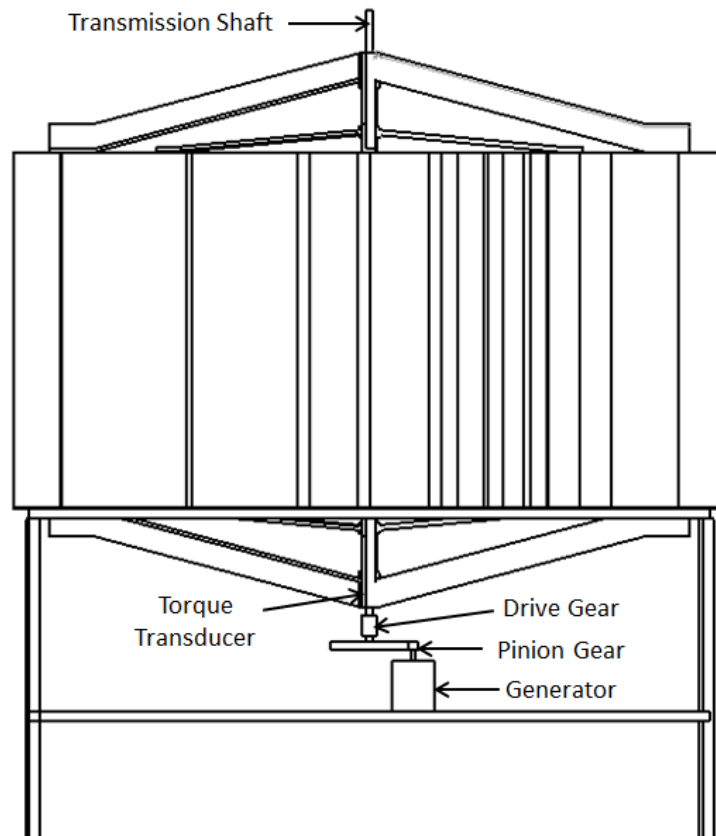
Figure 3.9 Wind Turbine System

The wind turbine is mounted on a square box section profile frame. The square frame is fabricated from 40mm x 40mm x 4mm box section steel and fillet welded together such that it is structurally rigid. The machine is mounted to the top surface of the frame and is held in place using eight equally spaced M10 x 60mm cap head bolts. To allow for easy access and adjustment of the machines position relative to the wind tunnel exit, the frame work uses castor wheels such that the machine can be aligned in any orientation. During operation the frame work is lifted off the ground using adjustment screws which are located on mounting platforms such that the machine is stable at high wind and rotational speeds.

3.4.1. Transmission System

The turbine consists of two zones namely the stator blade ring and the inner rotor ring each containing twelve blades. Both blade zones are held in place using four angled support sections which minimize flexing during operation. The rotor assembly is located on a central transmission shaft which in turn is located with two bearing housings at the top and bottom as shown on the above figure. To keep the transmission shaft fixed, two holes are placed in both the upper and lower bearing carriers. Using four M10 grub screws both the rotor and transmission are held at fixed position with zero slip. To transfer power from the shaft to the generator a simple gearing arrangement is used to increase generator shaft speed by a ratio of 8.3:1 relative to the input shaft. The gearing arrangement used in this setup consists of a pair of matched, lightened and balanced spur gears which are synchronised with a total tooth to tooth backlash of 150μm as shown in figure 3.10.
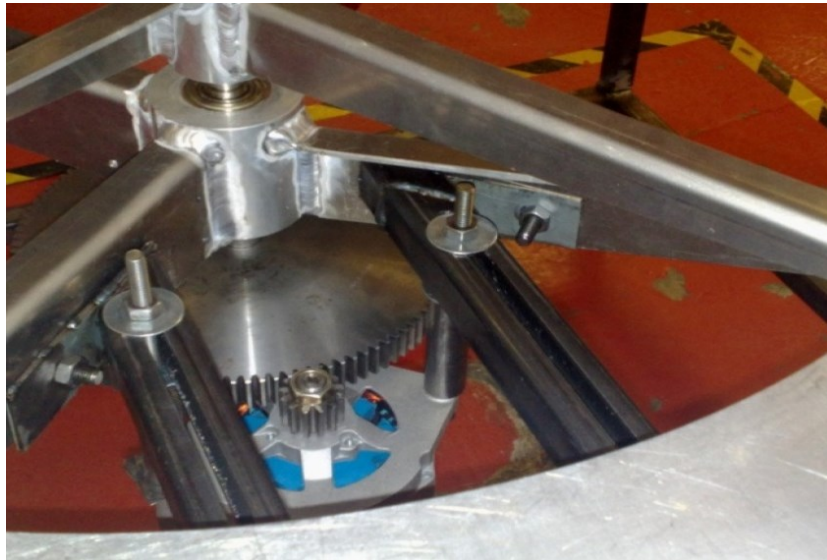
Figure 3.10 Transmission System

3.4.2. Power Generation

The power generation system used at the output of the turbine transmission shaft is described in the following section. This generation system contains the generator, power analyser, rectifier, resistive load and data acquisition system. Using this system it is possible to generate AC current, control wind turbine rotor speed and sample real-time instantaneous three phase current and voltage data. This system is depicted by figure 3.11.
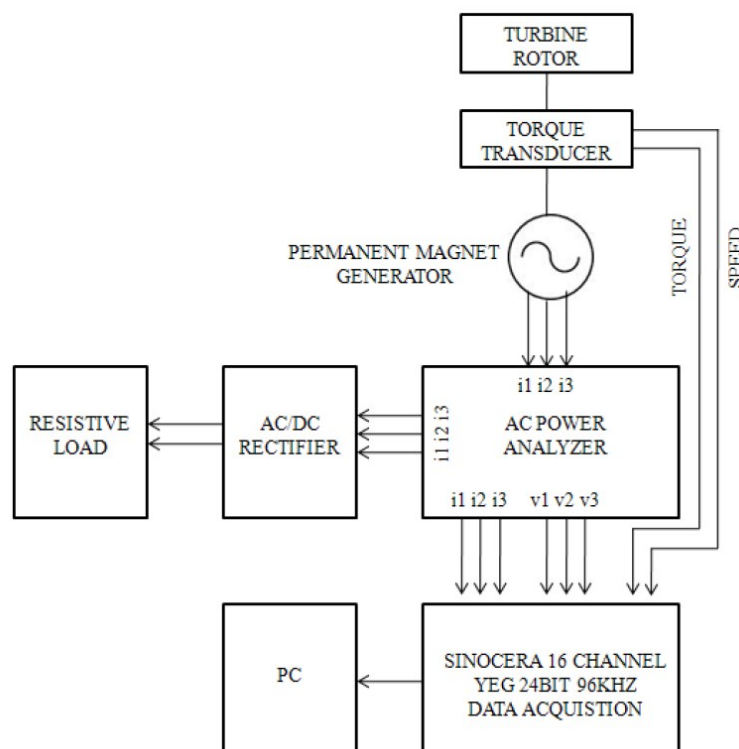
Figure 3.11 Power Generation System

Optimal Design of a Micro Vertical Axis Wind Turbine for Sustainable Urban Environment
By Kyooseon Park, School of Computing and Engineering, University of Huddersfield, UK (2013)

50

The three phase current output is connected to an AC power analyser which contains a series of current and voltage transducers and an individual power supply. As shown in the figure the primary three phase current enters the analyser where it is fed into an AC/DC rectifier such that a DC signal is produced. This rectifier is required given the type of resistive load bank that is used to control wind turbine rotor speed. On the opposite side of the analyser six terminals are present each with a linear 0-10v output. These terminals allow for acquisition of instantaneous current and voltage which in this case is connected to a high speed data acquisition system. Two further signals taken from the torque transducer unit namely torque and speed are fed into the data acquisition which is sampled with the electrical data. The output of this DAQ is then connected to a PC for post processing.

3.4.3. Complete System

The primary apparatus used for experimental studies is a low speed wind tunnel, which features a 0.6m x 0.6 test chamber and 0.8m diameter axial fan. Figure 3.12 depicts the working sections of the wind tunnel from a side elevation.
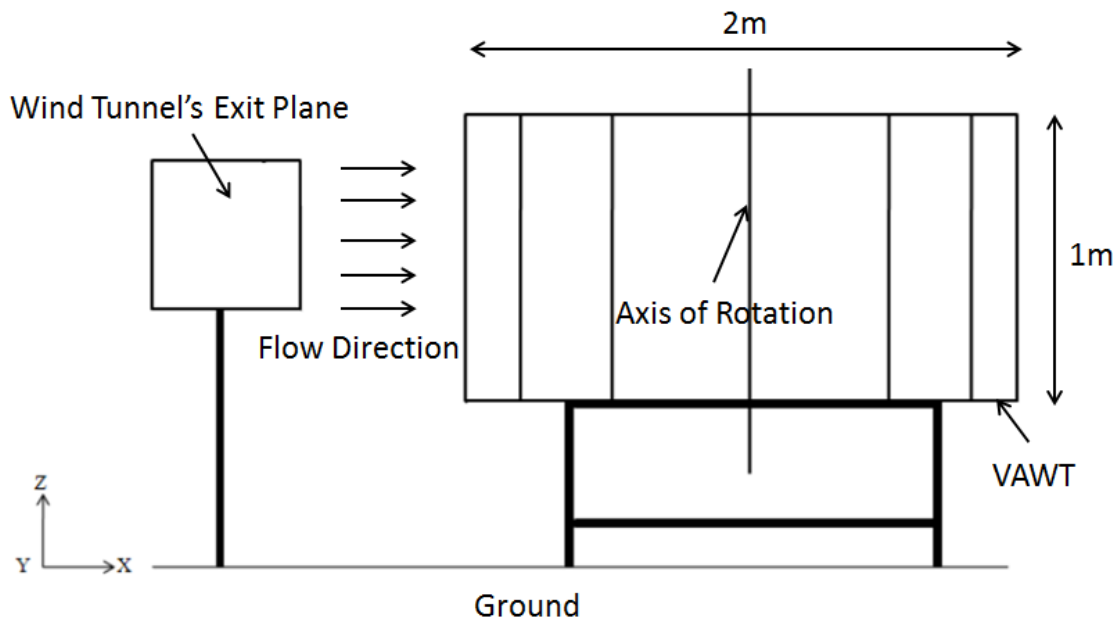
Figure 3.12 Wind Turbine System in XZ Plane

Furthermore, figure 3.13 shows the turbine from a plan view orientation in the XY plane. This view provides information of how the machine is constrained in an angular direction. Here, the turbine geometry is aligned to the test chamber wall using a parallel constraint between the outer chamber wall and a line that is fixed tangentially to the outer stator tip. This line is taken from the central axis of the turbine geometry and extended radially where it meets the stator tip face.
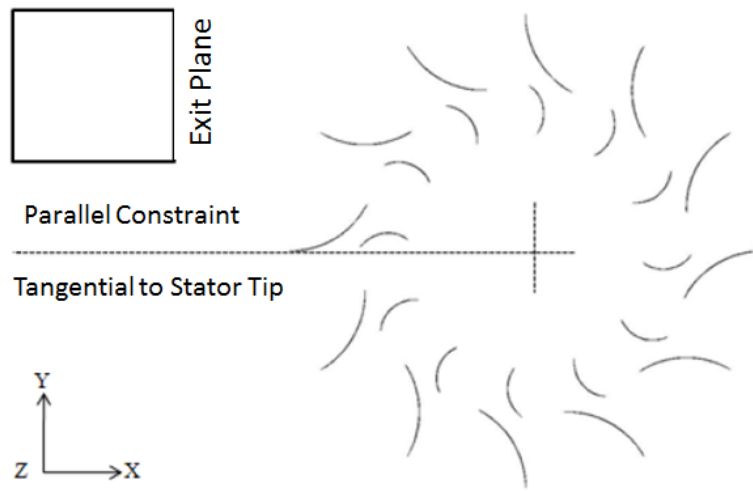
Figure 3.13 Wind Turbine System in XY Plane

3.4.4. Instrumentation and Specifications

The major instruments used are associated to flow and rotor torque/speed measurement. The fan, used to provide mass flow air through the wind tunnel, is of axial type operation using a pneumatic regulator to control the pitch of the blades. The specification of the unit is provided in table 3.3.

Table 3.3 Wind Tunnel's Axial Fan Specifications

Manufacturer	Woods Air Flow
Model Type	71KG/40A/F Class/380/420V
Air Pressure	1.76 Kg/cm^2
Speed Range	0 – 2950 rpm
Control Type	Varofoil Pneumatic

To obtain flow field data at the exit of the wind tunnel along with the angular distribution about the wind turbine a cobra head pressure probe has been used connected to a high speed data acquisition. The specifications of the Cobra Probe are provided in table 3.4.

Table 3.4 Cobra Probe's Specifications

Manufacturer	Turbulent Flow Instruments
Model	Cobra 1.5mm head
Number of Velocity Components	3
Conical Head Range	±45º
Frequency	1.25 kHz

Optimal Design of a Micro Vertical Axis Wind Turbine for Sustainable Urban Environment
By Kyooseon Park, School of Computing and Engineering, University of Huddersfield, UK (2013)

52

The generator used is of permanent magnet type and is connected to the wind turbine transmission shaft. The generator specification is provided in table 3.5.

Table 3.5 Power Generator's Specifications

Manufacturer	Wind Blue Power
Model	DC – 540
Number of Poles	7
Output	15A at 2000rpm using 12V battery

To characterize the performance of the turbine both torque and speed data is taken from the transducer unit mounted between the generator and the bottom bearing arrangement of the rotor as per figure 3.9. The specification of the torque transducer is provided in table 3.6.

Table 3.6 Torque/Speed Transducer's Specifications

Torque Rating	100N-m
Speed Rating	30,000rpm
Torque Scale Equation	Torque (N-mm)=20 * V
Speed Scale Equation	Speed (rpm)=V + 1.577/1.388
Overload Capacity	1.3 x rated torque, 2 x rated torque
Break Capacity	> 5 rated torque
Altering Torque	1 x rated torque
Protection Class	IP40
Speed Transducer	60 Pulses
Linearity Deviation	< 0.1% of full scale
Hysteresis	< 0.1% of full scale
Device Class according to DIN 51 309	Typ 0.2% (depends on measured value) > 20% rated torque
Limit Frequency	1 kHz
Output	±5V at rated torque
Load Resistance	>10kΩ
Nominal Temperature Range	+10ºC to +60ºC
Temperature Influence on Zero	0.05% / 10K
Torque Control Signal	100% ± .02%
Power Supply	16 – 30V DC
Current Consumption	110 mA

Optimal Design of a Micro Vertical Axis Wind Turbine for Sustainable Urban Environment
By Kyooseon Park, School of Computing and Engineering, University of Huddersfield, UK (2013)

53

Analogue data is obtained using a Sinocera AD convertor having the specifications provided in table 3.7.

Table 3.7 Data Acquisition's Specifications

Manufacturer	Sinocera
Model	YEG
Resolution	24Bit
Number of Channels	16
Sampling Frequency	96kHz
Accuracy	±0.4%

3.5. Summary

This chapter provides a summary of the CFD modelling techniques that have been used in the present study. In addition to the fluid flow governing equations, a special attention has been given to the solver settings being used. Boundary types and conditions have been mentioned in detail. Sliding mesh concept has been discussed in order to understand the modelling of this technique. The experimental setup, along with the specifications of the various instruments used, has been mentioned in detail.

CHAPTER 4
OPTIMISATION OF VERTICAL AXIS WIND TURBINES BASED ON BLADE ANGLES

Optimisation of a vertical axis wind turbine's design has been carried out, in the present chapter, based on the blade angles. Recent studies have shown that these angles can considerably affect the performance output of a VAWT. Hence, a thorough qualitative and quantitative analysis has been presented here that makes use of local flow parameters such as flow velocity and pressure. The effect of blade angles has been investigated on the global output parameters such as torque output and power output of a VAWT. Furthermore, a novel semi-empirical expression for torque coefficient has been developed that takes into account the effect of the blade angles and hence, is the highlight of this chapter.

Optimal Design of a Micro Vertical Axis Wind Turbine for Sustainable Urban Environment
By Kyooseon Park, School of Computing and Engineering, University of Huddersfield, UK (2013)

55

4.1. Mesh Independence Tests

As discussed in Chapter 3, three different meshes with 0.85, 1.7 and 3.4 million mesh elements were chosen for mesh independence testing. The results obtained, shown in table 4.1, depict that the difference in the average torque output of the VAWT is 6.6% between 0.85 and 1.7 million mesh elements whereas the difference between 1.7 and 3.4 million mesh elements is 1.5%. It can therefore be concluded that the mesh with 1.7 million elements is capable of accurately predicting the complex flow features in the vicinity of the VAWT and hence has been chosen for further analysis.

Table 4.1 Mesh Independence Results

Mesh Size (million)	Average Torque Output (N-m)	Percentage Difference (%)
0.85	20.17	
1.7	21.61	6.6
3.4	21.93	1.5

4.2. Validation of CFD Results

One of the most important steps while conducting numerical studies is the validation of the results. This means that the results obtained from the numerical simulations are compared against experimental findings to confidently authorise that the numerical model represents the physical model of the real world. Hence, all the geometric, flow and solver-related parameters/variables become important in validation studies.

For the present study, the numerical model has been validated against the experimental findings for the average torque output of a VAWT considered by Colley [30]. The size of the VAWT and the blade angles, from Colley's work, has been noted to accurately validate CFD results. The geometric details of the VAWT are shown in table 4.2:

Table 4.2 Geometric Details of the VAWT

Geometric Entity	Symbol	Value
Height of the VAWT	h	1m
Radius of Stator	r_s	1m
Radius of Rotor	r_r	0.7m
Radius of Core	r_c	0.5m
Stator Blade's inlet angle	β	90º
Stator Blade's outlet angle	α	11.689º
Rotor Blade's outlet angle	γ	28.2º
Rotor Blade's inlet angle	δ	32.357º

Optimal Design of a Micro Vertical Axis Wind Turbine for Sustainable Urban Environment
By Kyooseon Park, School of Computing and Engineering, University of Huddersfield, UK (2013)

56

In order to accurately validate the CFD model, same flow conditions have been specified as in Colley's study i.e. $\lambda=0.5$ and $v=4m/sec$. Figure 4.1 depicts the variations in the coefficient of pressure (C_p) between angular positions=270° to 360° of the VAWT at a radius of 1.025m, where C_p is defined as:

$$C_p = \frac{P - P_\infty}{0.5\rho v_\infty{}^2} \tag{4.1}$$

In equation (4.1), P is the local pressure, P_∞ is the free stream pressure (averaged at inlet boundary), ρ is the density of air and v_∞ is the free stream flow velocity (averaged at both inlet and outlet boundaries). It can be seen in figure 4.1 that the CFD model considered in the present study predicts the performance of a VAWT with reasonable accuracy. The average difference between the experimental and CFD results have been calculated to be less than 10%.
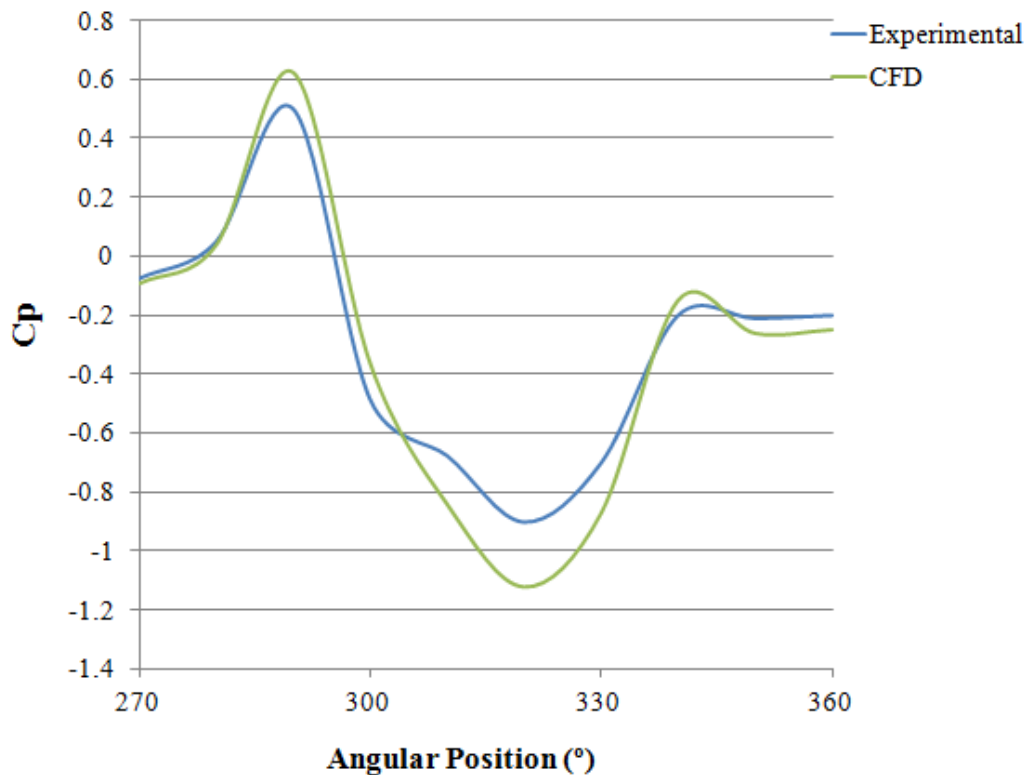
Figure 4.1 Variations in C_p between Experimental and CFD Models

Furthermore, figure 4.2 depicts the variations in the normalised flow velocity, where the velocity has been normalised with average flow velocity value between angular positions=270° to 360° of the VAWT at a radius of 1.025m. It has been shown that the velocity variations predicted by the CFD model, considered in the present study, have a close agreement with that measured experimentally.

Optimal Design of a Micro Vertical Axis Wind Turbine for Sustainable Urban Environment
By Kyooseon Park, School of Computing and Engineering, University of Huddersfield, UK (2013)

57
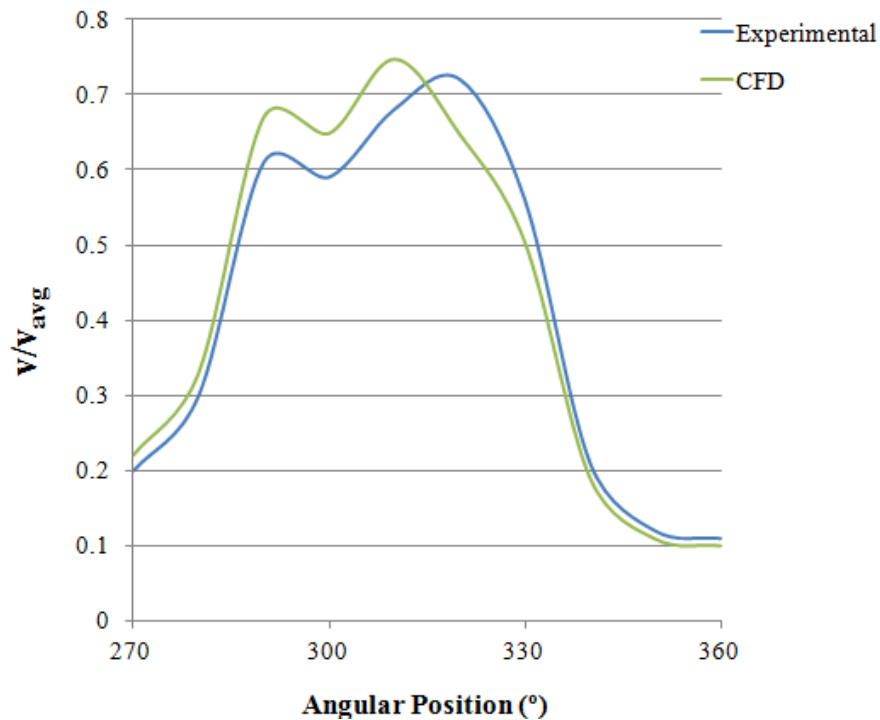
Figure 4.2 Variations in normalised flow velocity between Experimental and CFD Models

4.3. Performance Output of the VAWT

Before analysing the effect of the blade angles on the performance output of a vertical axis wind turbine, it is necessary to first analyse the flow structure in the vicinity of the VAWT so that important flow features can be described and an overall understanding of the local flow structure is established.

Figure 4.3(a) depicts the pressure variations in the vicinity of a VAWT having blade angles of $\alpha=1.689^{\circ}$, $\gamma=18.2^{\circ}$ and $\delta=22.357^{\circ}$ at 0° angular position of the VAWT. It is evident from the figure that the windward side of the VAWT has regions of high pressure whereas the leeward side of the VAWT shows comparatively lower pressure. This is due to the fact that the as the incident flow strikes the windward side of the VAWT, it transfers a large portion of its momentum to the blades in the said region. Due to concave shape of the blades at the windward side of the VAWT, the pressure forces are exerted on the blades of the VAWT. Similarly, due to no-slip boundary condition at the blades, viscous forces are being exerted on the blades of the VAWT. Under the action of the pressure and the viscous forces, the blades of the VAWT rotate.

Optimal Design of a Micro Vertical Axis Wind Turbine for Sustainable Urban Environment
By Kyooseon Park, School of Computing and Engineering, University of Huddersfield, UK (2013)

58
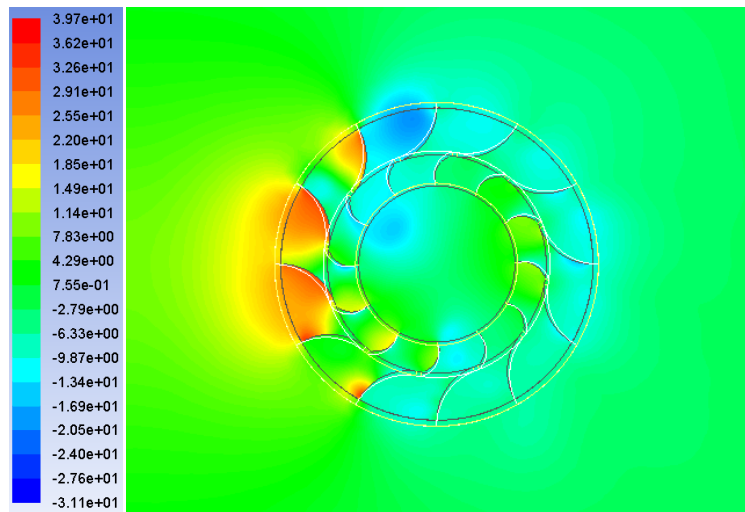
Figure 4.3(a) Pressure variations at 0⁰ angular position of the VAWT having α=1.689⁰, γ=18.2⁰ and δ=22.357⁰

As a major portion of the incident flow is being blocked at the windward side of the VAWT due to the orientation of the blades, a relatively low pressure region is observed at the leeward side of the VAWT. It can be further noticed that the upper section depicts lower pressure than the lower section. This is because the blockage effect is more severe on the upper windward section as compared to lower windward section of the VAWT due to the orientation of the blades. Hence, the flow enters the core region through the passages formed in the lower windward section of the VAWT.

In order to further analyze the flow structure in the vicinity of the aforementioned VAWT, velocity variations are being depicted in figure 4.3(b). It can be seen that the flow velocity is higher at those locations where the flow passes through the passages formed due to the orientation of the blades. These passages are formed at the lower windward side of the VAWT. The flow then enters the core region and exits through the upper leeward section. Due to the blade orientation, the flow is restricted to exit the VAWT through the lower leeward section due to the blade's orientation, hence creating a low velocity region.
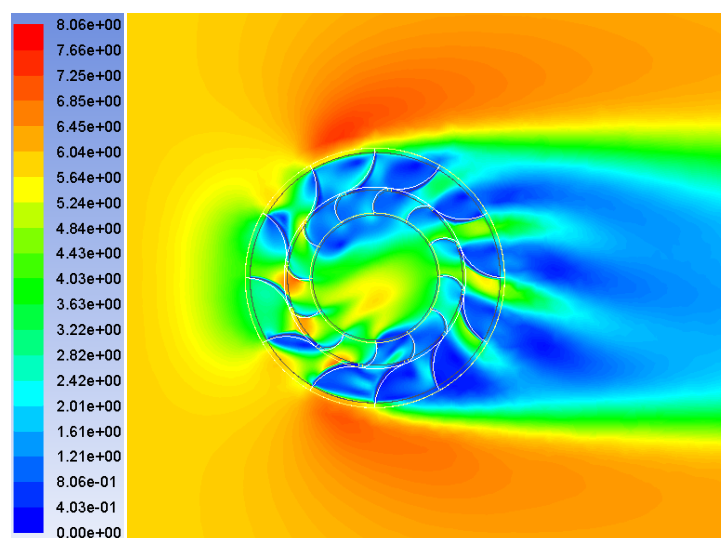
Figure 4.3(b) Velocity variations at 0⁰ angular position of the VAWT having α=1.689⁰, γ=18.2⁰ and δ=22.357⁰

Optimal Design of a Micro Vertical Axis Wind Turbine for Sustainable Urban Environment
By Kyooseon Park, School of Computing and Engineering, University of Huddersfield, UK (2013)

59

An important point to note at this moment is that the formation of the flow passages changes as the angular position of the VAWT changes. This can be seen in figure 4.4(a & b) where two different flow passages combinations are shown. It can be noticed that the path taken by the incident flow is different in the cases shown and is dependent on the angular position of the VAWT. Consequently, the performance output of the VAWT will also be seen to be dependent on the angular position.
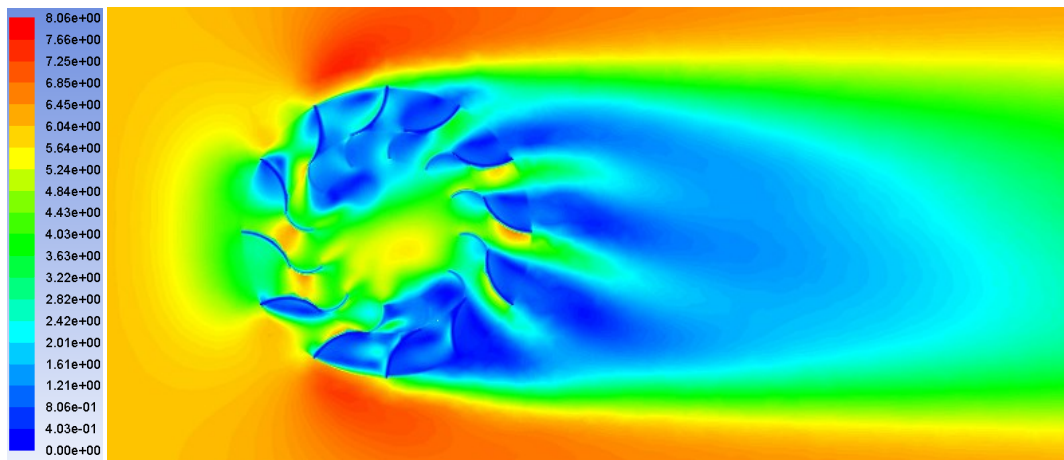
(a)
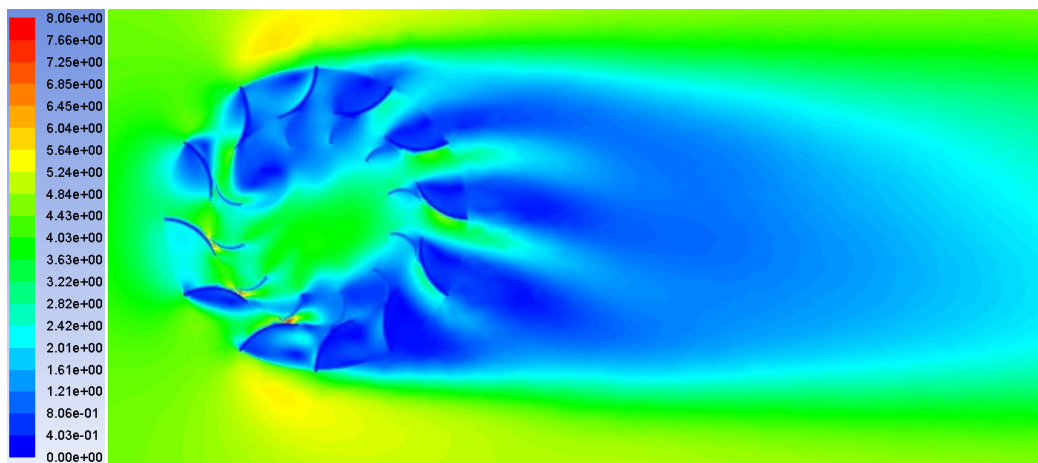
(b)

Figure 4.4 Velocity variations of the VAWT having α=1.689⁰, γ=18.2⁰ and δ=22.357⁰ at (a) 18⁰ (b) 15⁰ angular position of the VAWT

In order to quantify the performance output of the VAWT considered here, the instantaneous torque output for one revolution of the VAWT has been plotted in figure 4.5. It can be seen that the torque output of the VAWT is cyclic with the number of peaks/valleys equal to the number of rotor and stator blades. It is observed that the amplitude of instantaneous torque output of the VAWT decreases as the angular position of the VAWT increases. This is due to the orientation of the blades within the VAWT.

Optimal Design of a Micro Vertical Axis Wind Turbine for Sustainable Urban Environment
By Kyooseon Park, School of Computing and Engineering, University of Huddersfield, UK (2013)

60
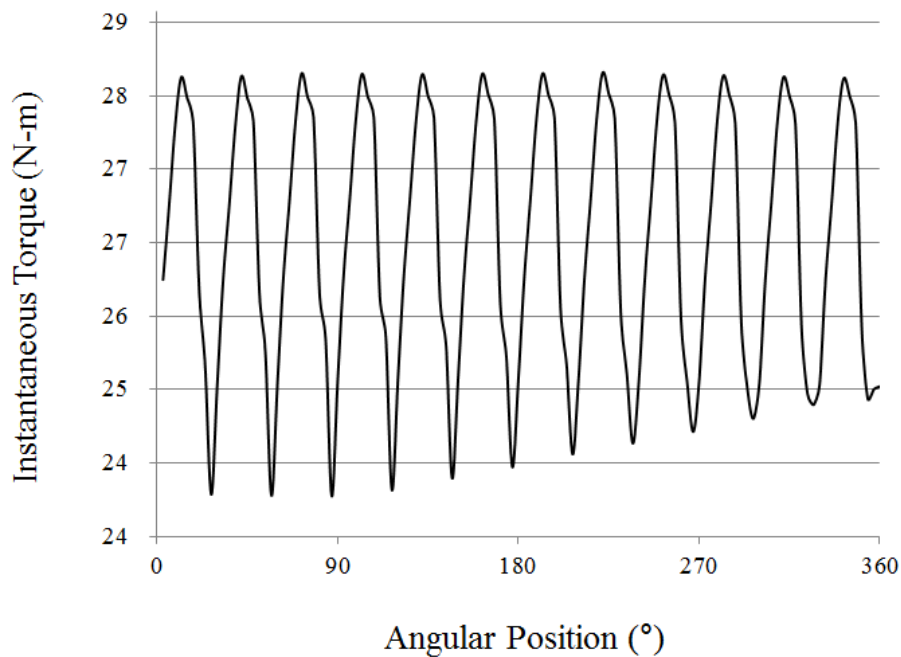
Figure 4.5 Instantaneous torque output of the VAWT having α=1.689°, γ=18.2° and δ=22.357°

In order to understand the dynamics behind the trend observed in instantaneous torque output of the VAWT, it is essential to analyse the flow structures and the angular positions of the VAWT that correspond to the peaks and valleys observed in figure 4.5. Figures 4.6(a & b) show the pressure and velocity variations in the vicinity of the VAWT at that angular position which corresponds to the peaks in the instantaneous torque output of the VAWT. It can be seen that peaks in the instantaneous torque output of the VAWT appear when the rotor and the stator blades are in-line with each other. This results into large uniform passages for the incident flow, hence increasing the torque output. Comparing figure 4.6(a) with figure 4.3(a), it can be seen from the scale in both the figures that the maximum pressure has increased, increasing the torque output. Furthermore, comparing figure 4.6(b) with figure 4.4(b) suggests that larger flow passages are available at leeward section in figure 4.6(b) through which flow can take place.
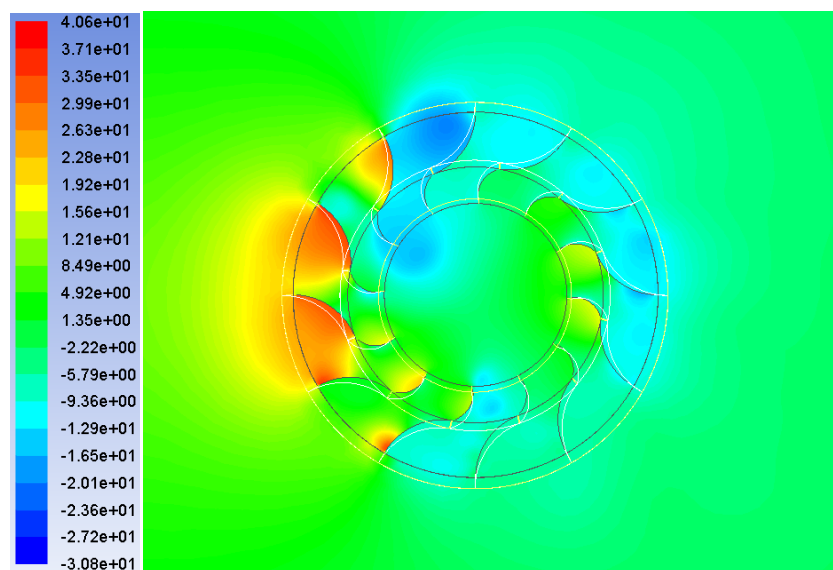
Figure 4.6(a) Pressure variations at peak instantaneous torque output of the VAWT

Optimal Design of a Micro Vertical Axis Wind Turbine for Sustainable Urban Environment
By Kyooseon Park, School of Computing and Engineering, University of Huddersfield, UK (2013)

61
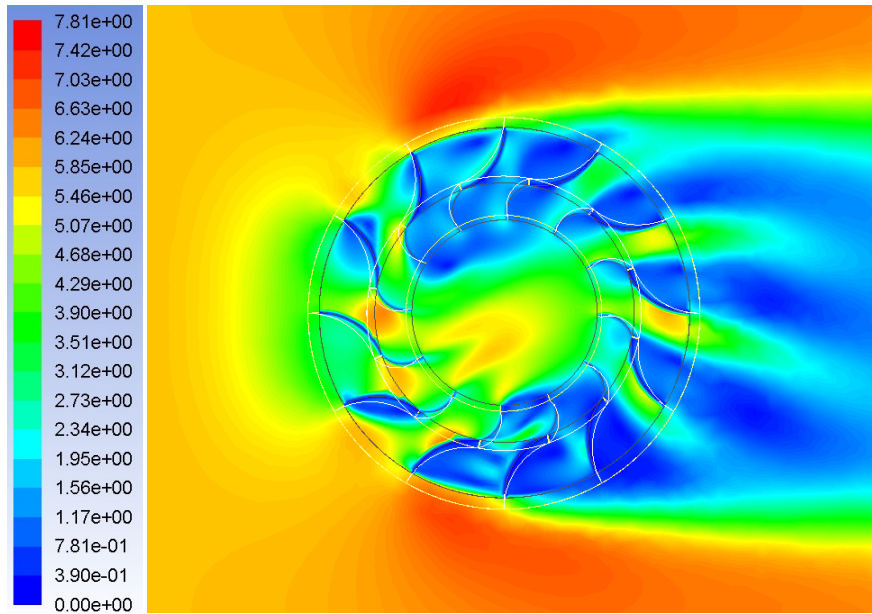
Figure 4.6(b) Velocity variations at peak instantaneous torque output of the VAWT

Figures 4.7(a & b) show the pressure and velocity variations in the vicinity of the VAWT at that angular position which corresponds to the valleys in the instantaneous torque output of the VAWT. It can be seen that valleys in the instantaneous torque output of the VAWT appear when the rotor and the stator blades are in such an orientation that forms non-uniform passages for the flow to take place. Comparing figure 4.7(a) with figure 4.6(a), it can be seen from the scale of both the figures that the maximum and minimum pressures have decreased significantly, decreasing the torque output of the VAWT. Furthermore, comparing figure 4.7(b) with figure 4.6(b) suggests that there is more blockage at both the windward and the leeward sections which results into reduced torque output of the VAWT.
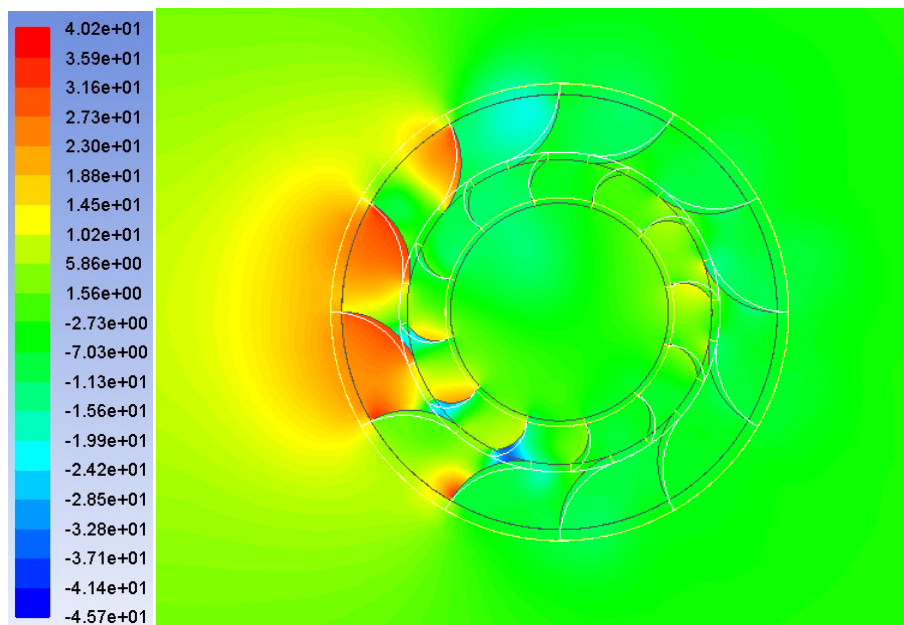
Figure 4.7(a) Pressure variations at lowest instantaneous torque output of the VAWT

Optimal Design of a Micro Vertical Axis Wind Turbine for Sustainable Urban Environment
By Kyooseon Park, School of Computing and Engineering, University of Huddersfield, UK (2013)

62
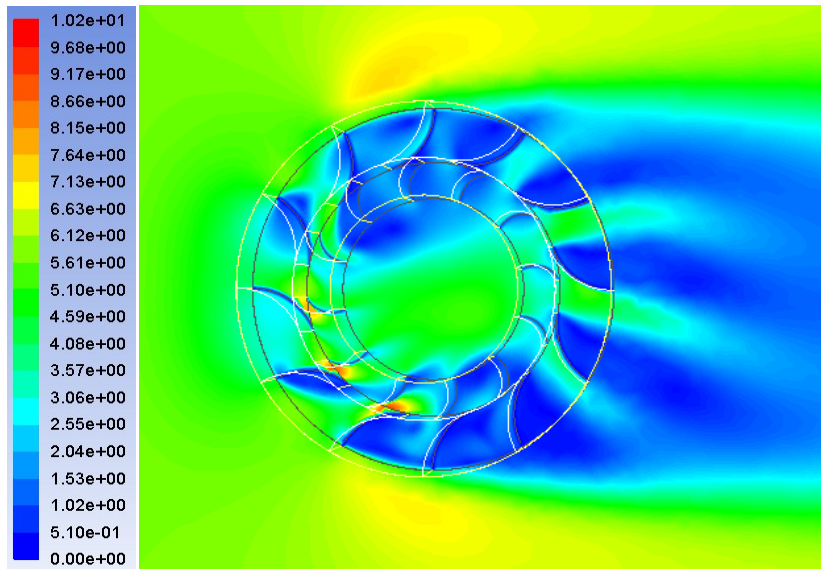
Figure 4.7(b) Velocity variations at lowest instantaneous torque output of the VAWT

Further quantifying the performance output of the aforementioned VAWT, table 4.3 shows the maximum, minimum, average, maximum amplitude and standard deviation in the instantaneous torque output shown in figure 4.3. The standard deviation shows how much variation exists from the average value and is defined as:

$$\text{Std. Dev.} = \sqrt{\frac{\sum (x - \bar{x})^2}{n - 1}} \tag{4.2}$$

A low standard deviation indicates that the data points tend to be very close to the mean whereas high standard deviation indicates that the data points are spread out over a large range of values.

Table 4.3 Statistical analysis of the instantaneous torque output of the VAWT having α=1.689⁰, γ=18.2⁰ and δ=22.357⁰

Torque Output	(N-m)
Maximum	28.36
Minimum	23.92
Average	26.60
Max - Min	4.44
Std. Dev.	1.37

After the general flow field analysis and discussions regarding the performance output of the VAWT, the effects of the blade angles, shown in figure 4.8, on the performance output have been discussed in the following sections.

Optimal Design of a Micro Vertical Axis Wind Turbine for Sustainable Urban Environment
By Kyooseon Park, School of Computing and Engineering, University of Huddersfield, UK (2013)

63
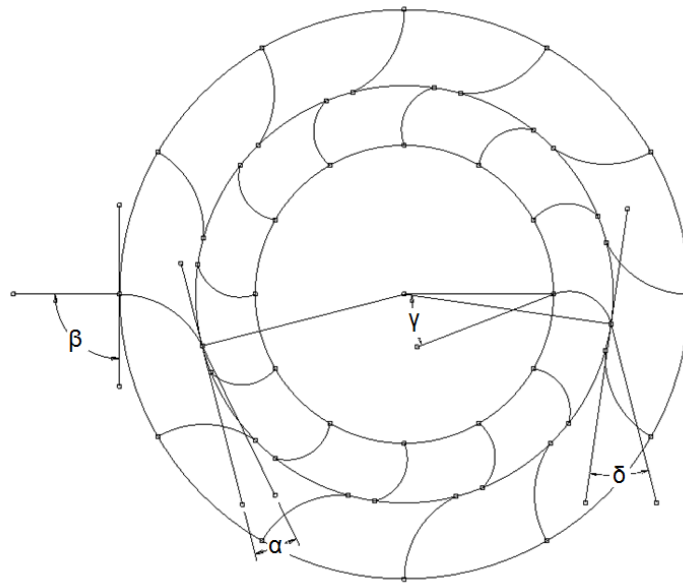
Figure 4.8 Blade Angles of a VAWT

4.4. Effect of α on the Performance Output of VAWT

In order to analyse the effect of α on the performance output of the VAWT, three α values of 1.689°, 11.689° and 21.689° have been chosen for the analysis purpose, keeping γ=18.2° and δ=32.357° constant. The complete set of results can be seen in Appendix 1. It is noteworthy at this point that only specific range of blade angles have been chosen in the present study (α from 1.689° to 21.689°, δ from 22.357° to 42.357° and γ from 18.2° to 38.2°) while β has been kept constant to 90°. β has been kept constant because of the design requirements that the incident flow and the stator blade's inlet should be in-line with each other. The range of other blade angles (α, δ and γ) has been chosen keeping in mind the difficulties in the manufacturing of such blades and integration of these blades with the in-house built VAWT shown in the previous chapter (under experimental setup section). Hence, a range of -10° to original VAWT to +10° has been chosen for analysis in the present study and all the results are valid in this range of angles only.

Figures 4.9(a & b) depicts the pressure and velocity variations in the vicinity of the VAWT for α=1.689°. It can be seen that there exists a high pressure region (going upto 39.5Pa) on the windward side of the VAWT whereas the pressure is lower on the leeward side of the VAWT. Furthermore, the pressure is comparatively low on the upper section as compared to the lower section due to the orientation of the blades.

Optimal Design of a Micro Vertical Axis Wind Turbine for Sustainable Urban Environment
By Kyooseon Park, School of Computing and Engineering, University of Huddersfield, UK (2013)

64
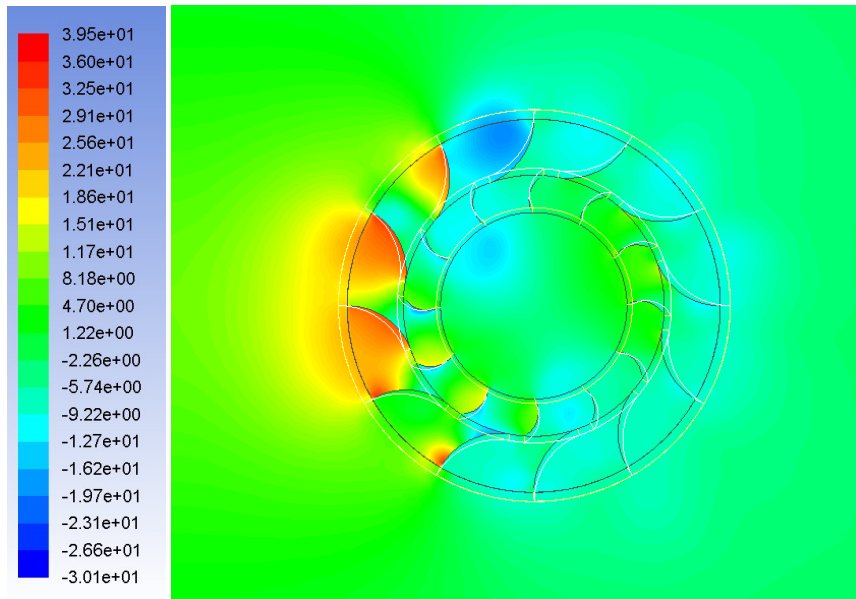
Figure 4.9(a) Pressure variations at 0° angular position of the VAWT having α=1.689°, γ=18.2° and δ=32.357°

Further analysing the flow structure in the vicinity of the VAWT, figure 4.9(b) depicts that the flow velocity is considerably high within the passages formed on the windward side due to the orientation of the blades. The velocity goes up to as high as 8.12m/sec where the incident flow velocity is 4m/sec. The reduction in the effective flow area, as these passages are formed, increases the flow velocity.
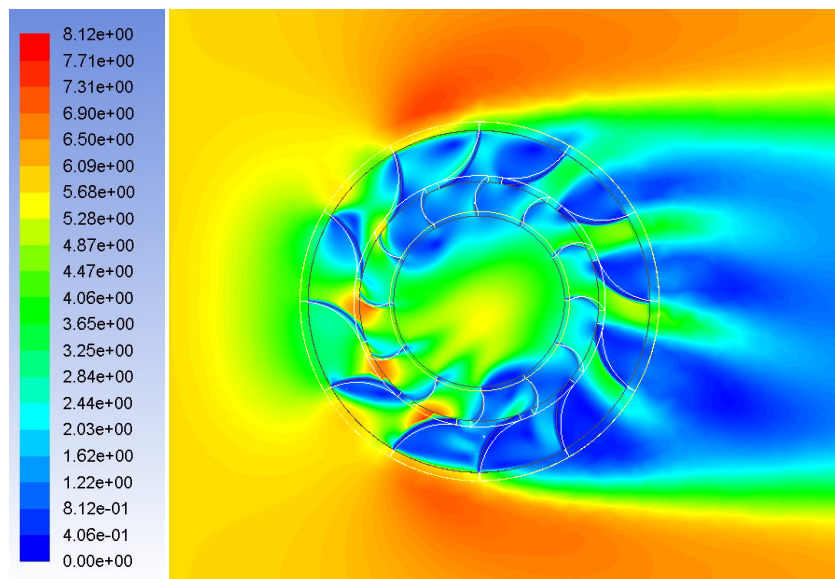
Figure 4.9(b) Velocity variations at 0° angular position of the VAWT having α=1.689°, γ=18.2° and δ=32.357°

In order to quantify the performance output of the VAWT considered here, the instantaneous torque output for one revolution of the VAWT has been plotted in figure 4.10. It can be seen that the torque output of the VAWT is cyclic with the number of peaks/valleys equal to the number of rotor and stator blades. It is observed that the amplitude of instantaneous torque output of the VAWT increases as the angular position of the VAWT increases. This is due to the orientation of the blades within the VAWT.

Optimal Design of a Micro Vertical Axis Wind Turbine for Sustainable Urban Environment
By Kyooseon Park, School of Computing and Engineering, University of Huddersfield, UK (2013)

65
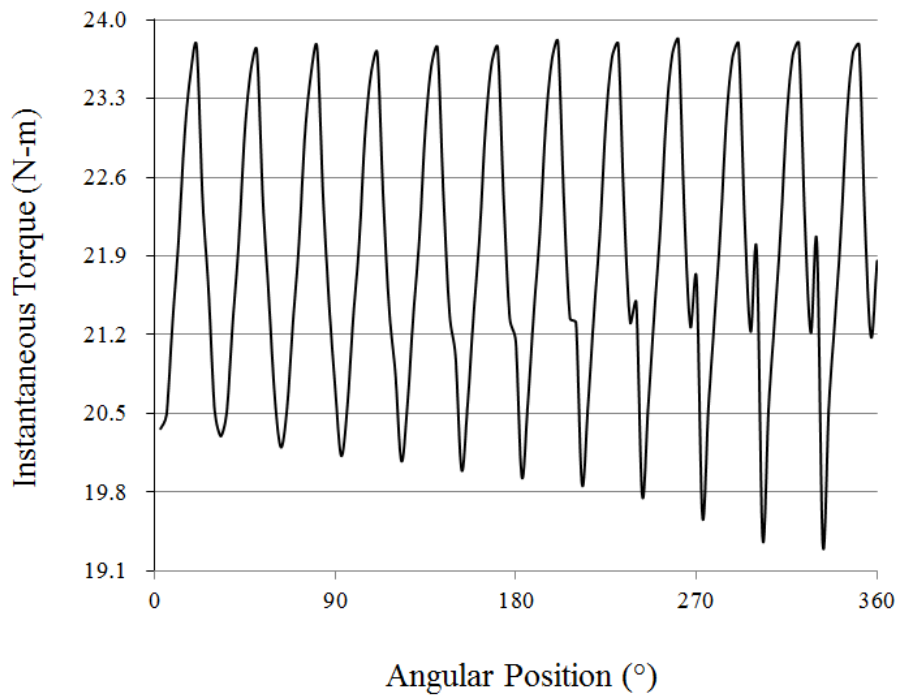
Figure 4.10 Instantaneous torque output of the VAWT having α=1.689⁰, γ=18.2⁰ and δ=22.357⁰

Further quantifying the performance output of the aforementioned VAWT, table 4.4 shows the maximum, minimum, average, maximum amplitude and standard deviation in the instantaneous torque output shown in figure 4.10.

Table 4.4 Statistical analysis of the instantaneous torque output of the VAWT having α=1.689⁰, γ=18.2⁰ and δ=32.357⁰

Torque Output	(N-m)
Maximum	23.81
Minimum	19.33
Average	21.93
Max - Min	4.49
Std. Dev.	1.23

Figures 4.11(a & b) depicts the pressure and velocity variations in the vicinity of the VAWT for α=11.689⁰, keeping γ=18.2⁰ and δ=32.357⁰ constant. In comparison with figure 4.9(a), it can be seen that the low pressure regions on the leeward side are bigger. Furthermore, the low pressure regions on the upper and lower sections penetrate much further into the core region of the VAWT. This low pressure in the core region forces the incident flow to exert more force on the blades of the VAWT, hence increasing its torque output.
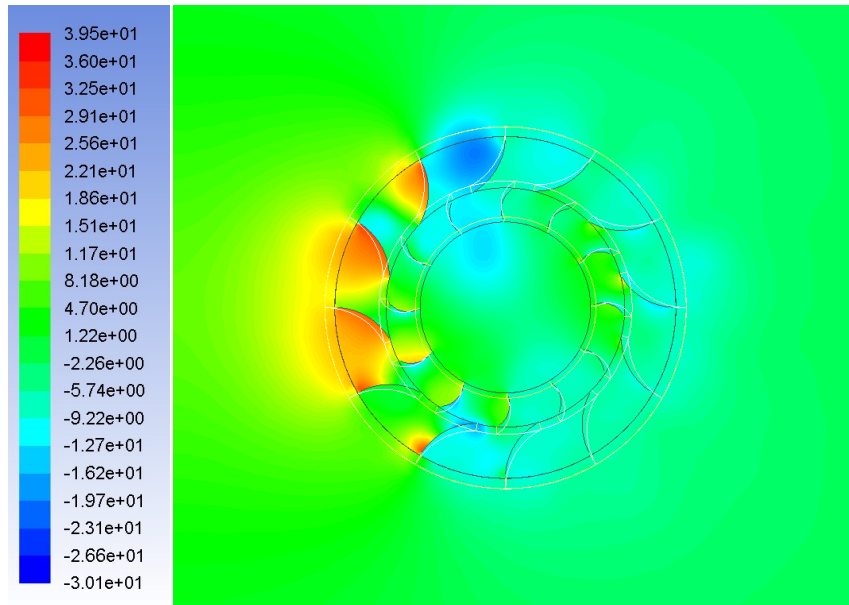
Figure 4.11(a) Pressure variations at 0⁰ angular position of the VAWT having α=11.689⁰, γ=18.2⁰ and δ=32.357⁰

Figure 4.11(b) depicts the flow velocity variations in the vicinity of the VAWT. In comparison with figure 4.9(b), it can be seen that the flow velocity is considerably lower in the passages formed on the windward side of the VAWT. This strengthens the argument given earlier regarding the exertion of higher forces on the blades due to more pressure difference between the windward side and the core region of the VAWT.
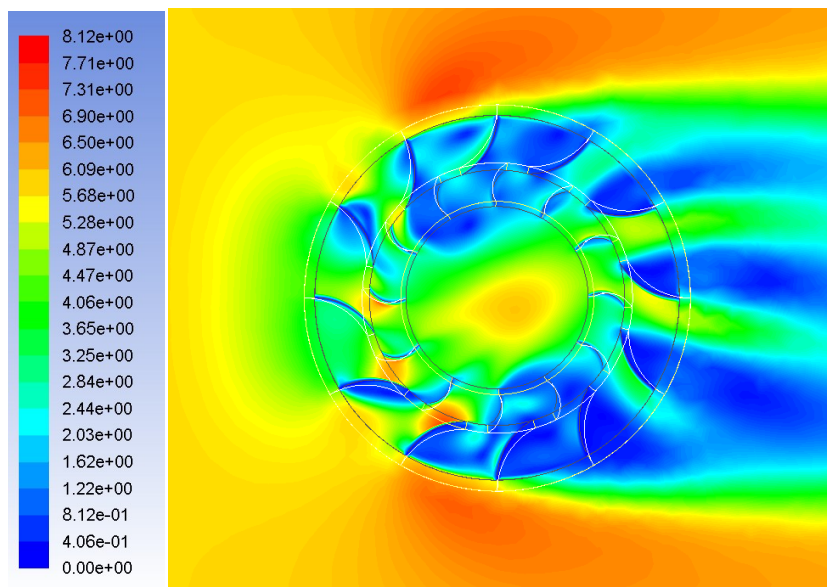
Figure 4.11(b) Velocity variations at 0⁰ angular position of the VAWT having α=11.689⁰, γ=18.2⁰ and δ=32.357⁰

The instantaneous torque output for one revolution of the VAWT has been plotted in figure 4.12. In comparison with figure 4.10, it can be clearly seen that the torque output of this model of the VAWT is considerably higher than the one discussed earlier having α=1.689⁰. Furthermore, it can be seen that the amplitude of instantaneous torque output remains constant in each cycle which is contrary to the trend observed earlier for α=1.689⁰.

Optimal Design of a Micro Vertical Axis Wind Turbine for Sustainable Urban Environment
By Kyooseon Park, School of Computing and Engineering, University of Huddersfield, UK (2013)

67
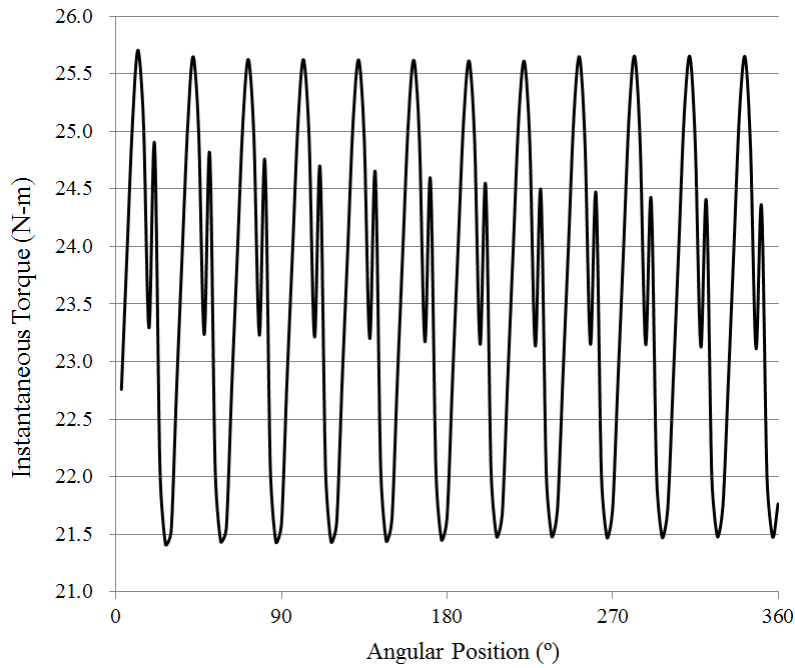
Figure 4.12 Instantaneous torque output of the VAWT having α=11.689°, γ=18.2° and δ=22.357°

Table 4.5 provides the statistical analysis of the torque output from the VAWT. It is noteworthy that the average torque output for α=11.689° is higher than for α=1.689° by 7.3%. Furthermore, it can also be seen that the maximum amplitude has decreased by 4.4% because of the uniform cycles observed in figure 4.12. Analyzing the standard deviations from both the models, it can be seen that the standard deviation is higher in case of α=11.689° as compared to α=1.689° although the maximum amplitude has reduced. This is because some additional peaks have been observed in figure 4.12. These peaks are much lower in magnitude than the standard peaks but still contribute significantly to the average torque output of the VAWT. It has been observed that these smaller peaks are formed when rotor blades come exactly in between two stator blades, forming two uniform, but smaller, flow passages. These passages are not that effective as a single large passage formed when both the rotor and the stator blades come in-line with each other, but still these passages contribute significantly to the performance output of the VAWT.

Table 4.5 Statistical analysis of the instantaneous torque output of the VAWT having α=11.689°, γ=18.2° and δ=32.357°

Torque Output	(N-m)
Maximum	25.71
Minimum	21.41
Average	23.53
Max - Min	4.29
Std. Dev.	1.45

Figures 4.13(a & b) depicts the pressure and velocity variations in the vicinity of the VAWT for α=21.689°, keeping γ=18.2° and δ=32.357° constant. In comparison with figure 4.11(a), it can be seen that the low pressure regions on the leeward side are even bigger and further penetrates into the core region of the VAWT. Hence, an increase in the torque output is expected.

Optimal Design of a Micro Vertical Axis Wind Turbine for Sustainable Urban Environment
By Kyooseon Park, School of Computing and Engineering, University of Huddersfield, UK (2013)

68
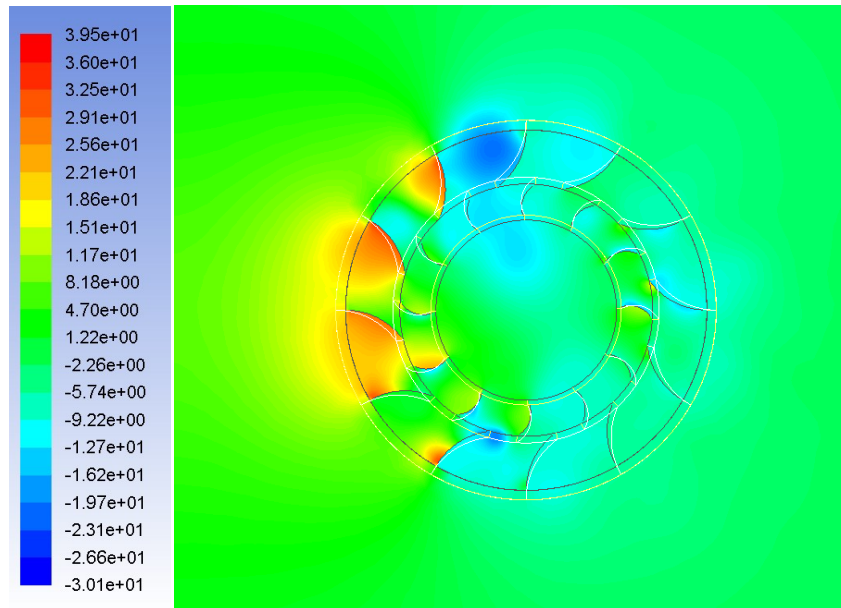
Figure 4.13(a) Pressure variations at 0⁰ angular position of the VAWT having α=21.689⁰, γ=18.2⁰ and δ=32.357⁰

Figure 4.13(b) depicts the flow velocity variations in the vicinity of the VAWT. In comparison with figure 4.11(b), it can be seen that the flow velocity is considerably higher in the core region of the VAWT while it is much lower on the windward side of the VAWT.
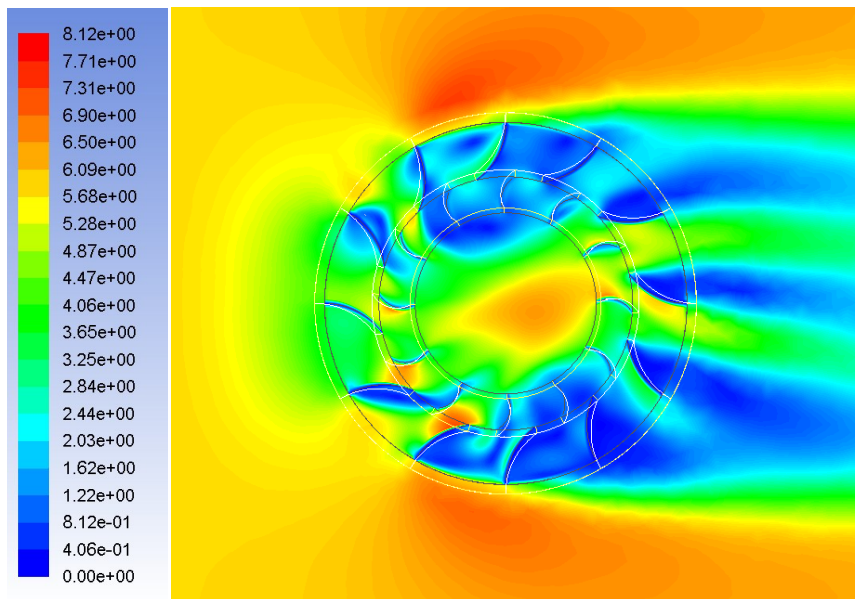
Figure 4.13(b) Velocity variations at 0⁰ angular position of the VAWT having α=21.689⁰, γ=18.2⁰ and δ=32.357⁰

The instantaneous torque output for one revolution of the VAWT having α=21.689⁰ has been plotted in figure 4.14. In comparison with figure 4.9, it can be seen that the torque output of this model of the VAWT is marginally higher than for α=11.689⁰. Furthermore, it can be seen that the smaller peaks are much more evident and have been shifted to the left side of the cycles. This is due to the orientation of the blades that forms passages.

Optimal Design of a Micro Vertical Axis Wind Turbine for Sustainable Urban Environment
By Kyooseon Park, School of Computing and Engineering, University of Huddersfield, UK (2013)

69
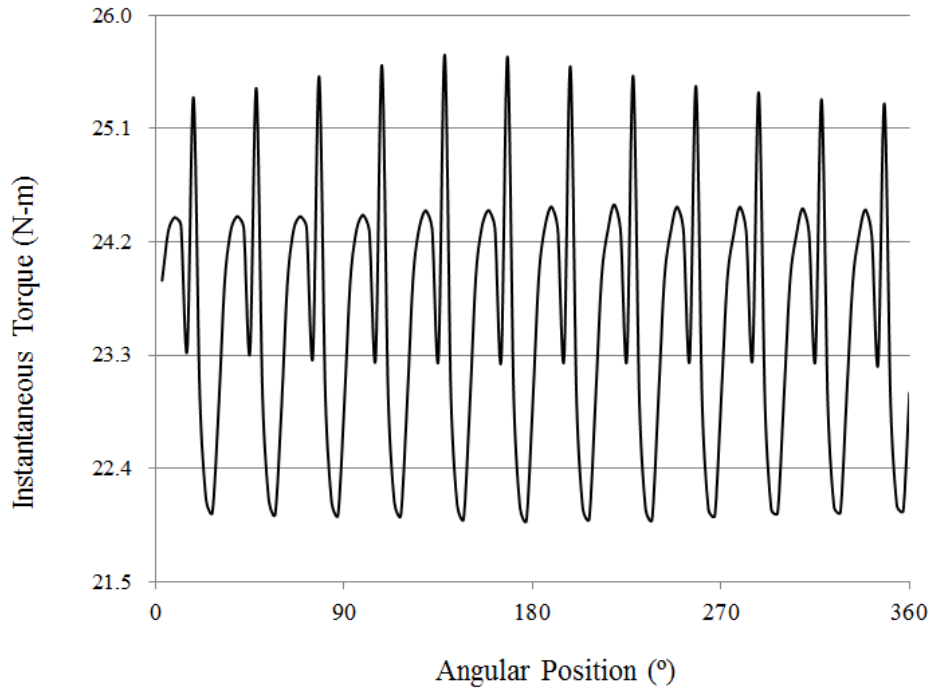
Figure 4.14 Instantaneous torque output of the VAWT having α=21.689⁰, γ=18.2⁰ and δ=22.357⁰

Table 4.6 provides the statistical analysis of the torque output from the VAWT. It is noteworthy that the average torque output for α=21.689° is marginally higher than for α=11.689° (by 0.17%). Analyzing the standard deviations from both the models, it can be seen that the standard deviation is higher in case of α=11.689° as compared to α=21.689°. This is due to the fact that the maximum amplitude of these smaller peaks in case of α=11.689° is 1.6 while it is 1.1 in case of α=21.689°. Hence, the overall standard deviation of the instantaneous torque output decreases for α=21.689°.

Table 4.6 Statistical analysis of the instantaneous torque output of the VAWT having α=21.689°, γ=18.2° and δ=32.357°

Torque Output	(N-m)
Maximum	25.69
Minimum	21.99
Average	23.57
Max - Min	3.70
Std. Dev.	1.05

Figure 4.15 depicts the instantaneous torque outputs of the aforementioned cases on a single scale for comparison purposes. It is evident that for α=1.689°, the torque output is considerably less than for the other two models. Comparing α=11.689° and α=21.689° reveals that although the maximum instantaneous torque output of α=11.689° is higher, its average torque output is still slightly lower than for α=21.689° because its minimum instantaneous torque output is considerably less than the minimum instantaneous torque output from α=21.689°.

Optimal Design of a Micro Vertical Axis Wind Turbine for Sustainable Urban Environment
By Kyooseon Park, School of Computing and Engineering, University of Huddersfield, UK (2013)

70
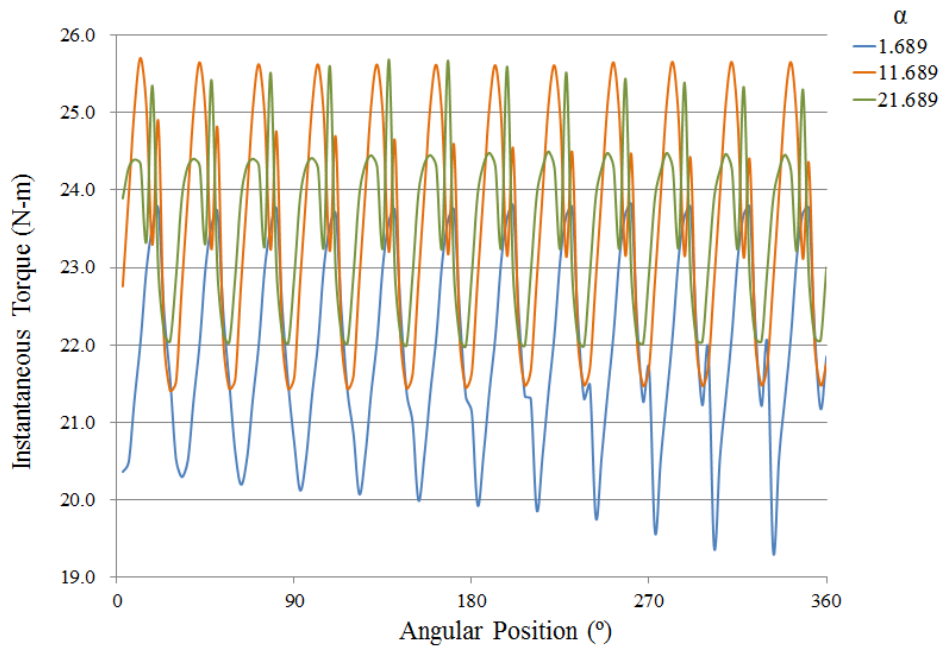
Figure 4.15 Instantaneous torque outputs of VAWT models having different α

As mentioned earlier, complete CFD results have been presented in Appendix 1. Figure 4.16 depicts some of these results where the effect of α can be clearly visualised. It can be seen that for a given γ and δ, as α increases, the average torque output and the average power output of the VAWT increases upto a certain point after which both these quantities start decreasing. Hence, there is an optimum value of α that corresponds to the maximum performance output of the VAWT, which in the present study is 16.689°. It is essential to mention here that the power of a VAWT can be represented by:

$$P = \omega * T \tag{4.3}$$

Where P is the power output, ω is the angular speed of the rotor blades and T is the torque output of the VAWT.
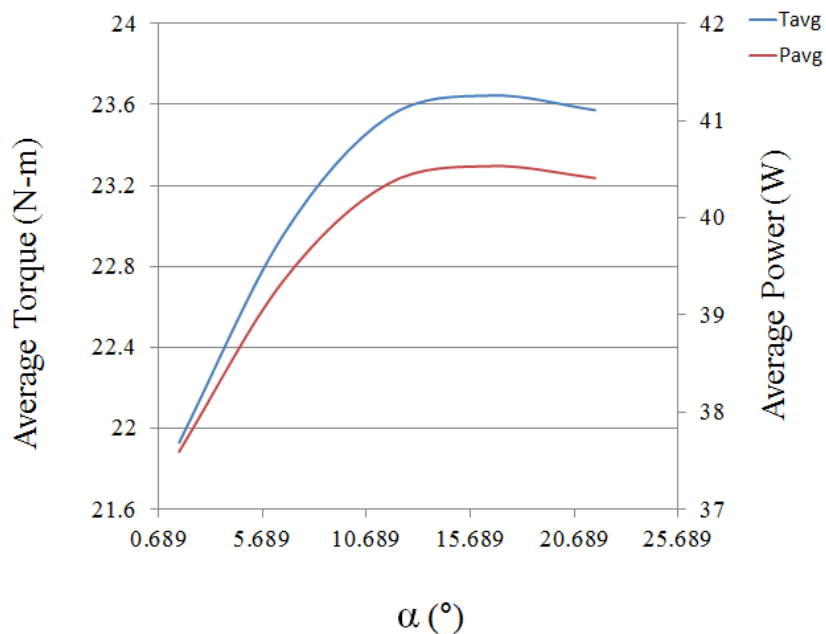
Figure 4.16 Effect of α on the performance output of VAWT

4.5. Effect of δ on the Performance Output of VAWT

In order to analyse the effect of δ on the performance output of the VAWT, three δ values of 22.357⁰, 32.357⁰ and 42.357⁰ have been chosen for the analysis purpose, keeping α=11.689⁰ and γ=28.2⁰ constant. The complete set of results can be seen in Appendix 1.

Figures 4.17(a & b) depicts the pressure and velocity variations in the vicinity of the VAWT for δ=22.357⁰. It can be seen that there exists a high pressure region (going upto 39.1Pa) on the windward side of the VAWT whereas the pressure is lower on the leeward side of the VAWT. Furthermore, the pressure is comparatively low on the upper section as compared to the lower section due to the orientation of the blades.
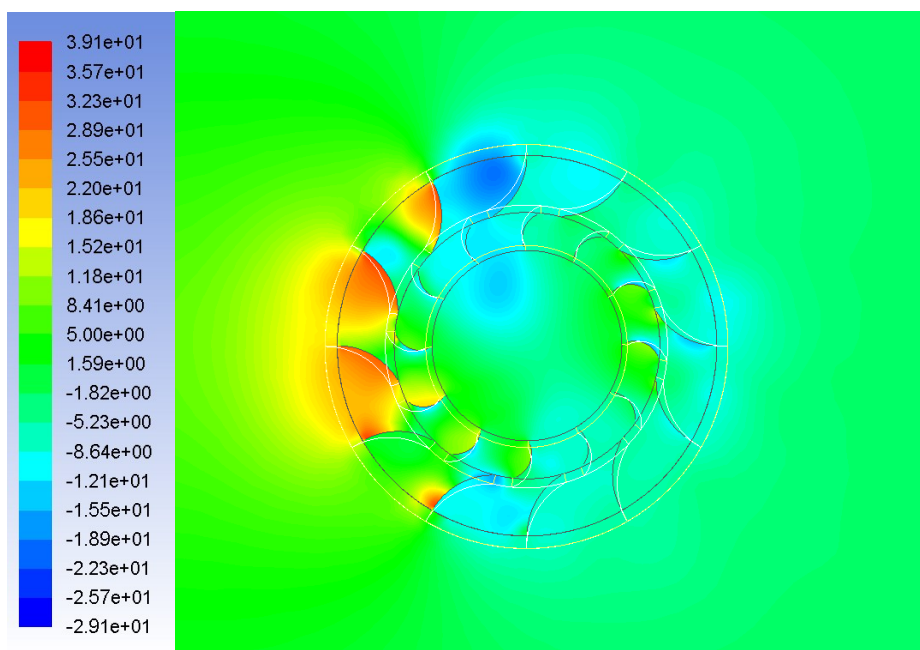
Figure 4.17(a) Pressure variations at 0⁰ angular position of the VAWT having α=11.689⁰, γ=28.2⁰ and δ=22.357⁰

Further analysing the flow structure in the vicinity of the VAWT, figure 4.17(b) depicts that the flow velocity is considerably high within the passages formed on the windward side due to the orientation of the blades. The velocity goes up to as high as 9.21m/sec where the incident flow velocity is 4m/sec. The reduction in the effective flow area, as these passages are formed, increases the flow velocity.

Optimal Design of a Micro Vertical Axis Wind Turbine for Sustainable Urban Environment
By Kyooseon Park, School of Computing and Engineering, University of Huddersfield, UK (2013)

72
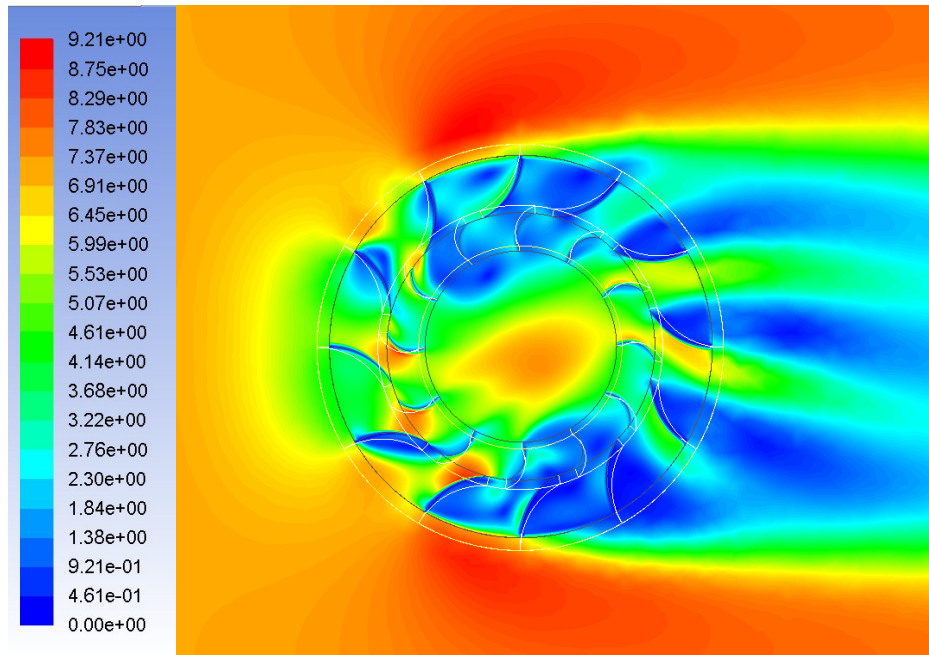
Figure 4.17(b) Velocity variations at 0⁰ angular position of the VAWT having α=11.689⁰, γ=28.2⁰ and δ=22.357⁰

In order to quantify the performance output of the VAWT considered here, the instantaneous torque output for one revolution of the VAWT has been plotted in figure 4.18. It can be seen that the torque output of the VAWT is cyclic with the number of peaks/valleys equal to the number of rotor and stator blades. It is observed that there are smaller peaks present in the first five cycles which is due to the orientation of the blades within the VAWT.
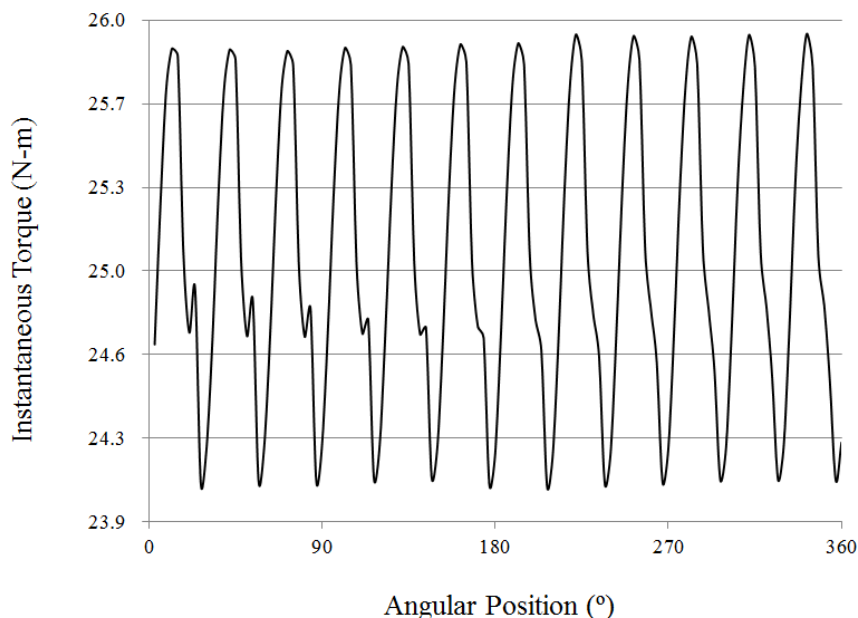
Figure 4.18 Instantaneous torque output of the VAWT having α=11.689⁰, γ=28.2⁰ and δ=22.357⁰

Further quantifying the performance output of the aforementioned VAWT, table 4.7 shows the maximum, minimum, average, maximum amplitude and standard deviation in the instantaneous torque output shown in figure 4.18.

Optimal Design of a Micro Vertical Axis Wind Turbine for Sustainable Urban Environment
By Kyooseon Park, School of Computing and Engineering, University of Huddersfield, UK (2013)

73

Table 4.7 Statistical analysis of the instantaneous torque output of the VAWT having α=11.689⁰, γ=28.2⁰ and δ=22.357⁰

Torque Output	(N-m)
Maximum	25.94
Minimum	24.05
Average	25.01
Max - Min	1.90
Std. Dev.	0.62

Figures 4.19(a & b) depicts the pressure and velocity variations in the vicinity of the VAWT for δ=32.357⁰, keeping γ=28.2⁰ and α=11.689⁰ constant. In comparison with figure 4.17(a), it can be seen that in the upper section of the VAWT, the low pressure region is significantly smaller in size and the pressure is considerably higher as compared to one observed in case of δ=22.357⁰. This increase in pressure on the upper section reduces the exertion of forces on the blades of the VAWT, hence, degrading its performance output.
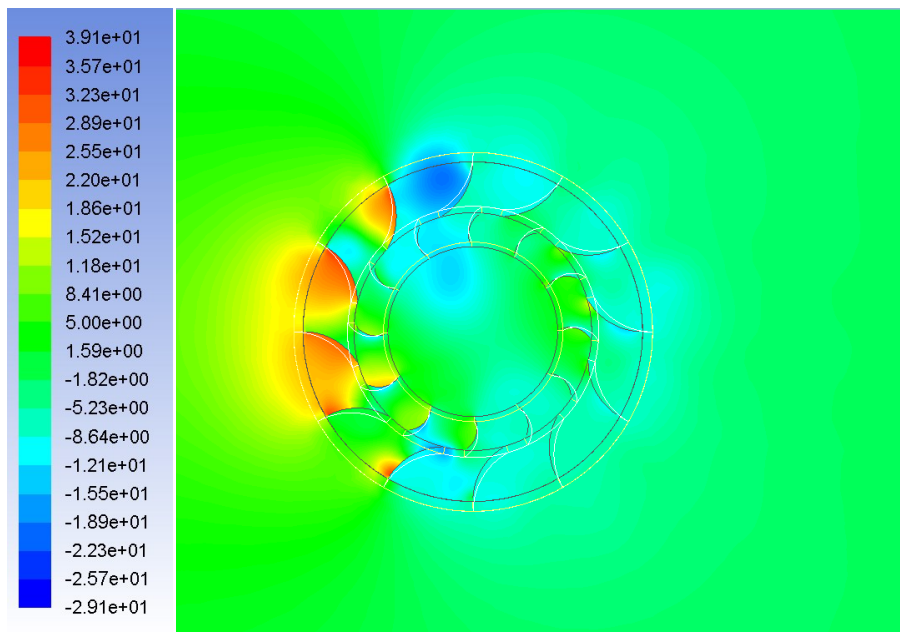
Figure 4.19(a) Pressure variations at 0⁰ angular position of the VAWT having α=11.689⁰, γ=28.2⁰ and δ=32.357⁰

Figure 4.19(b) depicts the flow velocity variations in the vicinity of the VAWT. In comparison with figure 4.17(b), it can be seen that the flow velocity is considerably lower in the whole flow domain shown in the figure. This lower flow velocity observed in the vicinity of the VAWT tries to slow down the VAWT, hence, reducing its torque and power outputs.

Optimal Design of a Micro Vertical Axis Wind Turbine for Sustainable Urban Environment
By Kyooseon Park, School of Computing and Engineering, University of Huddersfield, UK (2013)

74
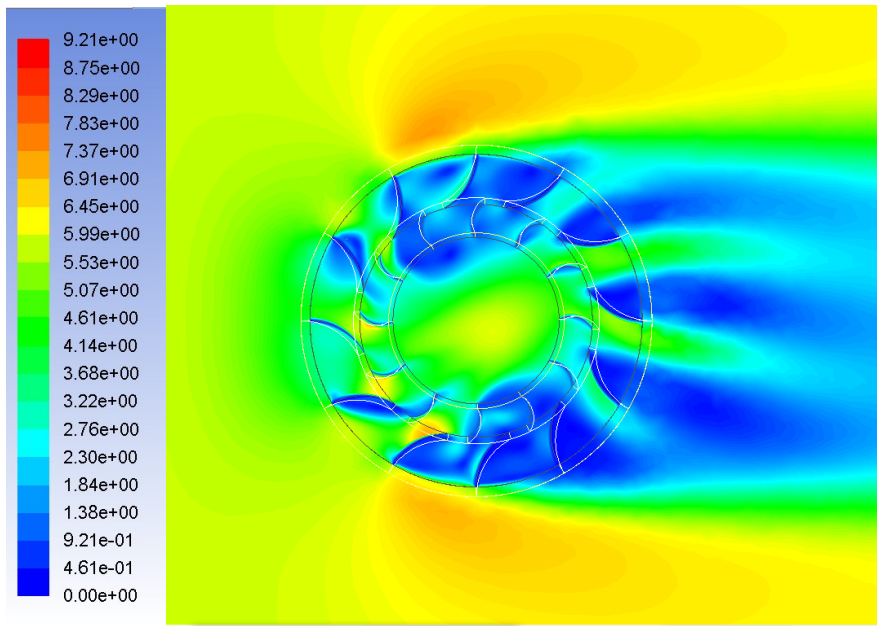
Figure 4.19(b) Velocity variations at 0° angular position of the VAWT having α=11.689°, γ=28.2° and δ=32.357°

The instantaneous torque output for one revolution of the VAWT has been plotted in figure 4.20. In comparison with figure 4.18, it can be clearly seen that the torque output of this model of the VAWT is considerably lower and the cycles have seemed to be shifted downwards on the same plot. Furthermore, it can be also be seen that there exists smaller peaks on each cycle and their amplitude is significantly higher than observed in the case of δ=22.357°. This suggests that the standard deviation would be much higher for δ=32.357° as compared to δ=22.357°.
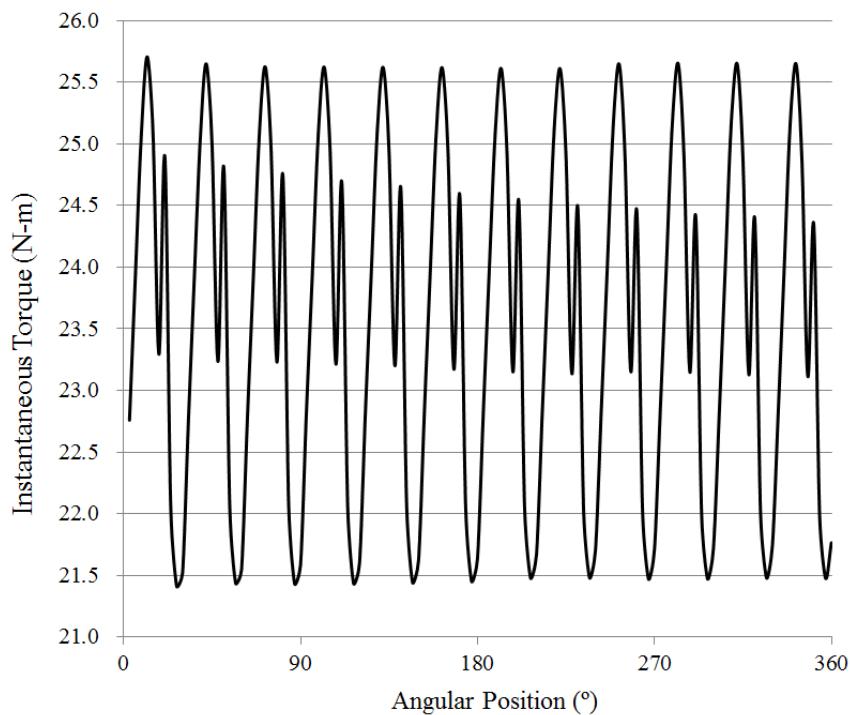
Figure 4.20 Instantaneous torque output of the VAWT having α=11.689°, γ=28.2° and δ=32.357°

Optimal Design of a Micro Vertical Axis Wind Turbine for Sustainable Urban Environment
By Kyooseon Park, School of Computing and Engineering, University of Huddersfield, UK (2013)

75

Table 4.8 provides the statistical analysis of the torque output from the aforementioned VAWT. It is can be seen clearly that the average torque output for δ=32.357⁰ is considerably lower than for δ=22.357⁰ (by 6%). Analyzing the standard deviations from both the models, it can be seen that the standard deviation is higher in case of δ=32.357⁰ as compared to δ=22.357⁰ as mentioned earlier.

Table 4.8 Statistical analysis of the instantaneous torque output of the VAWT having α=11.689⁰, γ=28.2⁰ and δ=32.357⁰

Torque Output	(N-m)
Maximum	25.71
Minimum	21.41
Average	23.53
Max - Min	4.29
Std. Dev.	1.45

Figures 4.21(a & b) depicts the pressure and velocity variations in the vicinity of the VAWT for δ=42.357⁰, keeping γ=28.2⁰ and α=11.689⁰ constant. In comparison with figure 4.19(a), it can be seen that the pressure on the windward side is higher whereas on the leeward side is considerably lower. This means that the pressure gradients in the vicinity of the VAWT are much more severe that might give rise to unwanted vibrations and structural damage. Furthermore, it is also expected that the amplitude of torque output would be significantly higher than observed in the previous cases.
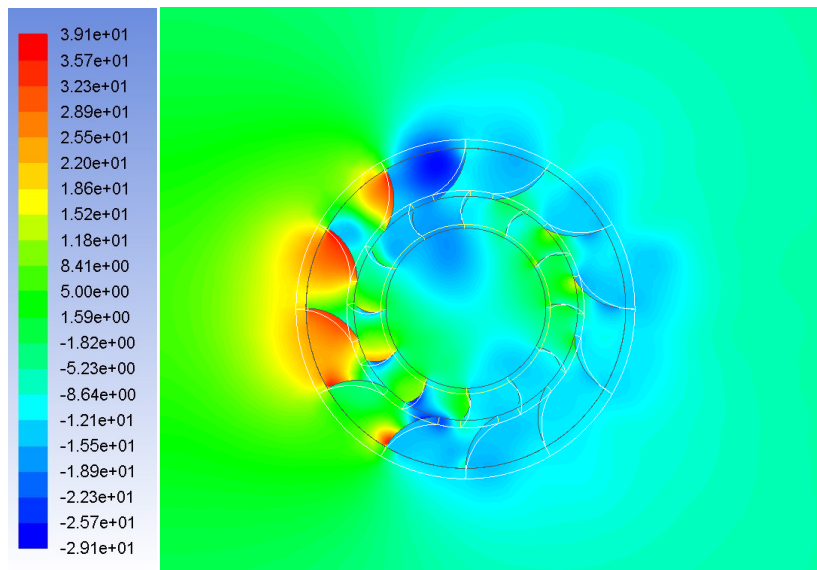
Figure 4.21(a) Pressure variations at 0⁰ angular position of the VAWT having α=11.689⁰, γ=28.2⁰ and δ=42.357⁰

Figure 4.21(b) depicts the flow velocity variations in the vicinity of the VAWT. In comparison with figure 4.19(b), it can be seen that the flow velocity is appreciably higher in the flow passages on the windward side of the VAWT. The reduction in the effective flow area, as these passages are formed, increases the flow velocity.

Optimal Design of a Micro Vertical Axis Wind Turbine for Sustainable Urban Environment
By Kyooseon Park, School of Computing and Engineering, University of Huddersfield, UK (2013)

76
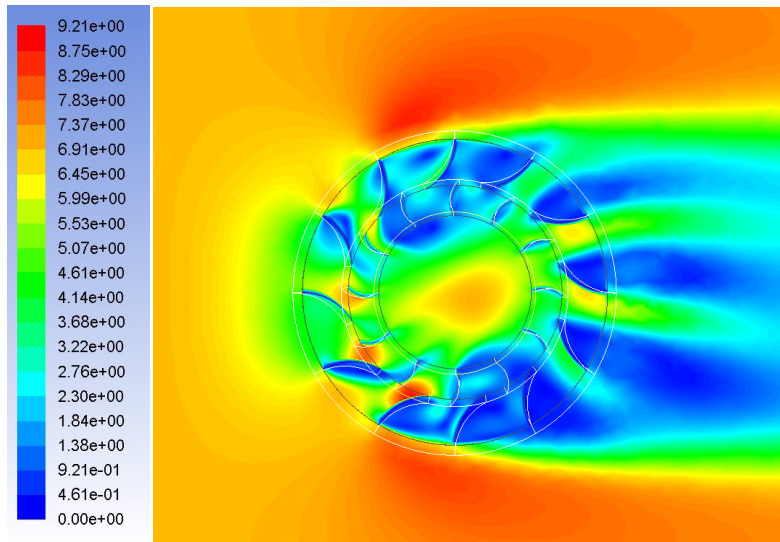
Figure 4.21(b) Velocity variations at 0⁰ angular position of the VAWT having α=11.689⁰, γ=28.2⁰ and δ=42.357⁰

The instantaneous torque output for one revolution of the VAWT has been plotted in figure 4.22. In comparison with figure 4.20, it can be clearly seen that the torque output of this model of the VAWT is considerably lower. Furthermore, it can be also be seen that the torque output is cyclic with no intermediate peaks (as observed earlier).
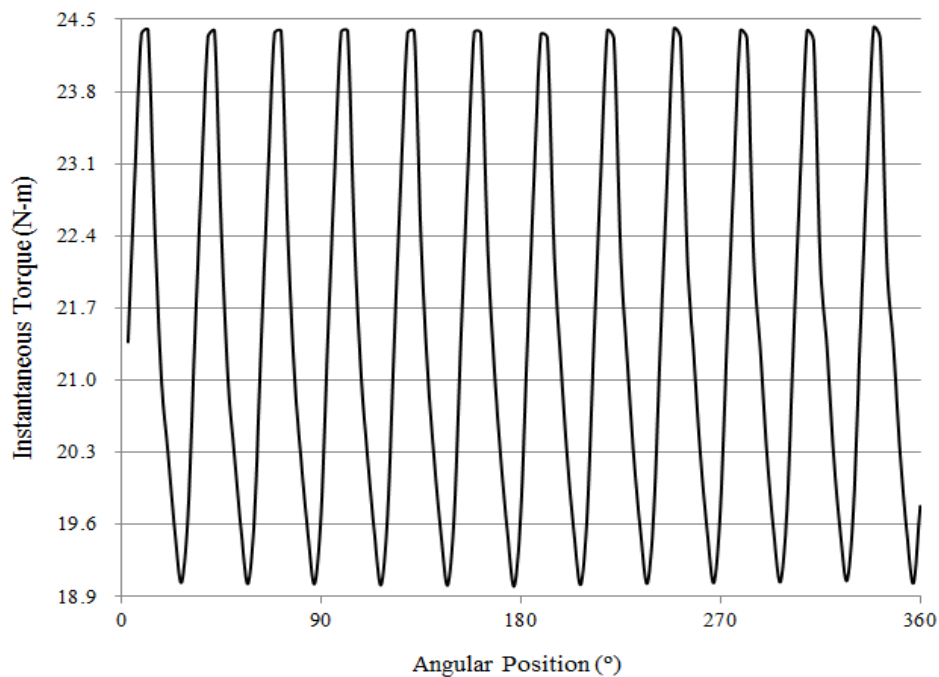
Figure 4.22 Instantaneous torque output of the VAWT having α=11.689⁰, γ=28.2⁰ and δ=42.357⁰

Table 4.9 provides the statistical analysis of the torque output from the aforementioned VAWT. It is can be seen clearly that the average torque output for δ=42.357⁰ is considerably lower than for δ=32.357⁰ (by 8.5%). Analyzing the standard deviations from both the models, it can be seen that the standard deviation is higher in case of δ=42.357⁰ as compared to δ=32.357⁰ as mentioned earlier.

Optimal Design of a Micro Vertical Axis Wind Turbine for Sustainable Urban Environment
By Kyooseon Park, School of Computing and Engineering, University of Huddersfield, UK (2013)

77

An important point to mention at this stage is that as δ increases, the amplitude of the torque output increases as well (125% from δ=22.357° to 32.57° and 26% from δ=32.357° to δ=42.357°)

Table 4.9 Statistical analysis of the instantaneous torque output of the VAWT having α=11.689°, γ=28.2° and δ=42.357°

Torque Output	(N-m)
Maximum	24.42
Minimum	19.00
Average	21.51
Max - Min	5.42
Std. Dev.	1.85

Figure 4.23 depicts the instantaneous torque outputs of the aforementioned cases on a single scale for comparison purposes. It is evident that for δ=22.357°, the torque output is considerably higher than for the other two models. Hence, it can be concluded that as δ increases, the torque output of the VAWT decreases. This trend is contrary to the one observed for α, where the torque output increases as α increases (upto a certain point). Furthermore, it can also be seen in the figure that the amplitude of torque output increases significantly as δ increases.
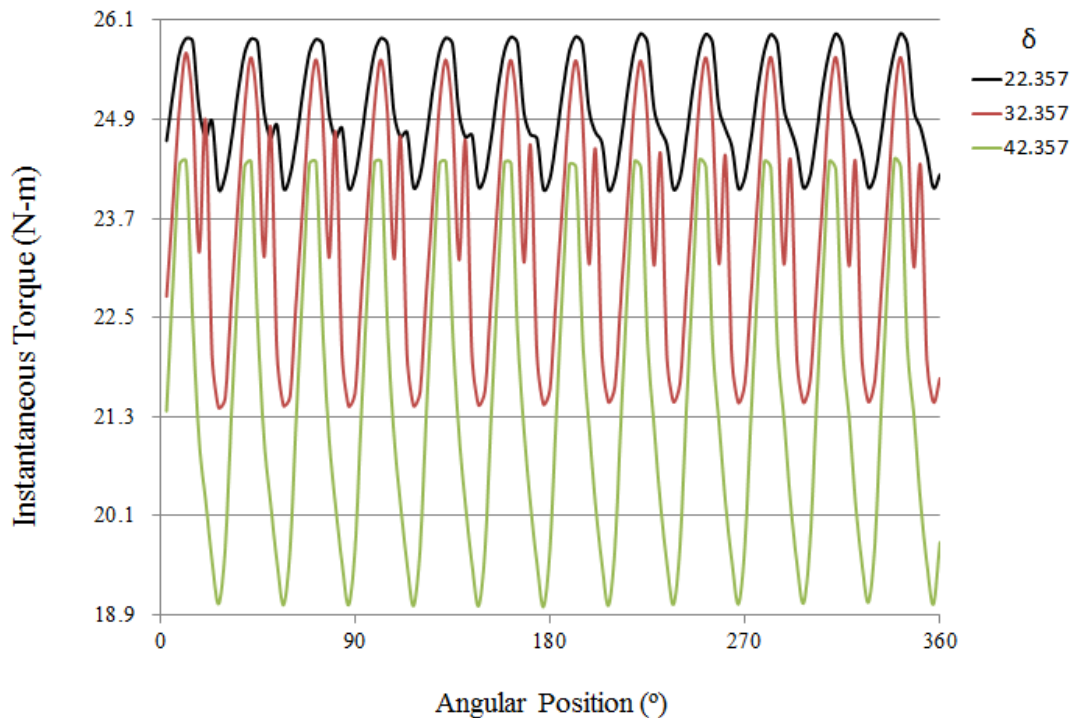
Figure 4.23 Instantaneous torque outputs of VAWT models having different δ

As mentioned earlier, complete CFD results have been presented in Appendix 1. Figure 4.24 depicts some of these results where the effect of δ can be clearly visualised. It can be seen that for a given γ and α, as δ increases, the average torque output and the average power output of the VAWT decreases almost linearly. Hence, lower δ means more torque and power outputs from the VAWT.
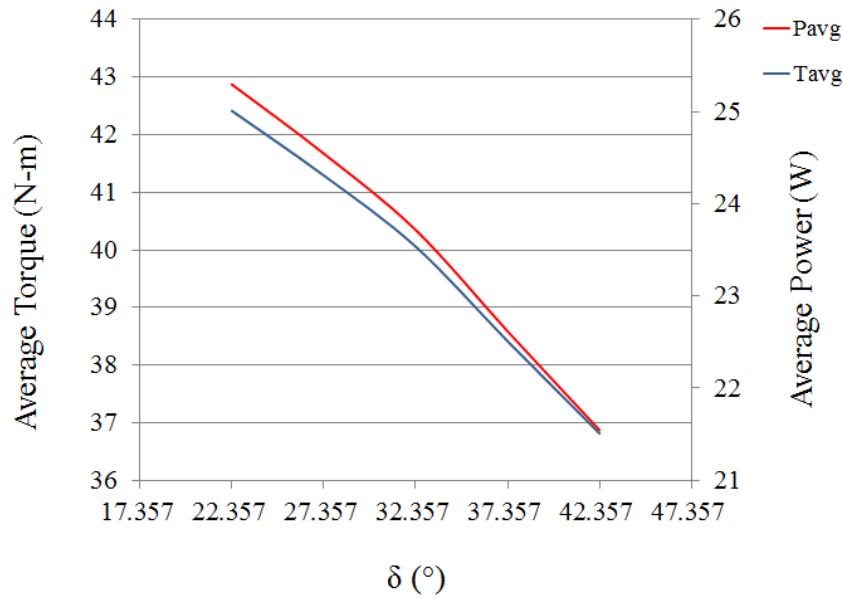
Figure 4.24 Effect of δ on the performance output of VAWT

4.6. Effect of γ on the Performance Output of VAWT

In order to analyse the effect of δ on the performance output of the VAWT, three γ values of 18.2°, 28.2° and 38.2° have been chosen for the analysis purpose, keeping α=11.689° and δ=32.357° constant. The complete set of results can be seen in Appendix 1.

Figures 4.25(a & b) depicts the pressure and velocity variations in the vicinity of the VAWT for γ=18.2°. It can be seen that there exists a high pressure region (going upto 38.9Pa) on the windward side of the VAWT whereas the pressure is lower on the leeward side of the VAWT. Furthermore, the pressure is comparatively low on the upper section as compared to the lower section due to the orientation of the blades.
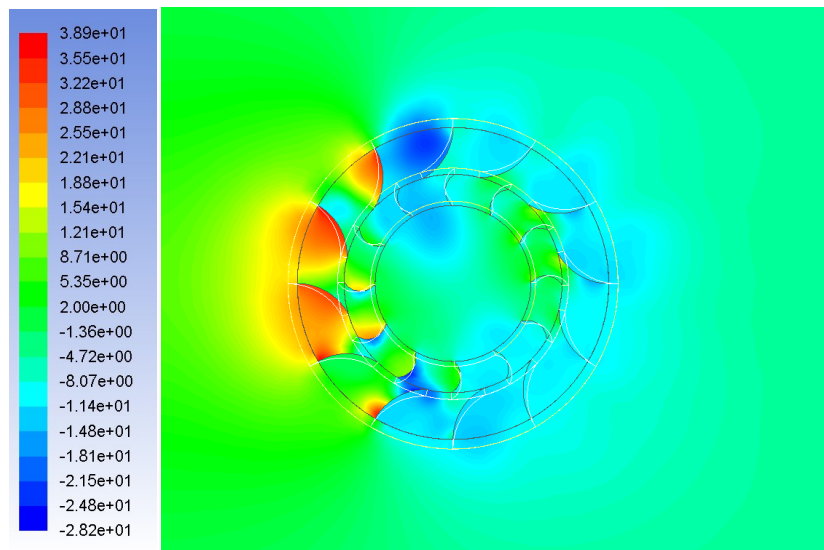
Figure 4.25(a) Pressure variations at 0° angular position of the VAWT having α=11.689°, γ=18.2° and δ=32.357°

Optimal Design of a Micro Vertical Axis Wind Turbine for Sustainable Urban Environment
By Kyooseon Park, School of Computing and Engineering, University of Huddersfield, UK (2013)

79

Further analysing the flow structure in the vicinity of the VAWT, figure 4.25(b) depicts that the flow velocity is considerably high within the passages formed on the windward side due to the orientation of the blades. The velocity goes up to as high as 8.28m/sec where the incident flow velocity is 4m/sec. The reduction in the effective flow area, as these passages are formed, increases the flow velocity.
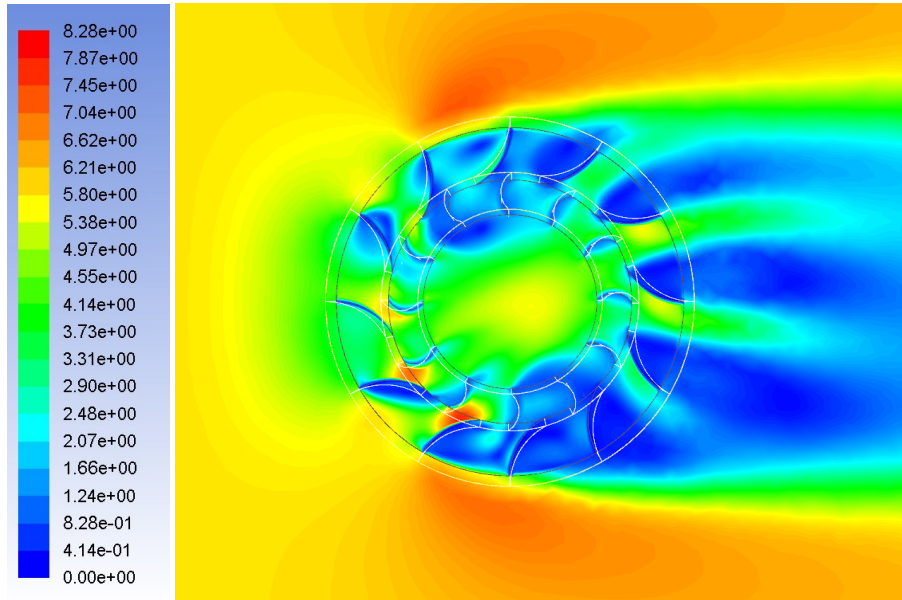
Figure 4.25(b) Velocity variations at 0⁰ angular position of the VAWT having α=11.689⁰, γ=18.2⁰ and δ=32.357⁰

In order to quantify the performance output of the VAWT considered here, the instantaneous torque output for one revolution of the VAWT has been plotted in figure 4.26. It can be seen that the torque output of the VAWT is cyclic with the number of peaks/valleys equal to the number of rotor and stator blades. The maximum torque output observed is 26.3N-m whereas the minimum is 22.5N-m.
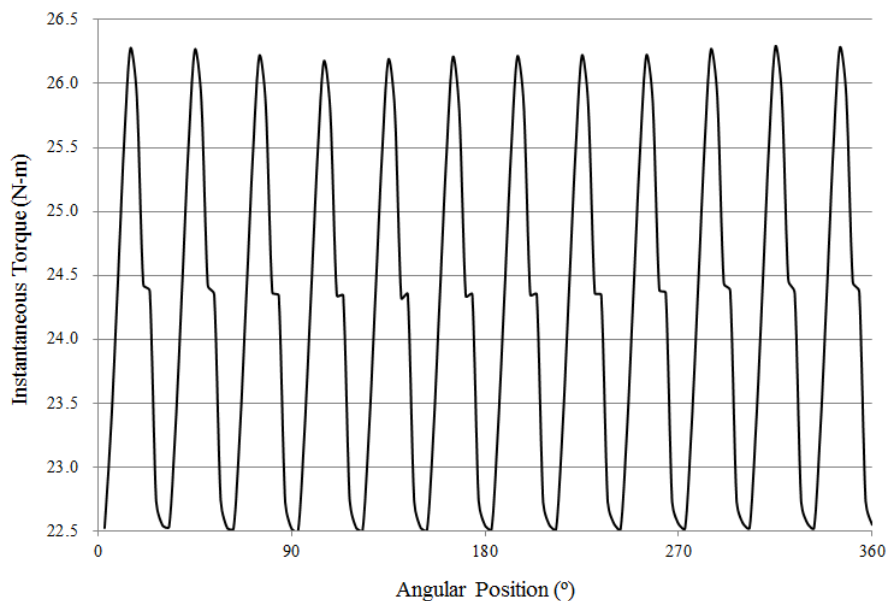
Figure 4.26 Instantaneous torque output of the VAWT having α=11.689⁰, γ=18.2⁰ and δ=32.357⁰

Optimal Design of a Micro Vertical Axis Wind Turbine for Sustainable Urban Environment
By Kyooseon Park, School of Computing and Engineering, University of Huddersfield, UK (2013)

80

Further quantifying the performance output of the aforementioned VAWT, table 4.10 shows the maximum, minimum, average, maximum amplitude and standard deviation in the instantaneous torque output shown in figure 4.26.

Table 4.10 Statistical analysis of the instantaneous torque output of the VAWT having α=11.689⁰, γ=18.2⁰ and δ=32.357⁰

Torque Output	(N-m)
Maximum	26.29
Minimum	22.50
Average	24.17
Max - Min	3.79
Std. Dev.	1.31

Figures 4.27(a & b) depicts the pressure and velocity variations in the vicinity of the VAWT for γ=28.2⁰, keeping δ=32.357⁰ and α=11.689⁰ constant. In comparison with figure 4.25(a), it can be seen that the pressure on the windward side of the VAWT is considerably lower and on the leeward side is appreciably higher than observed in case of γ=18.2⁰. This suggests that the average torque output from this VAWT model will be lower than for γ=18.2⁰
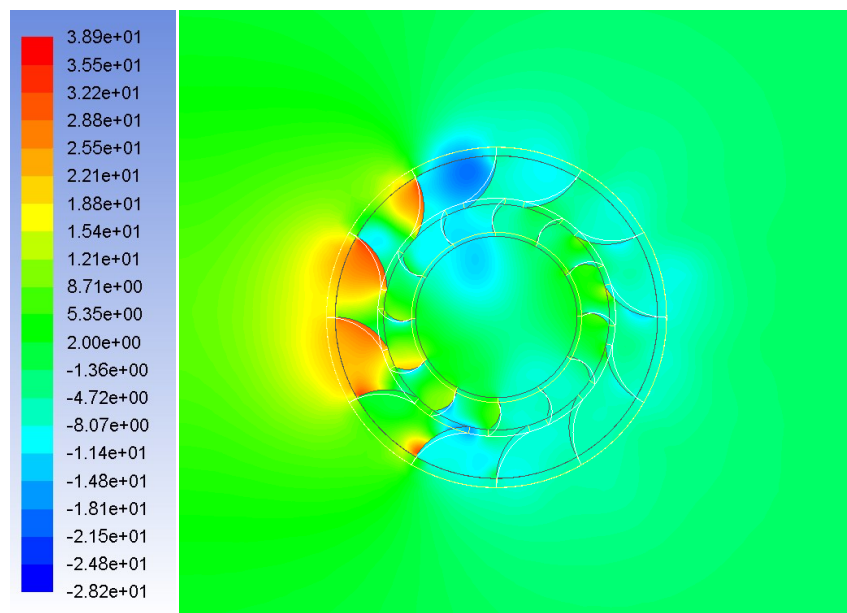
Figure 4.27(a) Pressure variations at 0⁰ angular position of the VAWT having α=11.689⁰, γ=28.2⁰ and δ=32.357⁰

Figure 4.27(b) depicts the flow velocity variations in the vicinity of the VAWT. In comparison with figure 4.25(b), it can be seen that the flow velocity is considerably lower in the flow passages on the windward side whereas the flow velocity is higher in the core region. This trend is consistent with the pressure distribution observed in figure 4.27(a) such that higher pressure corresponds to lower flow velocity and vice versa.

Optimal Design of a Micro Vertical Axis Wind Turbine for Sustainable Urban Environment
By Kyooseon Park, School of Computing and Engineering, University of Huddersfield, UK (2013)

81
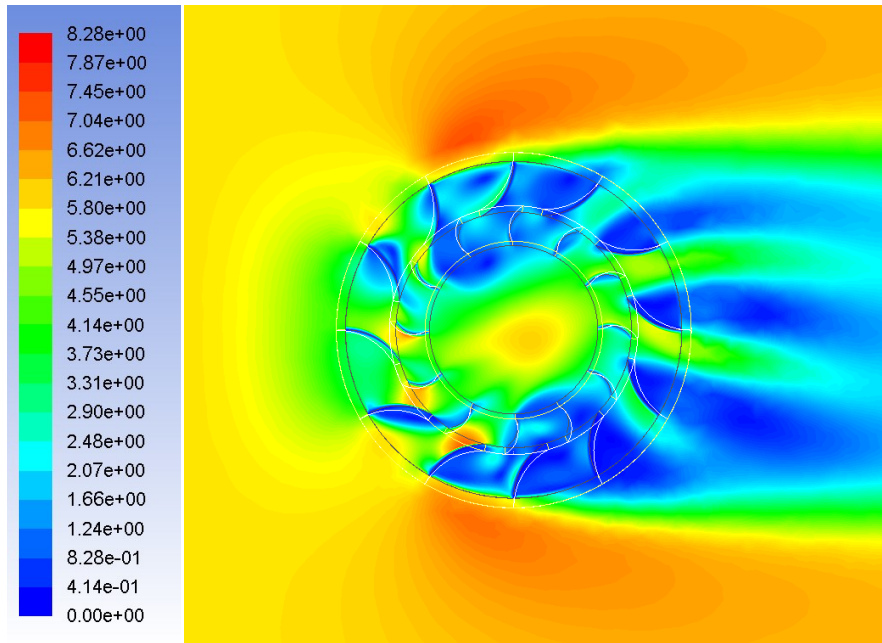
Figure 4.27(b) Velocity variations at 0⁰ angular position of the VAWT having α=11.689⁰, γ=28.2⁰ and δ=32.357⁰

The instantaneous torque output for one revolution of the VAWT has been plotted in figure 4.28. In comparison with figure 4.26, it can be clearly seen that there exists smaller peaks on each cycle and their amplitude decreases as the angular position of the VAWT increases. The presence of these additional peaks suggest that the standard deviation would be higher for γ=28.2⁰ as compared to γ=18.2⁰.
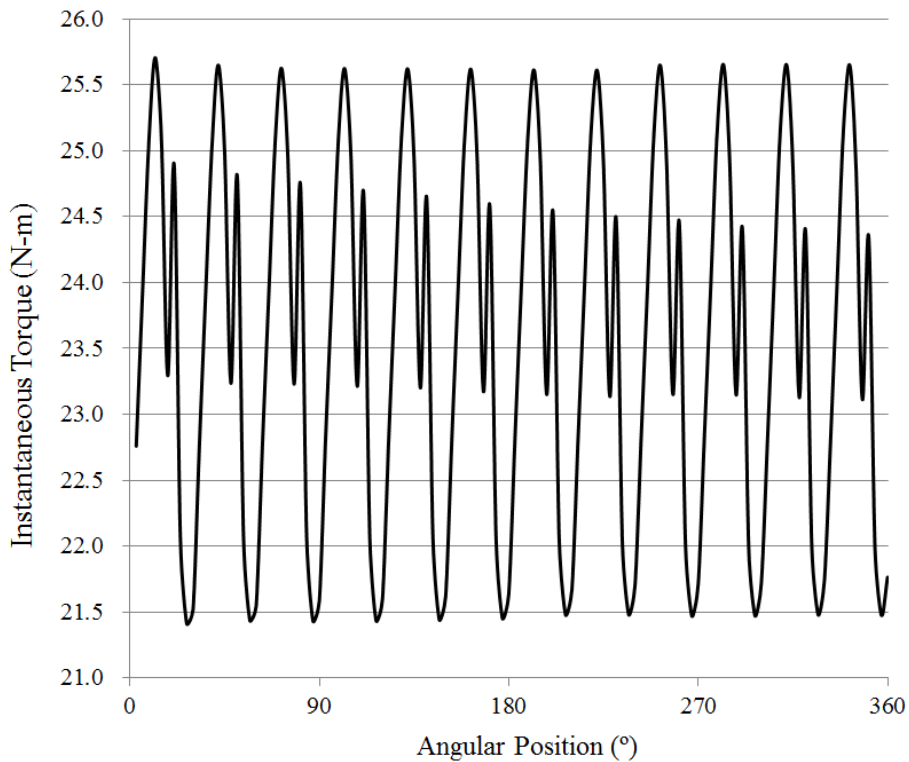
Figure 4.28 Instantaneous torque output of the VAWT having α=11.689⁰, γ=28.2⁰ and δ=32.357⁰

Optimal Design of a Micro Vertical Axis Wind Turbine for Sustainable Urban Environment
By Kyooseon Park, School of Computing and Engineering, University of Huddersfield, UK (2013)

82

Table 4.11 provides the statistical analysis of the torque output from the aforementioned VAWT. It is can be seen clearly that the average torque output for γ=28.2⁰ is lower than for γ=18.2⁰ (by 2.6%). Analyzing the standard deviations from both the models, it can be seen that the standard deviation is higher in case of γ=28.2⁰ as compared to γ=18.2⁰ as mentioned earlier.

Table 4.11 Statistical analysis of the instantaneous torque output of the VAWT having α=11.689⁰, γ=28.2⁰ and δ=32.357⁰

Torque Output	(N-m)
Maximum	25.71
Minimum	21.41
Average	23.53
Max - Min	4.29
Std. Dev.	1.45

Figures 4.29(a & b) depicts the pressure and velocity variations in the vicinity of the VAWT for γ=38.2⁰, keeping δ=32.357⁰ and α=11.689⁰ constant. In comparison with figure 4.27(a), it can be seen that the pressure on the windward side is slightly lower. This suggests that the average torque output from this VAWT model will be lower than for γ=28.2⁰
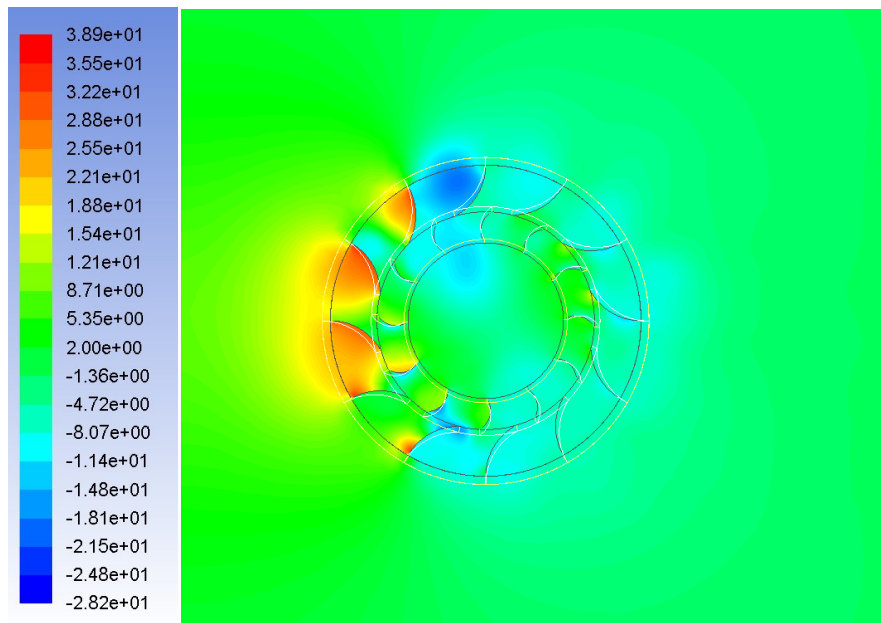
Figure 4.29(a) Pressure variations at 0⁰ angular position of the VAWT having α=11.689⁰, γ=38.2⁰ and δ=32.357⁰

Figure 4.29(b) depicts the flow velocity variations in the vicinity of the VAWT. In comparison with figure 4.27(b), it can be seen that the flow velocity is marginally higher in the flow passages on the windward side whereas it is slightly lower in the core region. This trend is consistent with the pressure distribution observed in figure 4.29(a) such that higher pressure corresponds to lower flow velocity and vice versa.

Optimal Design of a Micro Vertical Axis Wind Turbine for Sustainable Urban Environment
By Kyooseon Park, School of Computing and Engineering, University of Huddersfield, UK (2013)

83
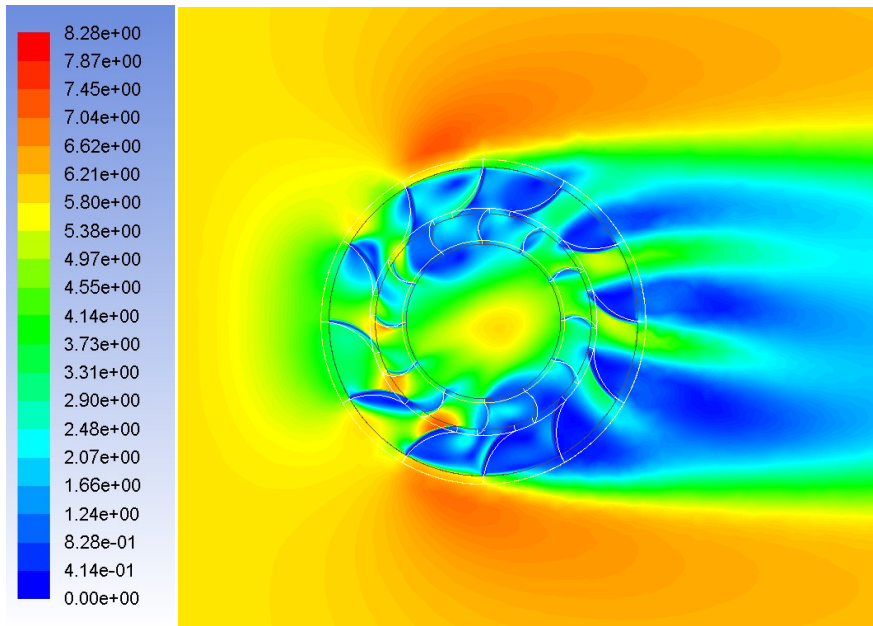
Figure 4.29(b) Velocity variations at 0⁰ angular position of the VAWT having α=11.689⁰, γ=38.2⁰ and δ=32.357⁰

The instantaneous torque output for one revolution of the VAWT has been plotted in figure 4.30. In comparison with figure 4.28, it can be seen that the torque output has shifted slightly to the lower side as the minimum torque output is 21N-m for γ=38.2⁰ as compared to 21.5N-m for γ=28.2⁰. Furthermore, it can be seen that the amplitude of the smaller peaks is considerably smaller, hence, it can be expected that the standard deviation would be lower for γ=38.2⁰ as compared to γ=28.2⁰.
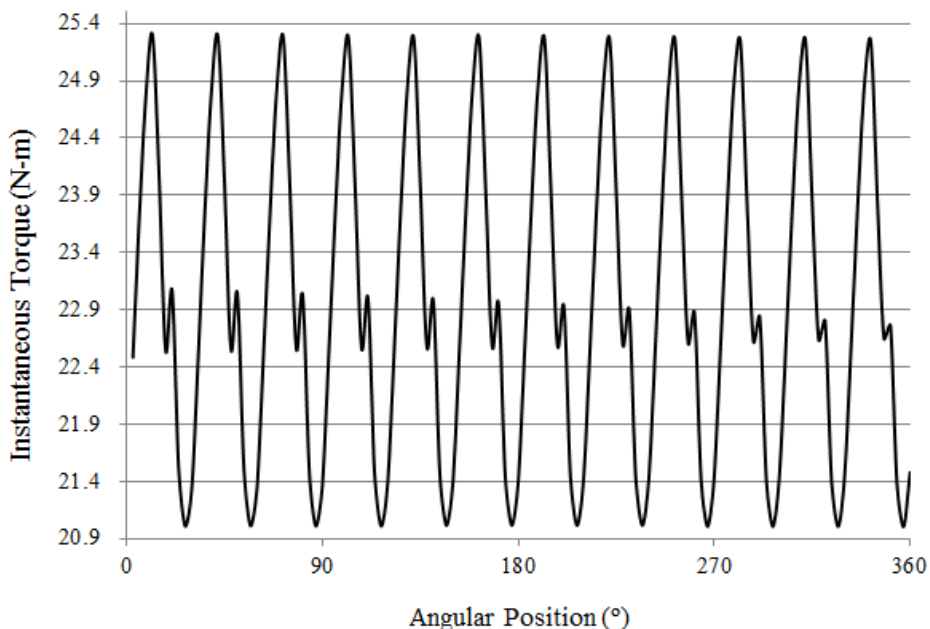
Figure 4.30 Instantaneous torque output of the VAWT having α=11.689⁰, γ=38.2⁰ and δ=32.357⁰

Table 4.12 provides the statistical analysis of the torque output from the aforementioned VAWT. It is can be seen clearly that the average torque output for γ=38.2⁰ is lower than for γ=28.2⁰ (by 2.3%). Analyzing the standard deviations from both the models, it can be seen that the standard deviation is higher in case of γ=38.2⁰ as compared to γ=28.2⁰ as mentioned earlier.

Optimal Design of a Micro Vertical Axis Wind Turbine for Sustainable Urban Environment
By Kyooseon Park, School of Computing and Engineering, University of Huddersfield, UK (2013)

84

Table 4.12 Statistical analysis of the instantaneous torque output for α=11.689⁰, γ=38.2⁰ and δ=32.357⁰ of the VAWT

Torque Output	(N-m)
Maximum	25.30
Minimum	21.00
Average	22.98
Max - Min	4.29
Std. Dev.	1.39

Figure 4.31 depicts the instantaneous torque outputs of the aforementioned cases on a single scale for comparison purposes. It is evident that for γ=18.2⁰, the torque output is considerably higher than for the other two models. Hence, it can be concluded that as γ increases, the torque output of the VAWT decreases. This trend is the same as observed for δ, where the torque output decreases as δ increases.
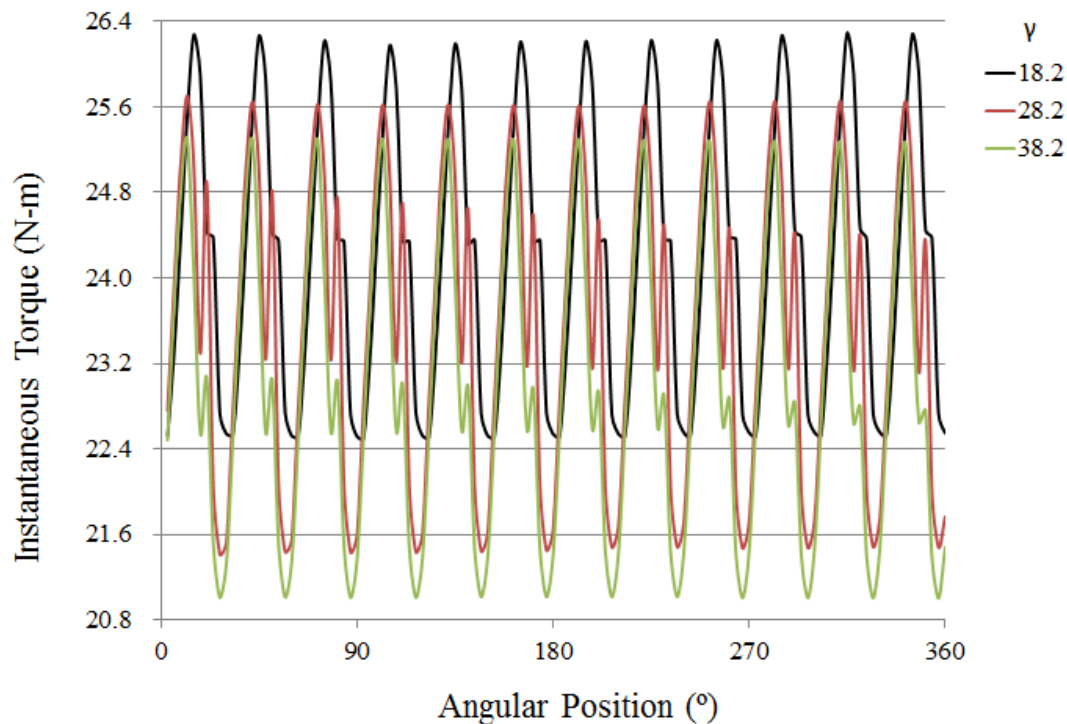
Figure 4.31 Instantaneous torque outputs of VAWT models having different γ

As mentioned earlier, complete CFD results have been presented in Appendix 1. Figure 4.32 depicts some of these results where the effect of γ can be clearly visualised. It can be seen that for a given α and δ, as γ increases, the average torque output and the average power output of the VAWT decreases. Hence, lower γ means more torque and power outputs from the VAWT. Furthermore, it can be seen that there are non-linearities in the curves that arises due to complex and transient interactions between the blades.

Optimal Design of a Micro Vertical Axis Wind Turbine for Sustainable Urban Environment
By Kyooseon Park, School of Computing and Engineering, University of Huddersfield, UK (2013)

85
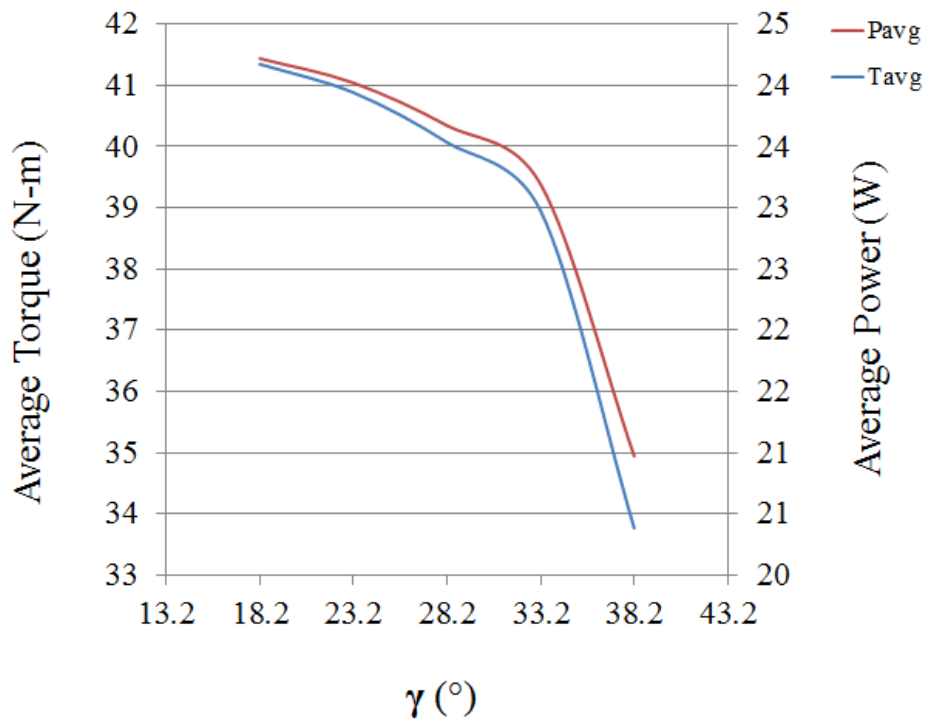
Figure 4.32 Effect of γ on the performance output of VAWT

4.7. Optimal VAWT Design

After carrying out detailed analysis on the performance output of various VAWT configurations, it has been shown that the optimal VAWT design, based on blade angles considered in the present study, is the one with α=16.689°, γ=18.2° and δ=22.357°. Figure 4.33(a & b) depict the pressure and velocity variations in the vicinity of the optimal VAWT design.
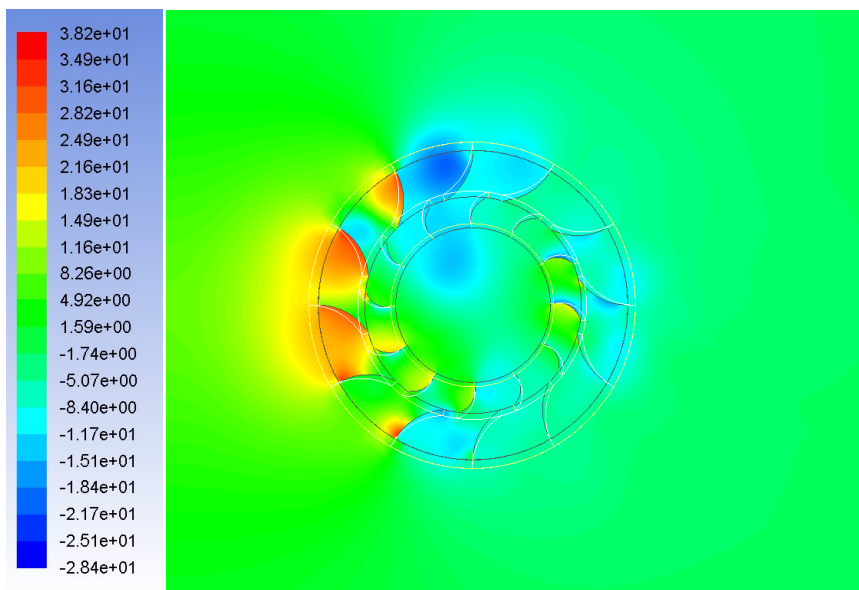
Figure 4.33(a) Pressure variations at 0° angular position of the VAWT having α=16.689°, γ=18.2° and δ=22.357°

Optimal Design of a Micro Vertical Axis Wind Turbine for Sustainable Urban Environment
By Kyooseon Park, School of Computing and Engineering, University of Huddersfield, UK (2013)

86
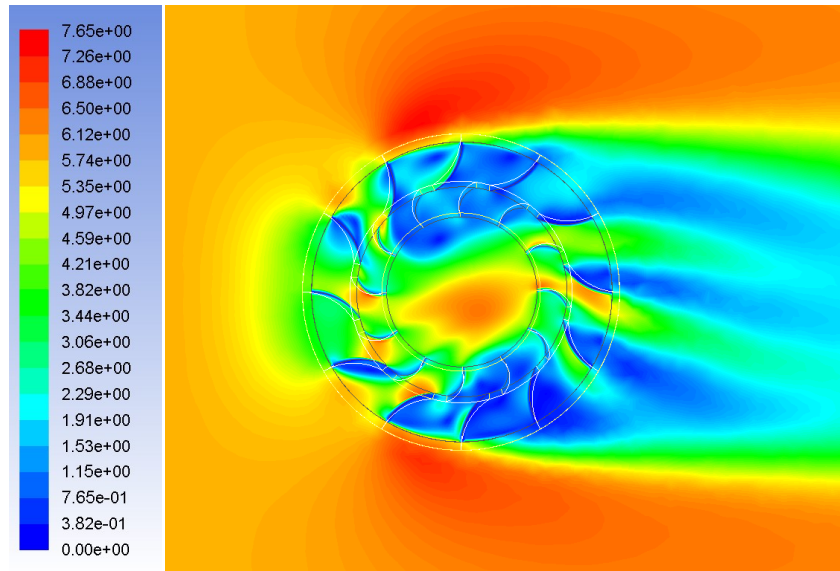
Figure 4.33(b) Velocity variations at 0⁰ angular position of the VAWT having α=16.689⁰, γ=18.2⁰ and δ=22.357⁰

Figure 4.33 depicts the instantaneous torque output for the optimised VAWT design. It can be seen that in between two consecutive peaks, there exists additional smaller peaks that are generated due to the formation of uniform passages between the rotor and the stator blades. High amplitude of these additional peaks leads to increased torque output from the VAWT.
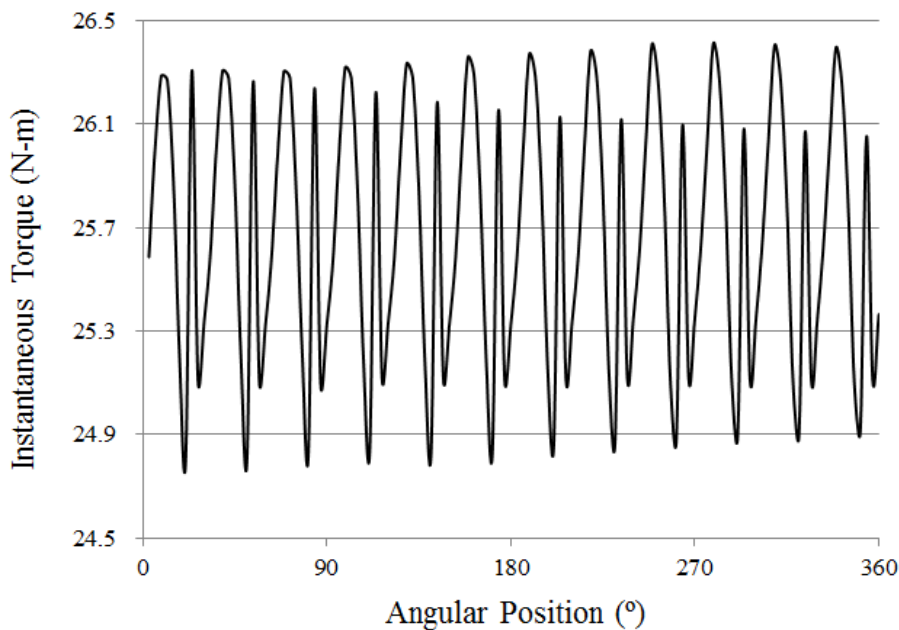
Figure 4.34 Instantaneous torque output of the VAWT having α=16.689⁰, γ=18.2⁰ and δ=22.357⁰

Table 4.13 summarises the statistical results for the optimised VAWT design. It can be observed that the standard deviation in the torque output is considerably low, This is because the maximum amplitude is quite small although the maximum torque output is very high. This means that the variations in the torque output in various cycles is appreciably lower as compared to many cases

Optimal Design of a Micro Vertical Axis Wind Turbine for Sustainable Urban Environment
By Kyooseon Park, School of Computing and Engineering, University of Huddersfield, UK (2013)

87

discussed in the previous sections. Hence, the optimised VAWT design presented here is being used to carry out various analyses in the next chapter.

Table 4.13 Statistical analysis of the instantaneous torque output of the VAWT having α=16.689⁰, γ=18.2⁰ and δ=22.357⁰

Torque Output	(N-m)
Maximum	26.41
Minimum	24.80
Average	25.67
Max - Min	1.61
Std. Dev.	0.51

4.8. Expression for C_T based on Blade Angles

A detailed investigation into the effect of the blade angles on the performance output of a VAWT has been carried out in the previous sections, where the range of blade angles is limited for practical purposes. The trends show that increase in α improves the performance of a VAWT whereas increase in δ and γ degrades the torque output of the VAWT. In order to quantify these results such that they can be used in the design process of a VAWT, multiple regression analysis has been carried out on the results obtained from CFD simulations. The need to modify the design process of the VAWT is that the design process presented in Chapter 1 is based on ideal flow theory. However, the CFD predicted results are real flow results and hence the ideal flow theory cannot be applied to these results.

The three variables included in the study are the angles (α, δ and γ) whereas the output parameter has been chosen to be non-dimensional torque output of the VAWT. This non-dimensional torque is commonly known as Coefficient of Torque and can be represented by:

$$C_T = \frac{T}{0.5\,\rho\,A\,r_r\,v^2}$$

(4.4)

Where T is the torque output of the VAWT, ρ is the density of air, A is the frontal area of the VAWT, r_r is the radius of the rotor blades and v is the incident flow velocity. Once torque output of the VAWT is known, coefficient of torque could be found out using equation (4.1). Re-arranging the above equation gives:

$$T = 0.5\,\rho\,A\,r_r\,v^2 C_T$$

(4.5)

In equation (4.4), C_T can be represented in terms of the blade angles of the VAWT that results in a particular torque output. This means that if C_T can be replaced with an equation representing blade angles of the VAWT in non-dimensional terms. Than for a required torque output of the VAWT, the blade angles can be calculated and vice versa. Author is not aware of any published literature in which such an expression has been developed for the design process.

$$C_T = f(\alpha, \delta, \gamma)$$

(4.6)

Optimal Design of a Micro Vertical Axis Wind Turbine for Sustainable Urban Environment
By Kyooseon Park, School of Computing and Engineering, University of Huddersfield, UK (2013)

88

After performing multiple regression analysis on the results obtained from CFD simulations (presented in Appendix 1), the following equation for the torque coefficient has been developed:

$$C_T = \frac{1.178 \frac{\alpha^{0.00184}}{\beta}}{\frac{\delta^{0.2123}}{\beta} \frac{\gamma^{0.1135}}{\beta}} \tag{4.7}$$

Where β is the Stator inlet angle and has a constant value of 90° as mentioned in Chapter 3. In order to check the validity of equation (4.7), the CFD results for C_T have been compared with C_T calculated from equation (4.7). It has been shown in figure 4.35 that more than 90% of the data lies within ±5% error band. The errors are due to the numerical diffusion within the solver and interaction between the rotor and stator blades.
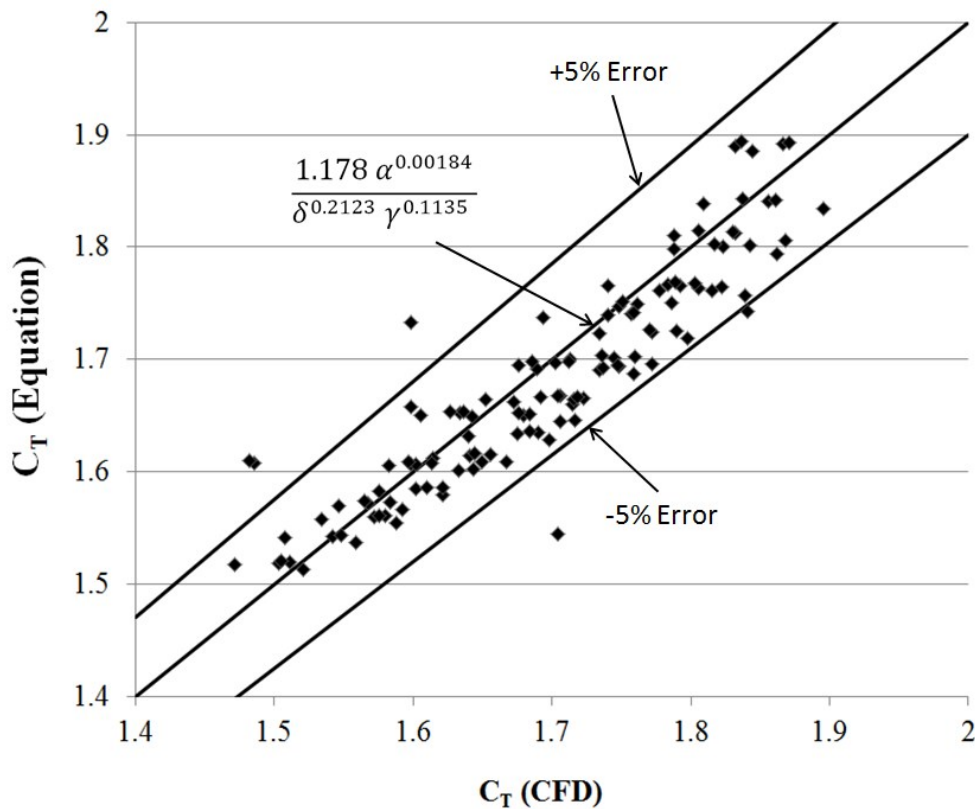
Figure 4.35 Validation of the equation (4.7)

The equation to calculate torque output of the VAWT will then be:

$$T = 0.589 \, \rho \, A \, r_r \, v^2 \left(\frac{\frac{\alpha^{0.00184}}{\beta}}{\frac{\delta^{0.2123}}{\beta} \frac{\gamma^{0.1135}}{\beta}} \right) \tag{4.8}$$

It should be noted down that equation (4.8) is only valid for the range of angles that has been considered in the present study.

Optimal Design of a Micro Vertical Axis Wind Turbine for Sustainable Urban Environment
By Kyooseon Park, School of Computing and Engineering, University of Huddersfield, UK (2013)

89

4.8.1. Validation of Equation 4.8

Calculate the blade angles of a Vertical Axis Wind Turbine using the following data:

A	2m^2	v	4m/sec	T	24N-m
r_r	0.7m				

Solution: Using equation (4.8):

$$24 = 0.589 * 1.225 * 2 * 0.7 * 16 * \left(\frac{\left(\frac{\alpha}{90}\right)^{0.00184}}{\left(\frac{\delta}{90}\right)^{0.2123} \left(\frac{\gamma}{90}\right)^{0.1135}} \right)$$

Taking the optimum value of α i.e. 16.689°, the remaining blade angles are computed to be:

$$\delta = 32.357^0 \quad and \quad \gamma = 18.2^0$$

4.9. Summary

A detailed investigation into the effect of the blade angles on the performance output of the vertical axis wind turbine has revealed the following results:

- The pressure and the velocity fields in the vicinity of the VAWT are highly unsymmetrical and non-uniform

- The instantaneous torque output of the VAWT consists of peaks and valleys equal to the number of blades of the VAWT

- Increase in α increases the performance output of the VAWT upto a certain value after which the torque output starts decreasing with increasing α

- Increase in δ decreases the performance output of the VAWT

- Increase in δ decreases the performance output of the VAWT

- The optimal VAWT design consists of α=16.689°, γ=18.2° and δ=22.357°

Furthermore, a novel semi-empirical correlation for C_T has been developed for various blade angles in this chapter.

Optimal Design of a Micro Vertical Axis Wind Turbine for Sustainable Urban Environment
By Kyooseon Park, School of Computing and Engineering, University of Huddersfield, UK (2013)

90

CHAPTER 5
OPTIMISATION OF VERTICAL AXIS WIND TURBINES BASED ON GEOMETRICAL FEATURES

Optimisation of the optimised vertical axis wind turbine, based on the results of Chapter 4, has been presented in this chapter. The effect of the number of blades, the size of rotor/stator regions and the height of the VAWT, on the performance output of the VAWT has been investigated in detail because these geometric features affect the start-up and shutdown of VAWTs. Both local and global parameters have been considered while describing these effects. It has been shown that these geometric parameters considerably affect the performance of a VAWT. Semi-empirical correlations for torque coefficient have been developed to take into account these effects. Furthermore, a novel torque prediction model has been developed that considers all the variables taken in both Chapter 4 and 5. This prediction model has been shown to be reasonably accurate in predicting torque output of a VAWT.

Optimal Design of a Micro Vertical Axis Wind Turbine for Sustainable Urban Environment
By Kyooseon Park, School of Computing and Engineering, University of Huddersfield, UK (2013)

91

5.1. Effect of Number of Rotor Blades

In the previous chapter, the design of a vertical axis wind turbine has been optimised on the basis of the blade angles. It has been shown that for blade angles of α=16.689⁰, γ=18.2⁰ and δ=22.357⁰, the torque and power outputs of VAWT are at their maximum. Hence, this design of the VAWT has been used in the present chapter to be optimised based on the number and size of both the rotor and the stator blades. This information will help the manufacturers to design VAWTs with maximum performance output.

In order to analyse the effect of the number of rotor blades on the performance output of a vertical axis wind turbine, three VAWT configurations have been chosen for analysis that constitute of 4, 8 and 12 rotor blades respectively while the number of stator blades have been fixed to be 12. Figure 5.1(a & b) depicts the pressure and velocity variations in the vicinity of the VAWT having 4 rotor blades. It can be seen in figure 5.1(a) that the windward side of the VAWT possess high pressure while the leeward side has lower pressure. Furthermore, it can be seen in figure 5.1(b) that the flow velocity is high on the windward side and the core region, while it is comparatively lower on the leeward side of the VAWT. It has also been observed, as previously, that the flow accelerates in the passages formed between the rotor and the stator blades on the windward side of the VAWT. These passages are formed due to the orientation and the angular position of the rotor blades.
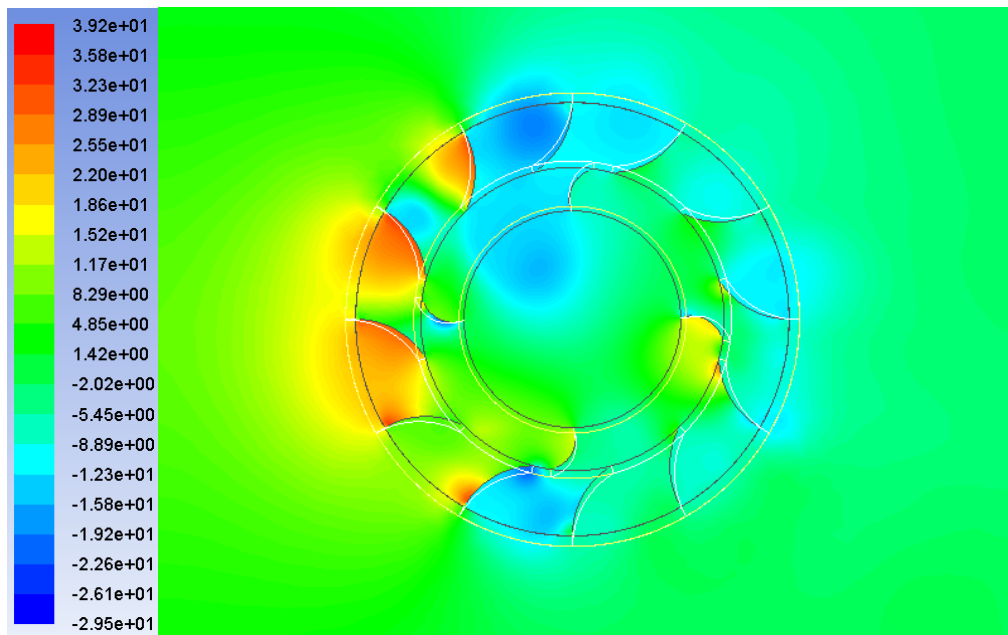
Figure 5.1(a) Pressure variations at 0⁰ angular position of the VAWT having 4 rotor blades

Further analysing figure 5.1(b) depicts that as there are less number of rotor blades than the number of stator blades, there are more large passages available for the incident flow to pass through at the windward side. Hence, the flow velocity is lower in those passages which are large, whereas the flow velocity is higher in the passages that are smaller (for the rotor blade present on the windward side).

Optimal Design of a Micro Vertical Axis Wind Turbine for Sustainable Urban Environment
By Kyooseon Park, School of Computing and Engineering, University of Huddersfield, UK (2013)

92
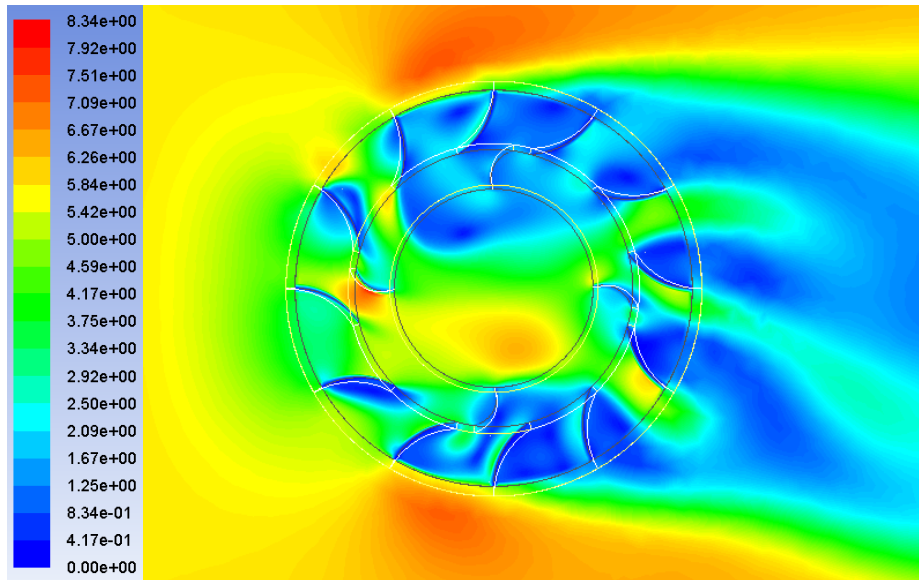
Figure 5.1(b) Velocity variations at 0° angular position of the VAWT having 4 rotor blades

Figure 5.2 depicts the instantaneous torque output of the VAWT having 4 rotor blades. It can be seen that the torque signals are cyclic and possesses 8 peaks, where 4 peaks are higher peaks and 4 are lower peaks. Higher peaks correspond to the orientation of the VAWT when a rotor blade is on the windward side of the VAWT (as shown in figure 5.1). The lower peaks correspond to that angular position of the VAWT when there is a large passage available for the incident flow on the windward side i.e. the rotor blades are at 75° angular position.
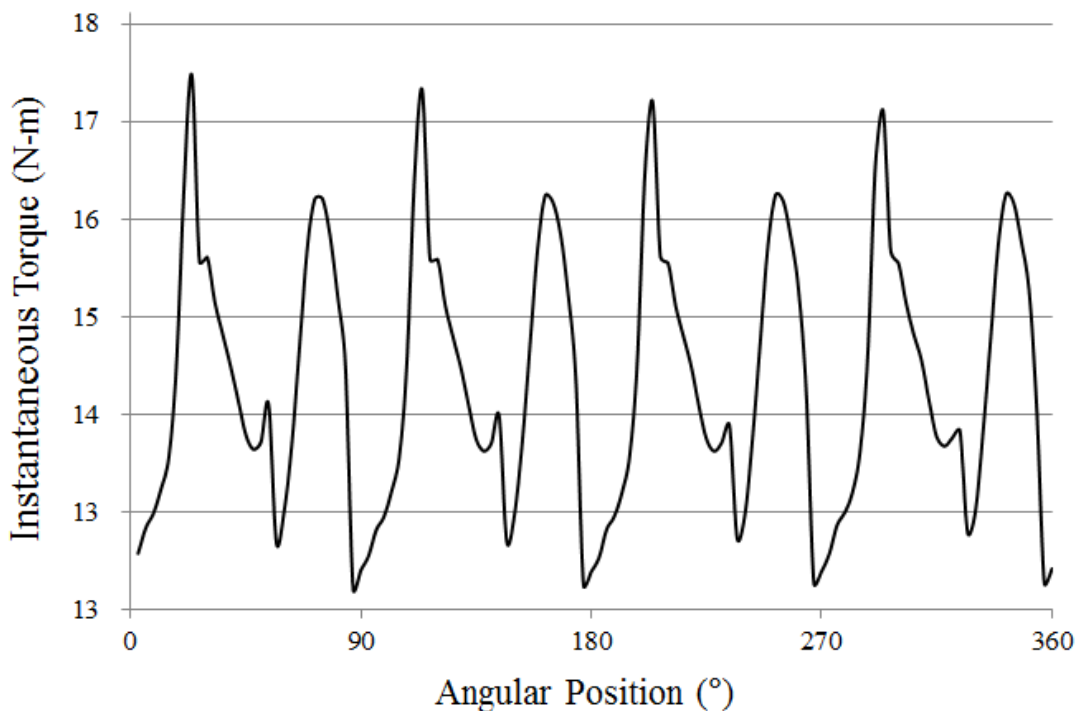
Figure 5.2 Instantaneous torque output of the VAWT having 4 rotor blades

5.3(a & b) depicts the pressure and velocity variations in the vicinity of the VAWT having 8 rotor blades. In comparison with figure 5.1(a), it can be seen in figure 5.3(a) that due to additional rotor blades, the pressure on the windward side of the VAWT has increased considerably. This happens because there is more resistance offered by the VAWT to the incident flow of air and hence more kinetic energy of the wind can be converted into the mechanical energy by the VAWT.
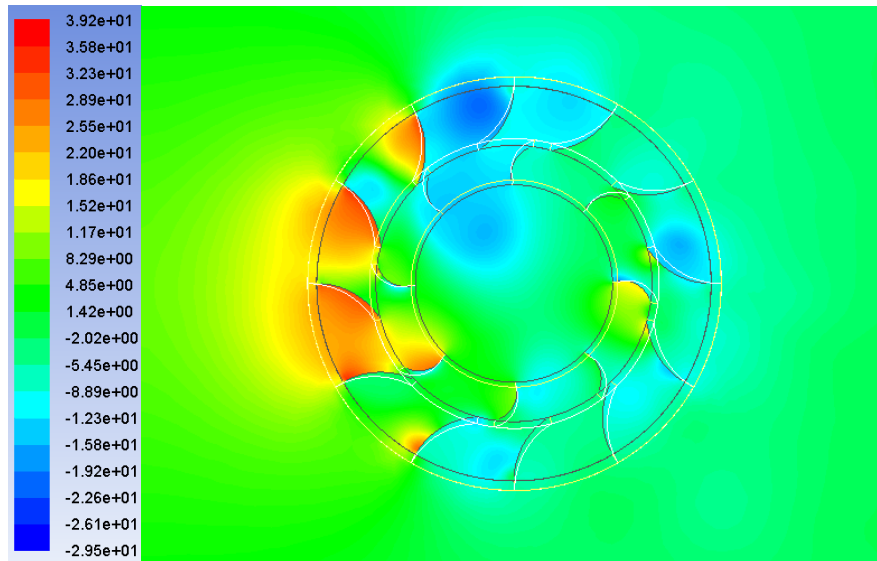
Figure 5.3(a) Pressure variations at 0° angular position of the VAWT having 8 rotor blades

Analysing the velocity variations in the vicinity of the VAWT having 8 rotor blades (figure 5.3(b)), it can be seen, in comparison with figure 5.1(b), that the flow velocity is appreciably lower on the windward side of the VAWT. It has been observed that due to higher number of rotor blades, there is less number of passages available for the flow to pass through the VAWT at the leeward sections. This suggests that the torque output of the VAWT will be considerably higher for 8 rotor blades as compared to 4 rotor blades.
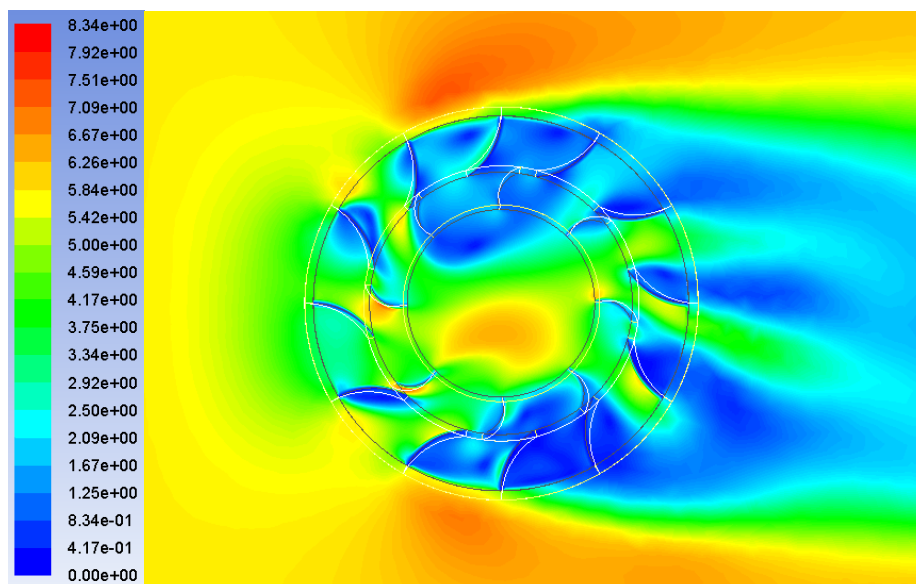
Figure 5.3(b) Velocity variations at 0° angular position of the VAWT having 8 rotor blades

Figure 5.4 depicts the instantaneous torque output of the VAWT having 8 rotor blades. As expected, in comparison with figure 5.2, it can be seen that the torque output has increased considerably. Furthermore, it can also be seen that there are 8 distinct peaks and valleys in the cyclic torque signals. As observed previously, the torque output suggests that the standard deviation in the torque output of the VAWT having 8 rotor blades will be higher than for 4 rotor blades.
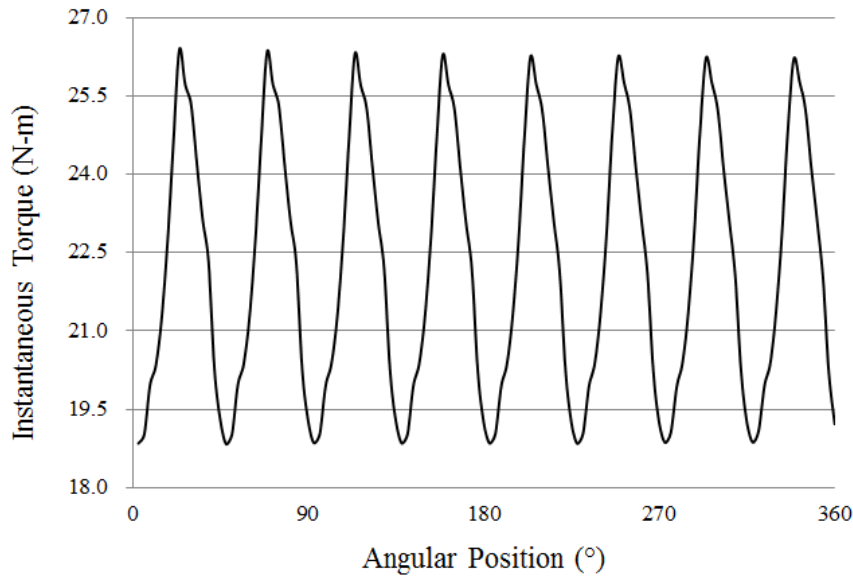
Figure 5.4 Instantaneous torque output of the VAWT having 8 rotor blades

5.5(a & b) depicts the pressure and velocity variations in the vicinity of the VAWT having 12 rotor blades. In comparison with figure 5.3(a), it can be seen in figure 5.5(a), due to additional rotor blades, the pressure on the leeward side of the VAWT is considerably lower. Furthermore, the pressure in the upper and the lower sections of the VAWT are higher than observed in case of 8 rotor blades. This means that the variations in the torque output of the VAWT will be significantly lower than for 8 rotor blades.
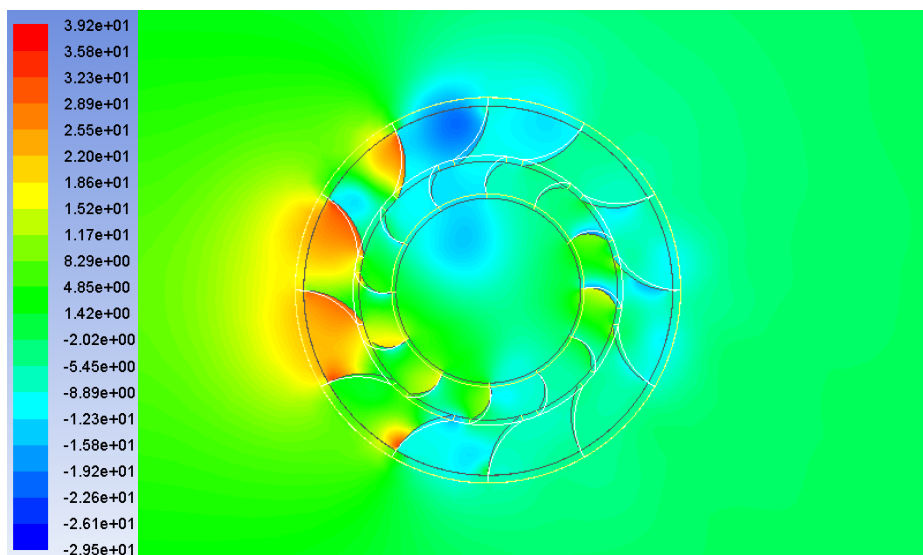
Figure 5.5(a) Pressure variations at 0° angular position of the VAWT having 12 rotor blades

Analysing the velocity variations in the vicinity of the VAWT having 12 rotor blades (figure 5.5(b)), it can be seen, in comparison with figure 5.3(b), that the flow velocity is considerably higher on the

windward side and the core region of the VAWT. Furthermore, the flow velocity on the upper and lower sections of the VAWT is slightly higher than for 8 rotor blades.
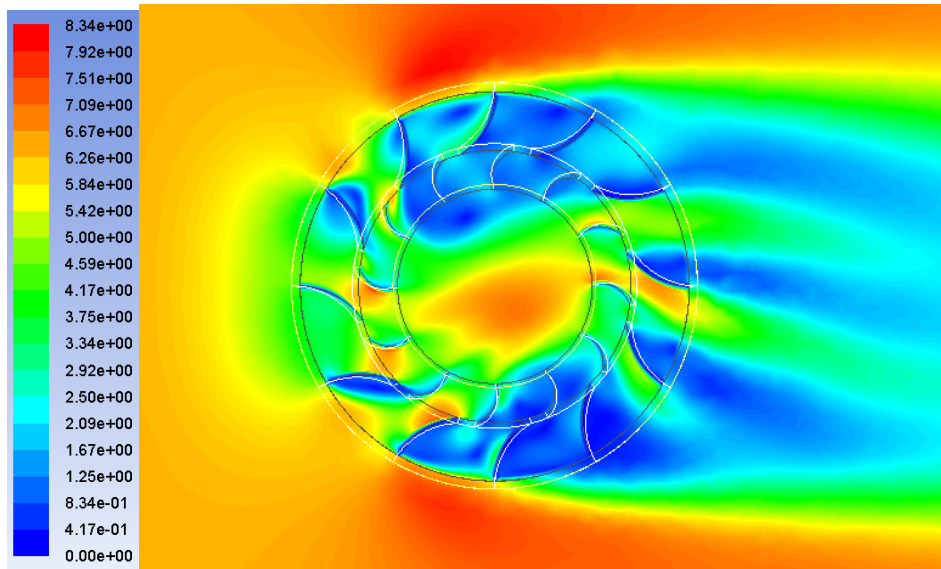
Figure 5.5(b) Velocity variations at 0⁰ angular position of the VAWT having 12 rotor blades

Figure 5.6 depicts the instantaneous torque output of the VAWT having 12 rotor blades. It can be seen that there are additional lower peaks, together with the expected 12 higher peaks corresponding to 12 rotor blades. The presence of these lower peaks suggests that the standard deviation of the torque output will be lower than for both 8 and 4 rotor blades because in 8 rotor blades case there were no lower peaks observed and in case of 4 rotor blades the lower peaks had considerably higher amplitude.
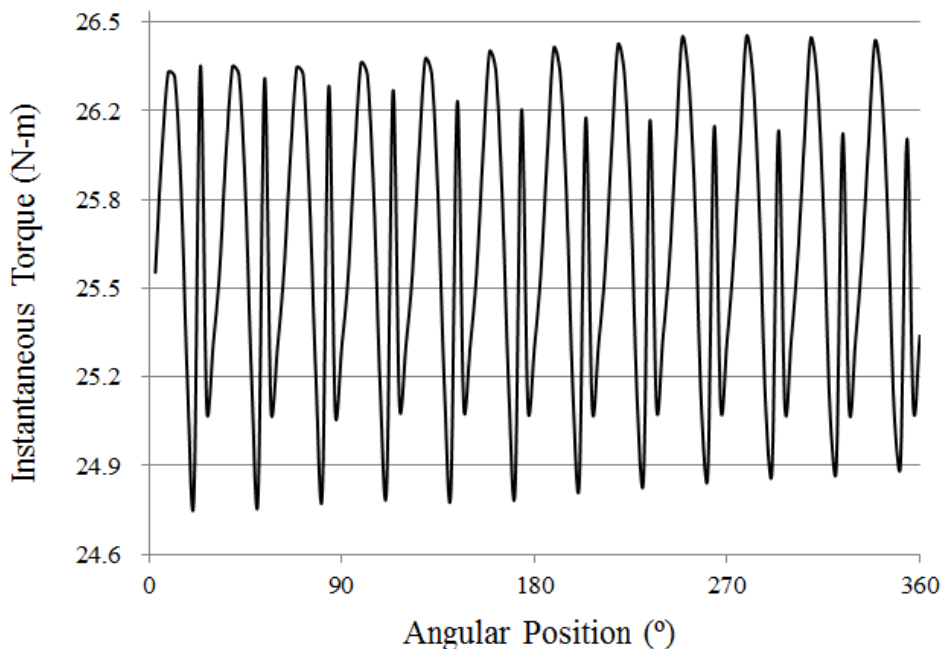
Figure 5.6 Instantaneous torque output of the VAWT having 12 rotor blades

Table 5.1 summarises the statistical results for the torque outputs of the VAWTs having various number of rotor blades. It can be seen that as the number of rotor blades increases, the average

Optimal Design of a Micro Vertical Axis Wind Turbine for Sustainable Urban Environment
By Kyooseon Park, School of Computing and Engineering, University of Huddersfield, UK (2013)

96

torque output (Tavg) also increases. Furthermore, the standard deviation (Std. Dev.) in the torque output is highest for 8 rotor blades and lowest for 12 rotor blades. It is also noteworthy that both the maximum (Tmax) and the minimum (Tmin) torques increase as the number of rotor blades increases.

Table 5.1 Effect of the number of rotor blades on the performance output of the VAWT

Number of Stator Blades	Number of Rotor Blades	Tmin (N-m)	Tmax (N-m)	Tavg (N-m)	Std. Dev.
12	4	12.68	17.43	14.61	1.19
12	8	18.83	26.38	22.22	2.49
12	12	24.80	26.41	25.67	0.51

Figure 5.7 depicts the instantaneous torque outputs of the VAWTs having different number of rotor blades. It can be seen that as the number of rotor blades increase, the torque output increases. Moreover, it has been observed that for 8 rotor blades, the variations in the cyclic torque output are considerably higher than the other two cases.
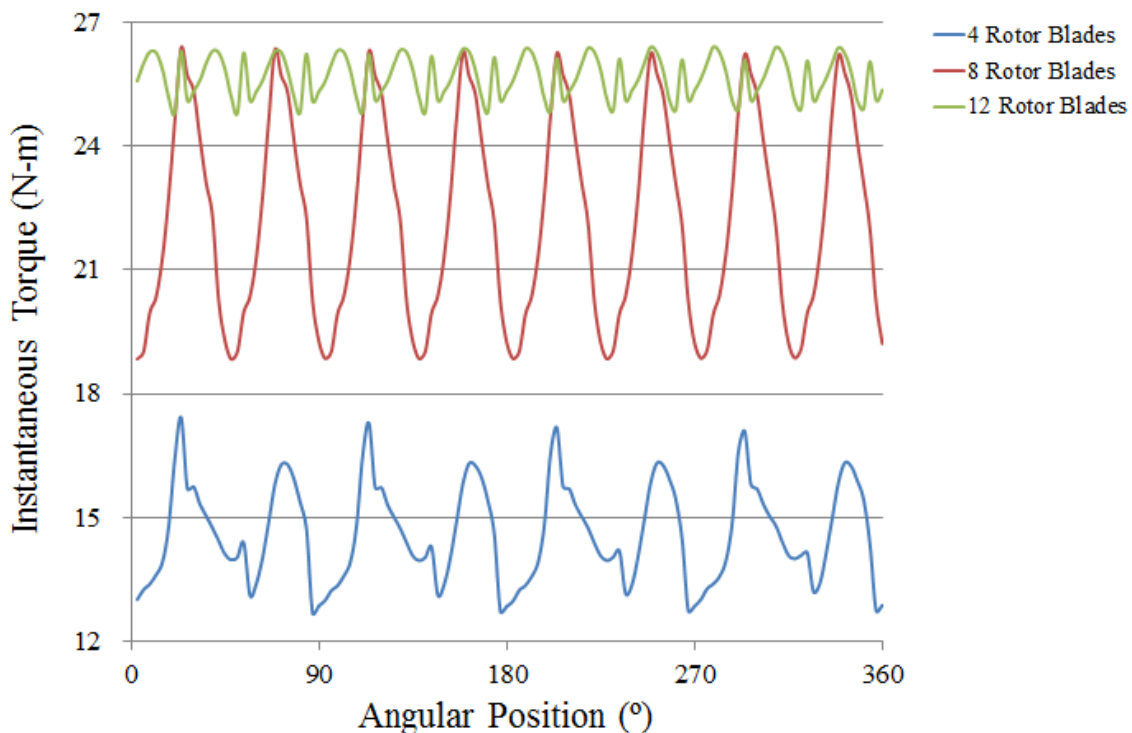
Figure 5.7 Instantaneous torque output of the VAWT having different number of rotor blades

Figure 5.8 depicts the effect of the number of rotor blades on the performance output of the VAWT. It can be seen that as the number of rotor blade increase, both the torque and the power outputs of the VAWT increases. Hence, in the present study, the optimised design of the VAWT is the one that has 12 rotor blades. Furthermore, it can be seen that there are non-linearities in the curves that arises due to complex and transient interactions between the blades.
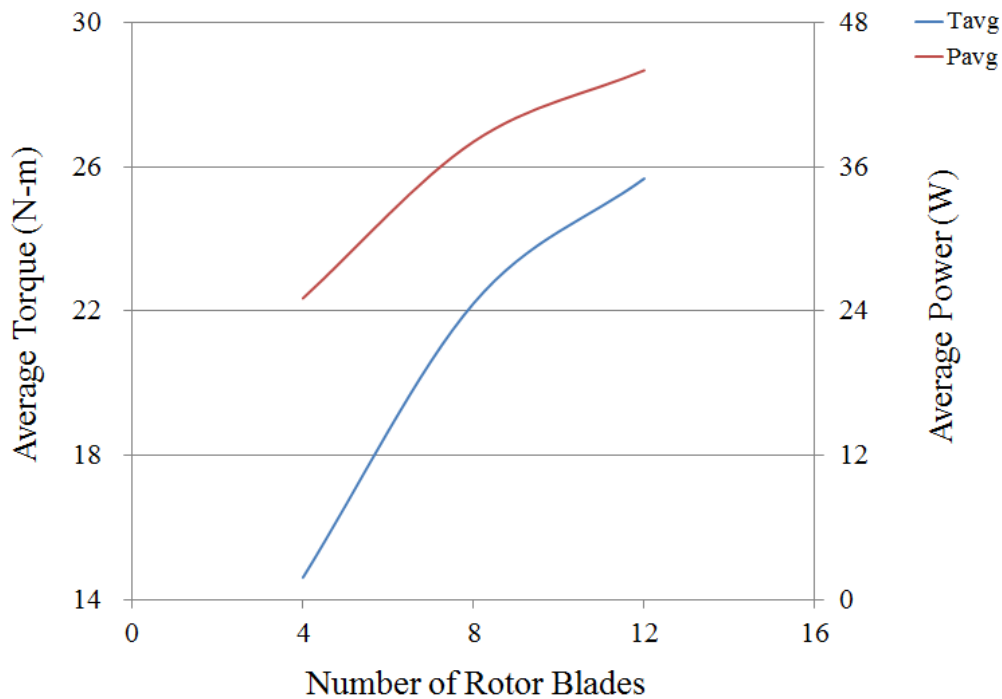
Figure 5.8 Effect of the number of rotor blades on the performance output of the VAWT

5.2. Effect of Number of Stator Blades

In order to analyse the effect of the number of stator blades on the performance output of a vertical axis wind turbine, three VAWT configurations have been chosen for analysis that constitute of 4, 8 and 12 stator blades respectively while the number of rotor blades have been fixed to be 12. Figure 5.9(a & b) depicts the pressure and velocity variations in the vicinity of the VAWT having 4 rotor blades. It can be seen in figure 5.9(a) that the windward side of the VAWT possess very high pressure while the leeward side has comparatively low pressure. Furthermore, it can be seen in figure 5.9(b) that the flow velocity is high on the windward side and the core region, while it is comparatively lower on the leeward side of the VAWT. It has also been observed that the flow accelerates in the passages formed between the rotor and the stator blades on the windward side of the VAWT. These passages are formed due to the orientation and the angular position of the rotor blades. Note that the formation of the flow passage from windward side to the leeward side is slightly inclined towards the upper section of the VAWT while in the previous cases; this inclination has mostly been towards the lower section of the VAWT. This is due to the orientation of the rotor and the stator blades.

Optimal Design of a Micro Vertical Axis Wind Turbine for Sustainable Urban Environment
By Kyooseon Park, School of Computing and Engineering, University of Huddersfield, UK (2013)

98
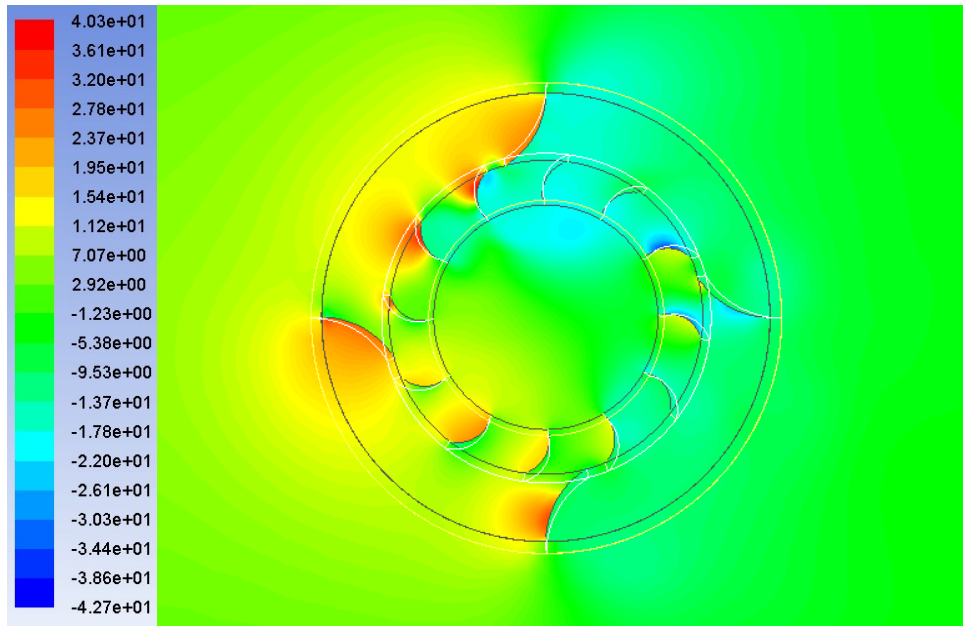
Figure 5.9(a) Pressure variations at 0⁰ angular position of the VAWT having 4 stator blades

Further analysing figure 5.9(b) depicts that as there are less number of rotor blades than the number of stator blades, there are more large passages available for the incident flow to pass through at the windward side.
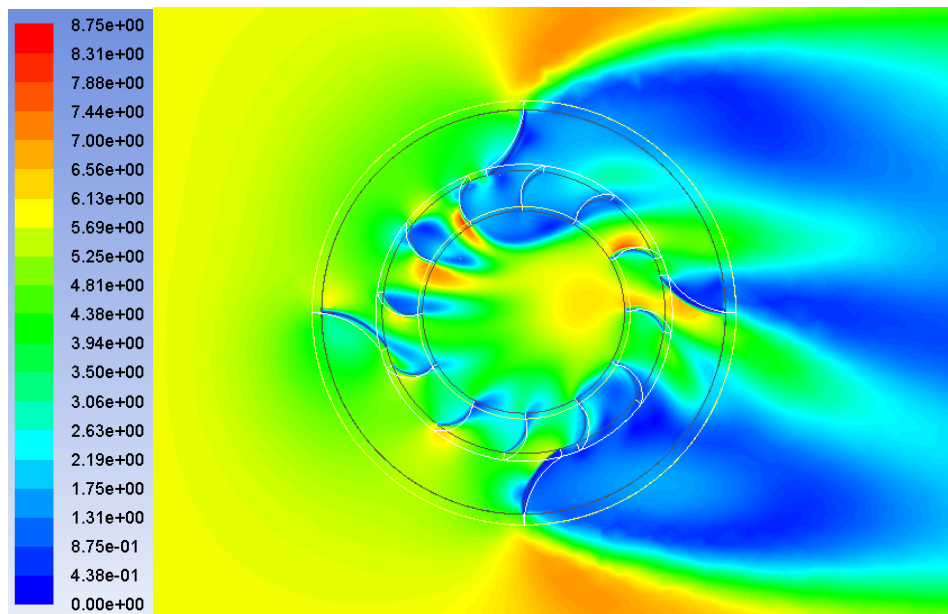
Figure 5.9(b) Velocity variations at 0⁰ angular position of the VAWT having 4 stator blades

Figure 5.10 depicts the instantaneous torque output of the VAWT having 4 stator blades. It can be seen that the torque signals are cyclic and possesses 24 peaks, where 12 peaks are higher peaks and 12 are lower peaks. Higher peaks correspond to the orientation of the VAWT when a stator blade is in-line with one of the rotor blades. The lower peaks correspond to that angular position of the VAWT when a stator blade is exactly in between two rotor blades, hence forming uniform passages for flow to take place.

Optimal Design of a Micro Vertical Axis Wind Turbine for Sustainable Urban Environment
By Kyooseon Park, School of Computing and Engineering, University of Huddersfield, UK (2013)

99
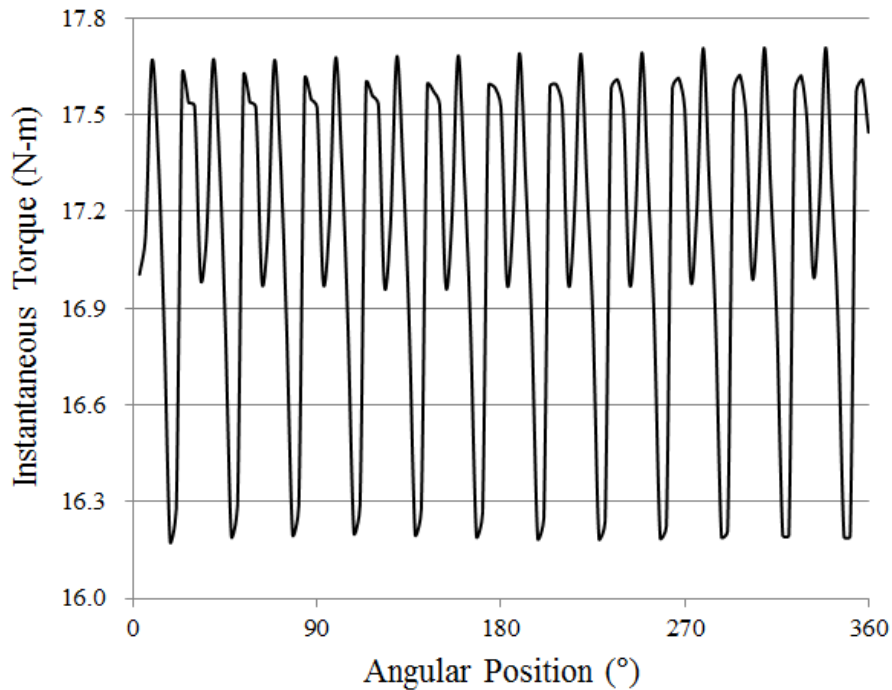
Figure 5.10 Instantaneous torque output of the VAWT having 4 stator blades

5.11(a & b) depicts the pressure and velocity variations in the vicinity of the VAWT having 8 stator blades. In comparison with figure 5.9(a), it can be seen in figure 5.11(a) due to additional stator blades, the pressure on both the windward and leeward sides of the VAWT is considerably higher. This is because there is more resistance offered by the VAWT to the incident flow of air and hence more kinetic energy of the wind can be converted into the mechanical energy by the VAWT.
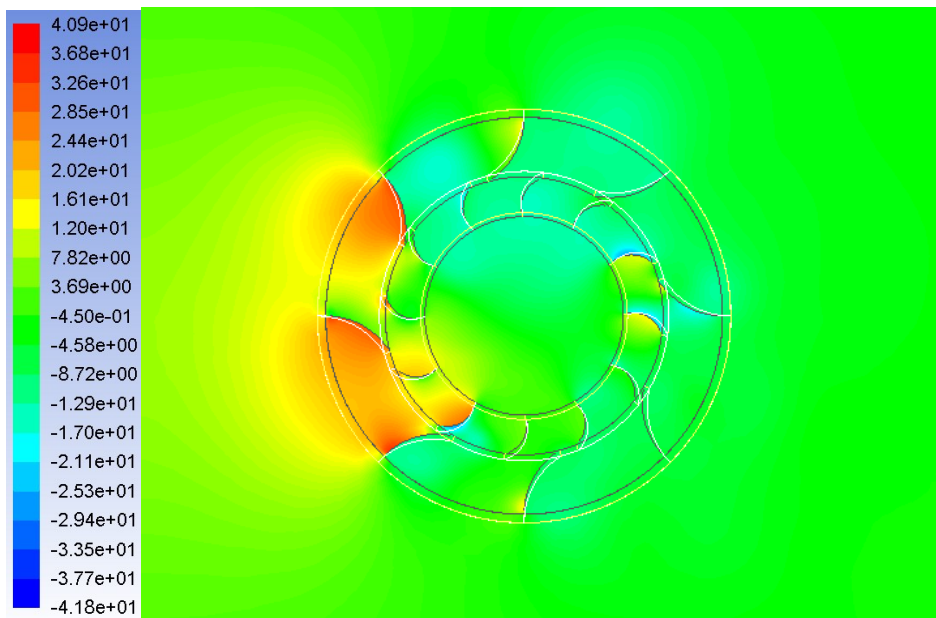
Figure 5.11(a) Pressure variations at 0° angular position of the VAWT having 8 stator blades

Analyzing the velocity variations in the vicinity of the VAWT having 8 stator blades (figure 5.11(b)), it can be seen, in comparison with figure 5.9(b), that the flow velocity is appreciably lower

Optimal Design of a Micro Vertical Axis Wind Turbine for Sustainable Urban Environment
By Kyooseon Park, School of Computing and Engineering, University of Huddersfield, UK (2013)

100

on both the windward and leeward sides of the VAWT. This suggests that the torque output of the VAWT will be considerably higher for 8 stator blades as compared to 4 stator blades.
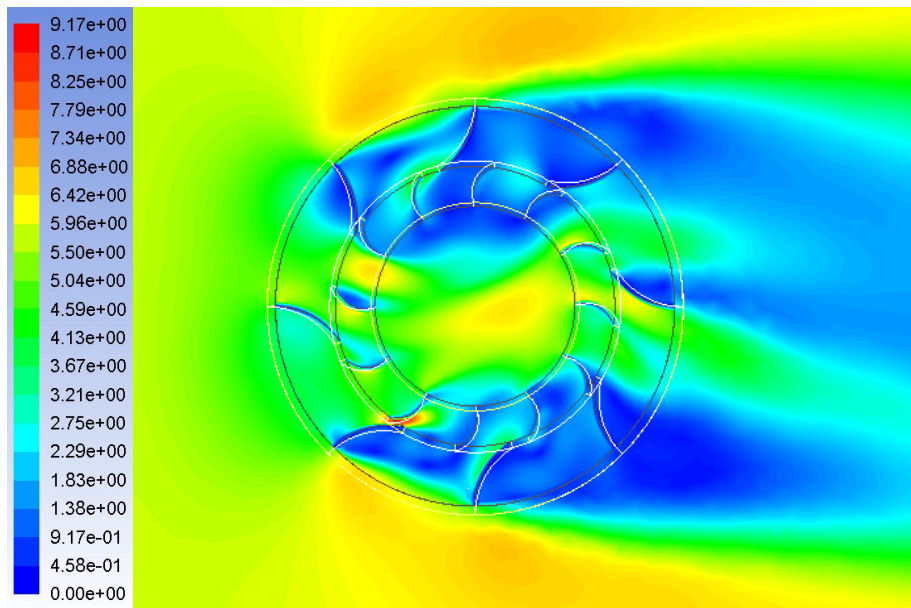
Figure 5.11(b) Velocity variations at 0° angular position of the VAWT having 8 stator blades

Figure 5.12 depicts the instantaneous torque output of the VAWT having 8 stator blades. As expected, in comparison with figure 5.10, it can be seen that the torque output has increased considerably. Furthermore, it can also be seen that there are 12 distinct peaks and valleys in the cyclic torque signals. As observed previously, the torque output suggests that the standard deviation in the torque output of the VAWT having 8 stator blades will be higher than for 4 stator blades.
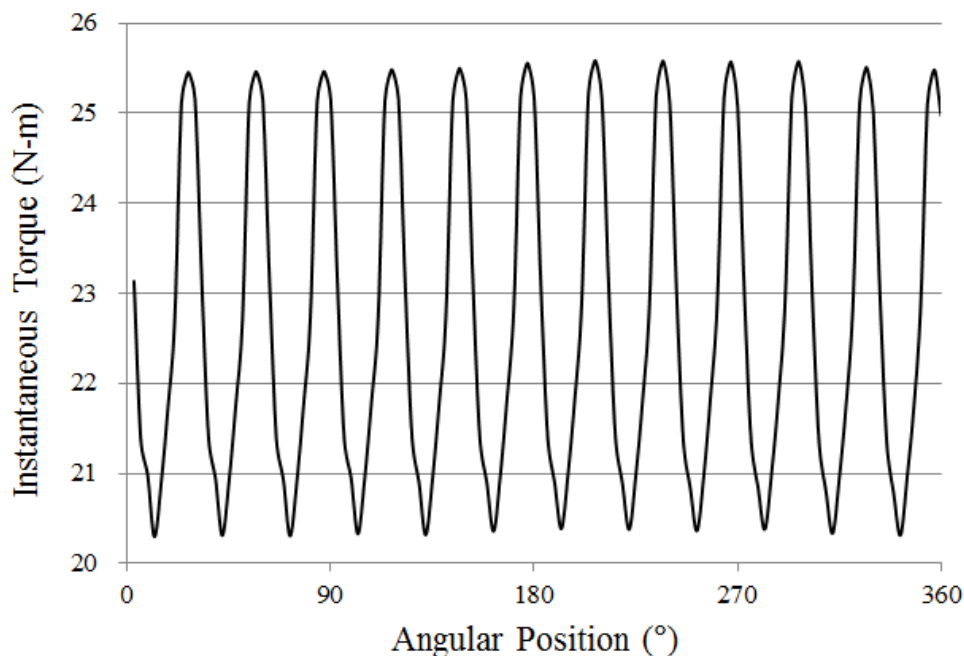
Figure 5.12 Instantaneous torque output of the VAWT having 8 stator blades

Optimal Design of a Micro Vertical Axis Wind Turbine for Sustainable Urban Environment
By Kyooseon Park, School of Computing and Engineering, University of Huddersfield, UK (2013)

101

5.13(a & b) depicts the pressure and velocity variations in the vicinity of the VAWT having 12 stator blades. In comparison with figure 5.11(a), it can be seen in figure 5.13(a), due to additional stator blades, the pressure on the leeward side of the VAWT is considerably lower. Furthermore, the pressure in the upper and the lower sections of the VAWT is very low. This means that the variations in the torque output of the VAWT will be significantly lower than for 8 stator blades.
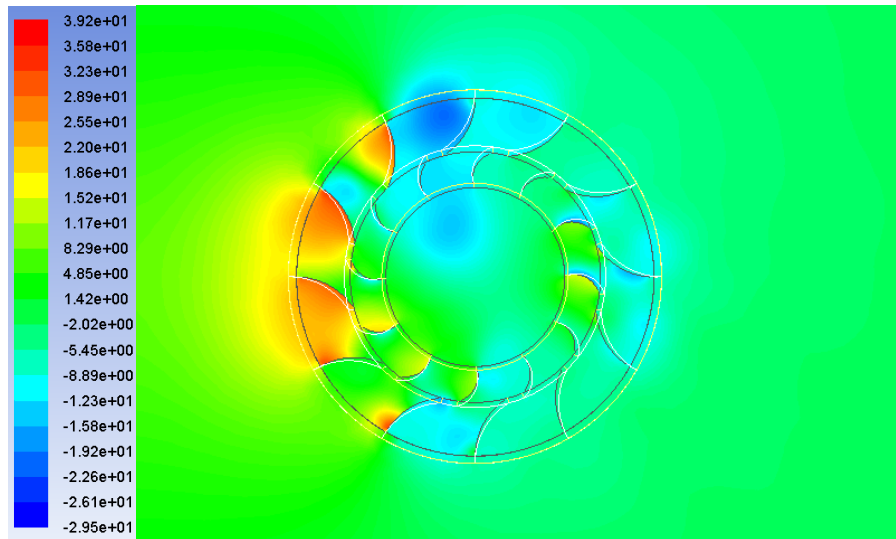
Figure 5.13(a) Pressure variations at 0° angular position of the VAWT having 12 stator blades

Analysing the velocity variations in the vicinity of the VAWT having 12 stator blades (figure 5.13(b)), it can be seen, in comparison with figure 5.1(b), that the flow velocity is considerably higher on the windward side and the core region of the VAWT. Furthermore, the flow velocity on the upper and lower sections of the VAWT is slightly higher than for 8 stator blades.
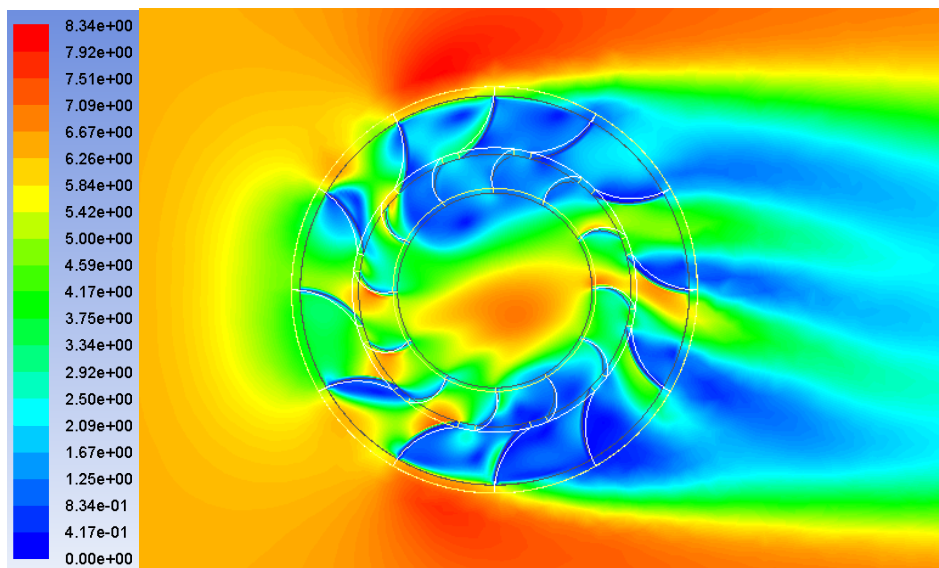
Figure 5.13(b) Velocity variations at 0° angular position of the VAWT having 12 stator blades

Figure 5.14 depicts the instantaneous torque output of the VAWT having 12 stator blades. It can be seen that there are additional lower peaks, together with the expected 12 higher peaks corresponding to 12 rotor blades. The presence of these lower peaks suggests that the standard deviation of the torque output will be considerably lower than for both 8 stator blades because there

Optimal Design of a Micro Vertical Axis Wind Turbine for Sustainable Urban Environment
By Kyooseon Park, School of Computing and Engineering, University of Huddersfield, UK (2013)

102

were no lower peaks observed in case of 8 stator blades. However, as the amplitude of lower peaks in case of both 4 and 12 stator blades is marginally different, it suggests that the difference in the standard deviation will also be marginally different.
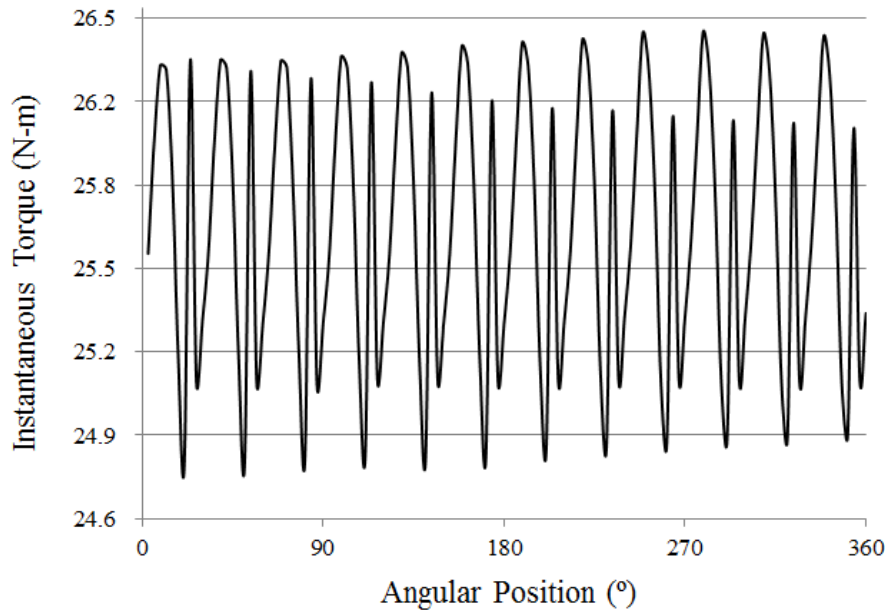
Figure 5.14 Instantaneous torque output of the VAWT having 12 stator blades

Table 5.2 summarises the statistical results for the torque outputs of the VAWTs having various number of stator blades. It can be seen that as the number of stator blades increases, the average torque output also increases. Furthermore, the standard deviation in the torque output is highest for 8 stator blades and lowest for 12 rotor blades as expected. It is also noteworthy that both the maximum and the minimum torques increase as the number of stator blades increases.

Table 5.2 Effect of the number of stator blades on the performance output of the VAWT

Number of Rotor Blades	Number of Stator Blades	Tmin (N-m)	Tmax (N-m)	Tavg (N-m)	Std. Dev.
12	4	16.18	17.71	17.12	0.52
12	8	20.30	25.58	22.70	1.85
12	12	24.80	26.41	25.67	0.51

Figure 5.15 depicts the instantaneous torque outputs of the VAWTs having different number of stator blades. It can be seen that as the number of stator blades increase, the torque output increases. Moreover, it has been observed that for 8 stator blades, the variations in the cyclic torque output are considerably higher than the other two cases.

Optimal Design of a Micro Vertical Axis Wind Turbine for Sustainable Urban Environment
By Kyooseon Park, School of Computing and Engineering, University of Huddersfield, UK (2013)

103
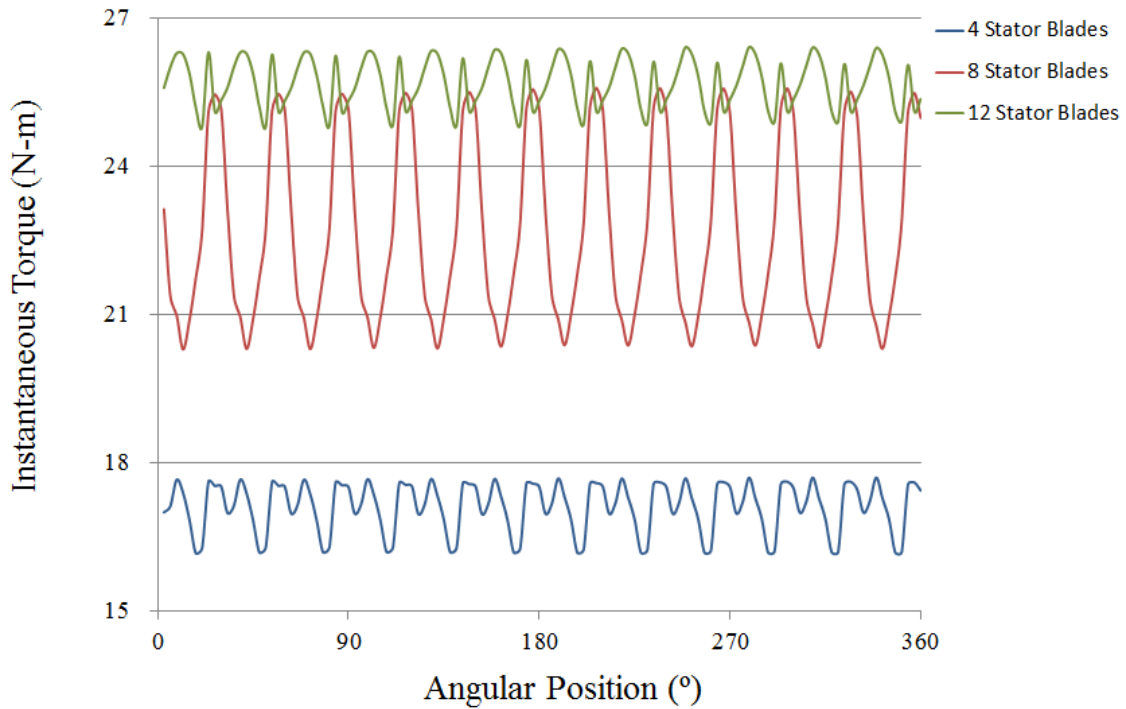
Figure 5.15 Instantaneous torque output of the VAWT having different number of stator blades

Figure 5.16 depicts the effect of the number of stator blades on the performance output of the VAWT. It can be seen that as the number of stator blade increase, both the torque and the power outputs of the VAWT increases. Hence, in the present study, the optimised design of the VAWT is the one that has 12 stator blades. Furthermore, it can be seen that there are non-linearities in the curves that arises due to complex and transient interactions between the blades.
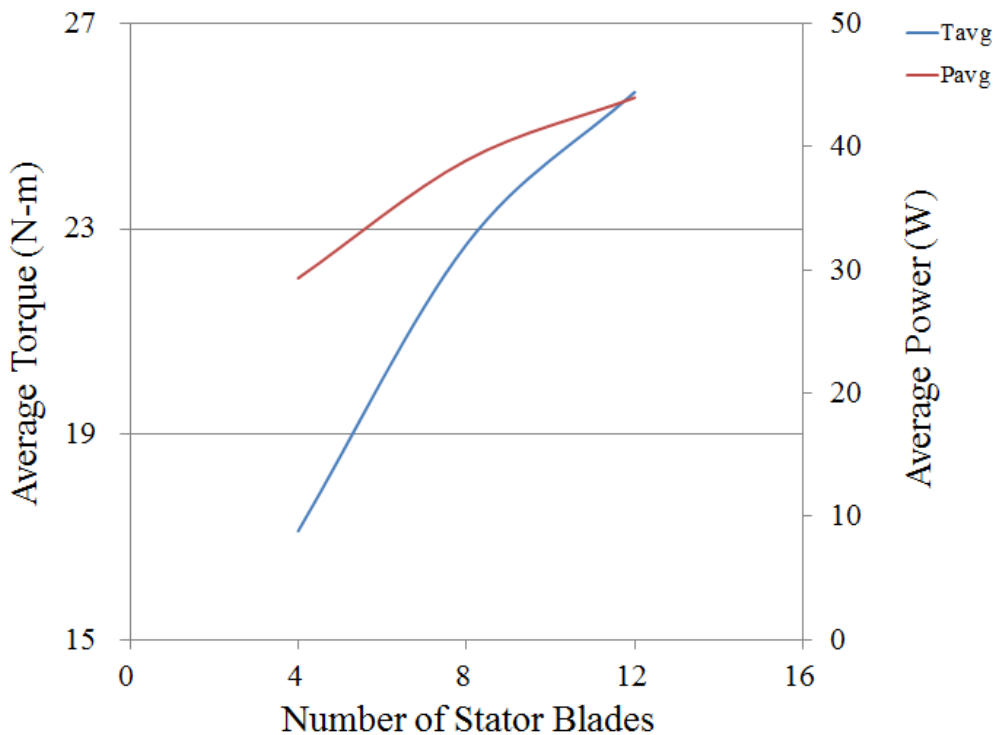
Figure 5.16 Effect of the number of stator blades on the performance output of the VAWT

104

5.3. Effect of Size of Rotor

In order to analyse the effect of the size of the rotor on the performance output of a vertical axis wind turbine, two VAWT configurations have been chosen for analysis that constitute of r_r-r_c=0.1m and 0.2m respectively while r_s-r_r has been kept constant to 0.3m. As discussed in the Chapter 3, r_s is the radius of the stator, r_r is the radius of the rotor and r_c is the radius of the core region (see figure 3.3).

Figure 5.17(a & b) depicts the pressure and velocity variations in the vicinity of the VAWT having r_r-r_c=0.1m. It can be seen in figure 5.17(a) that the windward side of the VAWT possess very high pressure while the leeward, upper and lower sections have comparatively low pressure. Furthermore, it can be seen in figure 5.17(b) that the flow velocity is high on the windward side and the core region, while it is comparatively lower on the leeward side of the VAWT. It has also been observed that the flow accelerates in the passages formed between the rotor and the stator blades on the windward side of the VAWT. These passages are formed due to the orientation and the angular position of the rotor blades.
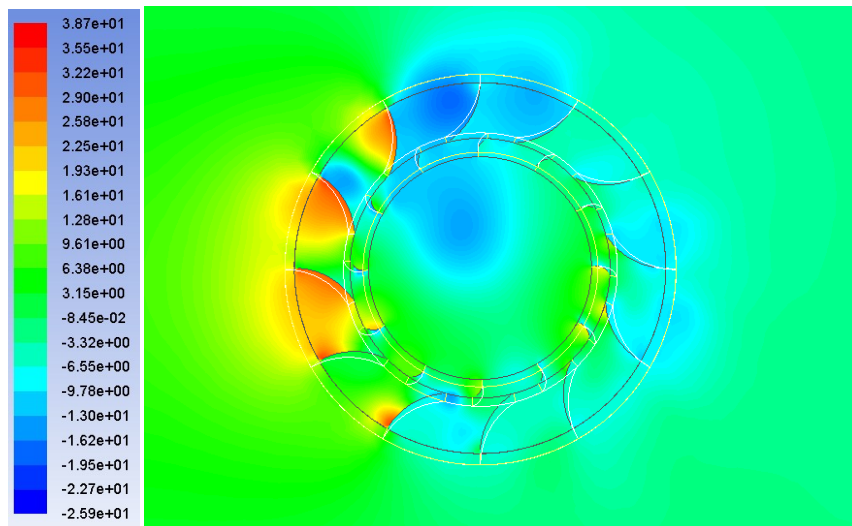
Figure 5.17 (a) Pressure variations at 0° angular position of the VAWT having r_r-r_c=0.1m
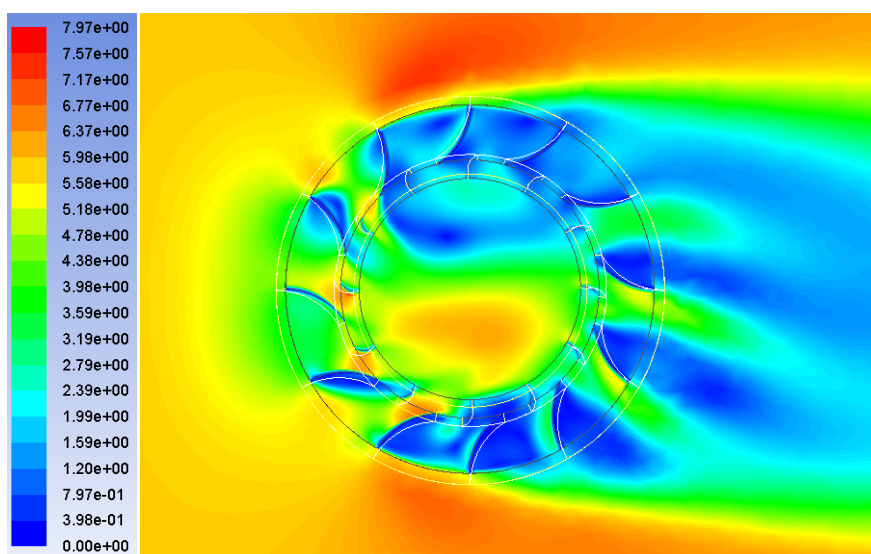
Figure 5.17 (b) Velocity variations at 0° angular position of the VAWT having r_r-r_c=0.1m

Optimal Design of a Micro Vertical Axis Wind Turbine for Sustainable Urban Environment
By Kyooseon Park, School of Computing and Engineering, University of Huddersfield, UK (2013)

105

Figure 5.18 depicts the instantaneous torque output of the VAWT having r_r-r_c=0.1m. It is noticed that the amplitude of the torque output increases as the angular position of the VAWT increases. Furthermore, each cycle contains two distinct peaks. As the angular position of the VAWT increases, the amplitude of the second peak in a cycle increases while the amplitude of the first peak remains constant. These non-uniform peaks contribute towards increase in the standard deviation of the torque output.
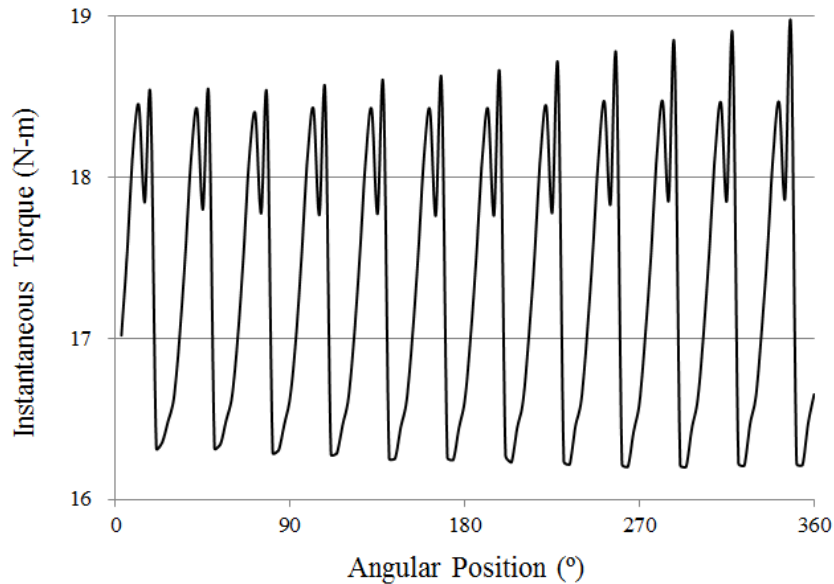
Figure 5.18 Instantaneous torque output of the VAWT having r_r-r_c=0.1m

Figure 5.19(a) depicts the variations in the pressure for the VAWT having r_r-r_c=0.2m i.e. the rotor size is twice than the previous case. It can be clearly seen by comparing figures 5.17(a) and 5.19(a) that the pressure in the whole flow domain is considerably high for r_r-r_c=0.2m. This is because the size of the rotor blades has increased and hence more wind's kinetic energy can be converted into mechanical energy.
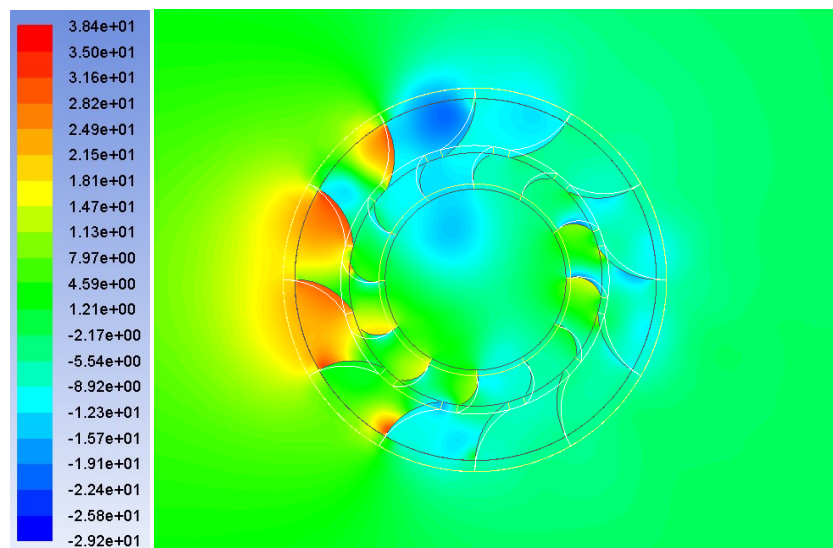
Figure 5.19 (a) Pressure variations at 0° angular position of the VAWT having r_r-r_c=0.2m

Analysing the velocity variations in the vicinity of the VAWT having r_r-r_c=0.2m (figure 5.19(b)), it can be seen, in comparison with figure 5.17(b), that the flow velocity is considerably higher on the

Optimal Design of a Micro Vertical Axis Wind Turbine for Sustainable Urban Environment
By Kyooseon Park, School of Computing and Engineering, University of Huddersfield, UK (2013)
106

windward side and the core region of the VAWT. Furthermore, the flow velocity on the upper and lower sections of the VAWT is slightly higher than for r_r-r_c=0.1m.
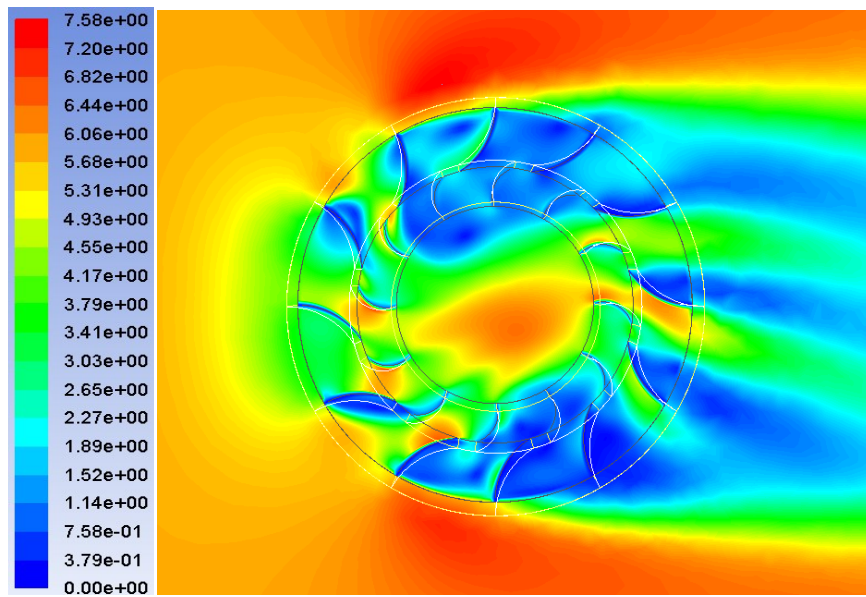
Figure 5.19 (b) Velocity variations at 0° angular position of the VAWT having r_r-r_c=0.2m

Figure 5.20 depicts the instantaneous torque output of the VAWT having r_r-r_c=0.2m. In comparison with figure 5.18, it can be clearly visualised that the torque output is considerably higher for r_r-r_c=0.2m i.e. bigger rotor corresponds to higher torque output of the VAWT. Furthermore, it can be seen that the amplitude of the second peaks decreases as the angular position of the VAWT increases. This trend is contrary to the one observed in case of r_r-r_c=0.1m.
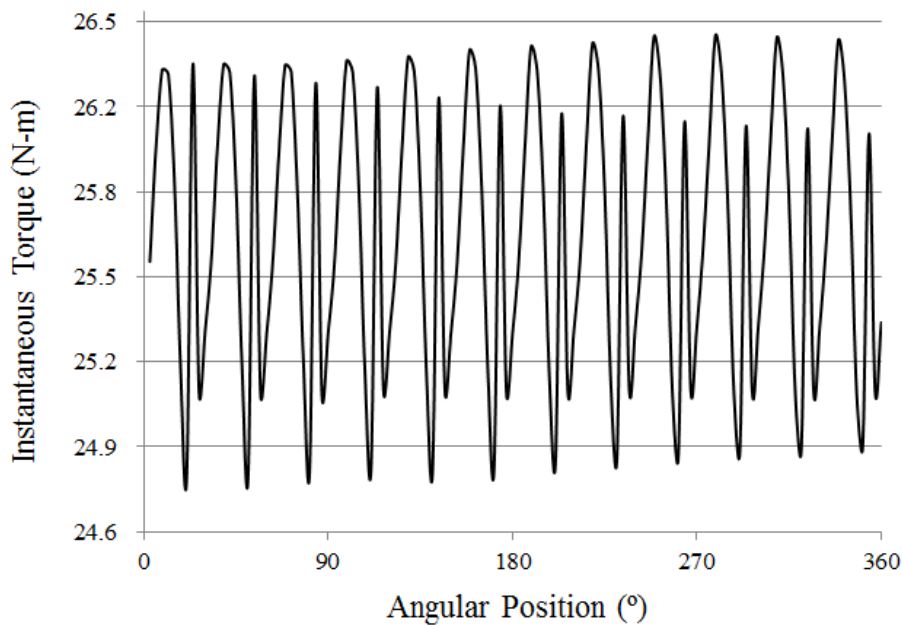
Figure 5.20 Instantaneous torque output of the VAWT having r_r-r_c=0.2m

Table 5.3 summarises the statistical results for the torque outputs of the VAWTs having different rotor sizes. It can be seen that as the size of rotor increases, the average torque output increases. Furthermore, the standard deviation in the torque output is higher for r_r-r_c=0.1m as expected. It is

Optimal Design of a Micro Vertical Axis Wind Turbine for Sustainable Urban Environment
By Kyooseon Park, School of Computing and Engineering, University of Huddersfield, UK (2013)
107

also noteworthy that both the maximum and the minimum torques increase as the rotor size increases.

Table 5.3 Effect of the size of rotor on the performance output of the VAWT

r_r-r_c (m)	Tmin (N-m)	Tmax (N-m)	Tavg (N-m)	Pavg (W)	Std. Dev.
0.1	16.20	18.94	17.32	29.69	0.87
0.2	24.80	26.41	25.67	44.01	0.51

Figure 5.21 depicts the instantaneous torque outputs of the VAWTs having different rotor sizes. It can be seen that as the size of rotor increase, the torque output increases significantly. Moreover, it has been observed that as the size of the rotor increases, the variations in the torque output decreases as expected.
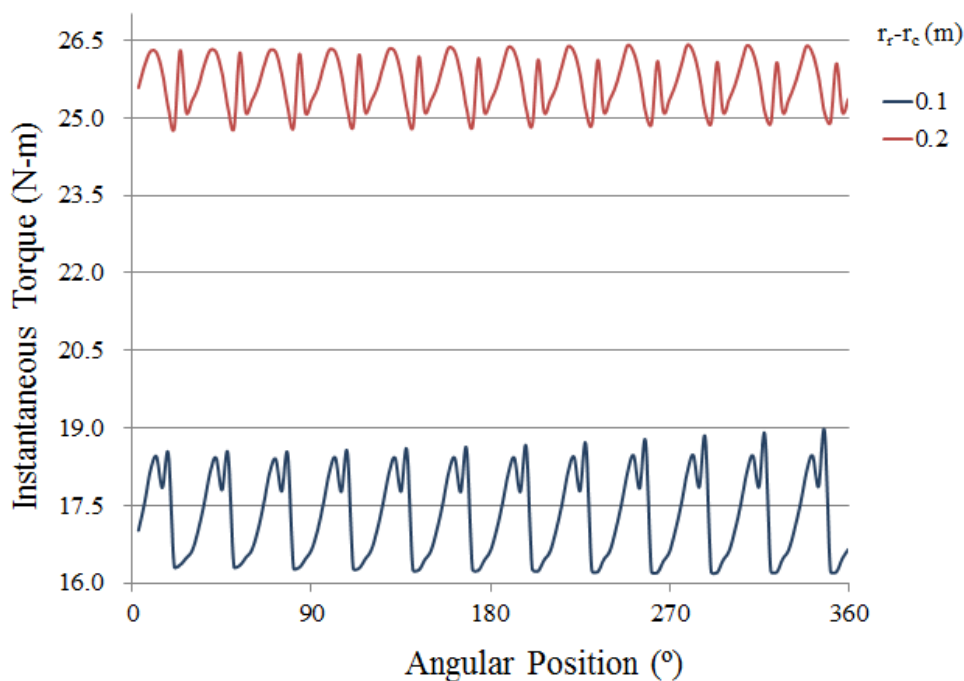
Figure 5.21 Instantaneous torque output of the VAWT having different size of rotor

Figure 5.22 depicts the effect of the size of rotor on the performance output of the VAWT. It can be seen that as the size of rotor increases, both the torque and the power outputs of the VAWT increases. Hence, in the present study, the optimised design of the VAWT is the one that has rotor size=0.2m.

Optimal Design of a Micro Vertical Axis Wind Turbine for Sustainable Urban Environment
By Kyooseon Park, School of Computing and Engineering, University of Huddersfield, UK (2013)

108
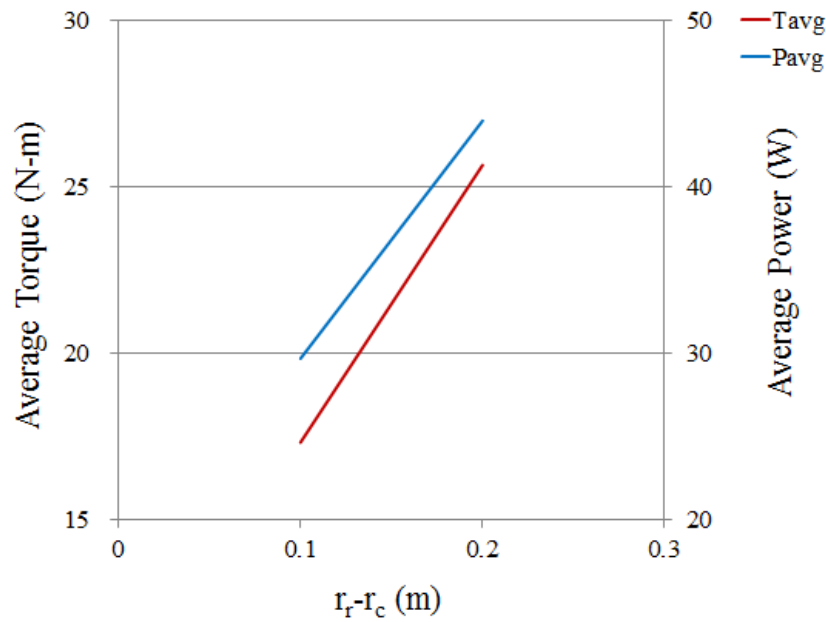
Figure 5.22 Effect of the size of rotor on the performance output of the VAWT

5.4. Effect of Size of Stator

In order to analyse the effect of the size of the stator on the performance output of a vertical axis wind turbine, four VAWT configurations have been chosen for analysis that constitute of r_s-r_r=0.1m, 0.2m, 0.3m and one with no stator (r_s-r_r=0m). r_r-r_c has been kept constant to 0.2m as mentioned in previous section. Figure 5.23(a & b) depicts the pressure and velocity variations in the vicinity of the VAWT having no stator. It can be seen in figure 5.23(a) that the windward side of the VAWT possess high pressure while the leeward, upper and lower sections have comparatively low pressure. Furthermore, it can be seen in figure 5.23(b) that the flow velocity is high on the windward side and the core region, while it is comparatively lower on the upper and lower sections of the VAWT. It has also been observed that the flow accelerates in the passages between the rotor blades on the windward side of the VAWT.
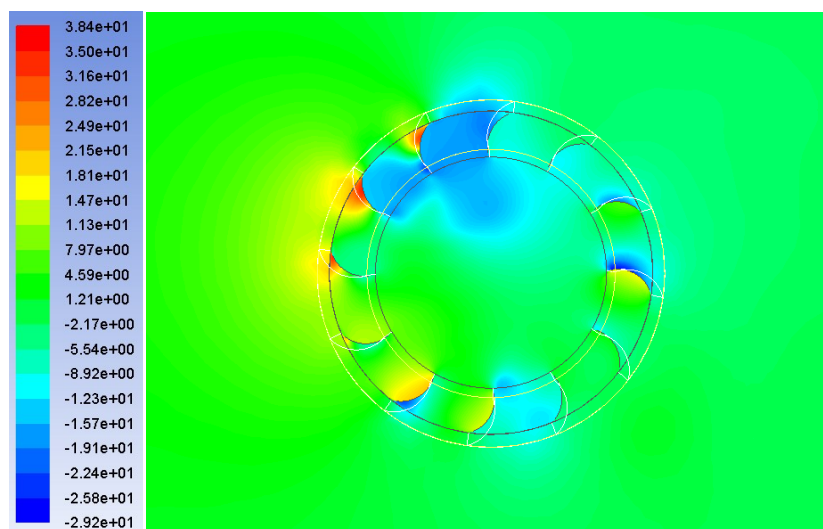
Figure 5.23 (a) Pressure variations at 0° angular position of the VAWT having no stator

Optimal Design of a Micro Vertical Axis Wind Turbine for Sustainable Urban Environment
By Kyooseon Park, School of Computing and Engineering, University of Huddersfield, UK (2013)

109
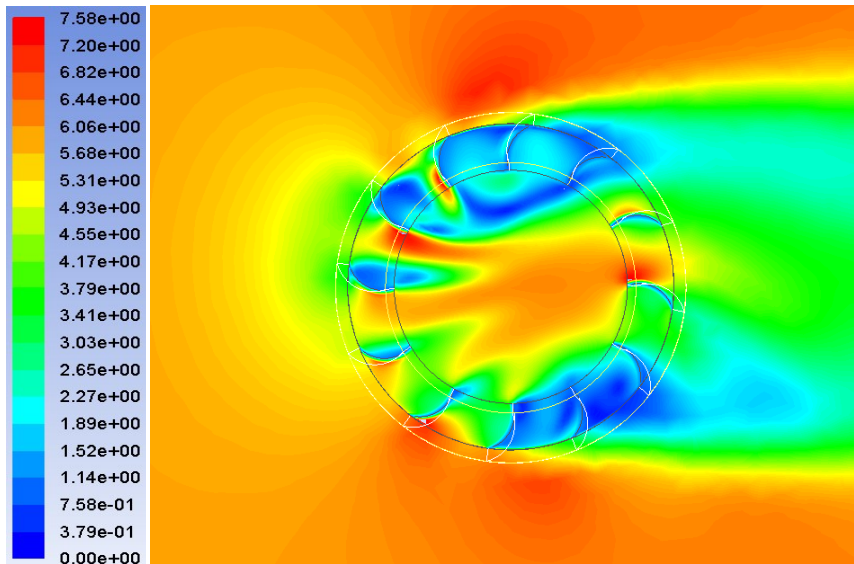
Figure 5.23 (b) Velocity variations at 0⁰ angular position of the VAWT having no stator

Figure 5.24 depicts the instantaneous torque output of the VAWT having no stator. It can be seen that due to the absence of the stator blades, there are no double peaks in the cycle torque output of the VAWT. The amplitude of the torque output remains constant throughout one complete revolution of the VAWT. The torque output varies between 11.5N-m and 13.5N-m and constitute of 12 peaks and valleys (because of 12 rotor blades present in the VAWT). It can noticed that as compared to the previous results, the torque output of the VAWT having no stator is considerably low, hence, degrading the performance output of the VAWT
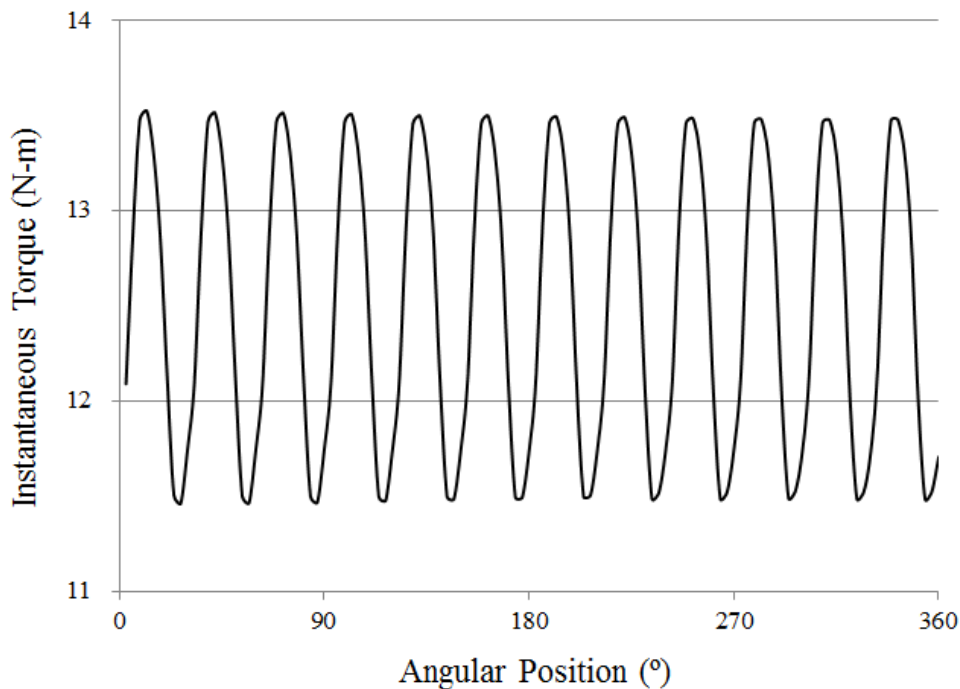
Figure 5.24 Instantaneous torque output of the VAWT having no stator

Optimal Design of a Micro Vertical Axis Wind Turbine for Sustainable Urban Environment
By Kyooseon Park, School of Computing and Engineering, University of Huddersfield, UK (2013)

110

Figure 5.25(a) depicts the variations in the pressure for the VAWT having r_s-r_r=0.1m. It can be clearly seen by comparing figures 5.23(a) and 5.25(a) that the area of thigh pressure on the windward side of the VAWT is much bigger for r_s-r_r=0.1m. Furthermore, pressure on the upper section of the VAWT is also considerably high.
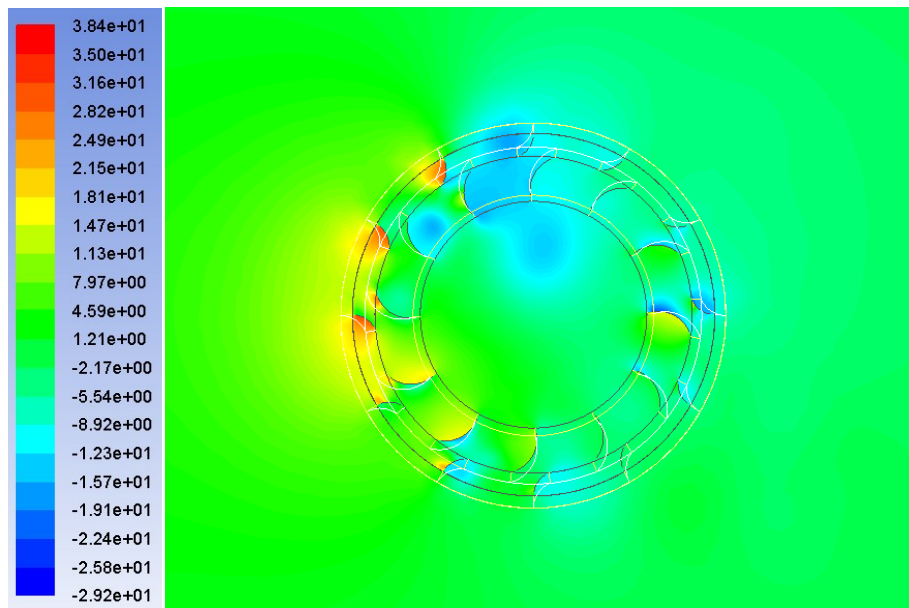
Figure 5.25 (a) Pressure variations at 0° angular position of the VAWT having r_s-r_r=0.1m

Analysing the velocity variations in the vicinity of the VAWT having r_s-r_r=0.1m (figure 5.25(b)), it can be seen, in comparison with figure 5.23(b), that the flow velocity is considerably lower on the windward side and the core region of the VAWT. Furthermore, the flow velocity on the upper and lower sections of the VAWT is also lower than for the VAWT having no stator.
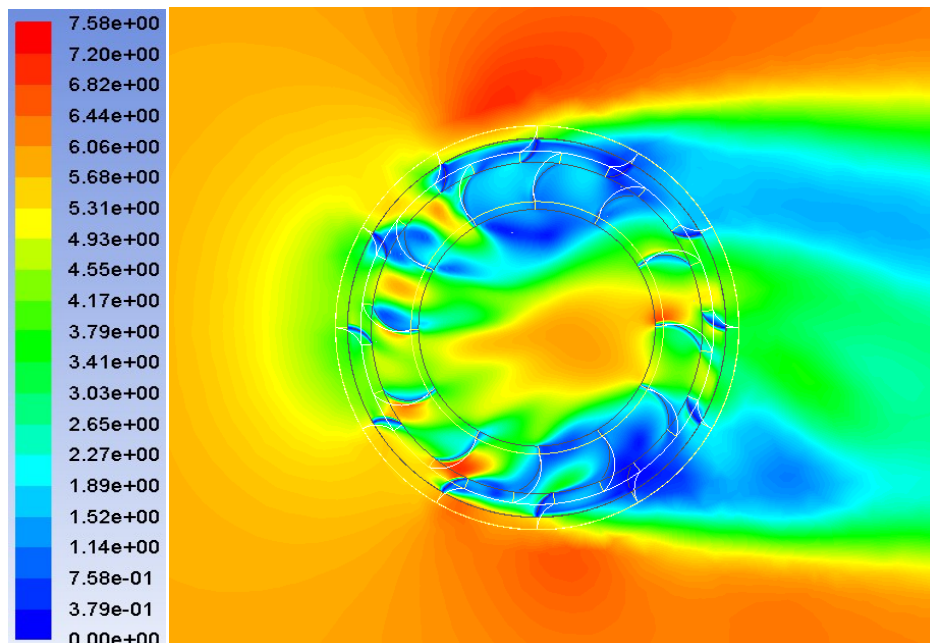
Figure 5.25 (b) Velocity variations at 0° angular position of the VAWT having r_s-r_r=0.1m

Figure 5.26 depicts the instantaneous torque output of the VAWT having r_s-r_r=0.1m. It can be seen, in comparison with figure 5.24, that the torque output of the VAWT has increased substantially.

Optimal Design of a Micro Vertical Axis Wind Turbine for Sustainable Urban Environment
By Kyooseon Park, School of Computing and Engineering, University of Huddersfield, UK (2013)

111

Furthermore, with the presence of stator blades, the variations in the torque output have also increased significantly. This suggests that the standard deviation in the torque output will be higher for r_s-r_r=0.1m as compared to no stator.
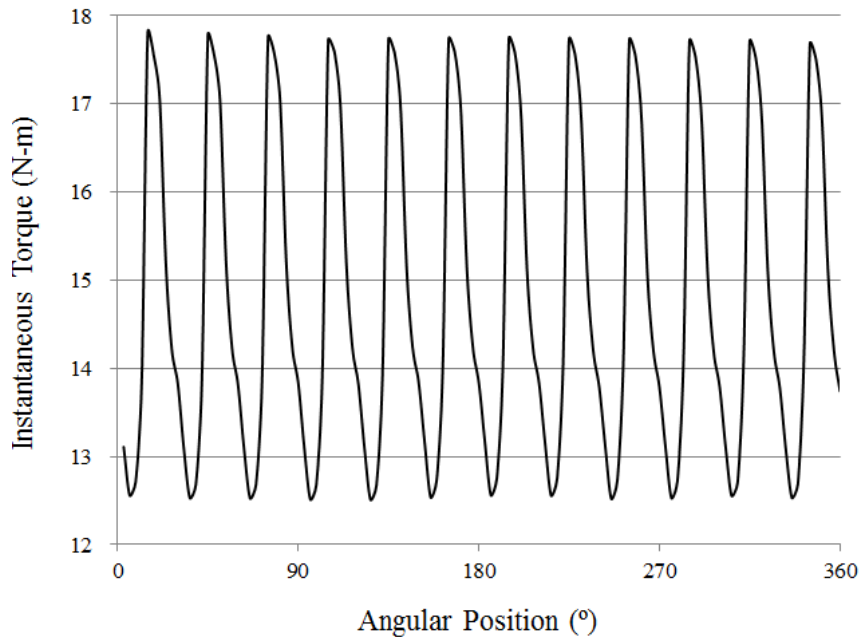
Figure 5.26 Instantaneous torque output of the VAWT having r_s-r_r=0.1m

Figure 5.27(a) depicts the variations in the pressure for the VAWT having r_s-r_r=0.2m. It can be clearly seen by comparing figures 5.25(a) and 5.27(a) that the area of thigh pressure on the windward side of the VAWT is much bigger for r_s-r_r=0.1m.
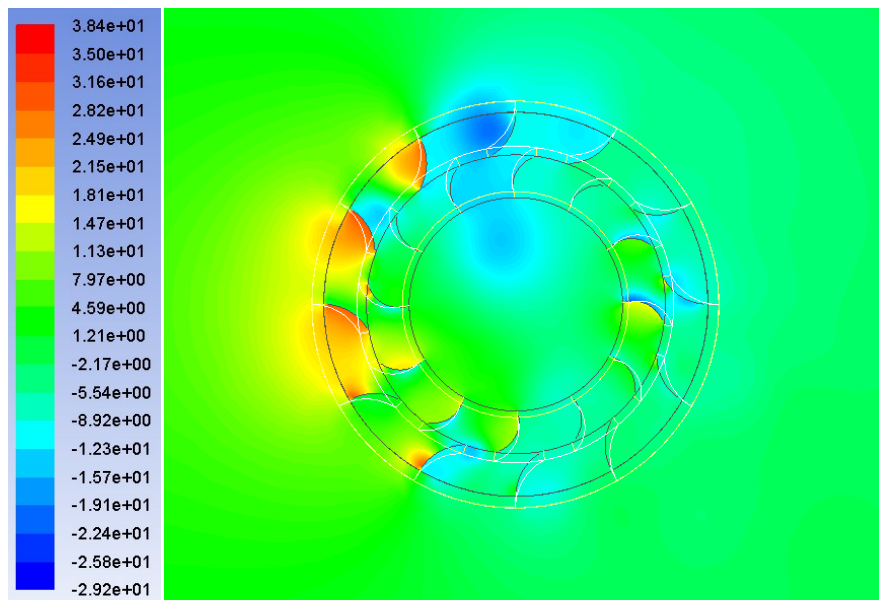
Figure 5.27 (a) Pressure variations at 0° angular position of the VAWT having r_s-r_r=0.2m

Analysing the velocity variations in the vicinity of the VAWT having r_s-r_r=0.2m (figure 5.27(b)), it can be seen, in comparison with figure 5.25(b), that the flow velocity is considerably lower on the windward side and the core region of the VAWT. Furthermore, the flow velocity on the leeward side of the VAWT is also lower than for r_s-r_r=0.1m.

Optimal Design of a Micro Vertical Axis Wind Turbine for Sustainable Urban Environment
By Kyooseon Park, School of Computing and Engineering, University of Huddersfield, UK (2013)

112
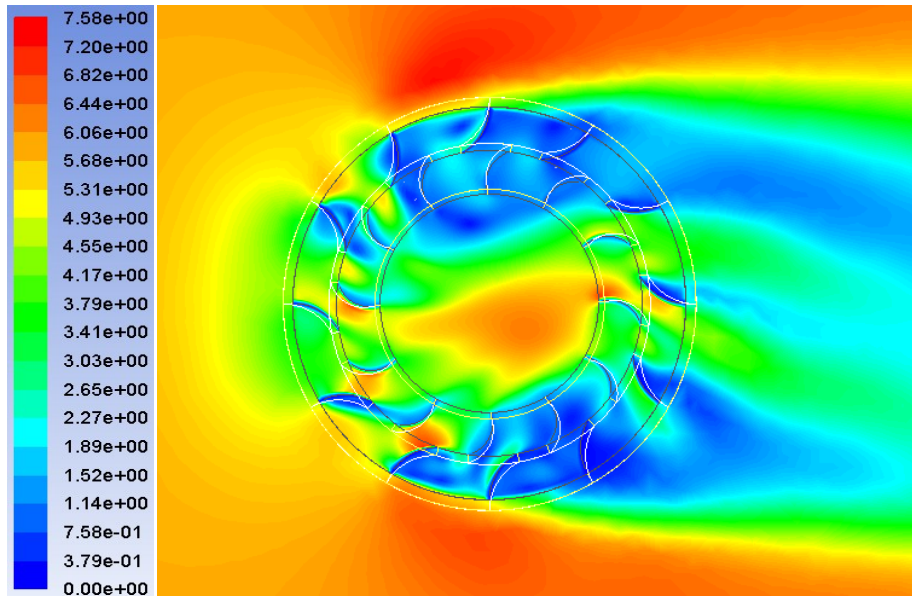
Figure 5.27 (b) Velocity variations at 0⁰ angular position of the VAWT having r_s-r_r=0.2m

Figure 5.28 depicts the instantaneous torque output of the VAWT having r_s-r_r=0.2m. It can be seen, in comparison with figure 5.26, that the torque output of the VAWT has increased substantially. Furthermore, the variations in the torque output have reduced significantly, suggesting that the standard deviation will be much smaller than for r_s-r_r=0.1m.
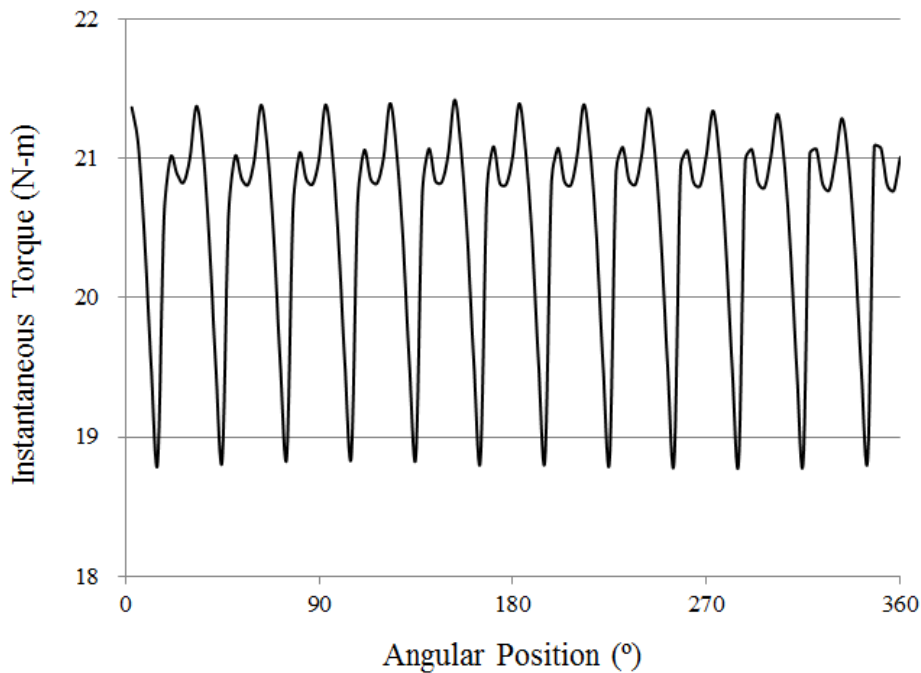
Figure 5.28 Instantaneous torque output of the VAWT having r_s-r_r=0.2m

Figure 5.29(a) depicts the variations in the pressure for the VAWT having r_s-r_r=0.3m. It can be clearly seen by comparing figures 5.27(a) and 5.29(a) that the area of thigh pressure on the windward side of the VAWT is much bigger for r_s-r_r=0.2m.

Optimal Design of a Micro Vertical Axis Wind Turbine for Sustainable Urban Environment
By Kyooseon Park, School of Computing and Engineering, University of Huddersfield, UK (2013)

113
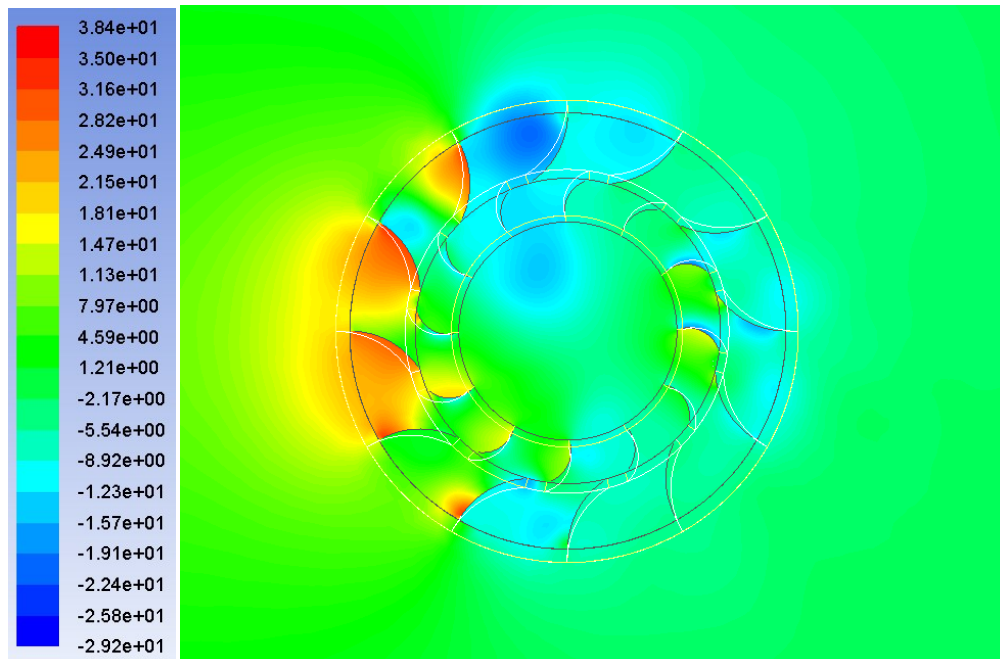
Figure 5.29 (a) Pressure variations at 0⁰ angular position of the VAWT having r_s-r_r=0.3m

Analysing the velocity variations in the vicinity of the VAWT having r_s-r_r=0.3m (figure 5.29(b)), it can be seen, in comparison with figure 5.27(b), that the flow velocity is considerably lower on the windward side and the core region of the VAWT. Furthermore, the flow velocity on the leeward side of the VAWT is also lower than for r_s-r_r=0.2m.
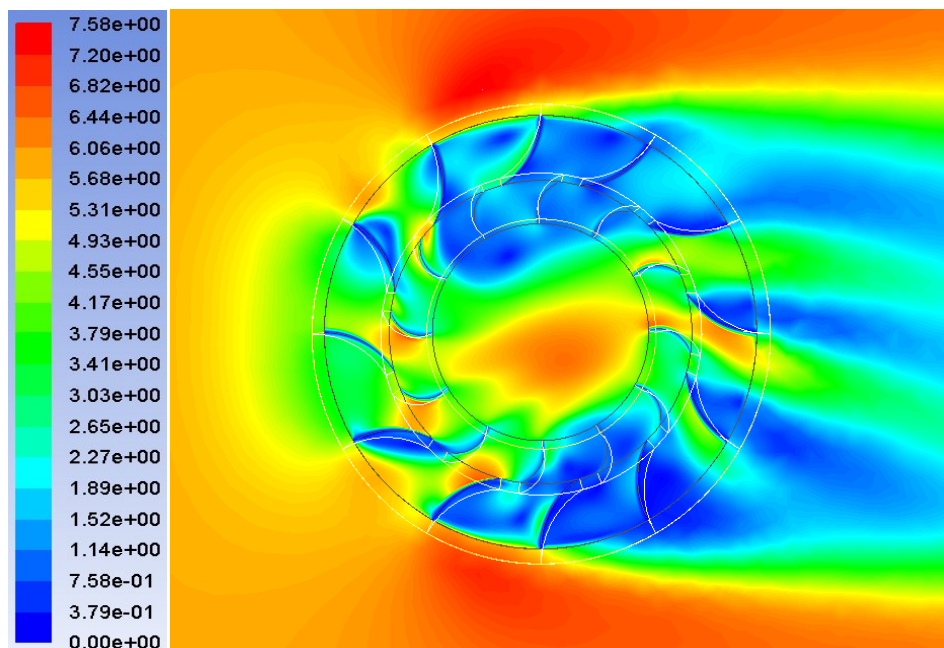
Figure 5.29 (b) Velocity variations at 0⁰ angular position of the VAWT having r_s-r_r=0.3m

Figure 5.30 depicts the instantaneous torque output of the VAWT having r_s-r_r=0.3m. It can be seen, in comparison with figure 5.28, that the torque output of the VAWT has increased substantially. Furthermore, the variations in the torque output have reduced significantly, suggesting that the standard deviation will be much smaller than for r_s-r_r=0.2m.

Optimal Design of a Micro Vertical Axis Wind Turbine for Sustainable Urban Environment
By Kyooseon Park, School of Computing and Engineering, University of Huddersfield, UK (2013)

114
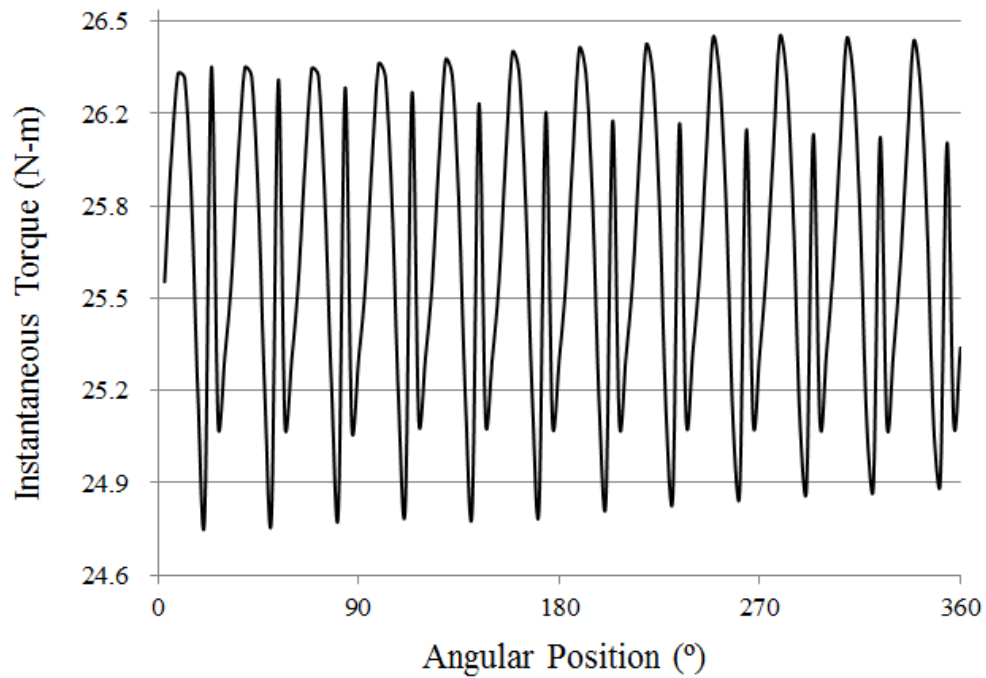
Figure 5.30 Instantaneous torque output of the VAWT having r_s-r_r=0.3m

Table 5.4 summarises the statistical results for the torque outputs of the VAWTs having different stator sizes. It can be seen that as the stator size increases, the average torque output increases. Furthermore, the standard deviation in the torque output is highest for r_s-r_r=0.1m as expected. It is also noteworthy that both the maximum and the minimum torques increase as the stator size increases.

Table 5.4 Effect of the size of stator on the performance output of the VAWT

r_s-r_r (m)	Tmin (N-m)	Tmax (N-m)	Tavg (N-m)	Pavg (W)	Std. Dev.
0 (No Stator)	10.96	13.02	11.99	20.56	1.31
0.1	12.51	17.81	14.78	25.33	1.88
0.2	18.32	20.92	20.07	34.41	0.75
0.3	24.80	26.41	25.67	44.01	0.51

Figure 5.31 depicts the instantaneous torque outputs of the VAWTs having different stator sizes. It can be seen that as the size of stator increase, the torque output increases significantly. Moreover, it has been observed that for r_s-r_r=0.1m, the variations in the torque output are highest as expected.

Optimal Design of a Micro Vertical Axis Wind Turbine for Sustainable Urban Environment
By Kyooseon Park, School of Computing and Engineering, University of Huddersfield, UK (2013)
115
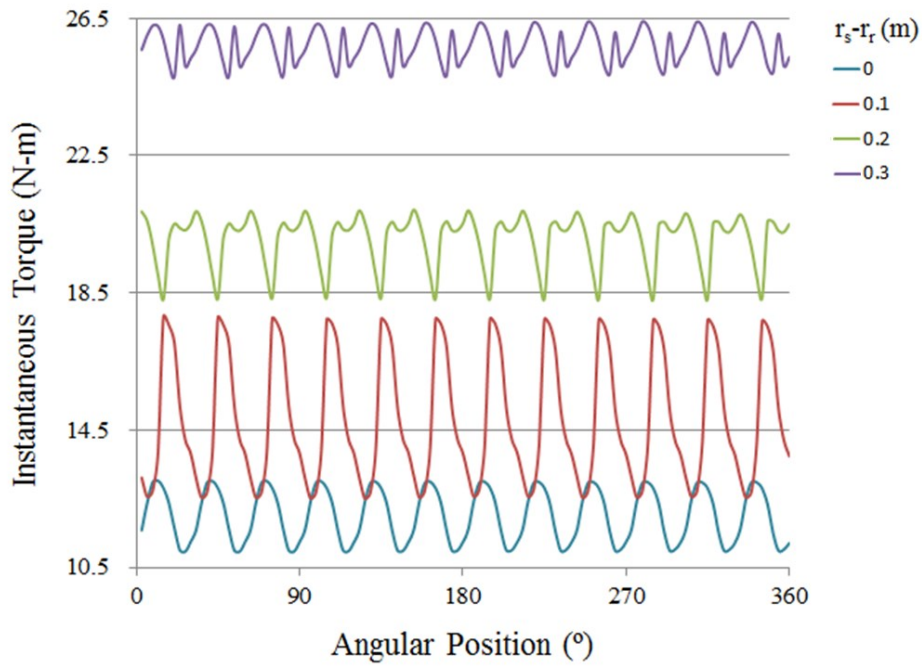
Figure 5.31 Instantaneous torque output of the VAWT having different size of stator

Figure 5.32 depicts the effect of the size of stator on the performance output of the VAWT. It can be seen that as the size of stator increases, both the torque and the power outputs of the VAWT increases. Hence, in the present study, the optimised design of the VAWT is the one that has stator size=0.3m. Furthermore, it can be seen that there are non-linearities in the curves that arises due to complex and transient interactions between the blades.
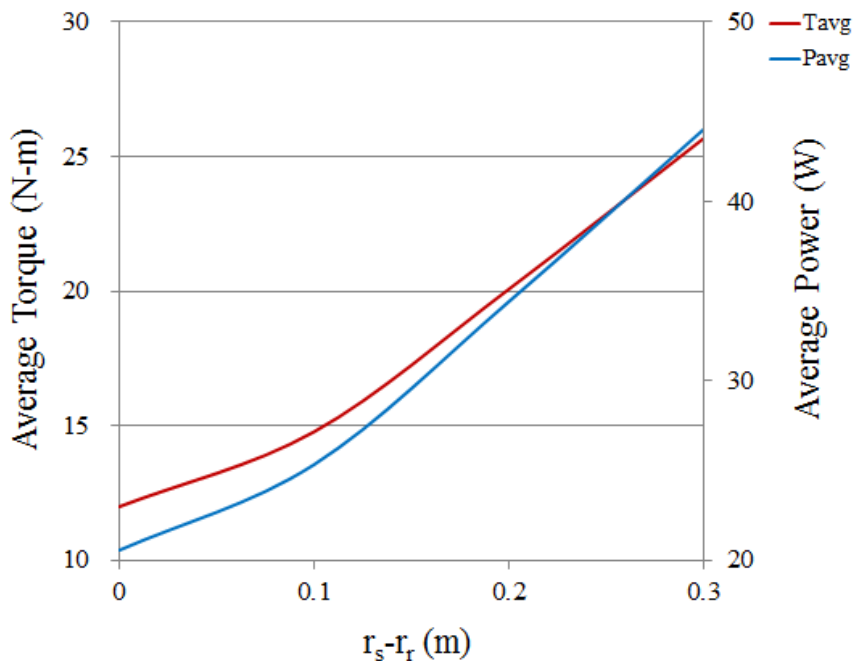
Figure 5.32 Effect of the size of stator on the performance output of the VAWT

Optimal Design of a Micro Vertical Axis Wind Turbine for Sustainable Urban Environment
By Kyooseon Park, School of Computing and Engineering, University of Huddersfield, UK (2013)

116

5.5.   Effect of Height of the VAWT

In order to analyse the effect of the height of a vertical axis wind turbine on its performance output, four VAWT configurations have been chosen for analysis that constitute of h=0.25m, 0.5m, 0.75m and 1m, where h represents height of the VAWT. Figure 5.33(a & b) depicts the pressure and velocity variations in the vicinity of the VAWT having a height of 0.25m. It can be seen in figure 5.33(a) that the windward side of the VAWT possess high pressure while the leeward, upper and lower sections have comparatively low pressure. Furthermore, it can be seen in figure 5.33(b) that the flow velocity is high on the windward side and the core region, while it is comparatively lower on the upper and lower sections of the VAWT. It has also been observed that the flow accelerates in the passages between the rotor blades on the windward side of the VAWT.
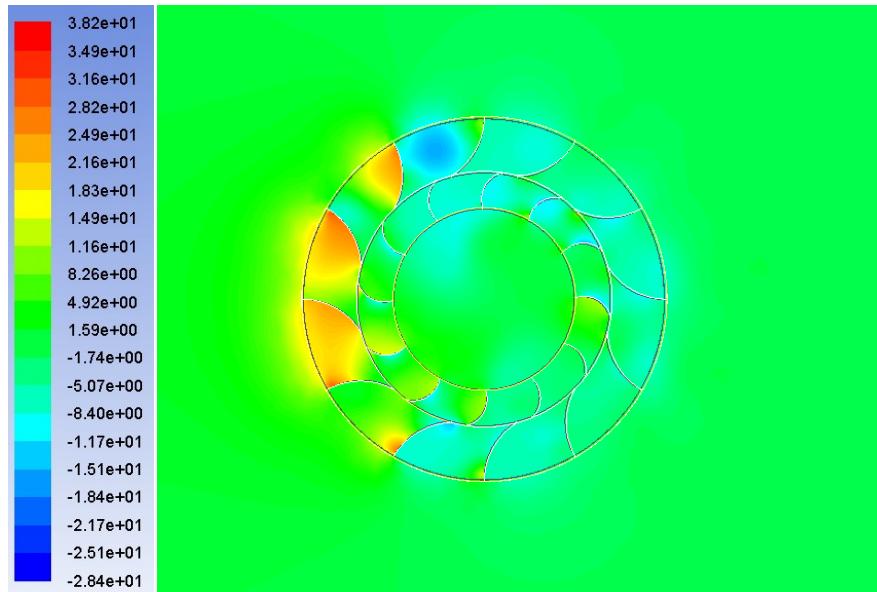
Figure 5.33(a) Pressure variations at 0° angular position of the VAWT having a height of 0.25m
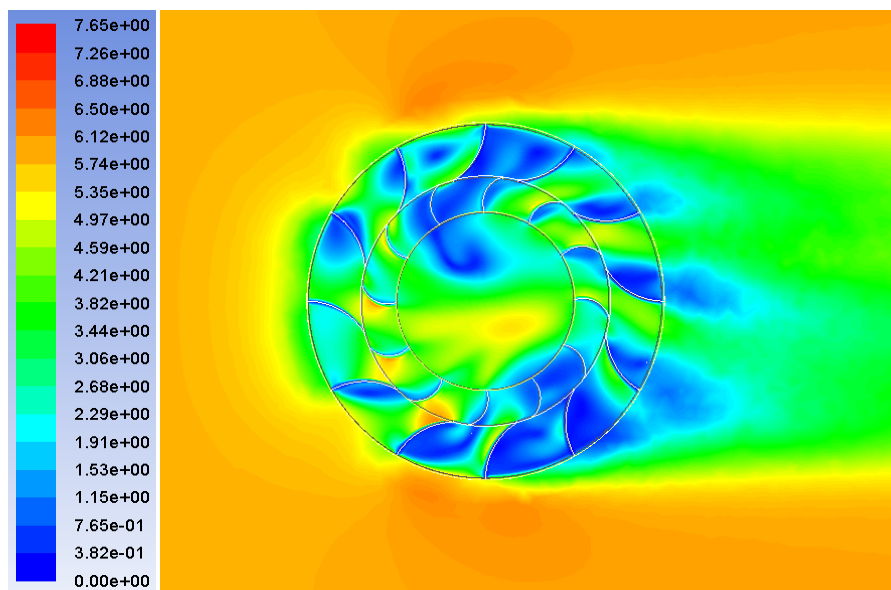
Figure 5.33(b) Velocity variations at 0° angular position of the VAWT having a height of 0.25m

Optimal Design of a Micro Vertical Axis Wind Turbine for Sustainable Urban Environment
By Kyooseon Park, School of Computing and Engineering, University of Huddersfield, UK (2013)

117

Figure 5.34 depicts the instantaneous torque output of the VAWT having a height of 0.25m. It is noticed that the amplitude of the torque output remains constant as the angular position of the VAWT increases. The number of peaks/valleys is the same as the number of rotor blades within the VAWT. Furthermore, each cycle contains two peaks, however, it can be clearly seen that the smaller peak has negligible effect on the overall torque output.
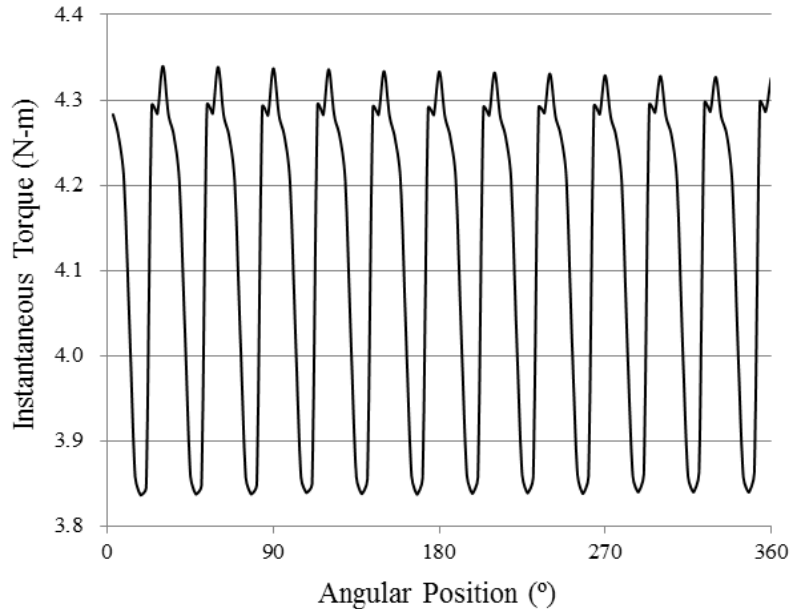
Figure 5.34 Instantaneous torque output of the VAWT having a height of 0.25m

Figure 5.35(a) depicts the variations in the pressure for the VAWT having a height of 0.5m. It can be seen by comparing figures 5.35(a) and 5.33(a) that the area of thigh pressure on the windward side of the VAWT is much bigger for h=0.5m. Furthermore, pressure on the upper section of the VAWT is considerably low than observed in case of h=0.25m.
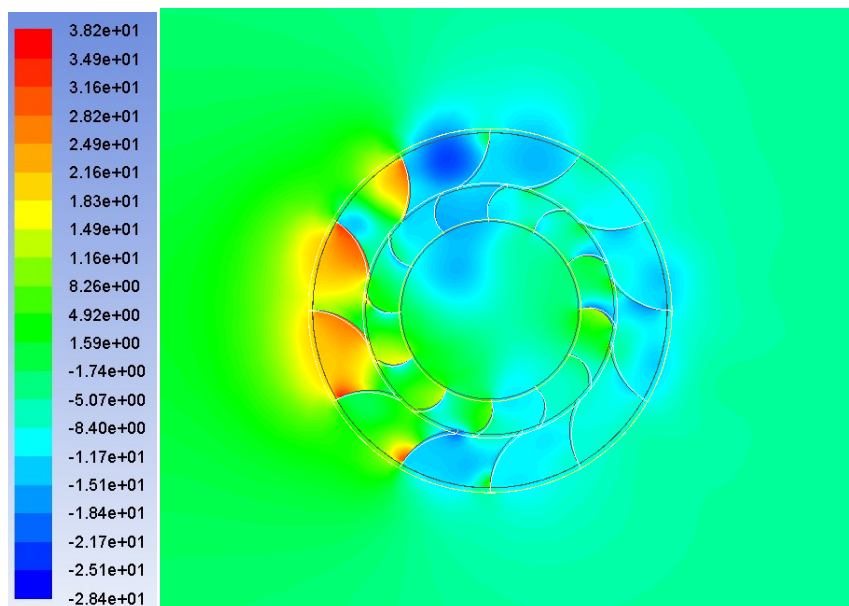
Figure 5.35(a) Pressure variations at 0° angular position of the VAWT having a height of 0.5m

Optimal Design of a Micro Vertical Axis Wind Turbine for Sustainable Urban Environment
By Kyooseon Park, School of Computing and Engineering, University of Huddersfield, UK (2013)

118

Analysing the velocity variations in the vicinity of the VAWT having a height of 0.5m (figure 5.35(b)), it can be seen, in comparison with figure 5.33(b), that the flow velocity is considerably lower on the windward side of the VAWT for h=0.5. Furthermore, the flow velocity on the upper section of the VAWT is relatively higher than for the VAWT having a height of 0.25m.
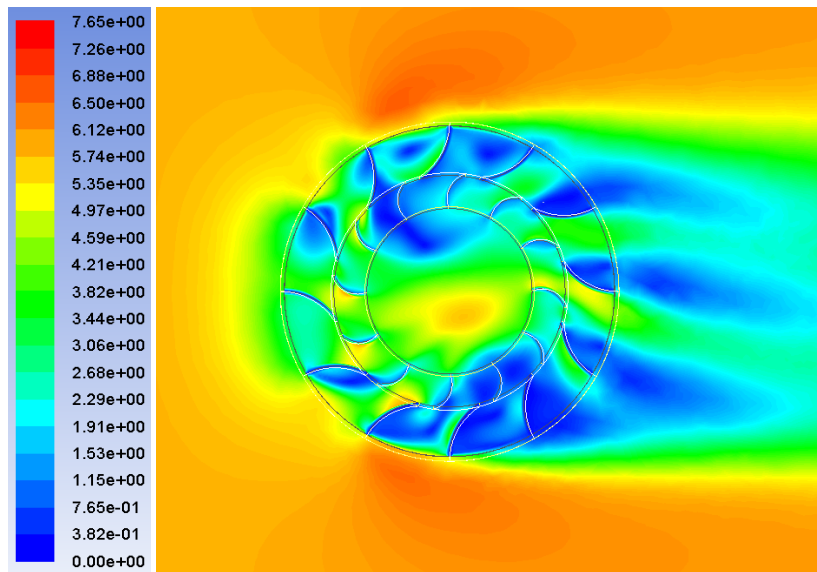
Figure 5.35(b) Velocity variations at 0° angular position of the VAWT having a height of 0.5m

Figure 5.36 depicts the instantaneous torque output of the VAWT having a height of 0.5m. It can be seen, in comparison with figure 5.34, that the torque output of the VAWT has increased substantially. Furthermore, it can be seen that there are two sets of distinct peaks in the torque output signals. The amplitude of the higher peaks decreases with the increase in the angular position of the VAWT, whereas, the amplitude of the lower peaks increases. Hence, the torque output is highly non-uniform for h=0.5m.
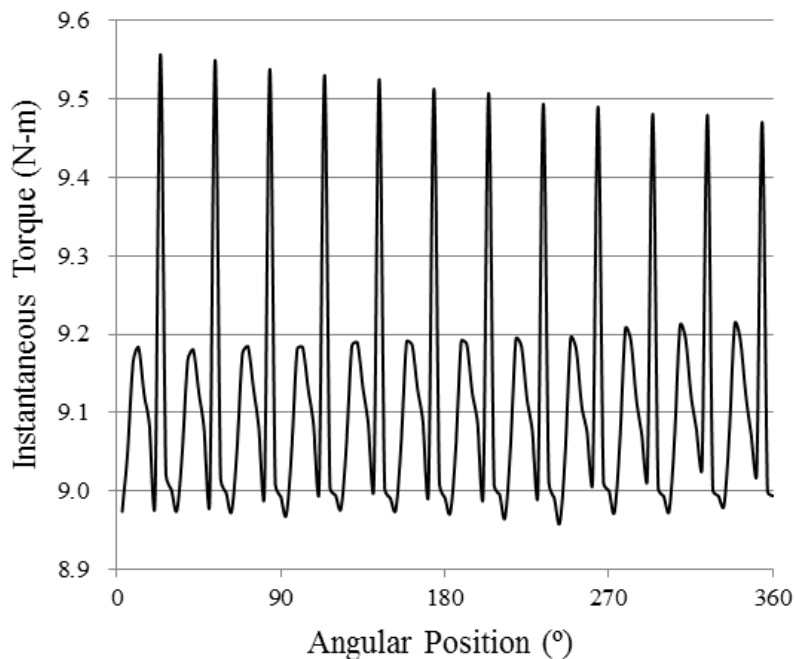
Figure 5.36 Instantaneous torque output of the VAWT having a height of 0.5m

Optimal Design of a Micro Vertical Axis Wind Turbine for Sustainable Urban Environment
By Kyooseon Park, School of Computing and Engineering, University of Huddersfield, UK (2013)
119

Figure 5.37(a) depicts the variations in the pressure for the VAWT having a height of 0.75m. It can be seen by comparing figures 5.37(a) and 5.35(a) that the area of thigh pressure on the windward side of the VAWT is bigger for h=0.75m. Furthermore, pressure on the upper section of the VAWT is considerably higher than observed in case of h=0.5m.
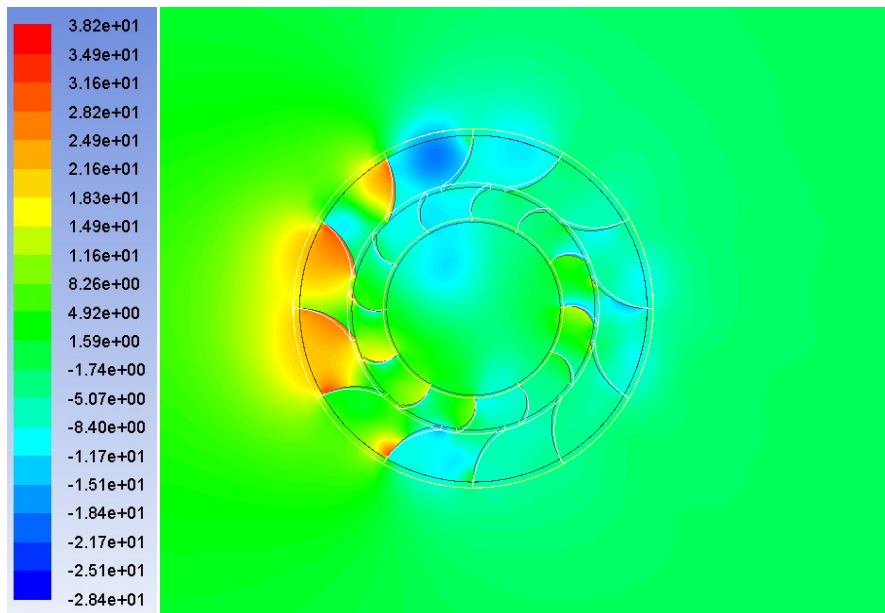
Figure 5.37(a) Pressure variations at 0⁰ angular position of the VAWT having a height of 0.75m

Analysing the velocity variations in the vicinity of the VAWT having a height of 0.75m (figure 5.37(b)), it can be seen, in comparison with figure 5.35(b), that the flow velocity is considerably higher in the core region of the VAWT for h=0.75. Furthermore, the flow velocity on the upper and lower sections of the VAWT is relatively higher than for the VAWT having a height of 0.5m.
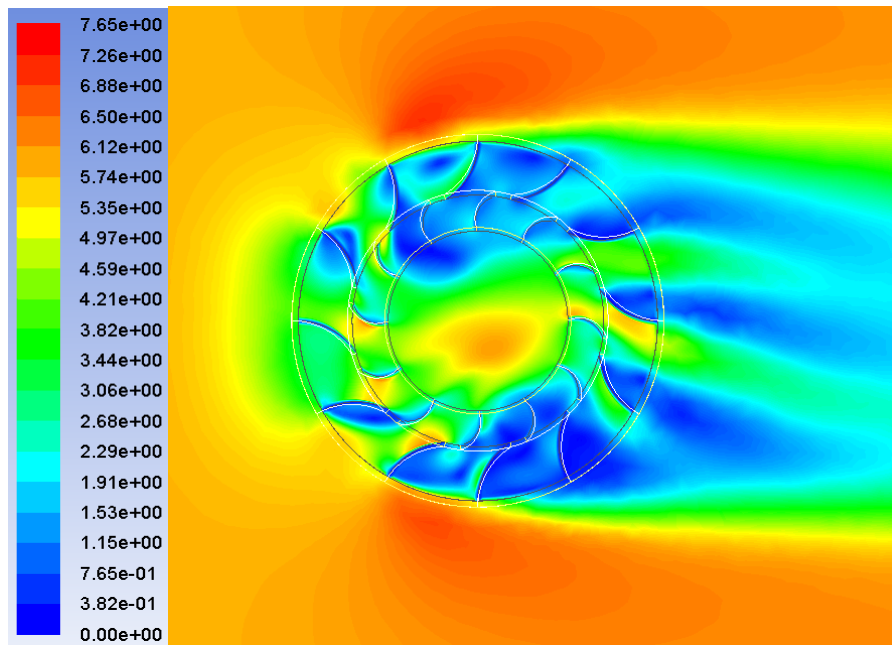
Figure 5.37(b) Velocity variations at 0⁰ angular position of the VAWT having a height of 0.75m

Optimal Design of a Micro Vertical Axis Wind Turbine for Sustainable Urban Environment
By Kyooseon Park, School of Computing and Engineering, University of Huddersfield, UK (2013)

120

Figure 5.38 depicts the instantaneous torque output of the VAWT having a height of 0.75m. It can be seen, in comparison with figure 5.36, that the torque output of the VAWT has increased considerably. Furthermore, it can be seen that there are two sets of distinct peaks in the torque output signals in this case as well. The amplitude of the higher peaks decreases with the increase in the angular position of the VAWT, whereas, the amplitude of the lower peaks increases. Hence, the torque output is also highly non-uniform for h=0.75m.
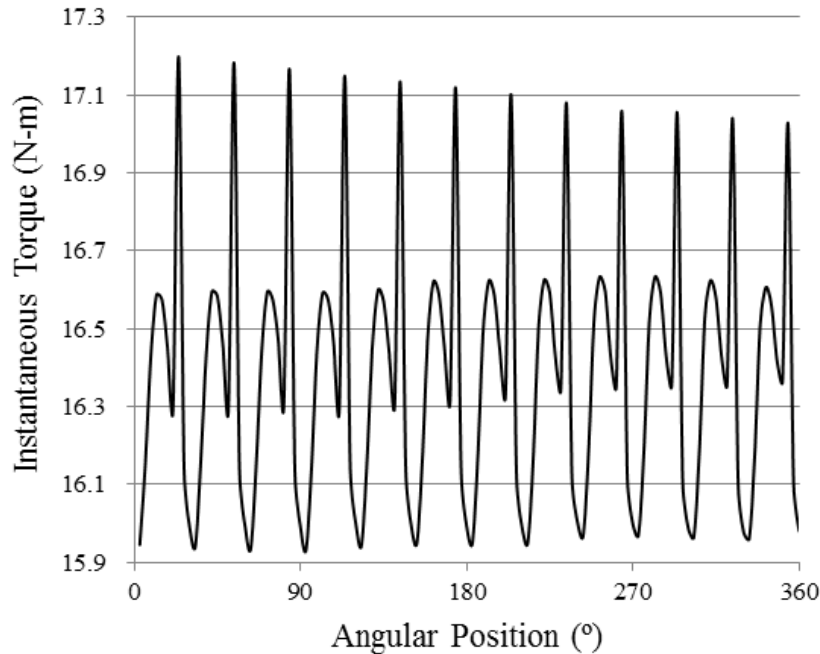
Figure 5.38 Instantaneous torque output of the VAWT having a height of 0.75m

Figure 5.39(a) depicts the variations in the pressure for the VAWT having a height of 1m. It can be seen by comparing figures 5.39(a) and 5.37(a) that the area of thigh pressure on the windward side of the VAWT is bigger for h=1m. Furthermore, pressure on the upper section of the VAWT is considerably lower than observed in case of h=0.75m.
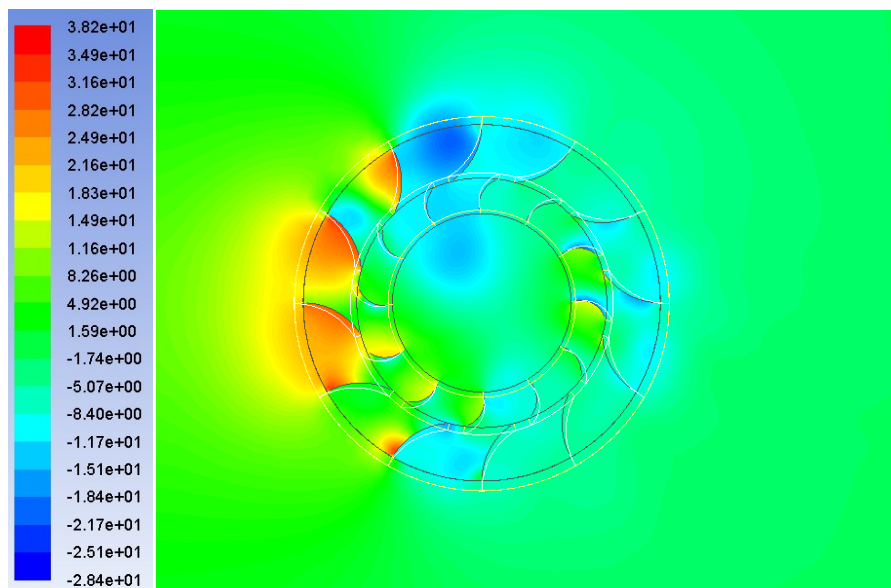
Figure 5.39(a) Pressure variations at 0° angular position of the VAWT having a height of 1m

Optimal Design of a Micro Vertical Axis Wind Turbine for Sustainable Urban Environment
By Kyooseon Park, School of Computing and Engineering, University of Huddersfield, UK (2013)
121

Analysing the velocity variations in the vicinity of the VAWT having a height of 1m (figure 5.39(b)), it can be seen, in comparison with figure 5.37(b), that the flow velocity is considerably higher in the core region and the flow passages on the windward side of the VAWT. Furthermore, the flow velocity on the upper and lower sections of the VAWT is relatively higher than for the VAWT having a height of 0.75m.
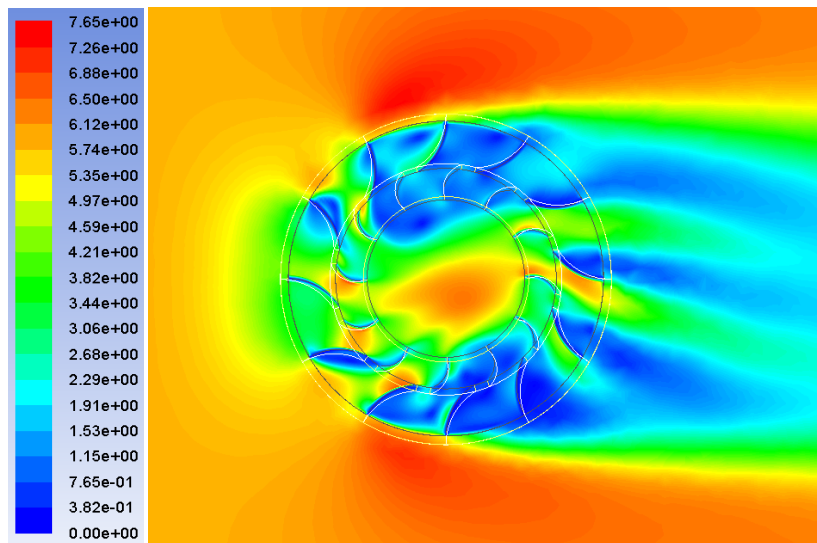
Figure 5.39(b) Velocity variations at 0° angular position of the VAWT having a height of 1m

Figure 5.40 depicts the instantaneous torque output of the VAWT having a height of 1m. It can be seen, in comparison with figure 5.38, that the torque output of the VAWT has increased appreciably. Furthermore, it can be seen that there are two sets of distinct peaks in the torque output signals. The amplitude of the higher peaks increases with the increase in the angular position of the VAWT, whereas, the amplitude of the lower peaks decreases. This trend is opposite to the one observed for h=0.5m and 0.75m. Hence, the torque output is also highly non-uniform for h=1m.
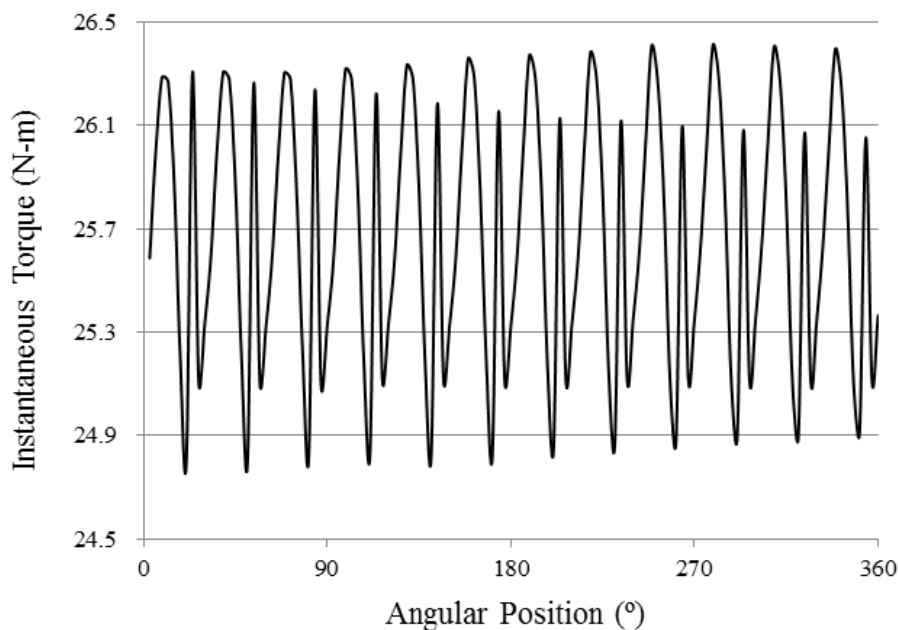
Figure 5.40 Instantaneous torque output of the VAWT having a height of 1m

Table 5.5 summarises the statistical results for the torque outputs of the VAWTs having different heights. It can be seen that as the height of the VAWT increases, the average torque output increases. Furthermore, the standard deviation in the torque output is highest for h=1m. It is also noteworthy that both the maximum and the minimum torques increase as the height of the VAWT increases.

Table 5.5 Effect of the height of the VAWT on its performance output

Height (m)	Tmin (N-m)	Tmax (N-m)	Tavg (N-m)	Pavg (N-m)	Std. Dev.
0.25	3.79	4.29	4.07	6.98	0.20
0.5	8.96	9.56	9.11	15.62	0.15
0.75	15.93	17.20	22.14	28.08	0.33
1	24.80	26.41	25.67	44.01	0.51

Figure 5.41 depicts the instantaneous torque outputs of the VAWTs having different heights. It can be seen that as the height of the VAWT increases, the torque output also increases significantly. Moreover, it has been observed that for h=1m, the variations in the torque output are highest as expected.
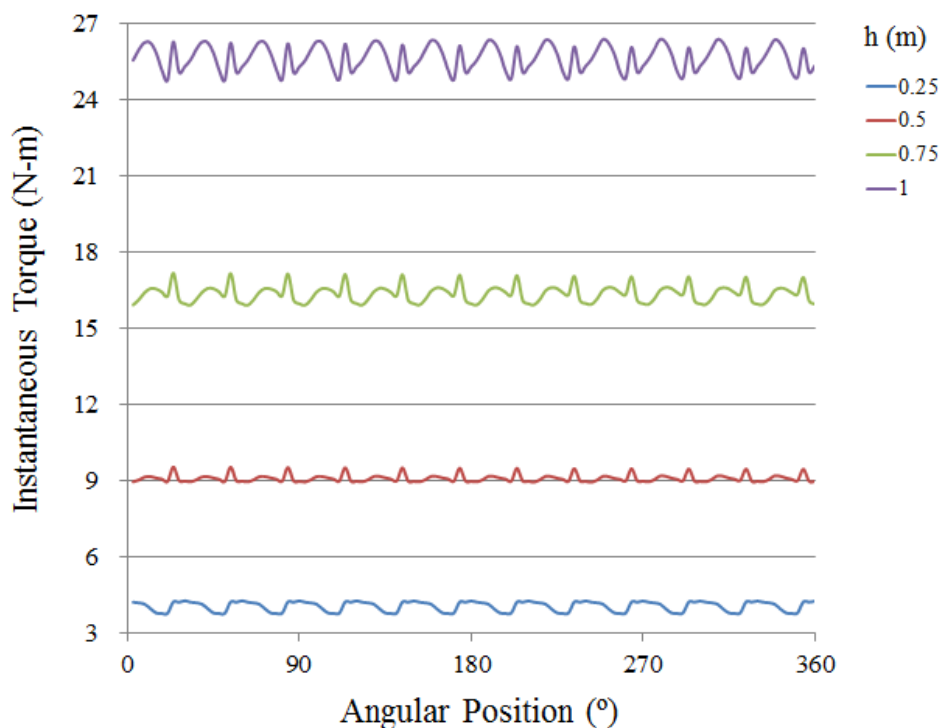
Figure 5.41 Instantaneous torque output of the VAWT having different heights

Figure 5.42 depicts the effect of the height of the VAWT on its performance output. It can be seen that as the height of the VAWT increases, both the torque and the power outputs VAWT increase. Hence, in the present study, the optimised design of the VAWT is the one that has a height of 1m. Furthermore, it can be seen that there are non-linearities in the curves that arises due to complex and transient interactions between the blades.

Optimal Design of a Micro Vertical Axis Wind Turbine for Sustainable Urban Environment
By Kyooseon Park, School of Computing and Engineering, University of Huddersfield, UK (2013)
123
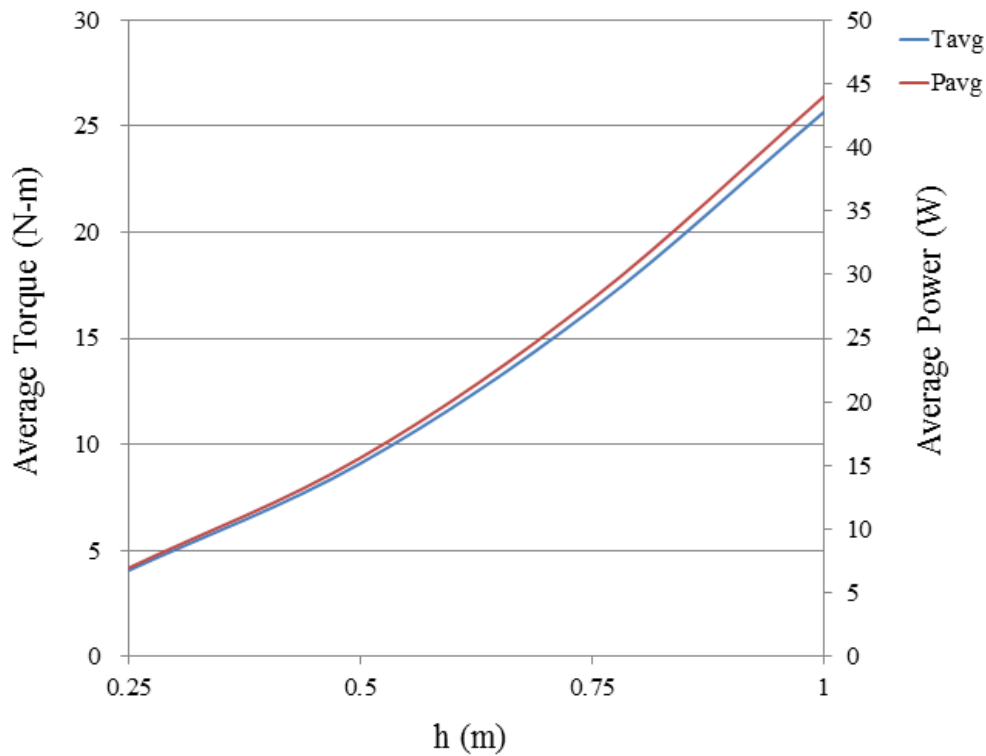
Figure 5.42 Effect of the height of the VAWT on its performance output

5.6. Expression for C_T based on Number of Blades

A detailed investigation into the effect of the number of blades on the performance output of a VAWT has been carried out in sections 5.1 and 5.2. The trends show that increase in the number of both the rotor and the stator blades increases the torque output of the VAWT. In order to quantify these results such that they can be used in the design process of a VAWT, multiple regression analysis has been carried out on the results obtained from CFD simulations. The two variables included in the study are the number of rotor and stator blades, whereas the output parameter has been chosen to be the torque coefficient.

After performing multiple regression analysis on the results obtained from CFD simulations (presented in Appendix 2), the following equation for the torque coefficient has been developed:

$$C_T = 0.056 \ NRB^{0.7838} \ NSB^{0.717} \tag{5.1}$$

where NSB and NRB corresponds to number of stator blades and number of rotor blades respectively.

In order to check the validity of equation (5.1), the CFD results for C_T have been compared with C_T calculated from equation (5.1). It has been shown in figure 5.43 that more than 90% of the data lies within ±10% error band. The errors are due to the numerical diffusion within the solver and interaction between the rotor and stator blades.

Optimal Design of a Micro Vertical Axis Wind Turbine for Sustainable Urban Environment
By Kyooseon Park, School of Computing and Engineering, University of Huddersfield, UK (2013)

124
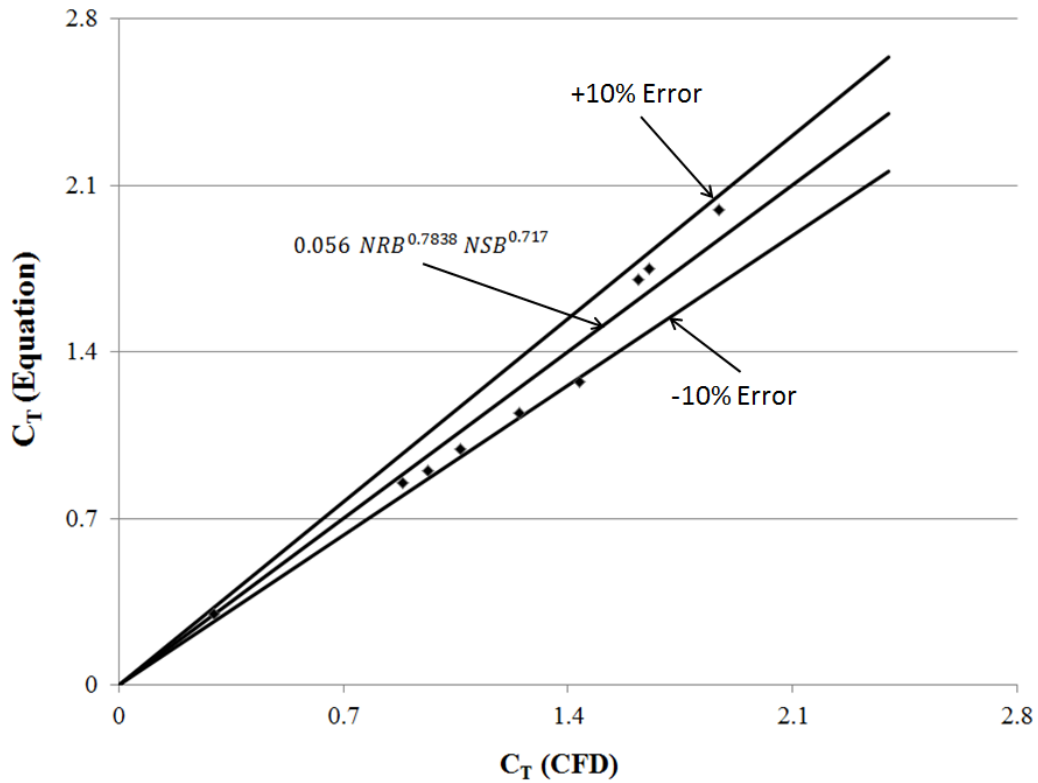
Figure 5.43 Validation of the equation (5.1)

The equation to calculate torque output of the VAWT will then be:

$$T = 0.028\,\rho\,A\,r_r\,v^2\,(NRB^{0.7838}\,NSB^{0.717})$$ (5.2)

5.6.1. Validation of Equation 5.2

Calculate the number of blades required in a Vertical Axis Wind Turbine for the following data:

A	2m^2	v	4m/sec	r$_r$	0.7m
T	32N-m				

Solution: Using equation (5.2):

$$32 = 0.028 * 1.225 * 2 * 0.7 * 16 * (NRB^{0.7838} * NSB^{0.717})$$

$$NRB = 12 \quad and \quad NSB = 12$$

Optimal Design of a Micro Vertical Axis Wind Turbine for Sustainable Urban Environment
By Kyooseon Park, School of Computing and Engineering, University of Huddersfield, UK (2013)

125

5.7. Expression for C_T based on Size of Rotor/Stator

A detailed investigation into the effect of the size of rotor and stator on the performance output of a VAWT has been carried out in sections 5.3 and 5.4. The trends show that increase in the size of both the rotor and the stator increases the torque output of the VAWT. In order to quantify these results such that they can be used in the design process of a VAWT, multiple regression analysis has been carried out on the results obtained from CFD simulations. The two variables included in the study are the size of rotor and stator, whereas the output parameter has been chosen to be the torque coefficient.

After performing multiple regression analysis on the results obtained from CFD simulations (tables 5.3 and 5.4), the following equation for the torque coefficient has been developed:

$$C_T = 10.23 \left(\frac{r_r - r_c}{r_t}\right)^{0.519} \left(\frac{r_s - r_r}{r_t}\right)^{0.744} \tag{5.3}$$

where r_s, r_r and r_t corresponds to radius of stator, radius of rotor and total radius of the VAWT respectively. Note that $r_s = r_t$.

In order to check the validity of equation (5.3), the CFD results for C_T have been compared with C_T calculated from equation (5.3). It has been shown in figure 5.44 that all of the data lies within ±5% error band.
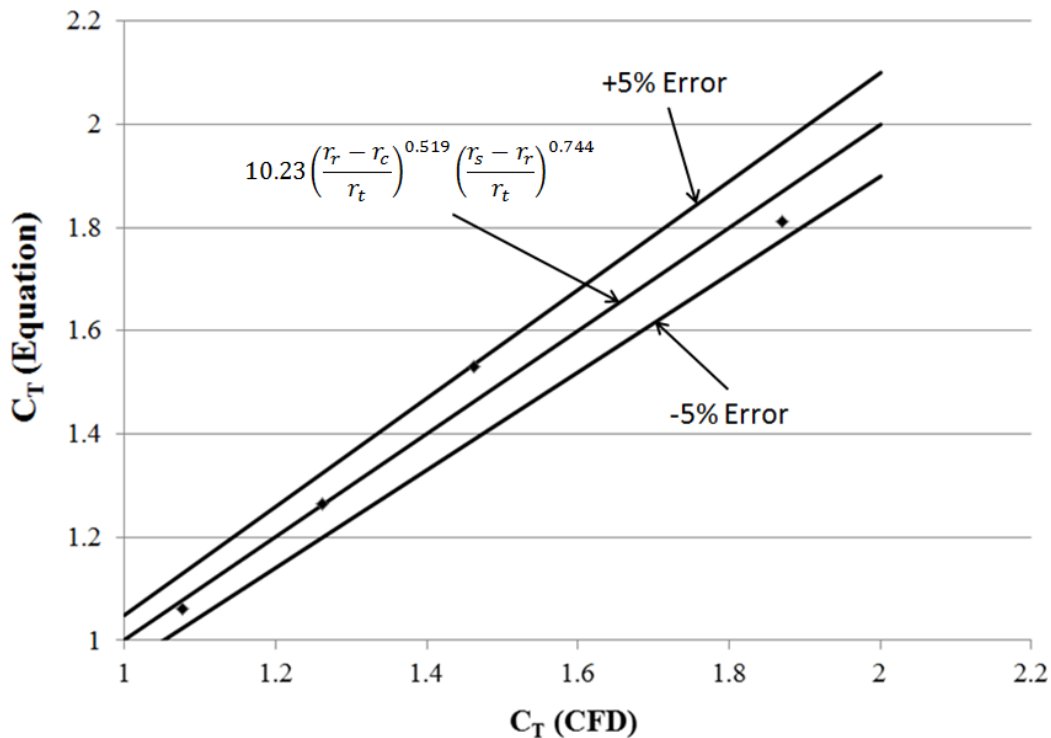
Figure 5.44 Validation of the equation (5.3)

The equation to calculate torque output of the VAWT will then be:

$$T = 5.115 \, \rho \, A \, r_r \, v^2 \left(\frac{r_r - r_c}{r_t}\right)^{0.519} \left(\frac{r_s - r_r}{r_t}\right)^{0.744} \tag{5.4}$$

Optimal Design of a Micro Vertical Axis Wind Turbine for Sustainable Urban Environment
By Kyooseon Park, School of Computing and Engineering, University of Huddersfield, UK (2013)

126

5.7.1. Validation of Equation 5.4

Calculate the size of the rotor and the stator section of a Vertical Axis Wind Turbine using the following data:

A	2m^2	v	4m/sec	T	21N-m

Solution: Using equation (5.4):

$$21 = 5.115 * 1.225 * 2 * r_r * 16 * \left(\frac{r_r - r_c}{r_t}\right)^{0.519} \left(\frac{r_s - r_r}{r_t}\right)^{0.744}$$

$$r_c = 0.5m \qquad r_r = 0.7m \quad \text{and} \quad r_s = r_t = 0.9m$$

5.8. Expression for C_T based on Height of the VAWT

A detailed investigation into the effect of the height of the VAWT on its performance output has been carried out in sections 5.5. The trends show that increase in the size of the height of the VAWT increases the torque output of the VAWT. In order to quantify the results such that they can be used in the design process of a VAWT, multiple regression analysis has been carried out on the results obtained from CFD simulations.

After performing multiple regression analysis on the results obtained from CFD simulations (table 5.5), the following equation for the torque coefficient has been developed:

$$C_T = 2.0167 \left(\frac{h}{r_t}\right)^{1.405} \tag{5.5}$$

where h si the height of the VAWT. In order to check the validity of equation (5.5), the CFD results for C_T have been compared with C_T calculated from equation (5.5). It has been shown in figure 5.45 that all of the data lies within ±10% error band. The errors are due to the numerical diffusion within the solver and interaction between the rotor and stator blades. The equation to calculate torque output of the VAWT will then be:

$$T = 1.0084 \, \rho \, A \, r_r \, v^2 \left(\frac{h}{r_t}\right)^{1.405} \tag{5.6}$$

5.8.1. Validation of Equation 5.6

Calculate the height of the Vertical Axis Wind Turbine using the following data:

A	2m^2	v	4m/sec	T	22N-m
r_r	0.7m	r_t	1m		

Optimal Design of a Micro Vertical Axis Wind Turbine for Sustainable Urban Environment
By Kyooseon Park, School of Computing and Engineering, University of Huddersfield, UK (2013)
127

Solution: Using equation (5.6):

$$22 = 1.0084 * 1.225 * 2 * 0.7 * 16 * \left(\frac{h}{1}\right)^{1.405}$$

$$h = 0.85m$$
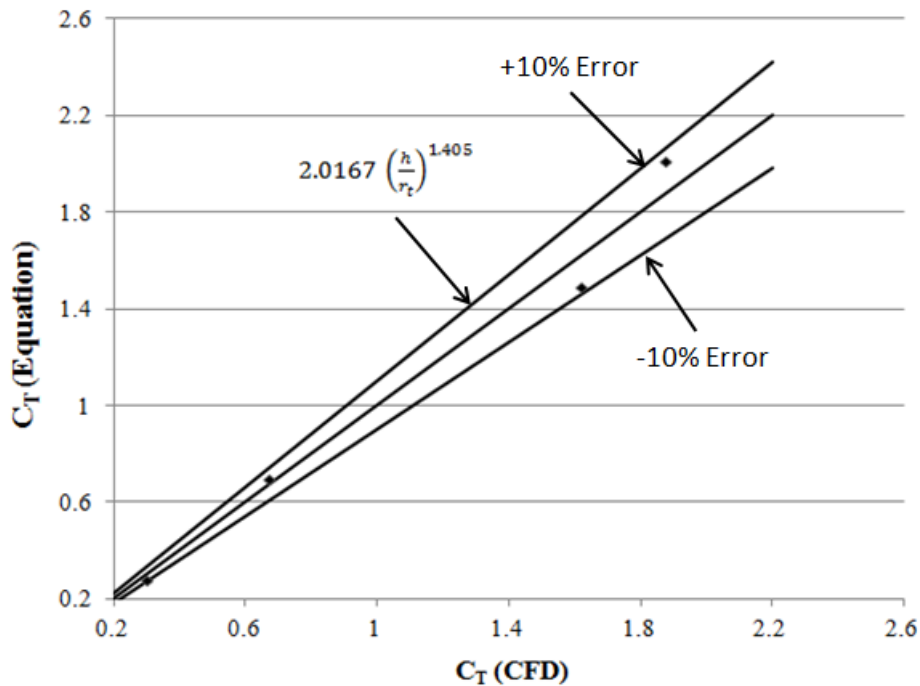
Figure 5.45 Validation of the equation (5.5)

5.9. Torque Prediction Model

Various semi-empirical correlations have been developed in the previous sections and Chapter 4. They deal with the blade angles, number of rotor/stator blades, size of rotor/stator blades and the height of the VAWT separately. However, VAWT designers are in need of a generic design tool that accommodates all these different parameters together. Hence, in order to meet the designer's requirements, a generic torque prediction model has been developed here for VAWTs.

After performing multiple regression analysis on the results obtained from CFD simulations, the following equation for the torque coefficient has been developed:

$$C_T = \frac{0.622 \left(\frac{\alpha}{\beta}\right)^{0.000106} \text{NSB}^{0.586} \text{NRB}^{0.653} \left(\frac{r_r - r_c}{r_t}\right)^{0.6168} \left(\frac{r_s - r_r}{r_t}\right)^{1.233} \left(\frac{h}{r_t}\right)^{1.37}}{\left(\frac{\delta}{\beta}\right)^{0.236} \left(\frac{\gamma}{\beta}\right)^{0.134}}$$

(5.7)

In order to check the validity of equation (5.7), the CFD results for C_T have been compared with C_T calculated from equation (5.7). It has been shown in figure 5.46 that more than 90% of the data lies within ±10% error band. The errors are due to the numerical diffusion within the solver and interaction between the rotor and stator blades.

Optimal Design of a Micro Vertical Axis Wind Turbine for Sustainable Urban Environment
By Kyooseon Park, School of Computing and Engineering, University of Huddersfield, UK (2013)

128
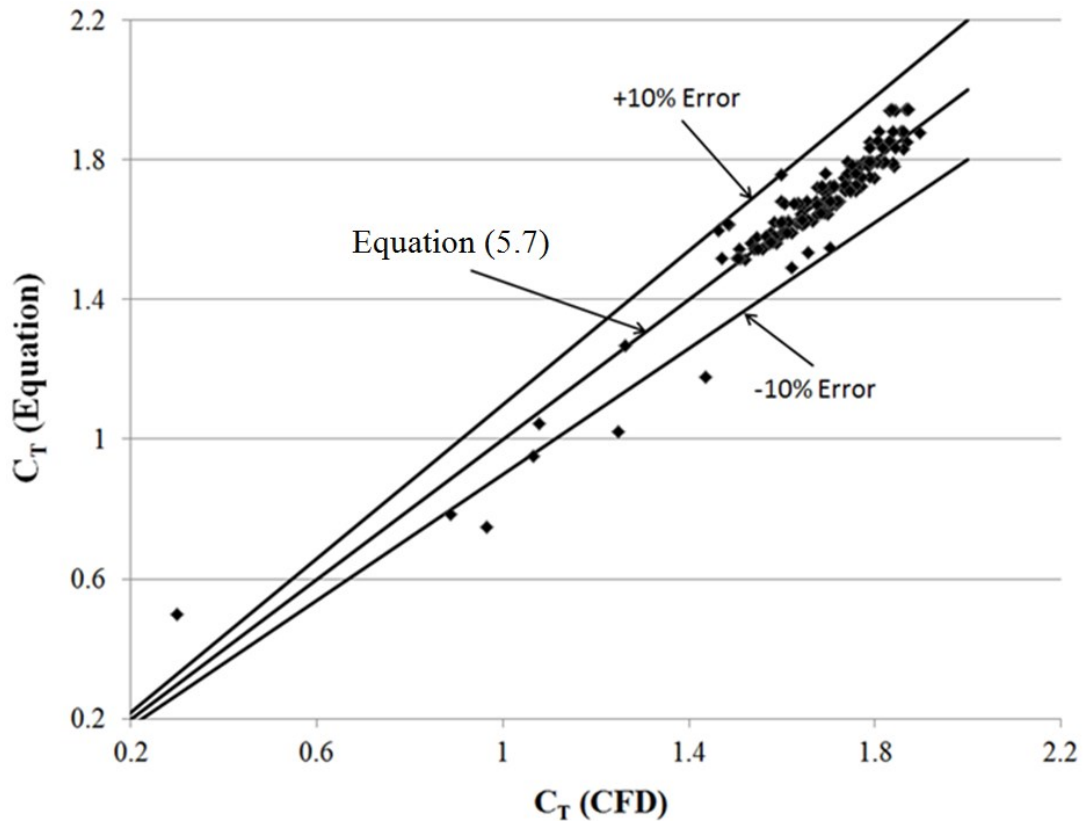
Figure 5.46 Validation of the equation (5.7)

The equation to calculate torque output of the VAWT will then be:

$$T = 0.311 \, \rho \, A \, r_r \, v^2 \left(\frac{\left(\frac{\alpha}{\beta}\right)^{0.000106} NSB^{0.586} \, NRB^{0.653}\left(\frac{r_r-r_c}{r_t}\right)^{0.6168}\left(\frac{r_s-r_r}{r_t}\right)^{1.233}\left(\frac{h}{r_t}\right)^{1.37}}{\left(\frac{\delta}{\beta}\right)^{0.236}\left(\frac{\gamma}{\beta}\right)^{0.134}} \right) \quad (5.8)$$

5.9.1. Design Example

Calculate the torque output of a Vertical Axis Wind Turbine using the following data:

v   4m/sec   T   22N-m

Solution: In order to design a VAWT that can generate 22N-m of torque, various geometrical parameters need to be found out such as blade angles, number of blades and the size of the VAWT. Hence, a step by step procedure has been presented here:

1. Fix α to its optimum value of 16.689⁰.

2. From design consideration, β is taken as 90⁰.

Optimal Design of a Micro Vertical Axis Wind Turbine for Sustainable Urban Environment
By Kyooseon Park, School of Computing and Engineering, University of Huddersfield, UK (2013)

129

3. From the cost and installation space considerations, decide what VAWT size is acceptable. Here, take both the height (h) and the total radius (r_t) of the VAWT as 1m.

4. Within the fixed overall size of the VAWT, keeping in mind the installation space required for drive shaft and the torque transducers etc. decide the size of the rotor and the core sections. Here, take r_r=0.7m and r_c=0.5m.

5. Fix the number of rotor and stator blades based on the average wind velocity at that location and the start-up torque required at that wind velocity. Here, 12 rotor and 12 stator blades have been taken (because this set generates maximum torque output).

6. Put the values calculated in steps 1 to 5 in equation (5.8). Using trial and error (or iterative method), calculate the sets of δ and γ that will generate the required torque output from the VAWT. The complete set of parameters that will generate torque output of 22N-m are presented in table 5.6.

Table 5.6 Predicted Geometrical Entities of the VAWT

h	1m
r_c	0.5m
r_r	0.7m
r_s	1m
α	16.689°
δ	35.357°
γ	35.2°
NRB	12
NSB	12

Scenario # 1: In the design example presented above, suppose the height of the VAWT is fixed at 0.75m, then the values of the geometric features that will result in a torque output of 22N-m, are presented in table 5.7:

Table 5.7 Predicted Geometrical Entities of the VAWT for a height of 0.75m

r_c	0.26m
r_r	0.7m
r_s	1m
α	16.689°
δ	22.357°
γ	18.2°
NRB	12
NSB	12

Optimal Design of a Micro Vertical Axis Wind Turbine for Sustainable Urban Environment
By Kyooseon Park, School of Computing and Engineering, University of Huddersfield, UK (2013)
130

Scenario # 2: In the design example presented above, suppose the number of stator blades is 8, then the values of the geometric features that will result in a torque output of 22N-m, are presented in table 5.8:

Table 5.8 Predicted Geometrical Entities of the VAWT for 8 Stator Blades

r_c	0.485m
r_r	0.7m
r_s	1m
α	16.689°
δ	22.357°
γ	18.2°
NRB	12
h	1m

Scenario # 3: In the design example presented above, suppose δ and γ are fixed at 32.357° and 28.2°, then the values of the geometric features that will result in a torque output of 22N-m, are presented in table 5.9:

Table 5.9 Predicted Geometrical Entities of the VAWT for 8 Stator Blades δ=25.357° and γ=20.2°

r_c	0.5m
r_r	0.64m
r_s	0.95m
α	1.689°
NRB	12
NRB	12
h	1m

Scenario # 4: In the design example presented above, suppose r_t is fixed at 0.9m, then the values of the geometric features that will result in a torque output of 22N-m, are presented in table 5.10:

Table 5.10 Predicted Geometrical Entities of the VAWT for r_t=0.9m

h	1m
r_r	0.7m
r_c	0.475m
α	16.689°
δ	22.357°
γ	18.2°
NRB	12
NSB	12

Optimal Design of a Micro Vertical Axis Wind Turbine for Sustainable Urban Environment
By Kyooseon Park, School of Computing and Engineering, University of Huddersfield, UK (2013)

131

5.10. Summary

A detailed investigation into the effect of the number of blades and size of the rotor/stator, on the performance output of the vertical axis wind turbine has revealed the following results:

- Increase in the number of rotor blades increases the performance output of the VAWT

- Increase in the number of stator blades increases the performance output of the VAWT

- Increase in the size of the rotor increases the performance output of the VAWT

- Increase in the size of the stator increases the performance output of the VAWT

- Increase in the height of the VAWT increases its performance output

Furthermore, a novel torque prediction model has been developed in this chapter.

Optimal Design of a Micro Vertical Axis Wind Turbine for Sustainable Urban Environment
By Kyooseon Park, School of Computing and Engineering, University of Huddersfield, UK (2013)

132

CHAPTER 6
Condition Based Monitoring of VERTICAL AXIS WIND TURBINES

Condition based health monitoring of vertical axis wind turbines has been an important topic of research for the past couple of decades. However, CFD based techniques have not been employed to detect the faults in the blades of a VAWT. Hence, condition monitoring aspect of CFD, applied to vertical axis wind turbines, is presented in this chapter. A detailed analysis of the results, obtained after performing CFD simulations, has been carried out in order to understand the complex flow structure in defective VAWTs. The effect of various geometric faults on the performance output of a VAWT has been investigated. It has been shown that CFD can be used as an effective tool to detect the faults in the blades of a VAWT.

Optimal Design of a Micro Vertical Axis Wind Turbine for Sustainable Urban Environment
By Kyooseon Park, School of Computing and Engineering, University of Huddersfield, UK (2013)

133

6.1. Introduction

Recent advancements in computational modelling namely CFD have allowed for complex simulation of fluid flow systems and in particular wind turbines. Although the use of CFD is relatively new its applications are developing with recent advancements made in the area of optimisation and diagnostics. Given improvements in computational hardware and its use as a simulation based condition monitoring tool is becoming more realistic. This therefore has the potential to reduce diagnostic costs from minimizing the amount of instrumentation required when obtaining machine signatures.

6.2. Effect of a Missing Rotor Blade

Figure 6.1(a & b) depicts the pressure and velocity variations in the vicinity of the VAWT having 12 rotor blades while the number of stator blades are kept constant at 12. This VAWT configuration has been termed here as healthy VAWT. It can be seen in figure 6.1(a) that the windward side of the VAWT possess very high pressure while the leeward side has comparatively low pressure. Furthermore, it can be seen in figure 6.1(b) that the flow velocity is high on the windward side and the core region, while it is comparatively lower on the leeward side of the VAWT. It has also been observed that the flow accelerates in the passages formed between the rotor and the stator blades on the windward side of the VAWT. These passages are formed due to the orientation and the angular position of the rotor blades.
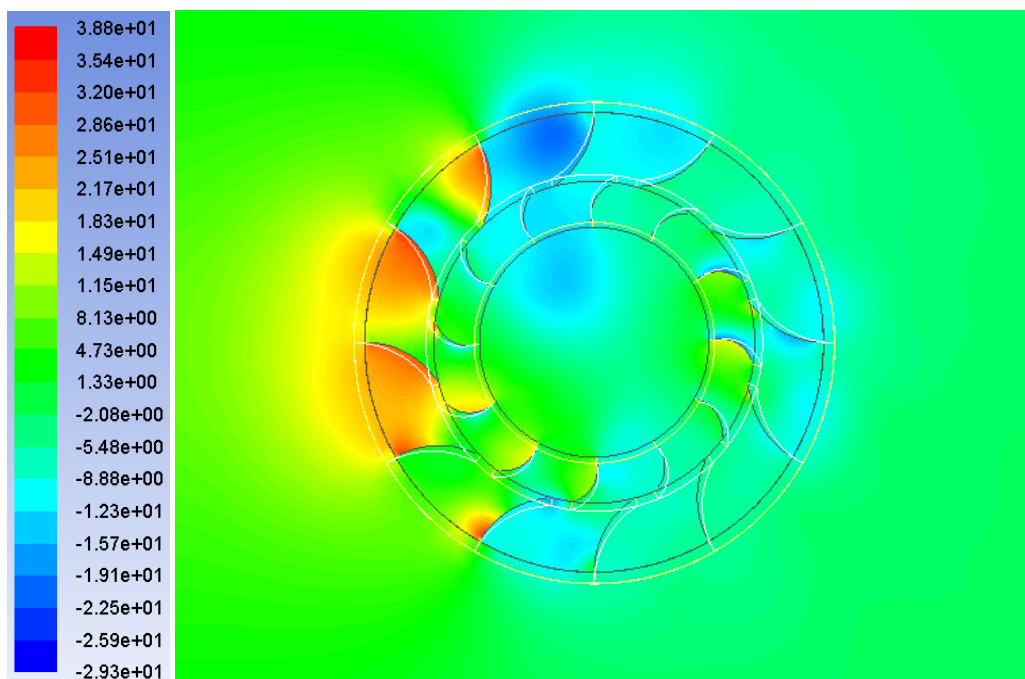
Figure 6.1 (a) Pressure variations at 0° angular position of the healthy VAWT

Optimal Design of a Micro Vertical Axis Wind Turbine for Sustainable Urban Environment
By Kyooseon Park, School of Computing and Engineering, University of Huddersfield, UK (2013)
134
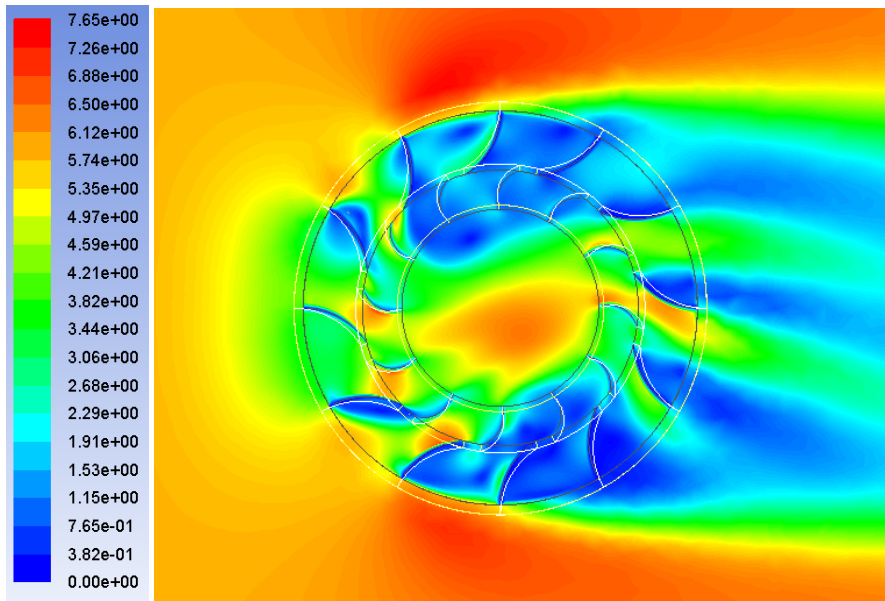
Figure 6.1 (b) Velocity variations at 0⁰ angular position of the healthy VAWT

Figure 6.2 depicts the instantaneous torque output of the healthy VAWT having 12 rotor blades. It can be seen that there are additional lower peaks, together with the expected 12 higher peaks corresponding to 12 rotor blades. Furthermore, it is observed that as the angular position of the VAWT increases, the amplitude of these lower peaks decreases.
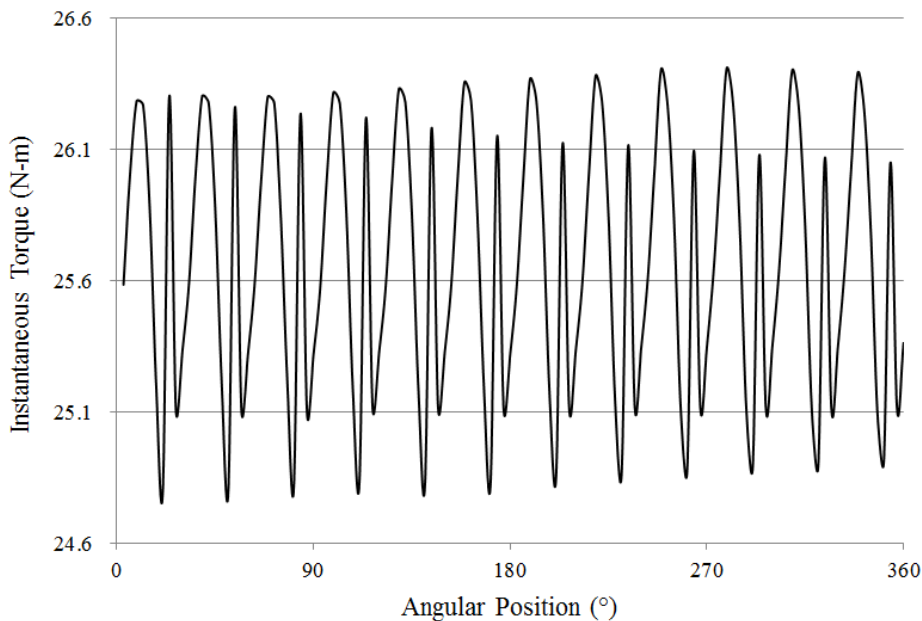
Figure 6.2 Instantaneous torque output for healthy VAWT

6.3(a & b) depicts the pressure and velocity variations in the vicinity of the VAWT having 11 rotor blades. This configuration of the VAWT is termed here as defective VAWT. In comparison with figure 6.1(a), it can be seen in figure 6.3(a) due to a missing rotor blade, the pressure in the rotor region decreases, giving rise to highly non-uniform pressure field.

Optimal Design of a Micro Vertical Axis Wind Turbine for Sustainable Urban Environment
By Kyooseon Park, School of Computing and Engineering, University of Huddersfield, UK (2013)

135
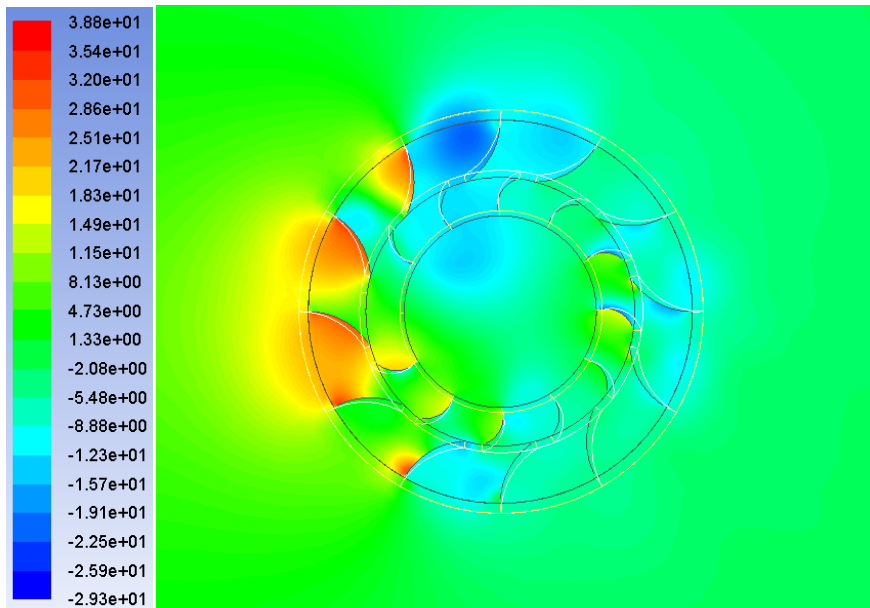
Figure 6.3 (a) Pressure variations at 0⁰ angular position of the defective VAWT missing a rotor blade

Figure 6.3(b), in comparison with figure 6.1(b), shows that due to a missing rotor blade of the VAWT, the flow velocity at the location of the missing rotor blade has reduced significantly. Furthermore, the flow velocity in the core region has also reduced.
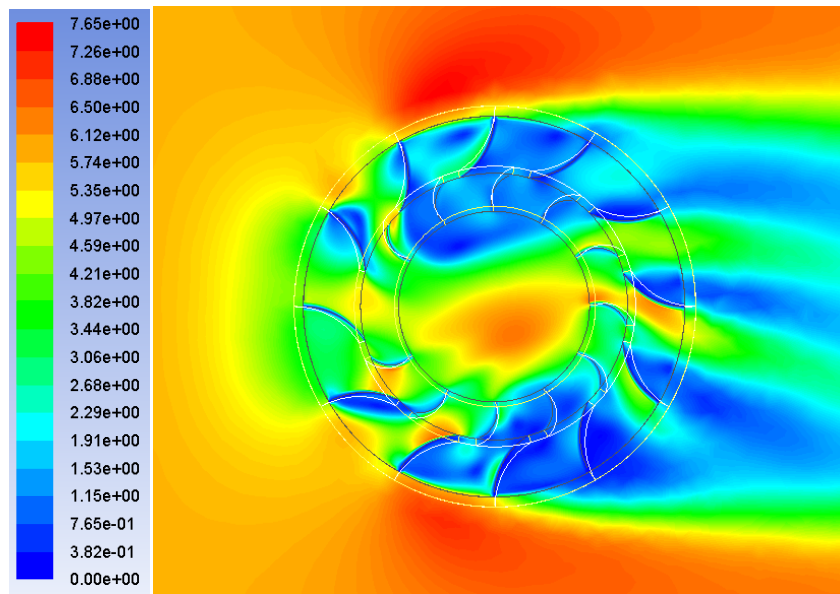
Figure 6.3 (b) Velocity variations at 0⁰ angular position of the defective VAWT missing a rotor blade

Figure 6.4 depicts the variations in the instantaneous torque output of the defective VAWT. It can be seen, in comparison with figure 6.2, that torque variations are non-uniform and there are no distinct peaks and valleys as observed in case of healthy VAWT. The amplitude of torque variations have increased substantially. Further analysing the instantaneous torque output reveals that there as a huge peak at 90⁰ angular position of the VAWT, while at 180⁰, there exists a deep valley.

Optimal Design of a Micro Vertical Axis Wind Turbine for Sustainable Urban Environment
By Kyooseon Park, School of Computing and Engineering, University of Huddersfield, UK (2013)
136
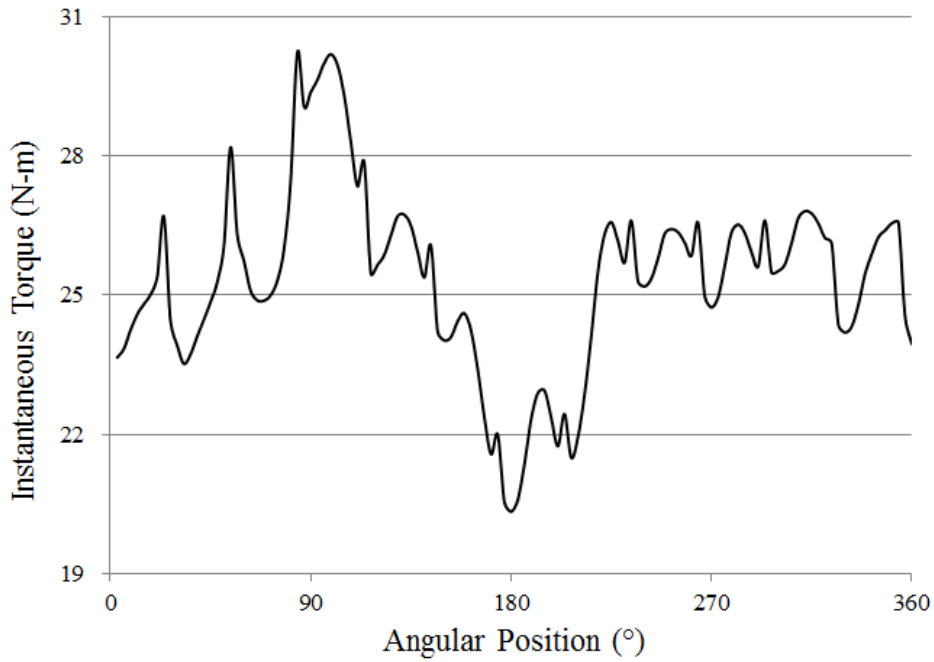
Figure 6.4 Instantaneous torque output for defective VAWT missing a rotor blade

Figure 6.5(a & b) depicts the velocity variations in the defective VAWT at those angular positions where a large peak and valley have been observed in figure 6.4. In comparison with figure 6.3(b), it can be seen that high peak corresponds to the orientation such that the rotor and the stator blades are in-line with each other, whereas, the deep valley exists at that orientation where the rotor blades are exactly in between the stator blades, forming uniform flow passages.
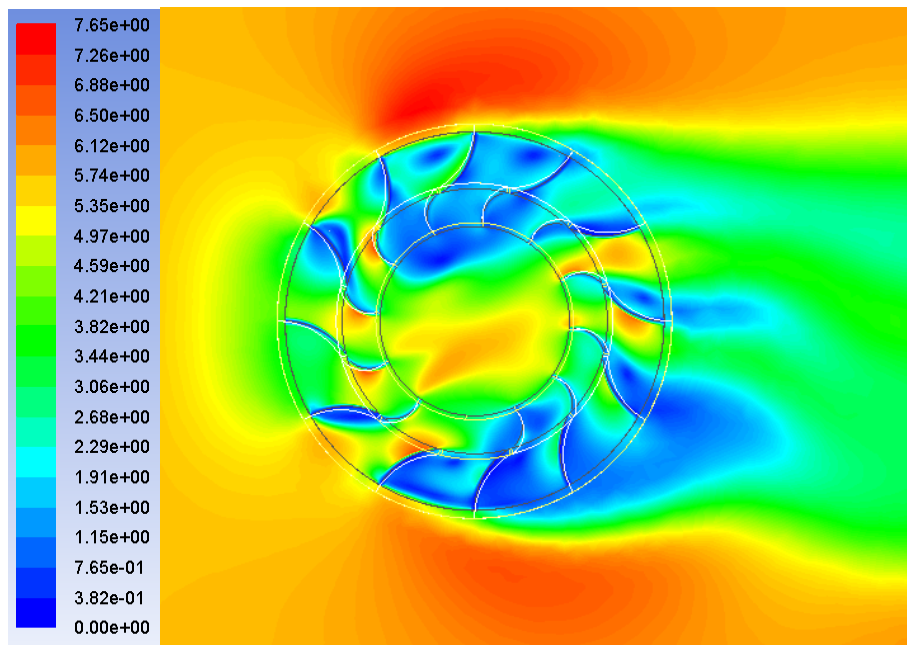
Figure 6.5 (a) Velocity variations at 90° angular position of the defective VAWT missing a rotor blade

Optimal Design of a Micro Vertical Axis Wind Turbine for Sustainable Urban Environment
By Kyooseon Park, School of Computing and Engineering, University of Huddersfield, UK (2013)

137
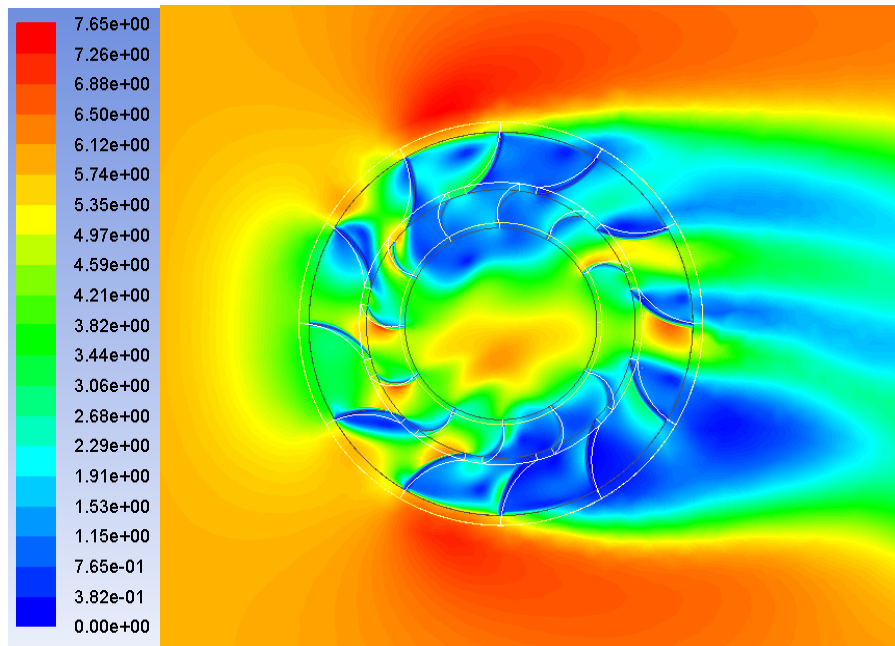
Figure 6.5 (a) Velocity variations at 180° angular position of the defective VAWT missing a rotor blade

Table 6.1 summarises the statistical results for the torque outputs from both the healthy and the defective VAWTs. It can be seen that a missing rotor blade degrades the performance output of the VAWT by decreasing its average torque and power outputs. Furthermore, it also noted that the maximum amplitude (Tmax−Tmin) for defective VAWT is considerably higher than for a healthy VAWT. The variations in the instantaneous torque output of the defective VAWT (figure 6.4) have resulted into a very high standard deviation.

Table 6.1 Effect of a missing rotor blade on the performance output of the VAWT

Number of Stator Blades	Number of Rotor Blades	Tmin (N-m)	Tmax (N-m)	Tavg (N-m)	Std. Dev.	Pavg (W)
12	12	24.80	26.41	25.67	0.51	44.00
12	11	18.20	31.89	25.11	4.76	43.05

Figure 6.6 depicts the instantaneous torque outputs of both the healthy and the defective VAWTs. By comparison, it can be seen that although the difference in the average torque outputs is very small, however, the variations in the torque output of the defective VAWT are quite severe that leads to the generation of vibrations in the VAWT. These unwanted vibrations can damage the structure of the VAWT, hence reducing the total useful remaining life of the VAWT.

Optimal Design of a Micro Vertical Axis Wind Turbine for Sustainable Urban Environment
By Kyooseon Park, School of Computing and Engineering, University of Huddersfield, UK (2013)

138
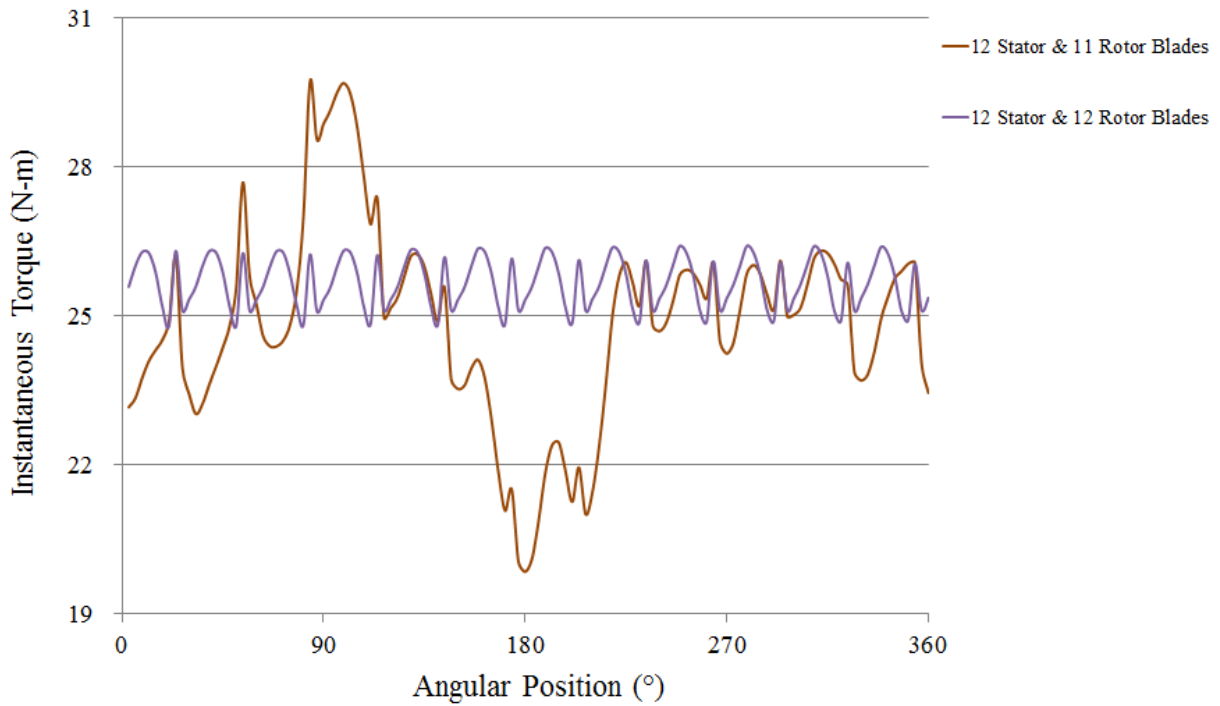
Figure 6.6 Instantaneous torque output of both the healthy and defective VAWTs

Figure 6.7 depicts the average power and torque outputs of both the healthy and the defective VAWTs. It can be seen that the missing rotor blade degrades the performance output of the VAWT by decreasing its average torque and power outputs.
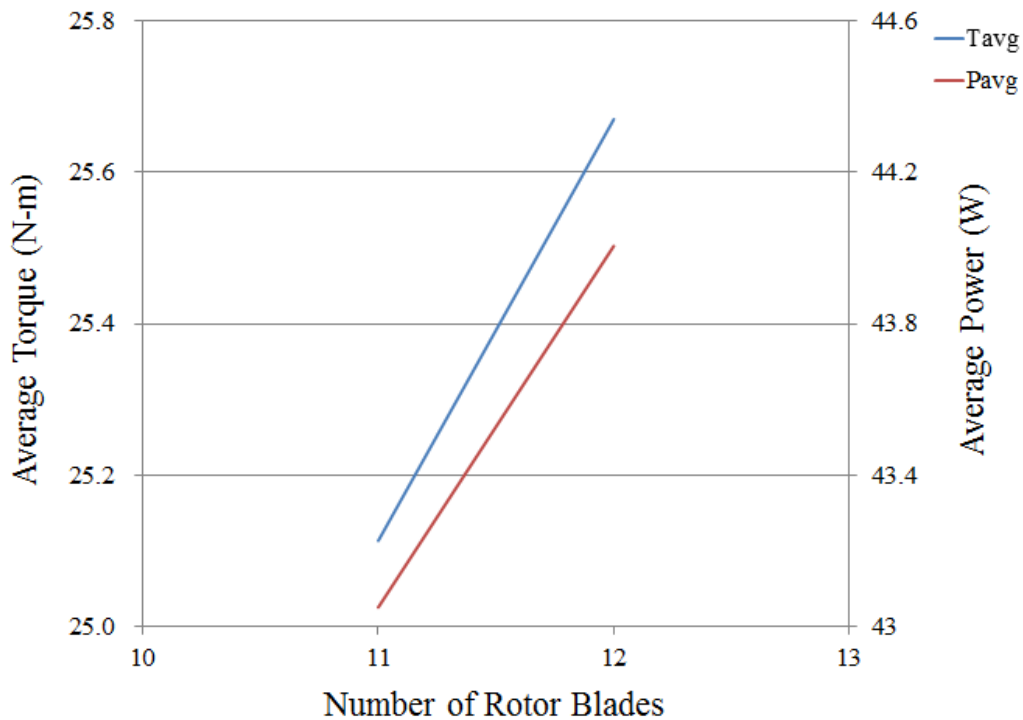
Figure 6.7 Effect of a missing rotor blade on the performance output of the VAWT

Optimal Design of a Micro Vertical Axis Wind Turbine for Sustainable Urban Environment
By Kyooseon Park, School of Computing and Engineering, University of Huddersfield, UK (2013)
139

6.3. Effect of a Missing Stator Blade

Figure 6.8(a & b) depicts the pressure and velocity variations in the vicinity of the VAWT having 12 stator blades while the number of rotor blades are kept constant at 12. This VAWT configuration has been termed here as healthy VAWT. It can be seen in figure 6.8(a) that the windward side of the VAWT possess very high pressure while the leeward side has comparatively low pressure. Furthermore, it can be seen in figure 6.8(b) that the flow velocity is high on the windward side and the core region, while it is comparatively lower on the leeward side of the VAWT. It has also been observed that the flow accelerates in the passages formed between the rotor and the stator blades on the windward side of the VAWT. These passages are formed due to the orientation and the angular position of the rotor blades.
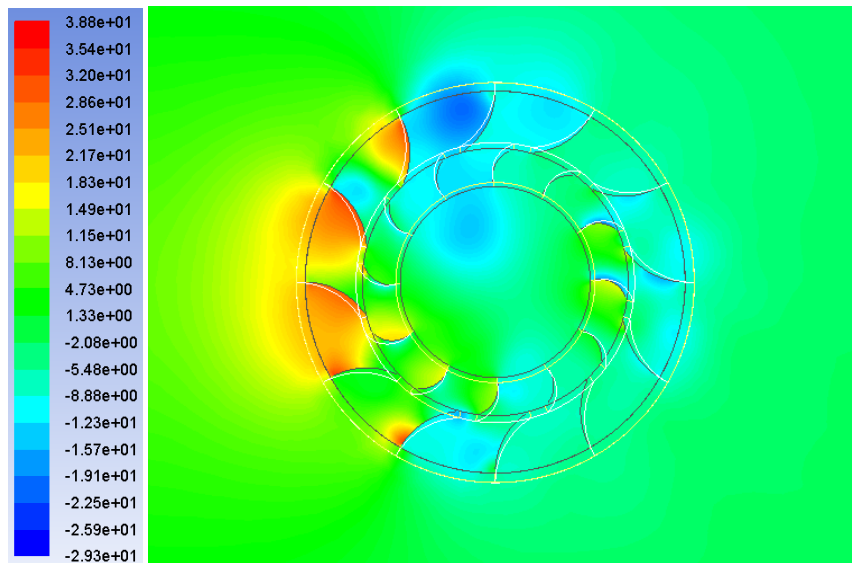
Figure 6.8 (a) Pressure variations at 0⁰ angular position of the healthy VAWT
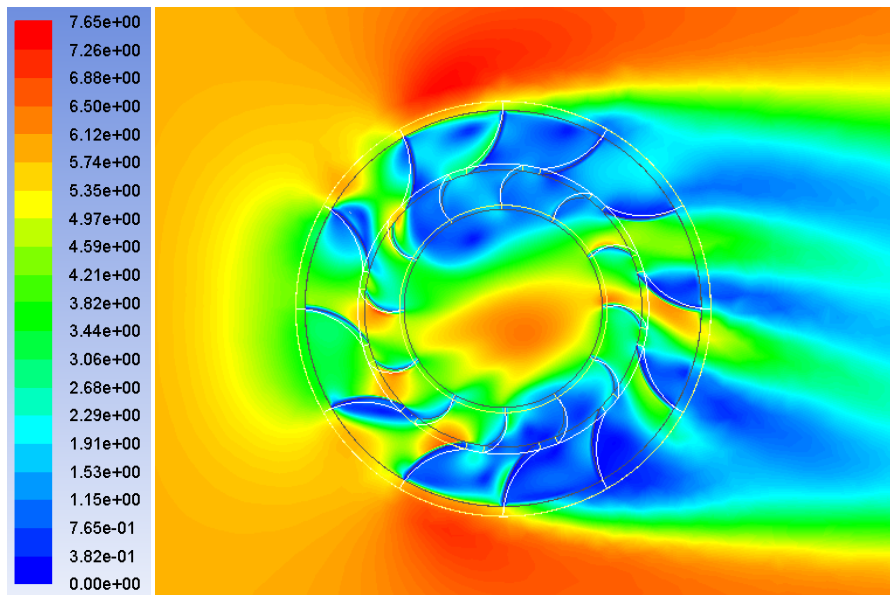
Figure 6.8 (b) Velocity variations at 0⁰ angular position of the healthy VAWT

Figure 6.9 depicts the instantaneous torque output of the healthy VAWT having 12 stator blades. It can be seen that there are additional lower peaks, together with the expected 12 higher peaks

Optimal Design of a Micro Vertical Axis Wind Turbine for Sustainable Urban Environment
By Kyooseon Park, School of Computing and Engineering, University of Huddersfield, UK (2013)
140

corresponding to 12 rotor blades. Furthermore, it is observed that as the angular position of the VAWT increases, the amplitude of these lower peaks decreases.
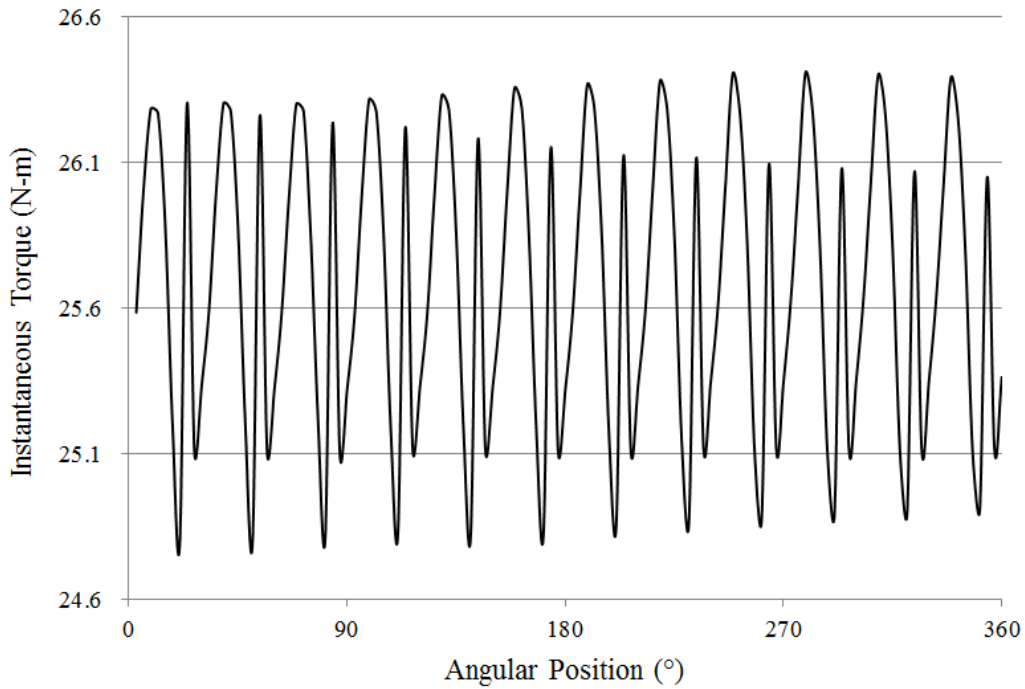
Figure 6.9 Instantaneous torque output for healthy VAWT

6.10(a & b) depicts the pressure and velocity variations in the vicinity of the VAWT having 11 stator blades. This configuration of the VAWT is termed here as defective VAWT. In comparison with figure 6.8(a), it can be seen in figure 6.10(a), due to a missing stator blade, the pressure in the stator region decreases, giving rise to highly non-uniform pressure field.
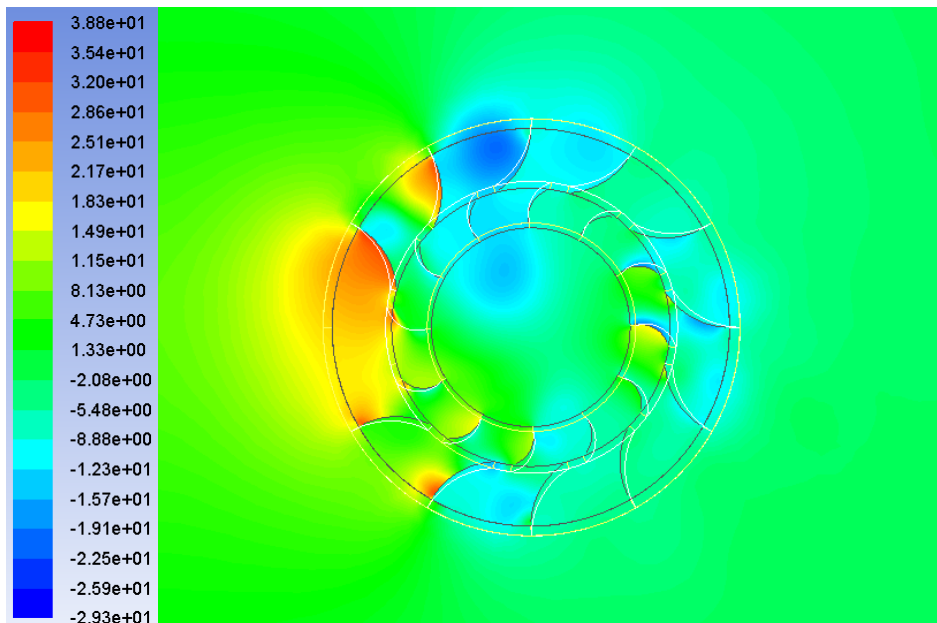
Figure 6.10 (a) Pressure variations at 0° angular position of the defective VAWT missing a stator blade

Optimal Design of a Micro Vertical Axis Wind Turbine for Sustainable Urban Environment
By Kyooseon Park, School of Computing and Engineering, University of Huddersfield, UK (2013)

141

Figure 6.10(b), in comparison with figure 6.8(b), shows that due to a missing stator blade of the VAWT, the flow velocity at the location of the missing stator blade has reduced significantly. Furthermore, the flow velocity in the core region has also reduced.
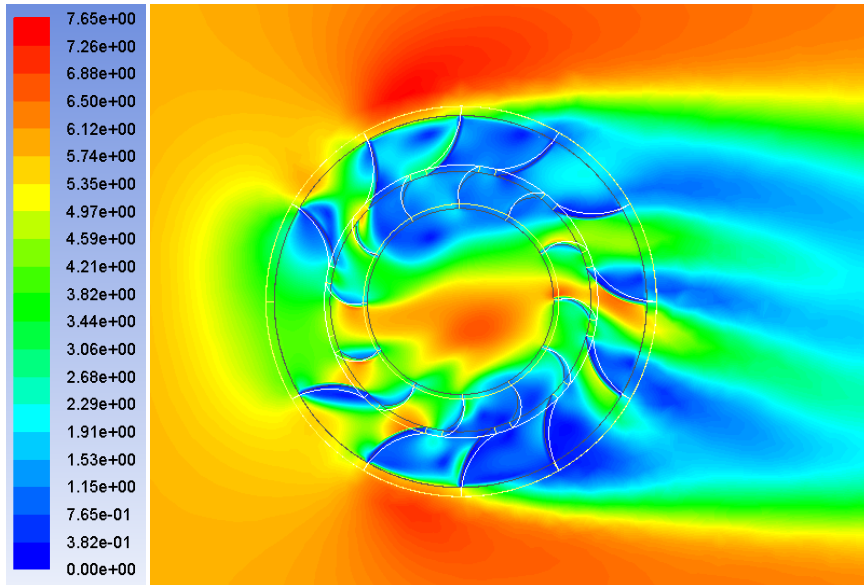
Figure 6.10 (b) Velocity variations at 0⁰ angular position of the defective VAWT missing a stator blade

Figure 6.11 depicts the variations in the instantaneous torque output of the defective VAWT having 11 stator blades. It can be seen, in comparison with figure 6.9, that there are 12 distinct peaks in the torque output that corresponds to the 12 rotor blades of the VAWT. Furthermore, it is observed that as the angular position of the VAWT increases, the amplitude of torque output decreases.
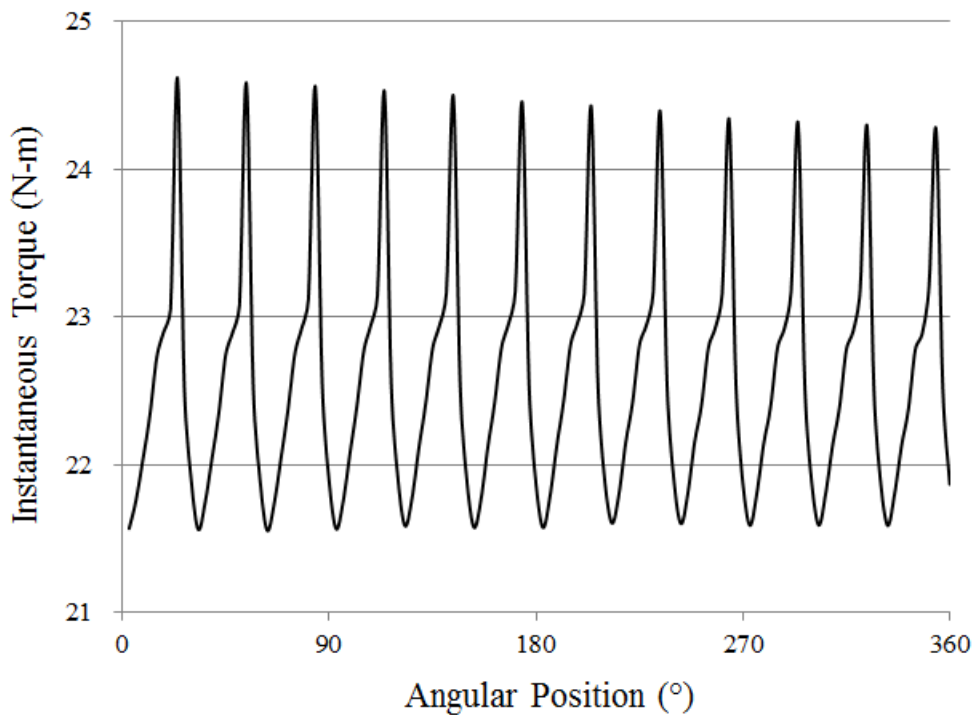
Figure 6.11 Instantaneous torque output for defective VAWT missing a stator blade

Optimal Design of a Micro Vertical Axis Wind Turbine for Sustainable Urban Environment
By Kyooseon Park, School of Computing and Engineering, University of Huddersfield, UK (2013)

142

Table 6.2 summarises the statistical results for the torque outputs of both the healthy and the defective VAWTs. It can be seen that a missing stator blade degrades the performance output of the VAWT by decreasing its average torque and power outputs. Furthermore, it also noted that the maximum amplitude (Tmax–Tmin) and standard deviation in the torque output for defective VAWT is considerably higher than for a healthy VAWT. Large variations in the instantaneous torque output of the defective VAWT (figure 6.11) have resulted into a very high standard deviation.

Table 6.2 Effect of a missing stator blade on the performance output of the VAWT

Number of Rotor Blades	Number of Stator Blades	Tmin (N-m)	Tmax (N-m)	Tavg (N-m)	Std. Dev.	Pavg (W)
12	12	24.80	26.41	25.67	0.51	44.00
12	11	19.84	29.73	24.85	1.98	42.60

Figure 6.12 depicts the instantaneous torque outputs of both the healthy and the defective VAWTs. By comparison, it can be seen the average torque output of the defective VAWT is substantially lower than of the healthy VAWT. Furthermore, the variations in the torque output of defective VAWT are much higher than for healthy VAWT.
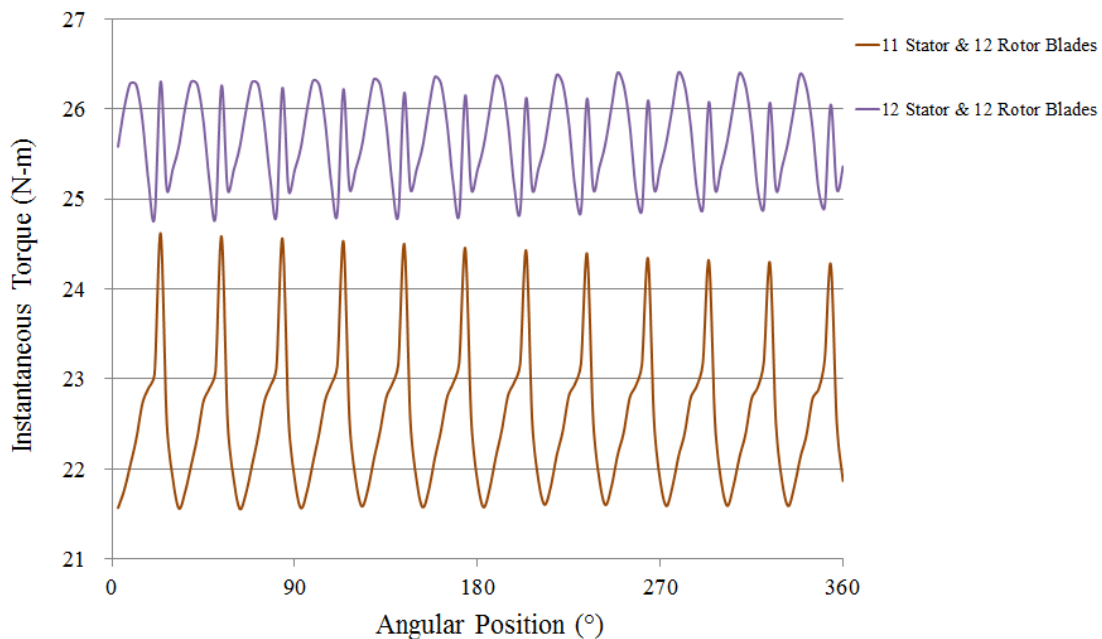
Figure 6.12 Instantaneous torque output of both the healthy and defective VAWTs

Figure 6.13 depicts the average power and torque outputs of both the healthy and the defective VAWTs. It can be seen that the missing stator blade degrades the performance output of the VAWT by decreasing its average torque and power outputs.

Optimal Design of a Micro Vertical Axis Wind Turbine for Sustainable Urban Environment
By Kyooseon Park, School of Computing and Engineering, University of Huddersfield, UK (2013)

143
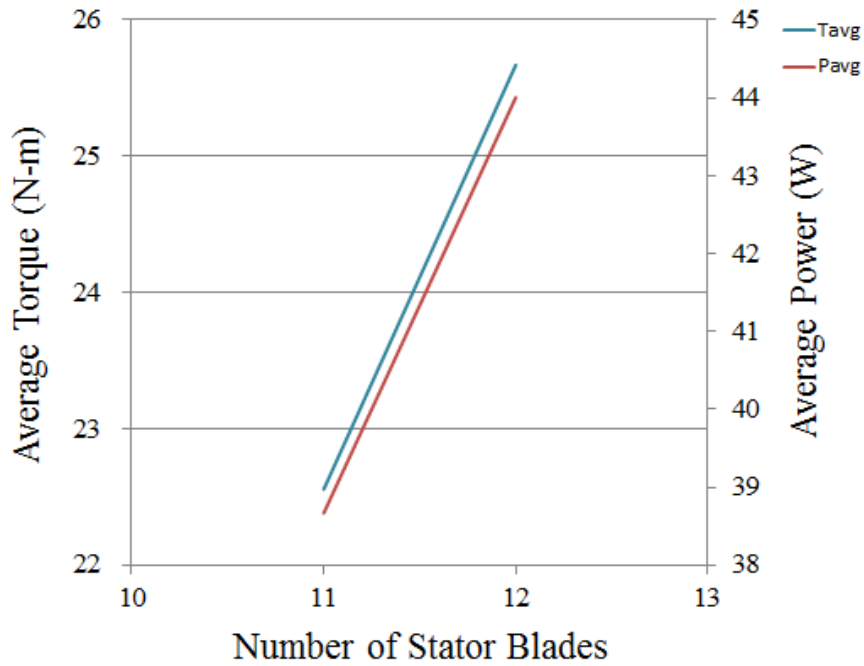
Figure 6.13 Effect of a missing stator blade on the performance output of the VAWT

In order to analyse the effect of a missing rotor and stator blade in detail, pressure and velocity fluctuations at strategically chosen points have been monitored. These locations/points are shown in figure 6.14. Furthermore, the coordinated of these points are summarised in table 6.3. It should be noted that these points are 50mm away from the inner and the outer boundaries of the VAWT.
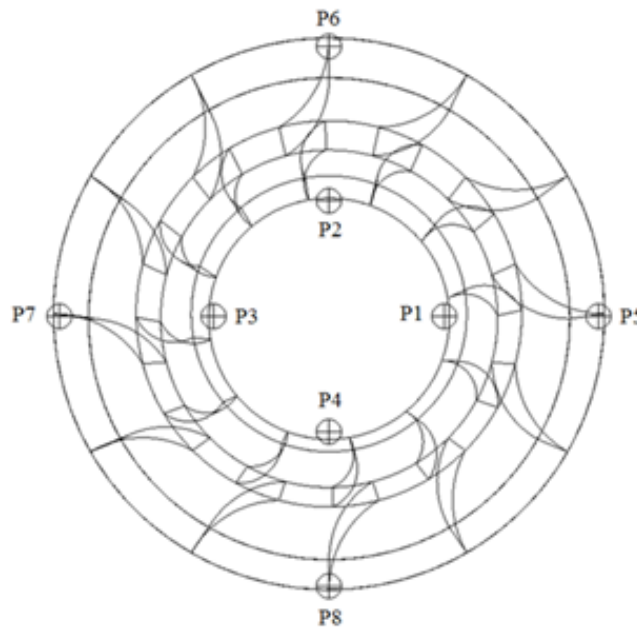
Figure 6.14 Points in the VAWT

Moreover, the monitoring of the pressure and the flow velocity has been carried out at three different angular positions of the VAWT such that the transient interaction between the rotor and the stator blades is captured. These angular positions corresponds to -9^0, 0^0 and 9^0, as shown in figure 6.15, where -9^0 indicates the angular position when rotor blades are 9^0 behind the stator

Optimal Design of a Micro Vertical Axis Wind Turbine for Sustainable Urban Environment
By Kyooseon Park, School of Computing and Engineering, University of Huddersfield, UK (2013)

144

blades, while approaching them in an anticlockwise manner. 0^0 corresponds to the angular position when both the rotor and the stator blades are in-line with each other i.e. the angular difference between the rotor and the stator blades is 0^0. Furthermore, 9^0 correspond to the angular position when rotor blades are 9^0 ahead of the stator blades.

Table 6.3 Coordinates of the Points

Point Number	x (m)	y (m)	z (m)
P1	0.45	0	0.5
P2	0	0.45	0.5
P3	-0.45	0	0.5
P4	0	0.45	0.5
P5	1.05	0	0.5
P6	0	1.05	0.5
P7	-1.05	0	0.5
P8	0	-1.05	0.5

The results are presented in figure 6.16(a &b) where figure 6.16(a) depicts the pressure fluctuations while figure 6.16(b) represents the velocity variations at points P1 to P8 for different angular positions of the VAWT. The green curves represent the healthy VAWT, red represent a missing rotor blade and the blue curves represent a missing stator blade. It can be seen in figure 6.16(a) that at most of the points, the difference in the pressure between the healthy and the defective VAWTs is negligibly small to be associated to the presence of defects in the VAWT. However, at P2, P3 and P6, the pressure is considerably lower for the VAWT having a rotor blade missing. These points are located near the upper section and downstream the windward side of the VAWT. It can be concluded that rotor blade faults are more severe in nature compared to the stator blade faults, as far as the pressure field in the vicinity of the VAWT is concerned.
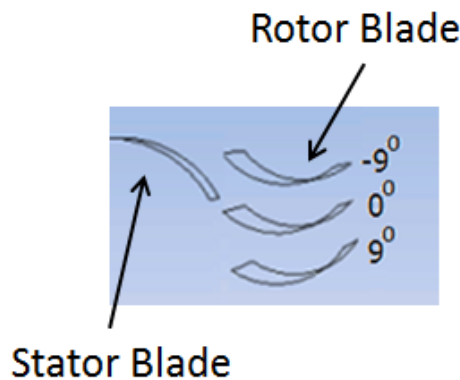
Figure 6.15 Angular positions of the rotor blade w.r.t. the stator blade

Analysing figure 6.16(b) suggests that stator blade faults are detected much better by velocity variations. Therefore, the differences can be visualised at P1, P6, P7 and P8 locations. Hence, it can be concluded that various faults in VAWTs are detectable by using CFD simulations; however, some faults are more sensitive to one flow variable whereas another fault is more sensitive to another flow variable. A more rigorous investigation is required to associate specific blade faults to specific flow parameters accurately.

Optimal Design of a Micro Vertical Axis Wind Turbine for Sustainable Urban Environment
By Kyooseon Park, School of Computing and Engineering, University of Huddersfield, UK (2013)

145

P1

P5

P2

P6

P3

P7

Optimal Design of a Micro Vertical Axis Wind Turbine for Sustainable Urban Environment
By Kyooseon Park, School of Computing and Engineering, University of Huddersfield, UK (2013)
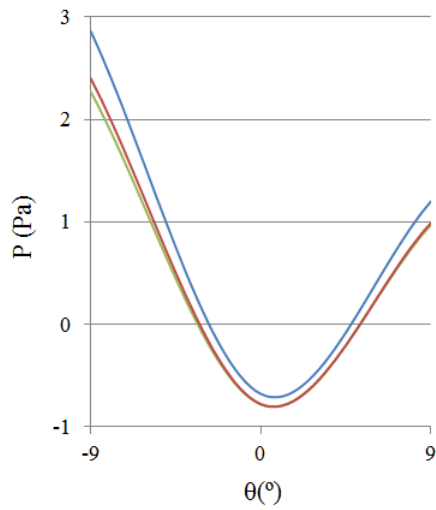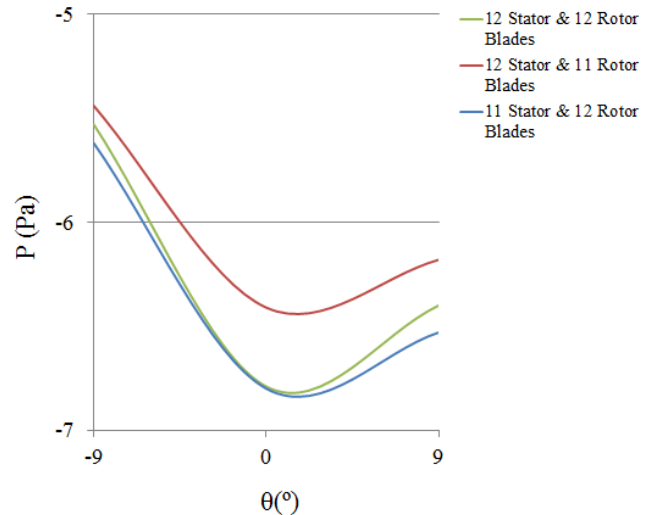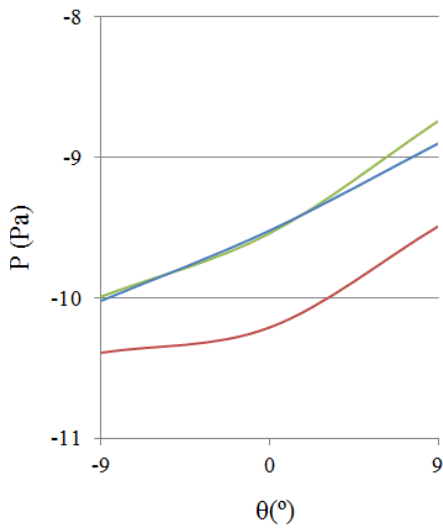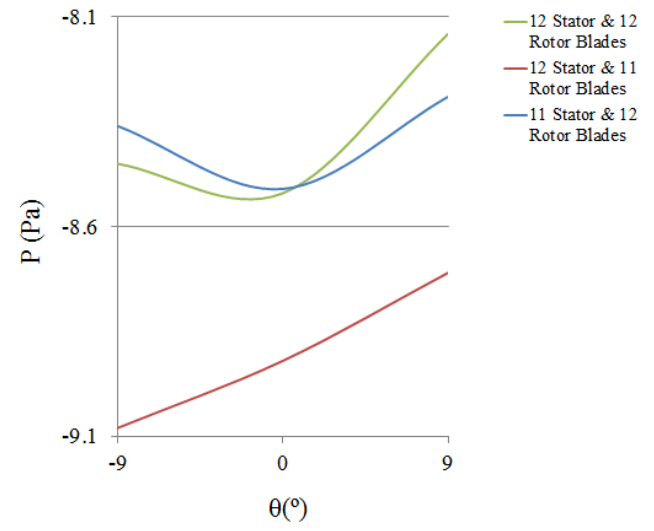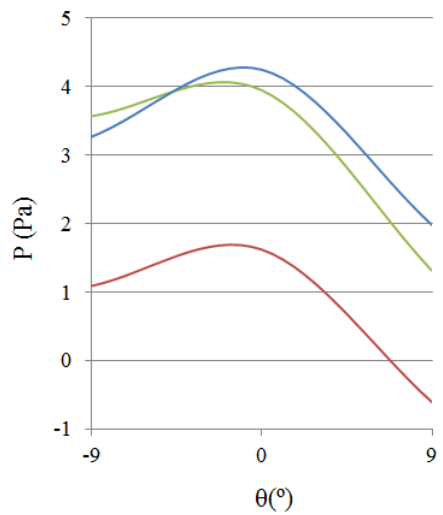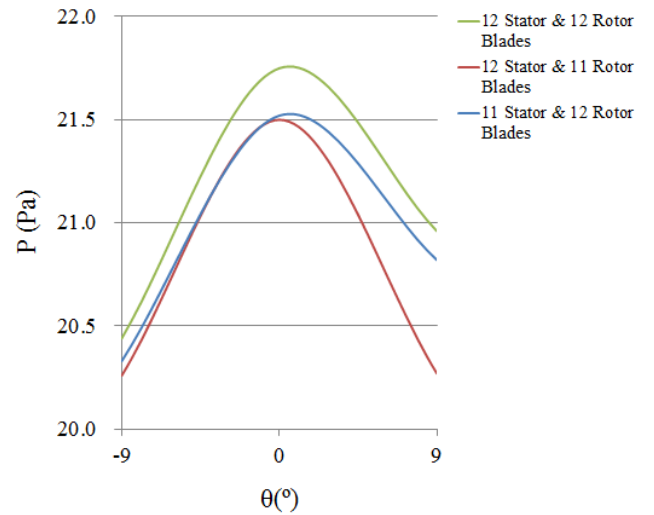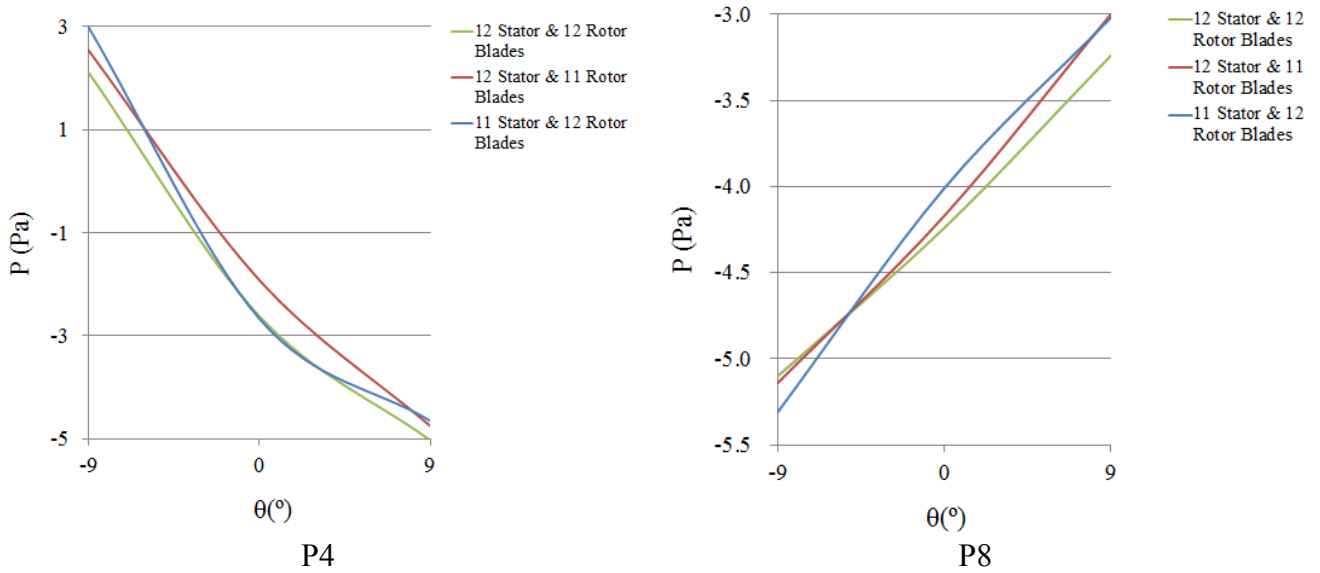
Figure 6.16 (a) Pressure fluctuations at the points for both healthy and defective VAWTs

Optimal Design of a Micro Vertical Axis Wind Turbine for Sustainable Urban Environment
By Kyooseon Park, School of Computing and Engineering, University of Huddersfield, UK (2013)

147
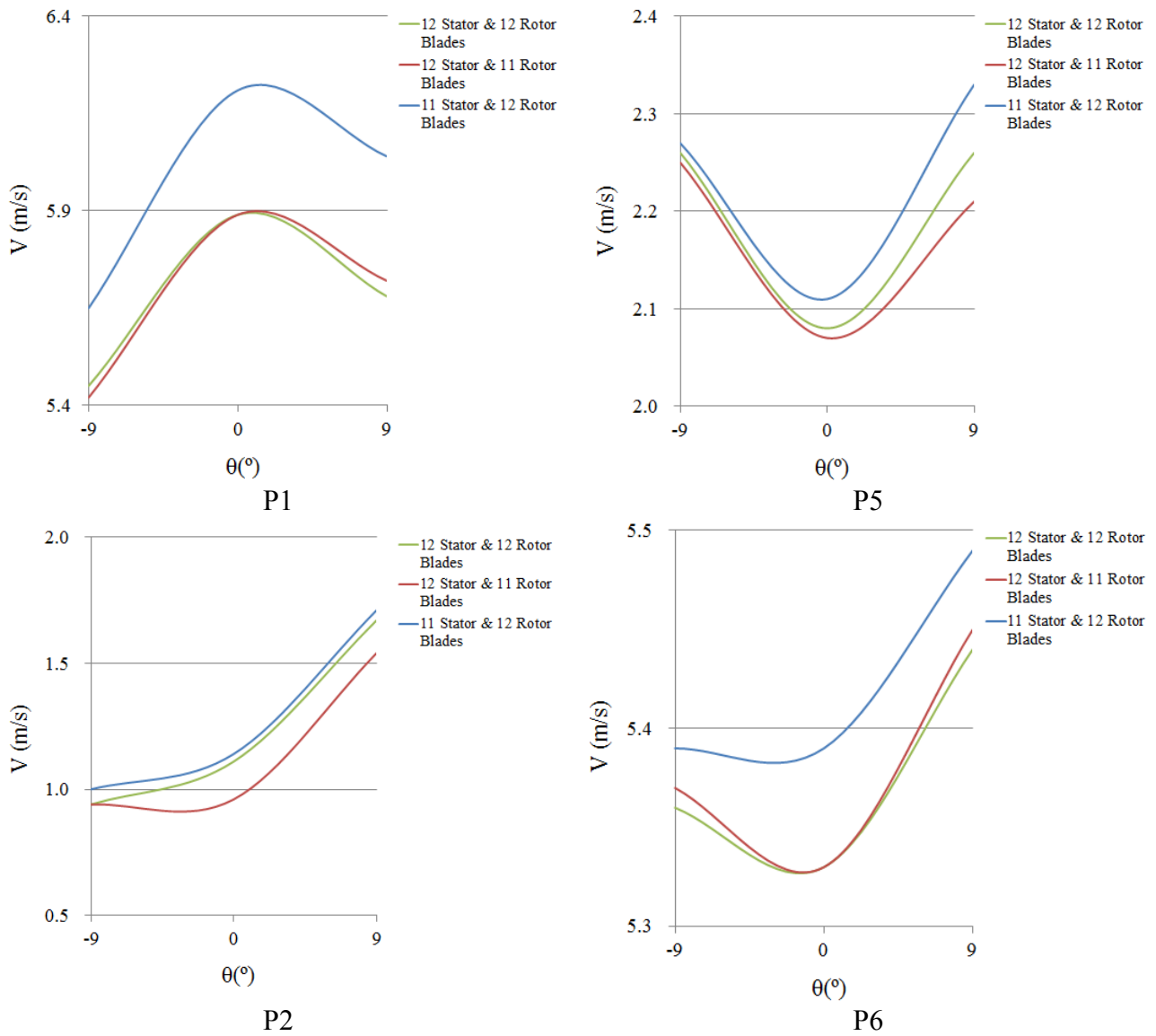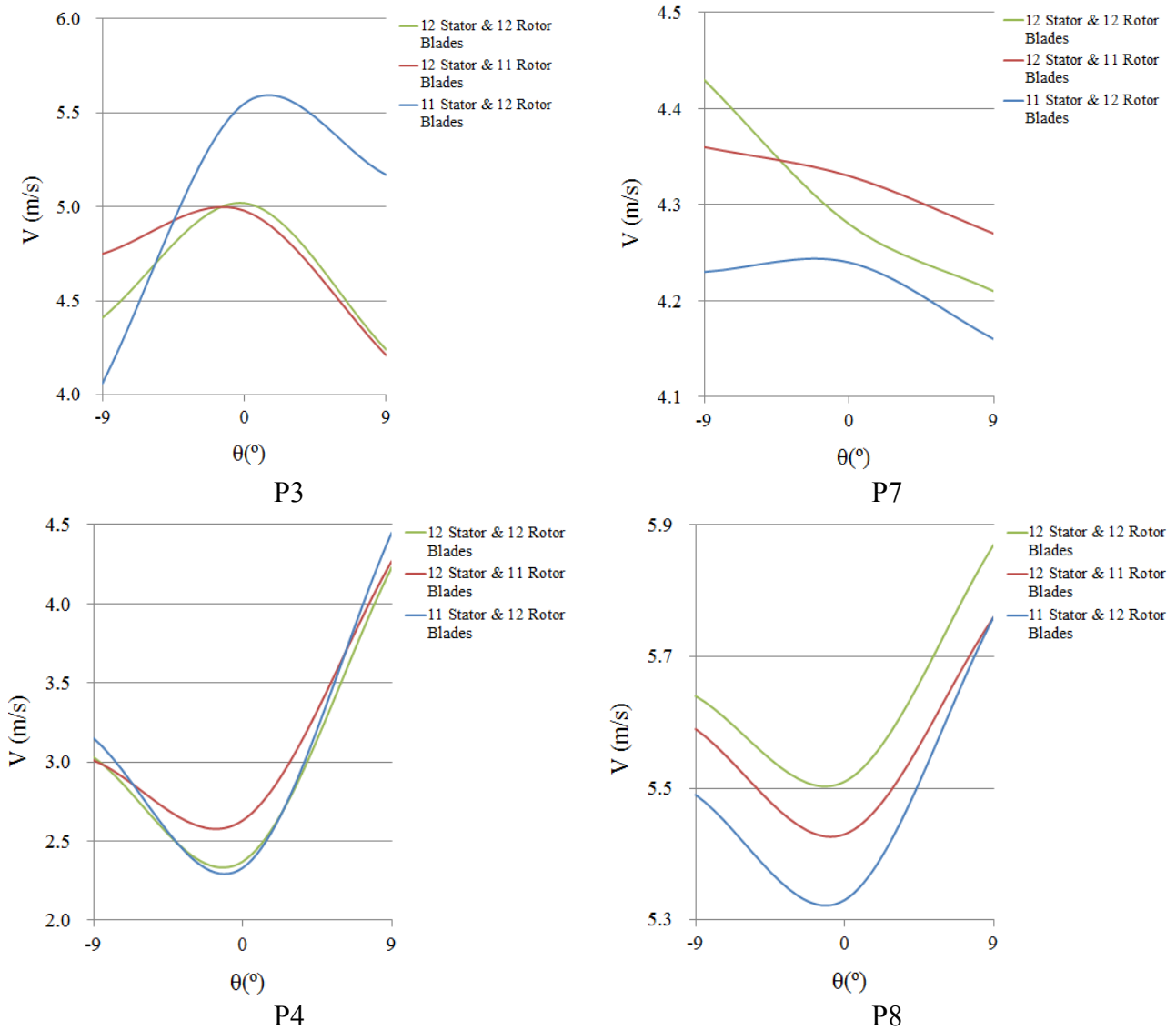
Figure 6.16 (b) Velocity variations at the points for both healthy and defective VAWTs

6.4. Effect of Slits in a Rotor Blade

In order to analyse the effects of slit in a rotor blade, on the performance output of the VAWT, various three different slit sizes have been chosen for analysis. These slit sizes correspond to 50mm, 100mm and 200mm, in the rotor blade that is present on the windward side of the VAWT. A defective VAWT with 50mm slit is shown in figure 6.17.

Optimal Design of a Micro Vertical Axis Wind Turbine for Sustainable Urban Environment
By Kyooseon Park, School of Computing and Engineering, University of Huddersfield, UK (2013)

148
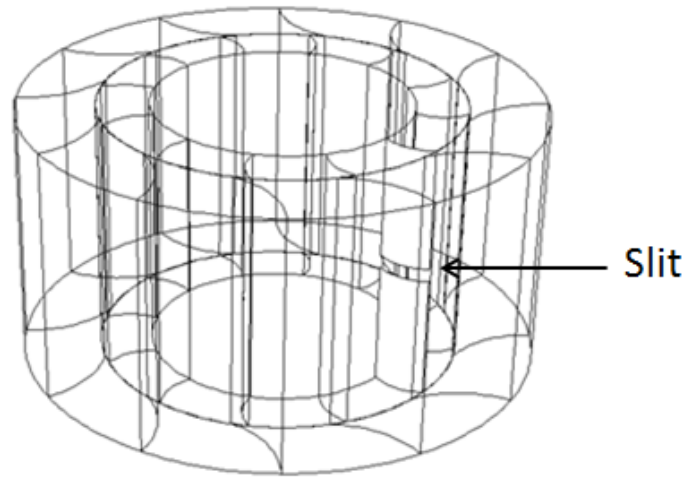
Figure 6.17 Slit in the Rotor Blade

Figure 6.18(a & b) depicts the pressure and velocity variations in the vicinity of the VAWT having no slit in the rotor blade. It can be seen in figure 6.18(a) that the windward side of the VAWT possess very high pressure while the leeward side has comparatively low pressure. Furthermore, it can be seen in figure 6.18(b) that the flow velocity is high on the windward side and the core region, while it is comparatively lower on the leeward side of the VAWT. It has also been observed that the flow accelerates in the passages formed between the rotor and the stator blades on the windward side of the VAWT. These passages are formed due to the orientation and the angular position of the rotor blades.
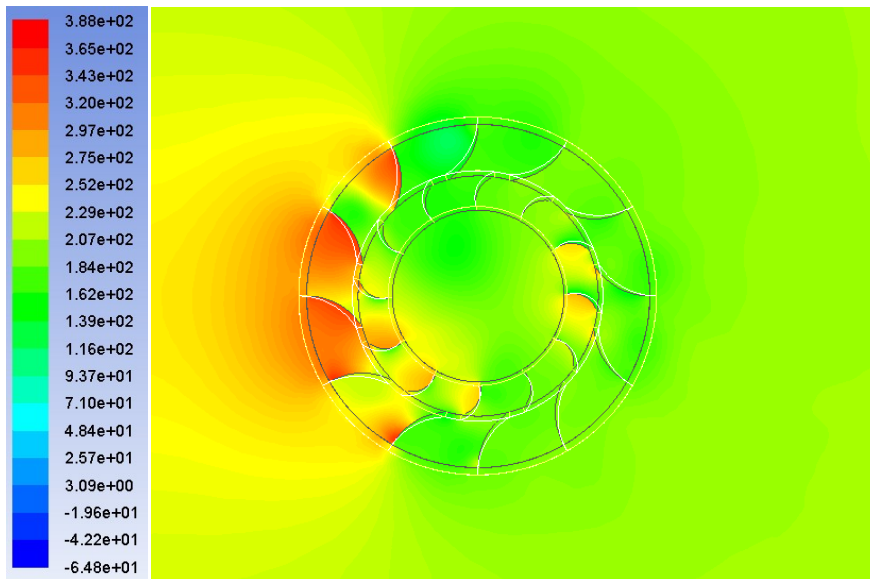
Figure 6.18 (a) Pressure variations at 0° angular position of the healthy VAWT

Optimal Design of a Micro Vertical Axis Wind Turbine for Sustainable Urban Environment
By Kyooseon Park, School of Computing and Engineering, University of Huddersfield, UK (2013)
149
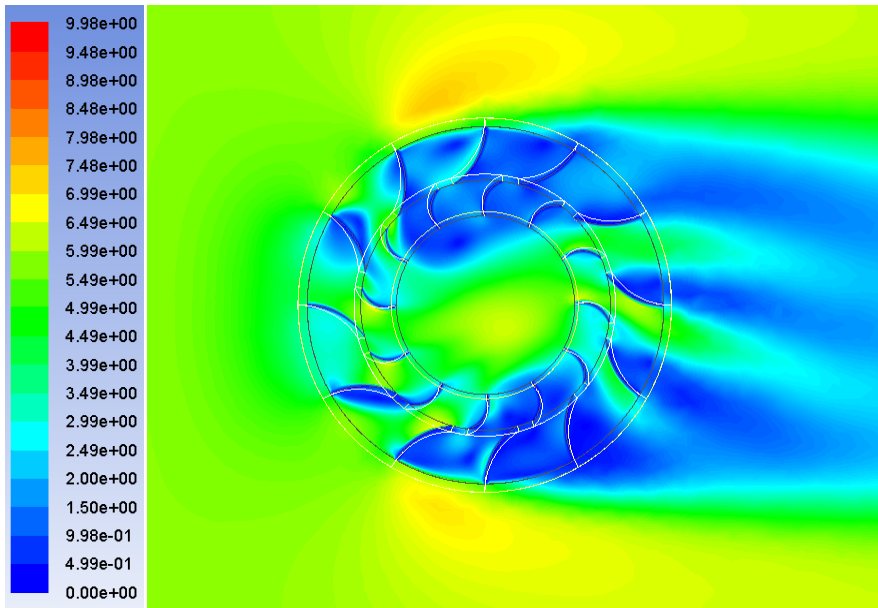
Figure 6.18 (b) Velocity variations at 0° angular position of the healthy VAWT

Figure 6.19 depicts the instantaneous torque output of the healthy VAWT. It can be seen that there are additional lower peaks, together with the expected 12 higher peaks corresponding to 12 rotor blades. Furthermore, it is observed that as the angular position of the VAWT increases, the amplitude of these lower peaks decreases.
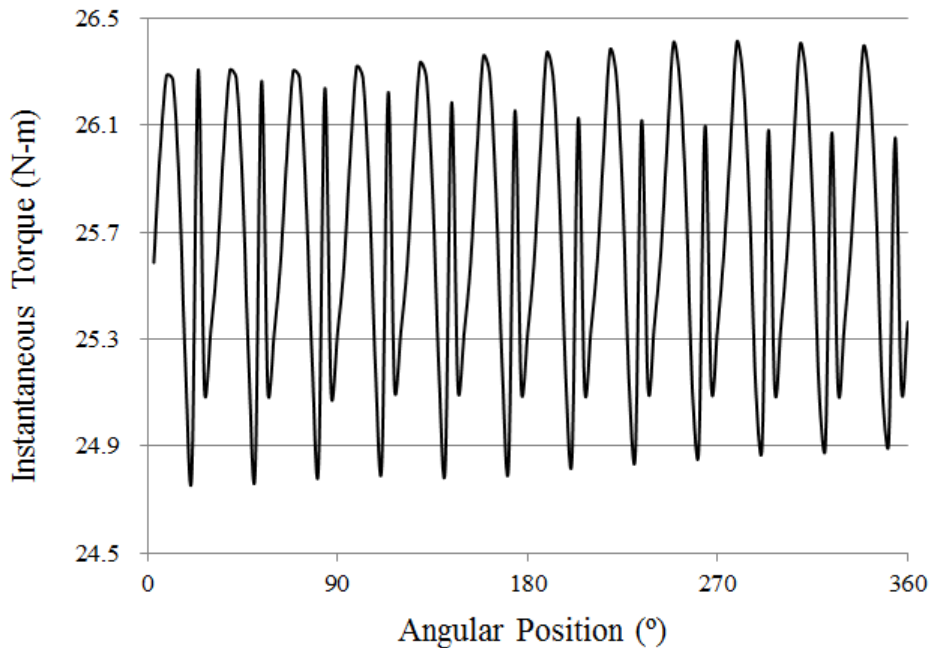
Figure 6.19 Instantaneous torque output for healthy VAWT

6.20(a & b) depicts the pressure and velocity variations in the vicinity of the defective VAWT having a 50mm slit in the rotor blade. In comparison with figure 6.18(a), it can be seen in figure 6.20(a) that due to a 50mm slit in the rotor blade, the pressure in the rotor region decreases, giving rise to highly non-uniform pressure field.

Optimal Design of a Micro Vertical Axis Wind Turbine for Sustainable Urban Environment
By Kyooseon Park, School of Computing and Engineering, University of Huddersfield, UK (2013)

150
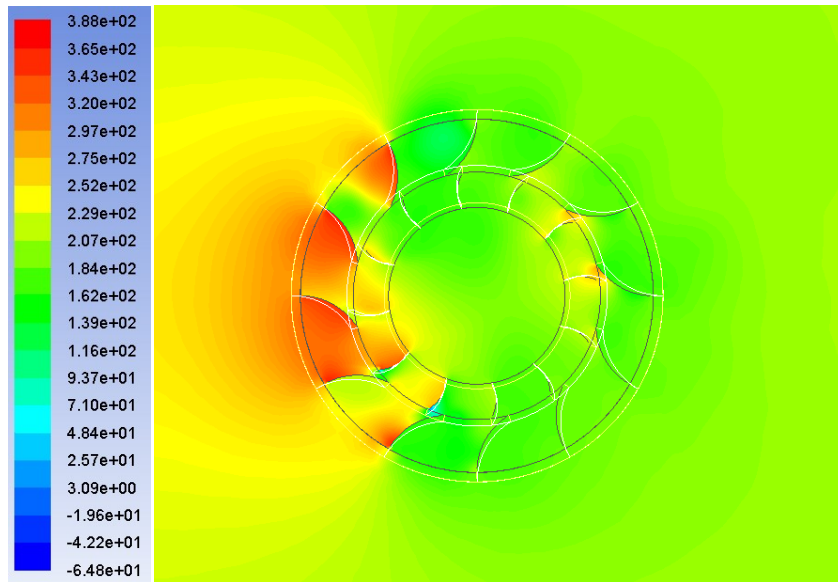
Figure 6.20 (a) Pressure variations at 0⁰ angular position of the defective VAWT having a 50mm Slit

Figure 6.20(b), in comparison with figure 6.18(b), shows that due to a 50mm slit in the rotor blade of the VAWT, the flow velocity at the location of the slit has increased marginally. Furthermore, the flow velocity in the core region and the upper section of the VAWT has also increased.
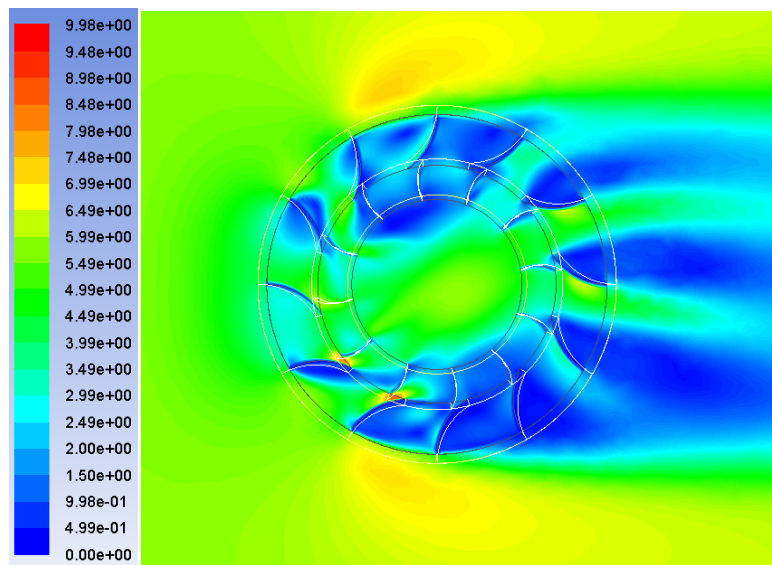
Figure 6.20 (b) Velocity variations at 0⁰ angular position of the defective VAWT having a 50mm Slit

Figure 6.21 depicts the variations in the instantaneous torque output of the defective VAWT having a 50mm slit in the rotor blade. It can be seen, in comparison with figure 6.19, that the instantaneous torque output of the defective VAWT is considerably lower than for the healthy VAWT. Furthermore, it has been observed that the variations in the torque output of the defective VAWT are significantly higher than for the healthy VAWT. The reason for the first cycle's torque output to be less than the other cycles is the presence of the slit at 0⁰ angular position of the VAWT. As the slit moves away from the windward side of the VAWT, its effect becomes less significant on the instantaneous torque output of the VAWT.

Optimal Design of a Micro Vertical Axis Wind Turbine for Sustainable Urban Environment
By Kyooseon Park, School of Computing and Engineering, University of Huddersfield, UK (2013)

151
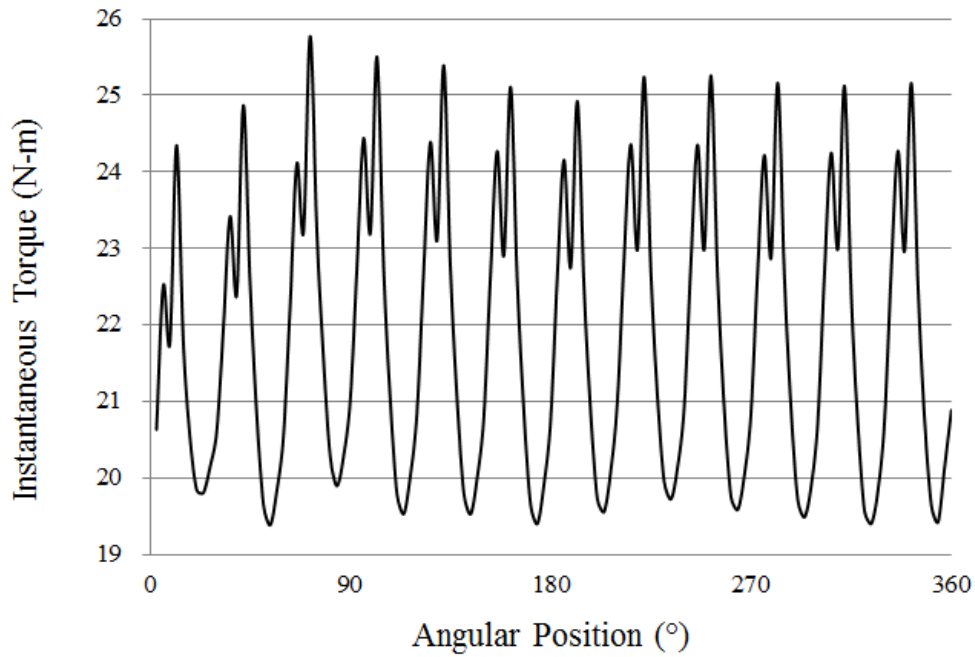
Figure 6.21 Instantaneous torque output for defective VAWT having a 50mm Slit

6.22(a & b) depicts the pressure and velocity variations in the vicinity of the defective VAWT having a 100mm slit in the rotor blade of the VAWT. In comparison with figure 6.20(a), it can be seen in figure 6.22(a) that due to a 100mm slit in the rotor blade, the pressure in the rotor region decreases further, and the pressure field in the vicinity of the VAWT is highly non-uniform.
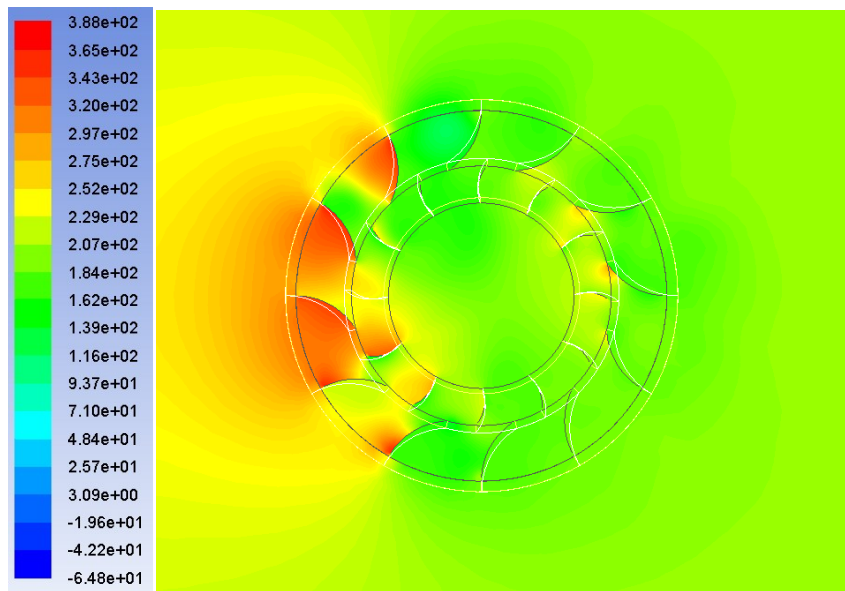
Figure 6.22 (a) Pressure variations at 0° angular position of the defective VAWT having a 100mm Slit

Figure 6.22(b), in comparison with figure 6.20(b), shows that due to a 100mm slit in the rotor blade of the VAWT, the flow velocity at the location of the slit has increased marginally. Furthermore, the flow velocity in the core region and the upper section of the VAWT has also increased.

Optimal Design of a Micro Vertical Axis Wind Turbine for Sustainable Urban Environment
By Kyooseon Park, School of Computing and Engineering, University of Huddersfield, UK (2013)

152
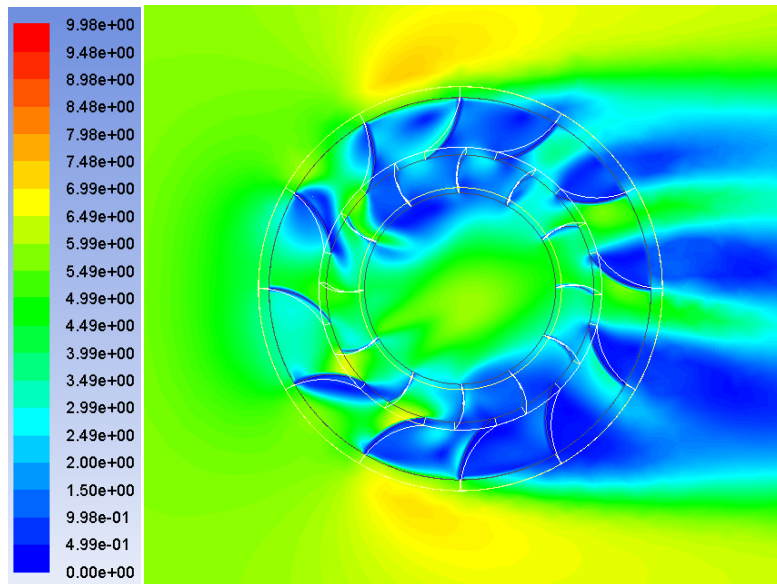
Figure 6.22 (b) Velocity variations at 0° angular position of the defective VAWT having a 100mm Slit

Figure 6.23 depicts the variations in the instantaneous torque output of the defective VAWT having a 100mm slit in the rotor blade. It can be seen, in comparison with figure 6.21, that the difference in the instantaneous torque output of the VAWT is negligibly small. However, the variations in the torque output are slightly higher, which suggests that the standard deviation for 100mm slit VAWT will be slightly higher than for 50mm slit VAWT. Furthermore, it has been observed that as the size of the slit increases, its effect remains significant for a wider range of angular positions of the VAWT.
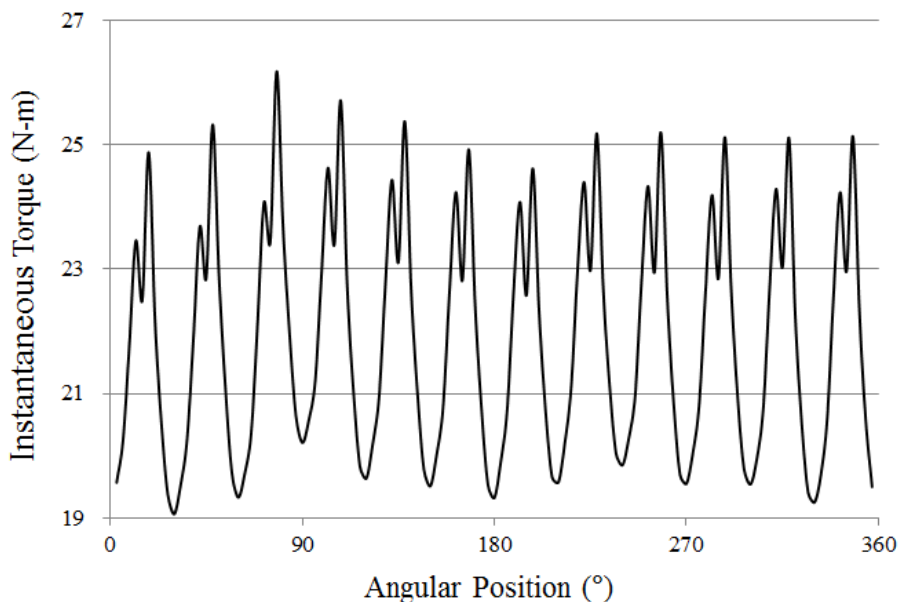
Figure 6.23 Instantaneous torque output for defective VAWT having a 100mm Slit

6.24(a & b) depicts the pressure and velocity variations in the vicinity of the defective VAWT having a 200mm slit in the rotor blade of the VAWT. In comparison with figure 6.22(a), it can be seen in figure 6.24(a) that due to a 100mm slit in the rotor blade, the pressure in the rotor region decreases further, giving rise to highly non-uniform pressure field.

Optimal Design of a Micro Vertical Axis Wind Turbine for Sustainable Urban Environment
By Kyooseon Park, School of Computing and Engineering, University of Huddersfield, UK (2013)

153
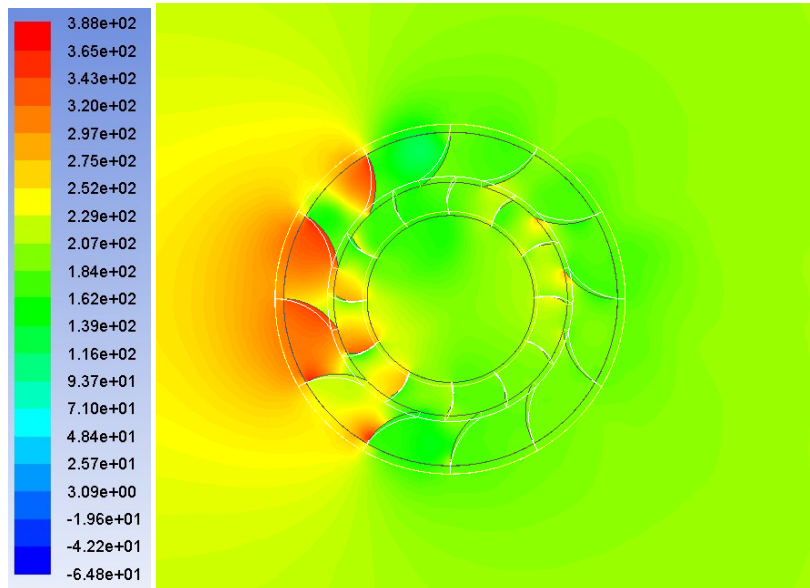
Figure 6.24 (a) Pressure variations at 0⁰ angular position of the defective VAWT having a 200mm Slit

Figure 6.24(b), in comparison with figure 6.22(b), shows that due to a 200mm slit in the rotor blade of the VAWT, the flow velocity at the location of the slit has increased marginally. Furthermore, the flow velocity in the core region and the upper section of the VAWT has also increased.
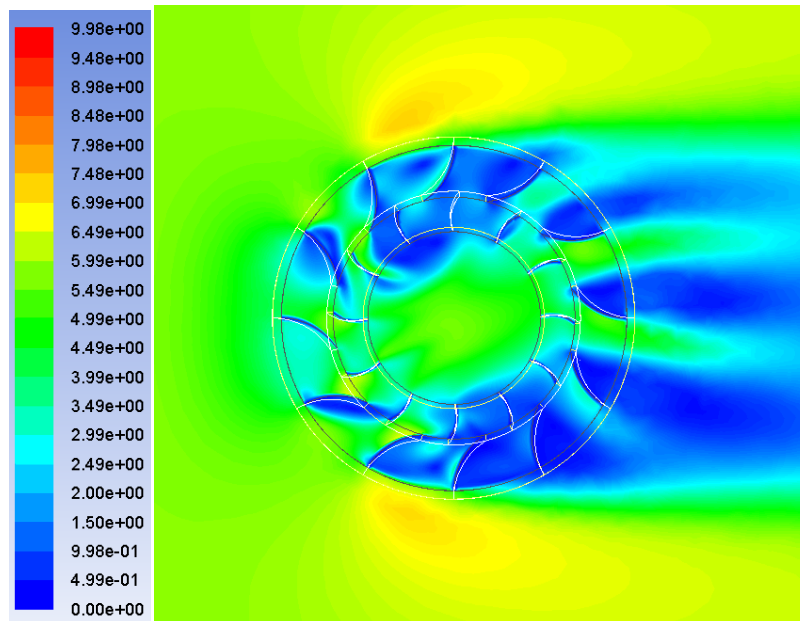
Figure 6.24 (b) Velocity variations at 0⁰ angular position of the defective VAWT having a 200mm Slit

Figure 6.25 depicts the variations in the instantaneous torque output of the defective VAWT having a 200mm slit in the rotor blade. It can be seen, in comparison with figure 6.23, that the instantaneous torque output of the defective VAWT with 200mm slit is slightly lower. Furthermore, it has been observed that the variations in the torque output of the defective VAWT with 200mm slit are significantly higher than for the 100mm slit.

Optimal Design of a Micro Vertical Axis Wind Turbine for Sustainable Urban Environment
By Kyooseon Park, School of Computing and Engineering, University of Huddersfield, UK (2013)
154
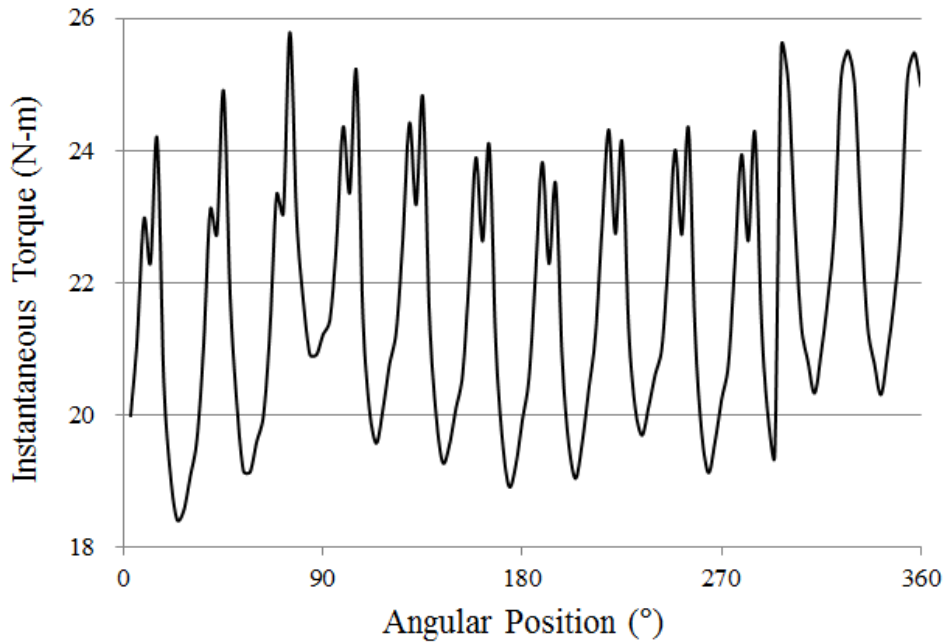
Figure 6.25 Instantaneous torque output for defective VAWT having a 200mm Slit

Table 6.4 presents the statistical analysis of the torque outputs of the healthy as well as defective VAWTs discussed above. It can be clearly seen that the presence of the defects in the rotor blade degrades the performance output of the VAWT significantly by reducing torque and power outputs and by increasing the standard deviation.

Table 6.4 Effect of Slit Size on the performance output of the VAWT

Slit Size (mm)	Tmin (N-m)	Tmax (N-m)	Tavg (N-m)	Pavg (W)	Std. Dev
0 (Healthy)	24.80	26.41	25.67	44.01	0.51
50	19.38	25.77	21.84	37.44	1.83
100	19.06	26.18	21.82	37.41	1.89
200	18.42	25.79	21.74	37.27	1.91

Figure 6.26 depicts the variations in the instantaneous torque outputs of the defective VAWTs. It can be seen that the torque variations are highly non-uniform. As the defect in the rotor blade gets bigger and bigger in size i.e. more severe, its impact on the performance output of the VAWT gets more and more significant. These non-uniform torque variations pose a great threat to the remaining useful life of the VAWT by degrading its structural integrity due to severe vibrations.

Optimal Design of a Micro Vertical Axis Wind Turbine for Sustainable Urban Environment
By Kyooseon Park, School of Computing and Engineering, University of Huddersfield, UK (2013)

155
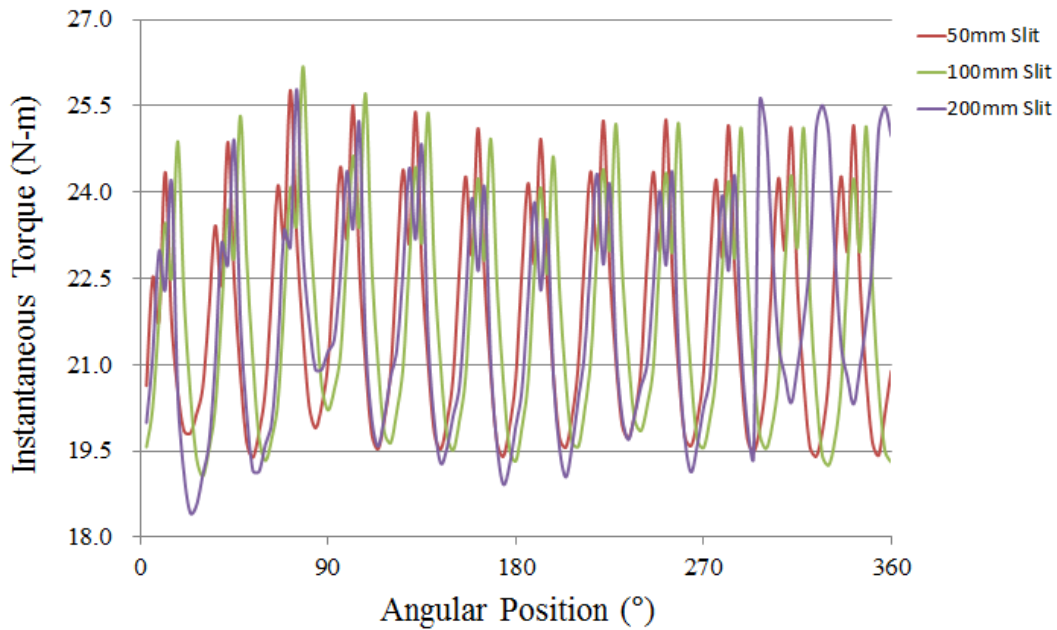
Figure 6.26 Instantaneous torque output of the defective VAWTs

Figure 6.27 depicts the variations in average torque and power outputs of the defective VAWTs. It can be seen that as the defect becomes larger in size, both the torque and power outputs of the VAWT reduces. Furthermore, it can be seen that there are non-linearities in the curves that arises due to complex and transient interactions between the blades.
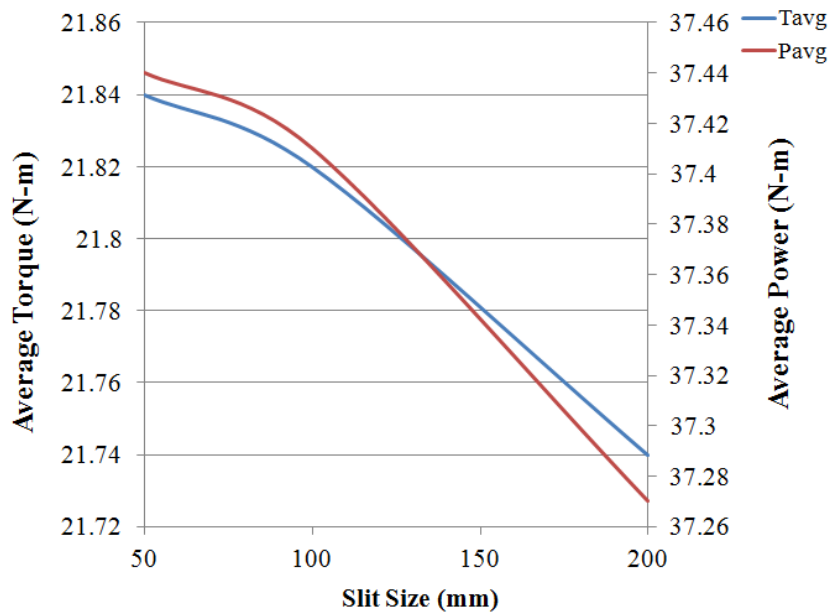
Figure 6.27 Effect of Slit Size on the performance output of the VAWT

Figure 6.28(a &b) depicts the variations in the pressure and the flow velocity at points mentioned in the previous section. It can be seen in figure 6.28(a) that there is significant pressure variations in the vicinity of the VAWT as the severity of the blade fault increases. For example, at location P1, as the angular position of the VAWT increases, the pressure decreases for 50mm slit VAWT. However, as the slit size increases (doubled and quadrupled), the trend of these variations become different. As the angular position of the VAWT increases, the pressure first increases until the rotor and the

Optimal Design of a Micro Vertical Axis Wind Turbine for Sustainable Urban Environment
By Kyooseon Park, School of Computing and Engineering, University of Huddersfield, UK (2013)

156

stator blades are in-line with each other. As the rotor blade leaves the stator blades, the pressure decreases. Hence, it is possible to detect the faults using CFD although the trends are highly non-uniform and it is suggested here that further studies should be conducted in the field of condition monitoring of VAWTs.

Analysing figure 6.28(b) suggests that blade faults are detected much better by velocity variations. The differences can be visualised at P1 and P7 locations where the flow velocity is lowest for the biggest slit. Hence, it can be concluded that some faults are more sensitive to one flow variable whereas another fault is more sensitive to another flow variable.

P1

P5

P2

P6

Optimal Design of a Micro Vertical Axis Wind Turbine for Sustainable Urban Environment
By Kyooseon Park, School of Computing and Engineering, University of Huddersfield, UK (2013)

157
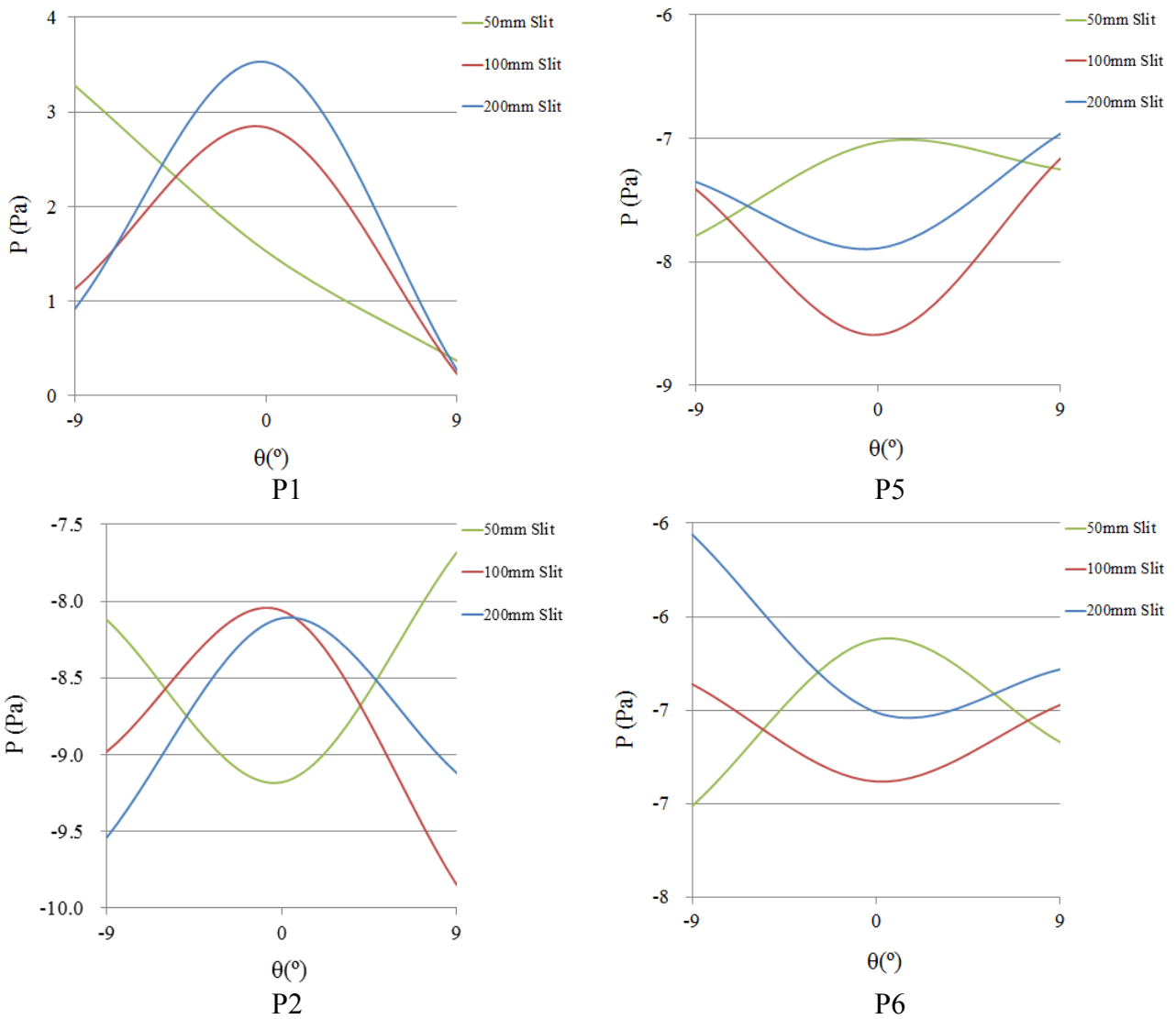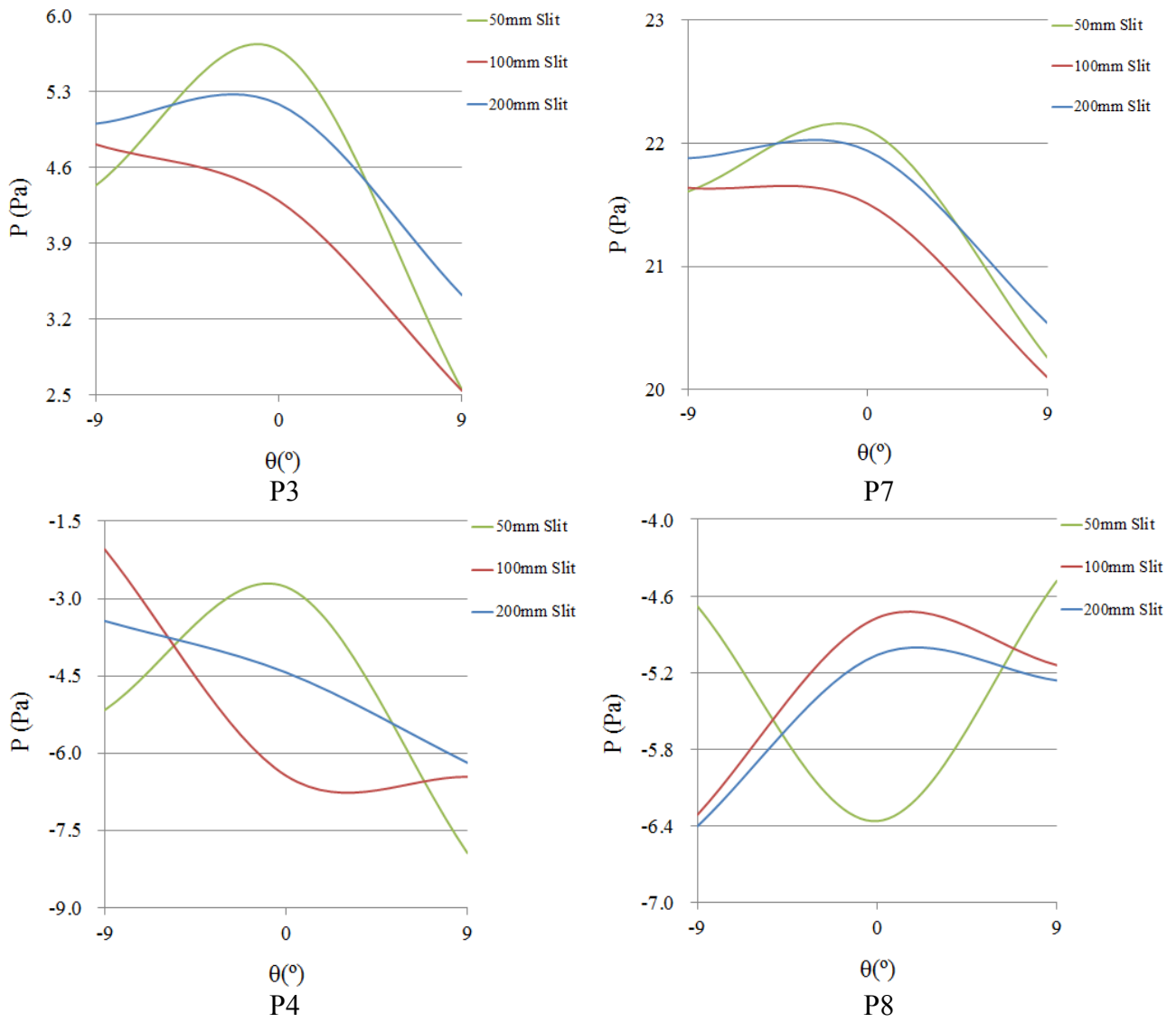
Figure 6.28 (a) Pressure fluctuations at the points for the defective VAWTs

Optimal Design of a Micro Vertical Axis Wind Turbine for Sustainable Urban Environment
By Kyooseon Park, School of Computing and Engineering, University of Huddersfield, UK (2013)

158
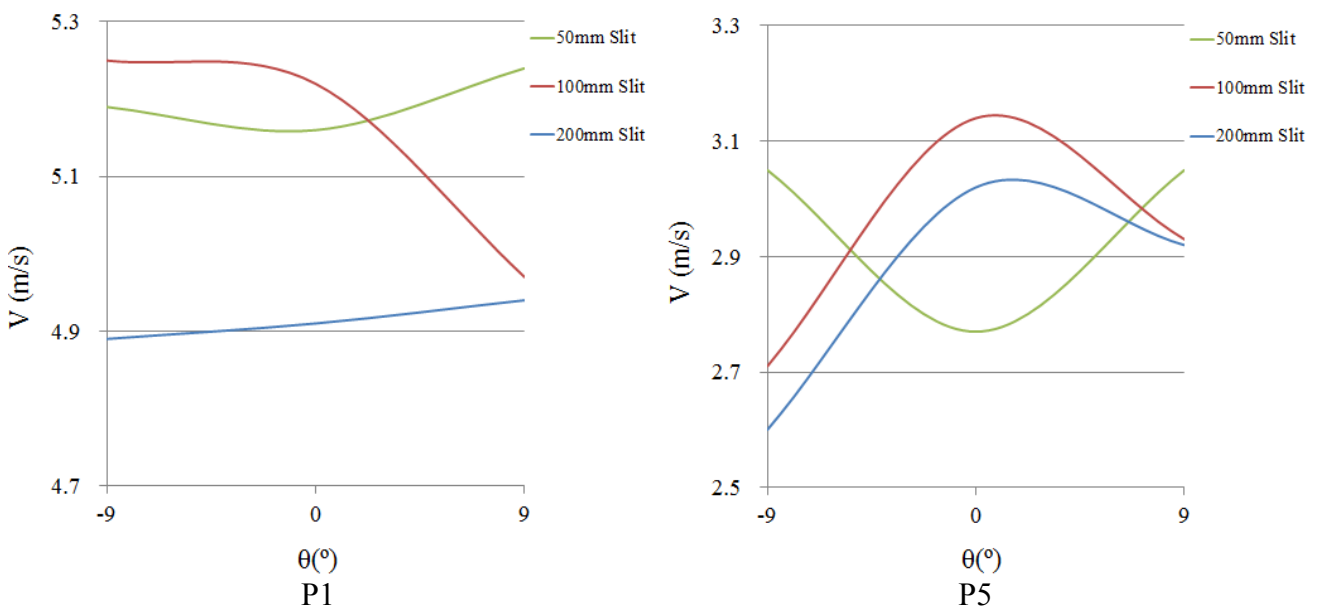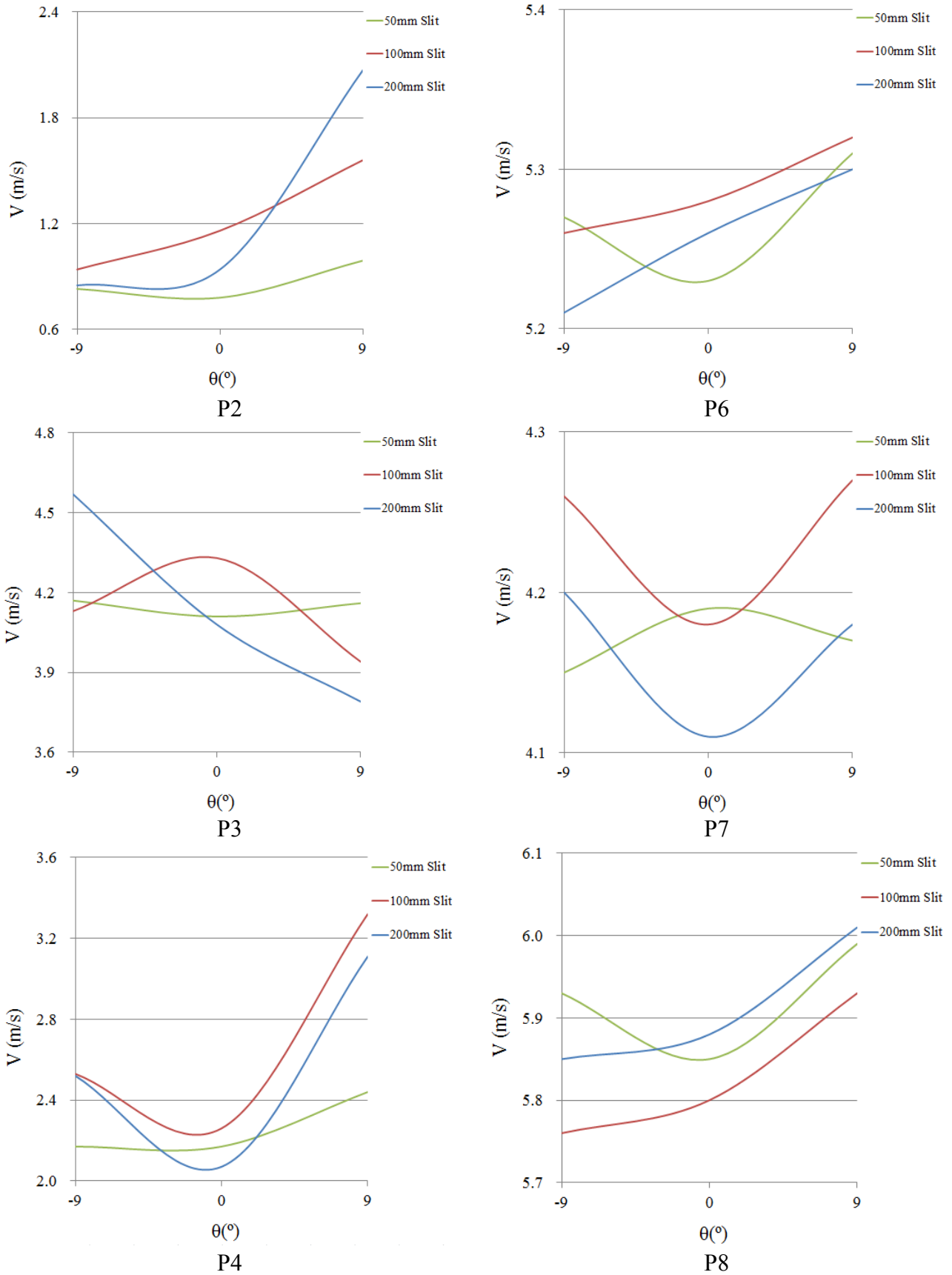
Figure 6.28 (b) Velocity fluctuations at the points for the defective VAWTs

Optimal Design of a Micro Vertical Axis Wind Turbine for Sustainable Urban Environment
By Kyooseon Park, School of Computing and Engineering, University of Huddersfield, UK (2013)

159

In this chapter CFD has been used for condition based health monitoring and fault detection in vertical axis wind turbines. Various blade faults have been generated numerically and the torque output of the VAWT monitored. It has been observed that a missing rotor or stator blade decreases the torque output of the VAWT. Furthermore, as the size of the slit increases, the torque output of the VAWT decreases. This shows that CFD has the capability of detecting blade faults within a VAWT and that the fluid flow parameters can be used to analyse these faults. It is hence concluded here that CFD can be used as an effective diagnostics tool in the future.

6.4. Summary

A detailed investigation into the effect of a missing blade and size of a slit in a rotor blade, on the performance output of the vertical axis wind turbine has revealed the following results:

- A missing rotor blade degrades the performance output of the VAWT

- A missing stator blade degrades the performance output of the VAWT

- Presence of a slit in a rotor blade degrades the performance output of the VAWT

- Increase in the size of the slit in a rotor blade increases the degradation of the performance output of the VAWT

Optimal Design of a Micro Vertical Axis Wind Turbine for Sustainable Urban Environment
By Kyooseon Park, School of Computing and Engineering, University of Huddersfield, UK (2013)
160

CHAPTER 7
Conclusions

From the results obtained in the previous chapters regarding the performance evaluation and fault detection in vertical axis wind turbines, detailed conclusions have been drawn in this chapter. The major achievements and contributions to the existing knowledge base are summarised and wherever possible referenced back to the initial aims of this study. Finally, the works carried out in this study are evaluated and requirements for future work in the area of VAWTs for sustainable urban environment are defined.

Optimal Design of a Micro Vertical Axis Wind Turbine for Sustainable Urban Environment
By Kyooseon Park, School of Computing and Engineering, University of Huddersfield, UK (2013)

161

7.1. Research Problem Synopsis

Use of wind turbines for sustainable urban environment is gaining more and more acceptance globally [1-6]. These machines need to be designed optimally for widespread commercial recognition [7-15]. Furthermore, there is a need to link the faults present in such machines to their performance output in such a way that online health monitoring of these machines is possible. In order to accomplish these goals, researchers have been trying to analyse the effects of various geometric parameters on the performance output of VAWTs. Diagnostics of VAWTs has however been limited to experimental results. With the advent of powerful computing machines and sophisticated software to analyse the flow fields, it has now become possible to computationally model a vertical axis wind turbine and analyse the flow within these machines under various operating conditions.

From a comprehensive review of the published literature, a number of limitations have been found out which are concerned with the aforementioned points. In order to accurately predict the flow behaviour in VAWTs, a set of aims and objectives have been formulated which define the scope of this research study. A summary of the primary aims of the thesis is provided in the following sections of this chapter along with the major achievements and contributions. For reference, the detailed objectives within each of these aims are given in Chapter 2.

7.2. Research Aims and Major Achievements

The main aims of the thesis defined from an extensive literature review in this area are as follows:

Research Aim # 1: Optimal Design of Vertical Axis Wind Turbines based on the Blade Angles

Achievement # 1: This study provides a detailed CFD based investigation on the optimisation of verticals axis wind turbines based on the blade angles. Three dimensional VAWT models having different stator blade outlet angles, rotor blade inlet angles and rotor blade outlet angles have been numerically simulated for the flow of air through them. Sliding mesh technique has been used in order to rotate the rotor blades. This technique captures the transient flow phenomena occurring during rotor/stator blade interaction and hence provides a more realistic approach for such applications.

Based on the detailed numerical investigations, both the pressure and the velocity fields in the vicinity of the VAWTs have been critically analysed, both qualitatively and quantitatively. Qualitative analysis makes use of the pressure and velocity contours whereas quantitative analysis makes use of the torque and power outputs of the VAWTs. The results presented give a clear picture of the flow behaviour in the flow domain. Furthermore, the effects of various blade angles on the performance output of the VAWTs have been rigorously analysed. As VAWT designers use the performance parameters for designing purposes, the present study makes use of the torque coefficient values for various cases under investigation in order to develop a semi-empirical correlation, which predicts the torque output of the VAWT for various geometric configurations mentioned above. The development of such a prediction model for the performance output of the VAWT that includes the effects of different blade angles is a major achievement of the present study. It has also been shown that this prediction model is reasonably accurate.

Optimal Design of a Micro Vertical Axis Wind Turbine for Sustainable Urban Environment
By Kyooseon Park, School of Computing and Engineering, University of Huddersfield, UK (2013)
162

Research Aim # 2: Optimal Design of Vertical Axis Wind Turbines based on Number of Rotor/Stator Blades and Size of Rotor/Stator

Achievement # 2: This study provides a detailed CFD based analysis on the optimisation of verticals axis wind turbines based on number of blades and the size of rotor/stator. Various VAWT models having different number of stator/rotor blades and size of stator/rotor sections of the VAWT have been numerically simulated until the solution has become statistically steady. Transient effects have been accurately captured during these simulations by using advanced modelling techniques such as sliding mesh. In this technique, the rotor blades physically move w.r.t. the axis of rotation and hence the geometric relationship between stator and rotor blades constantly changes.

Based on the detailed numerical examinations, both the pressure and the velocity fields in the vicinity of the VAWTs have been critically analysed, both qualitatively and quantitatively. It has been shown that both the pressure and the velocity variations in the vicinity of the VAWTs are highly unsymmetrical and non-uniform. It has also been shown that the number of stator/rotor blades and the size of the stator/rotor sections significantly affect the performance output of the VAWT. Based on the results from CFD simulations, semi-empirical correlations have been developed using advanced statistical tools. These semi-empirical relations relate the effects of the number of blades and the size of the rotor/stator sections to the performance output of the VAWT. Furthermore, a general torque prediction model has been developed using multiple regression analysis that takes into account all the aforementioned geometrical parameters such as blade angles, number of blades and size of sections. This prediction model is both robust and user-friendly and can be used by VAWT designers with relative ease.

Research Aim # 3: CFD Based Condition Monitoring of Vertical Axis Wind Turbines

Achievement # 3: This study provides a detailed CFD based investigation on the flow diagnostics and fault detection in verticals axis wind turbines. Various blade faults have been generated in the VAWT such as a missing stator blade, a missing rotor blade and slits in a rotor blade. Performance output of the VAWT models have been constantly monitored for several revolutions. It has been observed that CFD results are quite sensitive to blade faults. These faults seem to degrade the performance output of the VAWT considerably. Various statistical analyses have been provided that shows that CFD can be used as an effective tool in the near future for vertical axis wind turbine diagnostics and condition based health monitoring.

7.3. Thesis Conclusions

A comprehensive study has been carried out to support the existing literature regarding the optimisation and condition monitoring of vertical axis wind turbines for sustainable urban environment, and to provide novel additions to improve the current understanding of the design process and geometry related effects on the performance output of VAWTs. The major conclusions from each facet of this research study are summarized as follows:

Optimal Design of a Micro Vertical Axis Wind Turbine for Sustainable Urban Environment
By Kyooseon Park, School of Computing and Engineering, University of Huddersfield, UK (2013)
163

Research Objective # 1: To analyse the effect of the rotor blade angles on the performance output of a VAWT

Detailed CFD based investigations have been carried out to analyse the effects of the rotor blade inlet and exit angles on the performance output of the VAWT. It has been shown that the rotor blade angles (δ and γ) considerably affect the performance output of the VAWT. Increase in both these angles decreases the pressure and increases the flow velocity in the vicinity of the VAWT because decrease in these angles makes the rotor blades more flat, hence, offering less resistance to the flow. Furthermore, it has been observed that as both these angles increases, the torque and the power outputs of the VAWT decreases. Instantaneous torque outputs show that the amplitude of torque variations increases as these angles increase. Moreover, an increase in the standard deviation of the torque output has been noticed with the increase in both of these angles. Hence, it has been recommended here that while designing a VAWT, these angles should be kept small (δ=22.357° and γ=18.2° in this study). A novel torque prediction model has been developed, using statistical tools that links the performance output of the VAWT with δ and γ.

Research Objective # 2: To evaluate the effect of the stator blade exit angle on the performance output of a VAWT

Detailed CFD based investigations have been carried out to analyse the effects of the stator blade exit angle on the performance output of the VAWT. It has been shown that the stator blade exit angle (α) considerably affect the performance output of the VAWT. Increase in α increase the pressure and decreases the flow velocity in the vicinity of the VAWT. Hence, more torque is generated by the action of the aerodynamic forces on the blades of the VAWT. It has been observed that as α increase, the torque and the power outputs of the VAWT increases upto a certain limit after which they starts to decrease. Hence, there is an optimum value of α that generates maximum torque and power outputs of the VAWT. This angle has been found out to be 16.689°. Instantaneous torque output show that the amplitude of torque variations decreases as α increases. A novel torque prediction model has been developed, using statistical tools that links the performance output of the VAWT with α.

Research Objective # 3: To investigate the effect of the rotor size on the performance output of a VAWT

Detailed CFD based investigations have been carried out to analyse the effects of the size of rotor on the performance output of the VAWT. It has been shown that rotor size considerably affects the performance output of the VAWT. Increase in the size of rotor significantly increases the torque and the power outputs of the VAWT. It has also been noticed that a smaller rotor generates torque signals with higher amplitude of variations than a larger rotor. Furthermore, it has been shown that the standard deviation for a larger rotor is considerably lower than for a smaller rotor. A novel torque prediction model has been developed, using results from CFD simulations that links the performance output of the VAWT with the size of the rotor.

Optimal Design of a Micro Vertical Axis Wind Turbine for Sustainable Urban Environment
By Kyooseon Park, School of Computing and Engineering, University of Huddersfield, UK (2013)
164

Research Objective # 4: To formulate the effect of the stator size on the performance output of a VAWT

Detailed CFD based investigations have been carried out to analyse the effects of the size of stator on the performance output of the VAWT. It has been shown that stator size considerably affects the performance output of the VAWT. Increase in the size of stator significantly increases the torque and the power outputs of the VAWT. It has also been noticed that a smaller stator generates torque signals with higher amplitude of variations than a larger stator. Furthermore, it has been shown that the standard deviation for a larger stator is considerably lower than for a smaller stator. A novel torque prediction model has been developed, using results from CFD simulations that links the performance output of the VAWT with the size of the stator.

Research Objective # 5: To evaluate the effect of number of rotor blades on the performance of a VAWT

Detailed CFD based investigations have been carried out to analyse the effects of the number of rotor blades on the performance output of the VAWT. It has been shown that number of rotor blades considerably affects the performance output of the VAWT. Increase in the number of rotor blades significantly increases the torque and the power outputs of the VAWT. It has also been noticed that VAWT with less rotor blades generate torque signals with higher amplitude of variations than a VAWT with more rotor blades. Furthermore, it has been shown that the instantaneous torque output of the VAWT shows as many peaks and valleys as the number of rotor blades in the VAWT.

Research Objective # 6: To investigate the effect of number of stator blades on the performance of a VAWT

Detailed CFD based investigations have been carried out to analyse the effects of the number of stator blades on the performance output of the VAWT. It has been shown that number of stator blades considerably affects the performance output of the VAWT. Increase in the number of stator blades significantly increases the torque and the power outputs of the VAWT. It has also been noticed that VAWT with less stator blades generate torque signals with higher amplitude of variations than a VAWT with more stator blades. Furthermore, it has been shown that the instantaneous torque output of the VAWT shows as many peaks and valleys as the number of rotor blades in the VAWT and hence the stator blades have less impact on the instantaneous torque than rotor blades.

Research Objective # 7: To analyse the effect of a VAWT's height on its performance output

Detailed CFD based investigations have been carried out to analyse the effects of the height of the VAWT on its performance output. It has been shown that the height of the VAWT considerably affects its performance output. Increase in the height of the VAWT increases its torque and power outputs.

Optimal Design of a Micro Vertical Axis Wind Turbine for Sustainable Urban Environment
By Kyooseon Park, School of Computing and Engineering, University of Huddersfield, UK (2013)

165

Research Objective # 8: To analyse the effect of missing rotor blade on the performance output of a VAWT

Detailed CFD based investigations have been carried out to analyse the effects of a missing rotor blade on the performance output of the VAWT. It has been shown that a missing rotor blade considerably affects the performance output of the VAWT. A VAWT with a missing rotor blade generates less torque than a healthy VAWT. It has been shown that a missing rotor blade has a significant impact on the instantaneous torque output of the VAWT. Due to a missing rotor blade, the variations in the torque signals increase significantly, generating severe vibrations in the VAWT. This effect degrades the performance and decreases the remaining useful life of the VAWT. It has been observed that the standard deviation for a missing rotor blade is significantly higher than for a healthy VAWT.

Research Objective # 9: To investigate the effect of missing stator blade on the performance output of a VAWT

Detailed CFD based investigations have been carried out to analyse the effects of a missing stator blade on the performance output of the VAWT. It has been shown that a missing stator blade considerably affects the performance output of the VAWT. A VAWT with a missing stator blade generates less torque than a healthy VAWT. It has been shown that a missing stator blade has a significant impact on the instantaneous torque output of the VAWT. Due to a missing stator blade, the variations in the torque signals increase significantly. Furthermore, it has been observed that the standard deviation for a missing stator blade is significantly higher than for a healthy VAWT.

Research Objective # 10: to formulate the effect of rotor blade slits on the performance output of a VAWT

Detailed CFD based investigations have been carried out to analyse the effects of the presence and the size of slits present in a rotor blade, on the performance output of the VAWT. It has been shown that the presence of a slit in a rotor blade of the VAWT severely degrades the performance output of the VAWT by decreasing its torque and power generating capacities. It has also been shown that as the size of the slit increases, the performance output of the VAWT gets even more degraded. Furthermore, it has been observed that both pressure and velocity variations at strategically chosen locations can help detect blade faults in VAWTs. However, a more rigorous testing is required in order to quantify the effects of blade faults on the performance output of the VAWT.

7.4. Thesis Contributions

The major contributions of this research study are summarized below in which novelties of this research are described:

Contribution # 1

One of the major contributions of this study is the use of a novel modelling technique in order to rotate the rotor blades of the VAWT. This technique, known as Sliding Mesh, is capable of capturing the three dimensional transient complex fluid flow phenomena with much superior

Optimal Design of a Micro Vertical Axis Wind Turbine for Sustainable Urban Environment
By Kyooseon Park, School of Computing and Engineering, University of Huddersfield, UK (2013)

166

accuracy as compared to conventional modelling techniques available such as Single Reference Frame (SRF) and Multiple Reference Frame (MRF). It has been shown in the literature review of this study that most of the numerical studies on the performance evaluation of vertical axis wind turbines use the conventional modelling techniques because they are computationally less expensive than Sliding Mesh technique. However, in doing so, the accuracy of the predicted performance output of the VAWT is severely limited because the transient effects are not captured accurately. Using sliding mesh technique enables to actually rotate the rotor blades and capture the unsteady effects generated during the interaction between the stator and the rotor blades. Hence, the use of this technique is one of the major contributions of the present study.

Contribution # 2

Another major contribution of this study to the knowledge base regarding vertical axis wind turbines is the development of semi-empirical correlations and a torque prediction model that takes into account various geometric effects of the VAWT. Author is not aware of any published literature in which such correlations have been presented. In this study, five different expressions have been developed that link the geometrical features such as stator blade outlet angle, rotor blade inlet and outlet angles, number of rotor/stator blades, size of rotor/stator sections and height of the VAWT, to the performance output of the VAWT. Using CFD results, and applying advanced statistical tools on these results, a novel torque prediction model has been developed which takes the combined effects of the aforementioned parameters. This prediction model is both robust and user-friendly and hence can be used by VAWT designers with relative ease as shown in the design example.

Contribution # 3

The third major contribution of this study is the use of CFD tools towards condition based health monitoring and fault detection in vertical axis wind turbines. It has been shown in the present study that CFD is not only capable of detecting blade faults, but can also predict the severity of the fault/s. It has been observed that local flow parameters, such as pressure and flow velocity, can be used to detect variations in the performance output of the VAWT having blade defects. Hence, it is considered a major contribution of the present study.

7.5. Recommendations for Future Work

The design, optimization and diagnostics of vertical axis wind turbines, for sustainable urban environment, have been presented in the present study such that gaps identified in literature could be bridged. In light of the concluded remarks provided in the previous sections, a vast potential for further research in this particular area has been unlocked. The main areas identified for further work are described below which are associated to further performance-related analysis, design and optimization of VAWTs.

Optimal Design of a Micro Vertical Axis Wind Turbine for Sustainable Urban Environment
By Kyooseon Park, School of Computing and Engineering, University of Huddersfield, UK (2013)
167

Recommendation # 1

More advanced modelling techniques have now become available such as two degree of freedom model, six degree of freedom model etc. Using such models, the impact of flow on rotating bodies can be analysed with much better accuracy. In these techniques, the VAWT is treated as free a body, partially or completely, and the rotor blades revolve under the action of aerodynamic forces being generated on the blades. These advanced models do not require any inputs in terms of the rotor blade angular velocity. The aerodynamic forces acting on the blades are enumerated on-the-fly and necessary modifications are carried out for the orientation of the rotor blades. These advanced modelling techniques are indeed computationally very expensive and requires massive computational power. Furthermore, these tools require extra computational skills in terms of writing complex scripts to define the changing mesh structure and extraction of the data.

Recommendation # 2

Condition based health monitoring of vertical axis wind turbines is essential for its widespread commercial acceptability. A structured condition based health monitoring and fault detection system is required that can predict the faults in a VAWT. This leads toward predictive maintenance and hence a catastrophic structural damage can be avoided. The condition monitoring strategy includes the development of prediction models that links the severity and number of blade faults to the performance outputs of the VAWT. Such type of research can be carried out using advanced CFD tools but in order to do so high performance computing facilities are required that can handle the massive computational power required.

Recommendation # 3

It has been shown in the present study that errors arise in the prediction model due to certain elements like not considering the effect of the blade thickness in the computational model etc. These errors can be minimised by using an accurate blade profile rather than a simplified one. This can be achieved by using advanced CAD software and then integrating those designs with the computational fluid dynamics tools. However, the translation from CAD to CFD compromises some of the intricate details in the CAD model. Nowadays, advanced translators are available in the market that takes care of this issue. Hence, a real model of the blades will enable to remove some of the errors in the torque prediction model presented in this study.

Optimal Design of a Micro Vertical Axis Wind Turbine for Sustainable Urban Environment
By Kyooseon Park, School of Computing and Engineering, University of Huddersfield, UK (2013)
168

REFERENCES

[1]   GWEC (2007) Global Wind Energy Council available at

http://gwec.net/wp-content/uploads/2012/06/gwec-08-update_FINAL.pdf

[2]   EWEC (2009) Annual Report available at

http://www.ewea.org/fileadmin/files/library/publications/reports/Ewea_Annual_Report_2009.pdf

[3]   BTM Consultants (2007) World market update available at

http://www.btm.dk/public/WMU_2007_Sumarry.pdf

[4]   Walker, J. (2009) Renewable energies: How far can they take us?

[5]   WWEA (2008) World Wind Energy Report, Wind Energy Association, Bonn, Germany available at http://www.wwindea.org/home/images/stories/worldwindenergyreport2008_s.pdf

[6]   WWEA (2006) New World Record in Wind Power Capacity, Bonn, Germany available at

http://www.folkecenter.dk/mediafiles/folkecenter/pdf/2006_WWEA_Statistik.pdf

[7]   Lemming, J. (2009) Future wind energy technology and CO2 perspectives

[8]   BWEA (2009) England's Regional Renewable Energy Targets: Progress Report

[9]   EREC (2009) Renewable energy framework directive available at

http://www.erec.org/policy.html

[10]   Hassan, A. Y. Hil, D. R. (1986) Islamic Technology: An illustrated History, Cambridge University Press, ISBN 0-521-42239-6

[11]   Heier, S. (2004) Grid integration of Wind Energy Conversion Systems, Wiley

[12]   Leithead, W. E. (2007) Wind Energy, Philosophical translations of Royal Society, vol. 365, pp. 957 – 970

[13]   Clolow, R. (1999) Financial for Wind Energy, Renewable Energy, vol. 16, pp. 858 – 862

[14]   Mann, J. Sorensen, J. N. Mrthorst, P. E. (2008) Editorial Wind Energy, IOP Publishing

[15]   EWEA, EU energy policy post 2020 available at

http://www.ewea.org/fileadmin/files/library/publications/reports/EU_energy_policy_post_2020.pdf

[16]   Riegler, H. (2003) HAWT Vs VAWT, Re-Focus

[17]   B&Q   pulls   Wind   Turbines   from   shelves,   available   at http://www.guardian.co.uk/business/2009/feb/06/windpower

[18]   Eccleston, P. Urban wind turbines may be waste of time, The Telegraph

Optimal Design of a Micro Vertical Axis Wind Turbine for Sustainable Urban Environment
By Kyooseon Park, School of Computing and Engineering, University of Huddersfield, UK (2013)

174

[19]   Akhmatov, V. (2007) Influence of Wind Direction on Intense Power Fluctuations in Large Offshore Windfarms in the North Sea, Wind Engineering, vol. 31, pp. 59 – 64

[20]   Eriksson, S. Bernhoff, H. Leijon, M. (2008) Evaluation of different turbine concepts for wind power, Renewable and Sustainable Energy Reviews, vol. 12, pp. 1419 – 1434

[21]   Blackwell, B. (1974) The Vertical Axis Wind Turbine: How it works, Sandia Laboratories, no. SLA-74–0160

[22]   Darrieus, G. (1931) Turbine Having It's Rotating Shaft Transverse to the Flow of the Current, United States Patent No.1

[23]   Savonius, S. (1931) The S-Rotor and its applications, Mechanical Engineering, vol. 53, pp. 333 – 338

[24]   Modi, V. Fernando, M. (1989) On the Performance of the Savonius Wind Turbine, Journal of Solar Energy Engineering, vol.111/71

[25]   Sheldahl, R. (1978) Wind Tunnel performance data for two and three bucket savonius rotors, Journal of Energy, vol. 2, pp. 160 – 164

[26]   Sivasegaram, S. (1978) Secondary parameters affecting the performance of resistance-type vertical-axis wind rotors, available at http://adsabs.harvard.edu/abs/1978WiEng...2...49S.

[27]   Clayton, B. (1978) Observations of the flow in and around Savonius and Darrieus rotors, Proceedings of the First British Wind Energy Association Conference, Cranfield, pp. 24 – 31

[28]   Fujisawa, N. Shirai, H. Mizuno, Y. (1987) Hot wire anemometer measurements of flow fields around savonius rotors in open circuit wind tunnel, Laser and hot wire/film velocimetries and their applications, pp.109 – 122

[29]   Walker, S. L. (2011) Building mounted wind turbines and their suitability for the urban scale: A review of methods of estimating urban wind resource, Energy and Buildings, vol. 43, pp. 1852 – 1862

[30]   Colley. G. (2013) Design, Operation and Diagnostics of a Vertical Axis Wind Turbines, Ph. D. Thesis, University of Huddersfield, U.K.

[31]   Peacock, A. D. Jenkins, D. Ahadzi, M. Berry, A. Turan, S. (2008) Micro wind turbines in the UK domestic sector, Energy and Buildings, vol. 40, pp. 1324 – 1333

[32]   Herbert, G. M. J. Iniyan, S. Sreevalsan, E. Rajapandian, S. (2007) A review of wind energy technologies, Renewable and Sustainable Energy Reviews, vol. 11, pp. 1117 – 1145

[33]   Hameed, Z. Hong, Y. S. Cho, Y. M. Ahn, S. H. Song, C. K. (2009) Condition monitoring and fault detection of wind turbines and related algorithms: A review, Renewable and Sustainable Energy Reviews, vol. 13, pp. 1 – 39

[34]   Hameed, Z. Ahn, S. H. Cho, Y. M. (2010) Practical aspects of a condition monitoring system for a wind turbine with emphasis on its design, system architecture, testing and installation, Renewable Energy, vol. 35, pp. 879 – 894

Optimal Design of a Micro Vertical Axis Wind Turbine for Sustainable Urban Environment
By Kyooseon Park, School of Computing and Engineering, University of Huddersfield, UK (2013)

175

[35]   Caselitz, P. Giebhardt, J. Advanced maintenance and repair for offshore wind farms using fault prediction techniques, ISET, Division of Energy Conversion and Control Engineering, Germany

[36]   European Standards Institution (2010) EN 13306 Maintenance Terminology

[37]   Ribrant, J. Bertling, L. M. (2007) Survey of Failures in Wind Power Systems With Focus on Swedish Wind Power Plants During 1997–2005, IEEE Transactions on Energy Conversion, vol. 22, pp. 167 – 173

[38]   Kahrobaee, S. Asgarpoor, S. (2011) Risk-based Failure Mode and Effect Analysis for wind turbines (RBFMEA), North American Power Symposium (NAPS), pp.1 – 7

[39]   Khan, M. M. Iqbal, M. T. Khan, F. (2005) Reliability and condition monitoring of a wind turbine, in Canadian Conference on Electrical and Computer Engineering, pp. 1978 – 1981

[40]   Baird, J. P. Pender, S. F. (1980) Optimisation of a Vertical Axis Wind Turbine for Small Scale Applications, 7th Australasian Hydraulics and Fluid Mechanics Conference, 18 – 22 August, Brisbane, Australia

[41]   Travis, J. C. (2010) Aerodynamic Shape Optimisation of a Vertical Axis Wind Turbine, M.Sc. Thesis, University of Texas at Arlington, U.S.A.

[42]   Yonghai, H. Zhengmin, T. Shanshan, W. (2009) A New Type of VAWT and Blade Optimiztion, Technology and Innovation Conference (ITIC), Xian, China

[43]   Aron, Z. (2007) Optimization of a Savonius Rotor Vertical-Axis Wind Turbine for Use in Water Pumping System in Rural Honduras, B.Sc. Thesis, Massachesetts Institute of Technology, U.S.A.

[44]   Leal. C. H. V. (2008) Optimization of the efficiency of a Savonius wind turbine for urban media using a genetic algorithm, M.Sc. Thesis, Instituto Tecnológico Y De Estudios Superiores De Monterrey

[45]   Samuel, B. W. (2010) Vertical Axis Wind Turbine with Continuous Blade Angle Adjustment, B.Sc. Massachusetts Institute of Technology, U.S.A.

[46]   Paul, C. K. Mark, H. W. (1981) Effects of Blade Preset Pitch/Offset on Curved-Blade Darrieus Vertical Axis Wind Turbine Performance, Sandia Report, Sandia National Laboratories Albuquerque, NM 87185, U.S.A.

[47]   Colley, G. Mishra, R. Rao, H. V. Woolhead, R. (2010) Effect of rotor blade position on Vertical Axis Wind Turbine performance, International Conference on Renewable Energies and Power Quality, (ICREPQ'10), 23 – 25 March, Granada, Spain

[48]   Wirachai, R. (2004) Optimisation of Vertical Axis Wind Turbines, M.Sc. Thesis, School of Engineering and Technology, Northumbria University, U.K.

[49]   Manabu, T. Hideki, K. Takao, M. Yasunari K. Michiaki, O. Atsushi, M. (2009) A Straight-bladed Vertical Axis Wind Turbine with a Directed Guide Vane Row Effect of Guide Vane Geometry on the Performance, Journal of Thermal Science, vol. 18, pp. 54 − 57

Optimal Design of a Micro Vertical Axis Wind Turbine for Sustainable Urban Environment
By Kyooseon Park, School of Computing and Engineering, University of Huddersfield, UK (2013)

176

[50]   Marco, R. C. Stefano, D. B. Ernesto, B. (2012) Effect of Blade Number on a Straight Bladed Vertical Axis Darreius Wind Turbine, World Academy of Science, Engineering and Technology, vol. 61

[51]   Chein-Chang C. and Cheng-Hsiung K. (2012) Effects of pitch angle and blade camber on flow characteristics and performance of small-size Darrieus VAWT, Journal of Visualisation, vol. 16, pp. 65 – 74

[52]   Soraghan, C. Leithead, W. Jamieson, P. (2013) Influence of Lift to Drag Ratio on Optimal Aerodynamic Performance of Straight Blade Vertical Axis Wind Turbines, European Wind Energy Association Annual Conference, Vienna, Austria

[53]   Pope, K. Rodrigues, V. Doylea, R. Tsopelas, A. Gravelsins, R. Naterer, G. F. Tsang, E. (2010) Effects of stator vanes on power coefficients of a zephyr vertical axis wind turbine, Renewable Energy, vol. 35, pp. 1043 – 1051

[54]   Howell, R. Qin, N. Edwards, J. Durrani, N. (2010) Wind tunnel and numerical study of a small vertical axis wind turbine, Renewable Energy, vol. 35, pp. 412 – 422

[55]   Neumann, D. (1991) Fault diagnosis on machine-tools by estimation of signal spectra, Proceedings of IFAC Symposium. (SAFEPROCESS)

[56]   Widodo, A. Yang, B. S. Gu, D. S. Choi, B. K. (2009) Intelligent fault diagnosis system of induction motor based on transient current signal, Mechatronics, vol. 19, pp. 680 – 689

[57]   Kar, C. Mohanty, A. R. (2006) Monitoring gear vibrations through motor current signature analysis and wavelet transform, Mechanical Systems and Signal Processing, vol. 20, pp. 158 – 187

[58]   Tan, C. K. Irving, P. Mba, D. (2007) A comparative experimental study on the diagnostic and prognostic capabilities of acoustics emission, vibration and spectrometric oil analysis for spur gears, Mechanical Systems and Signal Processing, vol. 21, pp. 208 – 233

[59]   Treetrong, J. Sinha, J. K. Gu, F. G. Ball, A. (2009) Bispectrum of stator phase current for fault detection of induction motor, ISA Transactions, vol. 48, pp. 378 – 382

[60]   Schoen, R. Habetler, T. Kamran, F. Bartfield, R. (1995) Motor bearing damage detection using stator current monitoring, Industry Applications, IEEE Transactions on, vol. 31, pp. 1274 – 1279

[61]   Lijun, W. Lili, M. Yongliang, H. (2010) The application of Lifting Wavelet Transform in the Fault Diagnosis of Reciprocating Air Compressor, International Conference on Intelligent System Design and Engineering Application

[62]   Fiedler, A. J. Tullis, S. (2009) Blade Offset and Pitch Effects on a High Solidity Vertical Axis Wind Turbine, Wind Engineering, vol. 33, pp. 237 – 246

[63]   Colley, G. Mishra, R., Rao, H. V. Woolhead, R. (2009) Performance evaluation of three cross flow vertical axis wind turbine configurations, Proceedings of Computing and Engineering Annual Researchers' Conference, Huddersfield, U.K.

[64]   Ghatage, S. V. Joshi, J. B. (2012) Optimisation of Vertical Axis Wind Turbine: CFD Simulations and Experimental Measurements, The Canadian Journal of Chemical Engineering, vol. 90

Optimal Design of a Micro Vertical Axis Wind Turbine for Sustainable Urban Environment
By Kyooseon Park, School of Computing and Engineering, University of Huddersfield, UK (2013)

177

[65]   Preen, R. J. Bull, L. (2012) Towards the Evolution of Novel Vertical-Axis Wind Turbines

[66]   Castillo, J. (2011) Small-Scale Vertical Axis Wind Turbine design, B.Sc. Thesis, Tampere University of Applied Sciences

[67]   Paraschivoiu, I. Trifu, O. Saeed, F. (2009) H-Darrieus Wind Turbine with Blade Pitch Control, International Journal of Rotating Machinery

[68]   Ramkissoon, R. Manohar, K. (2013) Increasing the Power Output of the Darrieus Vertical Axis Wind Turbine, British Journal of Applied Science & Technology, vol. 3, pp. 77 – 90

[69]   Beri, H. Yao, Y. (2011) Effect of Camber Airfoil on Self Starting of Vertical Axis Wind Turbine, Journal of Environmental Science and Technology, pp. 302 – 312

[70]   Zhang, L. X. Liang, Y. B. Liu, X. H. Jiao, Q. F. Guo, J. (2013) Aerodynamic Performance Prediction of Straight-Bladed Vertical Axis Wind Turbine Based on CFD, Hindawi Publishing Corporation, Advances in Mechanical Engineering

[71]   Hargreaves, D. M. Wright, N. G. (2006) On the use of the $k–\varepsilon$ model in commercial CFD software to model the neutral atmospheric boundary layer, Journal of Wind Engineering, and Industrial Aerodynamics, vol. 95, pp. 355 – 369

[72]   Li, S. Li, Y. (2010) Numerical Study on the Performance Effect of Solidity on the Straight-Bladed Vertical Axis Wind Turbine, Scientific Research Fund of Heilongjiang Provincial Education, Scientific Research Foundation for the Returned Overseas Chinese Scholars

[73]   Sabaeifard, P. Razzaghi, H. Forouzandeh, A. (2012) Determination of Vertical Axis Wind Turbines Optimal Configuration through CFD Simulations, International Conference on Future Environment and Energy, Singapore

[74]   Colley, G. (2010) Effect of rotor blade position on Vertical Axis Wind Turbine performance, International Conference on Renewable Energies and Power Quality, Granda, Spain

[75]   Shahzad, A. Asim, T. Park, K. Pradhan, S. Mishra, R. (2012) Numerical Simulations of Effects of Faults in a Vertical Axis Wind Turbine's Performance, 2nd International Workshop and Congress on eMaintenance, Lulea, Sweden

[76]   Park, K. Asim, K. Mishra, R. Pradhan, S. (2012) Condition Based Monitoring of Vertical Axis Wind Turbines using Computational Fluid Dynamics, 39th National Conference on Fluid Mechanics and Fluid Power, Surat, India

[77]   Versteeg, H. K. Malalasekera, W. (1995) An Introduction to Computational Fluid Dynamics, Longman Scientific and Technical, U.K., ISBN: 0131274988

[78]   Pozrikidis, C. (2001) Fluid Dynamics Theory, Computation and Numerical Simulation, Kluwer Academic Publishers, U.S.A., ISBN: 038795869X

[79]   Cebeci, T. Shao, J. P. Kafyeke, F. Laurendeau, E. (2005) Computational Fluid Dynamics for Engineers, Horizons Publishing, U.S.A., ISBN: 3540244514

[80]   Blazek, J. (2001) Computational Fluid Dynamics Principles and Applications, Elsevier, ISBN: 0080430090

Optimal Design of a Micro Vertical Axis Wind Turbine for Sustainable Urban Environment
By Kyooseon Park, School of Computing and Engineering, University of Huddersfield, UK (2013)

178

[81]   Lomax, H. Pulliam, T. H. Zingg, D. W. (2001) Fundamentals of Computational Fluid Dynamics, Springer, ISBN: 3540416072

[82]   Hoffmann, K. A. and Chiang, S. T. (2000) Computational Fluid Dynamics, Engineering Education System, U.S.A., ISBN: 0962373133

[83]   Munson, B. R. Young, D. F. Okiishi, T. H. (2002) Fundamentals of Fluid Mechanics", John Willey & Sons Inc., 4th ed., U.S.A., ISBN: 0471675822

[84]   Patankar, S. V. Spalding, D. B. (1972), A Calculation Procedure for Heat, Mass and Momentum Transfer in Three-Dimensional Parabolic Flows, Heat and Mass Transfer, vol. 15, pp. 1787 – 1806

[85]   Rauch, R. D. Batira, J. T. Yang, N. T. Y. (1991) Spatial Adaption Procedures on Unstructured Meshes for Accurate Unsteady Aerodynamic Flow Computations, Technical Report, American Institute of Aeronautics and Astronautics, vol. 91, pp. 1106

[86]   Barth, T. J. Jespersen, D. (1989) The Design and Application of Upwind Schemes on Unstructured Meshes, 27th Technical Report, Aerospace Sciences Meeting, Nevada

[87]   Venkatakrishnan, V. (1993) On the Accuracy of Limiters and Convergence to Steady State Solutions, Technical Report, American Institute of Aeronautics and Astronautics, vol. 93, pp. 880

[88]   Menter, F. R. (1994) Two-Equation Eddy-Viscosity Turbulence Models for Engineering Applications, American Institute of Aeronautics and Astronautics, vol. 32, pp. 1598 – 1605

[89]   Ansys   13.0.0   User   Guide   accessible   at http://www1.ansys.com/customer/content/documentation/130/wb2_help.pdf

Optimal Design of a Micro Vertical Axis Wind Turbine for Sustainable Urban Environment
By Kyooseon Park, School of Computing and Engineering, University of Huddersfield, UK (2013)
179

APPENDIX - 1

α (º)	γ (º)	δ (º)	Tmin (N-m)	Tmax (N-m)	Tavg (N-m)	Std. Dev.	Pavg (W)
1.689	18.2	22.357	22.1	27.24	25.3	1.53	43.36
		27.357	23.07	27.9	25.63	1.61	43.94
		32.357	22.33	28.01	25.25	1.79	43.29
		37.357	20.86	26.94	23.79	2.01	40.78
		42.357	19.71	26.66	23.55	2.05	40.38
	23.2	22.357	23.48	27.82	26.01	1.41	44.59
		27.357	22.07	27.64	25.23	1.67	43.26
		32.357	21.43	27.27	24.31	1.91	41.67
		37.357	20.68	26.48	23.41	1.91	40.13
		42.357	19.3	25.71	22.4	2.04	38.4
	28.2	22.357	26.82	24.3	25.54	1.37	43.78
		27.357	21.98	27.33	24.66	1.74	42.27
		32.357	19.33	23.81	21.93	1.23	37.59
		37.357	19.8	26.06	22.87	1.96	39.2
		42.357	19.2	25.54	21.85	2.06	37.46
	33.2	22.357	22.49	27.15	24.91	1.54	42.69
		27.357	21.95	26.82	24.13	1.65	41.37
		32.357	20.38	26.31	23.29	1.86	39.93
		37.357	19.73	25.88	22.24	1.99	38.12
		42.357	18.68	24.7	21.38	1.96	36.66
	38.2	22.357	19.33	23.81	21.93	1.23	37.59
		27.357	20.85	26.32	23.52	1.71	40.32
		32.357	19.95	25.66	22.54	1.86	38.65
		37.357	19.01	25.02	21.78	1.89	37.34
		42.357	18.54	24.19	20.86	1.98	35.76
6.689	18.2	22.357	23.98	26.27	25.13	0.72	43.07
		27.357	23.1	26.32	24.53	1.14	42.06
		32.357	21.63	26.26	23.98	1.68	41.11
		37.357	20.61	26.05	22.99	1.8	39.42
		42.357	19.38	25.41	22.02	2.03	37.74
	23.2	22.357	23.65	26.13	24.82	0.84	42.56
		27.357	22.38	26.32	24.38	1.43	41.79

Optimal Design of a Micro Vertical Axis Wind Turbine for Sustainable Urban Environment
By Kyooseon Park, School of Computing and Engineering, University of Huddersfield, UK (2013)

175

		32.357	21.35	26.24	23.5	1.61	40.28
		37.357	20.09	25.65	22.53	1.88	38.62
		42.357	18.69	25.3	21.71	2.2	37.22
	28.2	22.357	22.94	26.52	24.53	1.16	42.06
		27.357	21.98	26.11	23.79	1.37	40.79
		32.357	20.71	25.73	22.95	1.71	39.35
		37.357	19.3	25.47	22.15	2.05	37.97
		42.357	18.26	25.01	21.22	2.22	36.37
	33.2	22.357	22.46	25.73	23.88	1.09	40.94
		27.357	21.23	25.57	23.18	1.47	39.74
		32.357	19.84	25.48	22.5	1.87	38.57
		37.357	18.92	25.12	21.61	2.05	37.04
		42.357	17.73	24.39	20.68	2.2	35.45
	38.2	22.357	21.68	25.15	23.23	1.17	39.82
		27.357	20.32	25.21	22.67	1.63	38.85
		32.357	19.47	25.04	21.93	1.85	37.59
		37.357	18.39	24.52	21.04	2.02	36.07
		42.357	17.19	24	20.19	2.21	34.61
11.689	18.2	22.357	24.75	26.38	25.6	0.56	43.89
		27.357	23.8	26.41	25.14	0.94	43.1
		32.357	22.5	26.29	24.17	1.31	41.44
		37.357	21.28	25.79	23.36	1.52	40.04
		42.357	19.77	25.2	22.41	1.83	38.43
	23.2	22.357	24.5	26.36	25.46	0.63	43.65
		27.357	23.44	26.2	24.77	0.94	42.46
		32.357	22.14	26.02	23.94	1.31	41.04
		37.357	20.61	25.58	23.04	1.66	39.49
		42.357	19.43	25.03	21.98	1.79	37.69
	28.2	22.357	24.05	25.94	25.01	1.45	42.87
		27.357	22.85	25.95	24.31	1.05	41.67
		32.357	21.41	25.71	23.54	1.44	40.35
		37.357	20.23	25.24	22.51	1.61	38.59
		42.357	19	24.42	21.51	1.52	36.87
	33.2	22.357	23.41	25.62	24.47	0.74	41.94
		27.357	22.1	25.54	23.83	1.18	40.86
		32.357	21	25.3	22.98	1.39	39.39
		37.357	19.78	24.56	21.98	1.63	37.68
		42.357	18.22	24.17	21.15	2.03	36.26
	38.2	22.357	22.61	25.3	23.88	0.87	40.93

Optimal Design of a Micro Vertical Axis Wind Turbine for Sustainable Urban Environment
By Kyooseon Park, School of Computing and Engineering, University of Huddersfield, UK (2013)

		27.357	21.65	25.04	23.21	1.09	39.79
		32.357	18.53	21.85	20.38	1.1	34.94
		37.357	18.96	24.21	21.57	1.79	36.97
		42.357	18.21	23.77	20.62	1.8	35.34
16.689	18.2	22.357	24.8	26.41	25.67	0.51	44.01
		27.357	24.14	26.19	25.11	0.7	43.05
		32.357	22.7	26.68	24.51	1.22	42.02
		37.357	21.7	25.38	23.49	1.23	40.26
		42.357	20.43	24.65	22.45	1.39	38.49
	23.2	22.357	24.83	26.2	25.53	0.48	43.76
		27.357	23.6	27.06	25	0.96	42.86
		32.357	22.64	25.61	24.14	1.01	41.38
		37.357	21.34	24.95	23.1	1.19	39.59
		42.357	19.83	24.25	22.13	1.5	37.94
	28.2	22.357	24.36	27.29	25.28	0.73	43.33
		27.357	23.44	25.53	24.55	0.76	42.08
		32.357	22.16	25.11	23.64	0.97	40.53
		37.357	20.71	24.49	22.71	1.28	38.93
		42.357	19.54	23.89	21.72	1.5	37.24
	33.2	22.357	24.11	25.62	24.73	0.5	42.4
		27.357	22.9	24.99	23.98	0.69	41.11
		32.357	21.51	24.59	23.19	1.04	39.76
		37.357	20.4	24.03	22.24	1.25	38.13
		42.357	19.37	23.42	21.24	1.34	36.41
	38.2	22.357	23.51	24.62	24.11	0.38	41.32
		27.357	22.14	24.5	23.41	0.75	40.13
		32.357	21.13	23.99	22.63	0.98	38.79
		37.357	20.19	23.46	21.68	1.07	37.17
		42.357	18.97	22.72	20.73	1.26	35.54
21.689	18.2	22.357	24.08	25.89	25.19	0.51	43.19
		27.357	23.76	26.53	24.77	0.78	42.46
		32.357	22.78	25.06	24.02	0.79	41.18
		37.357	21.62	24.46	23.13	0.96	39.66
		42.357	20.13	24.78	22.31	1.47	38.25
	23.2	22.357	24.11	26.91	25.21	0.69	43.22
		27.357	23.84	25.29	24.59	0.54	42.15
		32.357	22.63	24.83	23.81	0.74	40.81
		37.357	21.11	25.28	22.99	1.26	39.4
		42.357	20.18	23.51	21.91	1.14	37.56

Optimal Design of a Micro Vertical Axis Wind Turbine for Sustainable Urban Environment
By Kyooseon Park, School of Computing and Engineering, University of Huddersfield, UK (2013)

		22.357	24.16	25.67	24.93	0.47	42.74
		27.357	23.52	24.97	24.29	0.51	41.65
	28.2	32.357	21.99	25.69	23.57	1.05	40.41
		37.357	21.12	23.8	22.56	0.94	38.68
		42.357	19.86	22.98	21.47	1.01	36.8
		22.357	23.77	25.2	24.54	0.37	42.06
		27.357	22.82	25.99	23.97	0.83	41.1
	33.2	32.357	21.97	24.03	23.1	0.71	39.59
		37.357	20.78	23.17	22.09	0.78	37.86
		42.357	22.67	24.37	23.38	0.48	40.09
		22.357	23.33	26.1	24.13	0.68	41.36
		27.357	22.67	24.37	23.38	0.48	40.09
	38.2	32.357	17.65	23.07	20.33	1.86	34.86
		37.357	20.18	22.8	21.61	0.81	37.04
		42.357	19.18	21.78	20.65	0.91	35.4

Optimal Design of a Micro Vertical Axis Wind Turbine for Sustainable Urban Environment
By Kyooseon Park, School of Computing and Engineering, University of Huddersfield, UK (2013)

178

APPENDIX - 2

Number of Stator Blades	Number of Rotor Blades	Tmin (N-m)	Tmax (N-m)	Tavg (N-m)	Std. Dev.
12	12	24.80	26.41	25.67	0.51
12	8	18.83	26.38	22.22	2.49
12	4	12.68	17.43	14.61	1.19
8	12	20.30	25.58	22.70	1.85
8	8	15.61	22.38	19.71	2.14
8	4	10.31	15.73	13.25	1.44
4	12	16.18	17.71	17.12	0.52
4	8	5.23	21.72	12.16	3.99
4	4	-1.82	7.52	4.10	2.47

Optimal Design of a Micro Vertical Axis Wind Turbine for Sustainable Urban Environment
By Kyooseon Park, School of Computing and Engineering, University of Huddersfield, UK (2013)

179

APPENDIX – 3A

12 Stator & 12 Rotor Blades	Static Pressure (Pa)		
	-9º	0º	9º
P1	2.27	-0.78	0.97
P2	-9.99	-9.54	-8.74
P3	3.57	3.95	1.31
P4	2.11	-2.62	-5.03
P5	-5.53	-6.79	-6.4
P6	-8.45	-8.52	-8.14
P7	20.44	21.75	20.96
P8	-5.1	-4.24	-3.24

12 Stator & 12 Rotor Blades	Velocity Magnitude (m/sec)		
	-9º	0º	9º
P1	5.45	5.89	5.68
P2	0.94	1.11	1.67
P3	4.41	5.02	4.24
P4	3.03	2.37	4.23
P5	2.26	2.08	2.26
P6	5.36	5.33	5.44
P7	4.43	4.28	4.21
P8	5.64	5.51	5.87

12 Stator & 11 Rotor Blades	Static Pressure (Pa)		
	-9º	0º	9º
P1	2.4	-0.78	0.99
P2	-10.39	-10.21	-9.49
P3	1.09	1.62	-0.61
P4	2.54	-1.92	-4.75
P5	-5.44	-6.41	-6.18
P6	-9.08	-8.92	-8.71
P7	20.26	21.5	20.27
P8	-5.14	-4.17	-3

12 Stator & 11 Rotor Blades	Velocity Magnitude (m/sec)		
	-9º	0º	9º
P1	5.42	5.89	5.72
P2	0.94	0.96	1.54
P3	4.75	4.98	4.21
P4	3.01	2.63	4.27
P5	2.25	2.07	2.21
P6	5.37	5.33	5.45
P7	4.36	4.33	4.27
P8	5.59	5.43	5.76

11 Stator & 12 Rotor Blades	Static Pressure (Pa)		
	-9º	0º	9º
P1	2.86	-0.68	1.2
P2	-10.02	-9.52	-8.9
P3	3.27	4.25	1.98
P4	2.99	-2.67	-4.65
P5	-5.62	-6.8	-6.53
P6	-8.36	-8.51	-8.29
P7	20.33	21.52	20.82
P8	-5.31	-4.01	-3.02

11 Stator & 12 Rotor Blades	Velocity Magnitude (m/sec)		
	-9º	0º	9º
P1	5.65	6.21	6.04
P2	1	1.14	1.71
P3	4.06	5.55	5.17
P4	3.15	2.33	4.45
P5	2.27	2.11	2.33
P6	5.39	5.39	5.49
P7	4.23	4.24	4.16
P8	5.49	5.33	5.76

Optimal Design of a Micro Vertical Axis Wind Turbine for Sustainable Urban Environment
By Kyooseon Park, School of Computing and Engineering, University of Huddersfield, UK (2013)

181

APPENDIX – 3B

50 mm Slit	Static Pressure (Pa)		
	-9º	0º	9º
P1	3.28	1.53	0.37
P2	-8.12	-9.18	-7.68
P3	4.43	5.68	2.55
P4	-5.16	-2.77	-7.93
P5	-7.79	-7.03	-7.25
P6	-7.01	-6.12	-6.67
P7	21.61	22.11	20.26
P8	-4.68	-6.36	-4.48

50mm Slit	Velocity Magnitude (m/sec)		
	-9º	0º	9º
P1	5.19	5.16	5.24
P2	0.83	0.78	0.99
P3	4.17	4.11	4.16
P4	2.17	2.17	2.44
P5	3.05	2.77	3.05
P6	5.27	5.23	5.31
P7	4.15	4.19	4.17
P8	5.93	5.85	5.99

100mm Slit	Static Pressure (Pa)		
	-9º	0º	9º
P1	1.13	2.84	0.23
P2	-8.98	-8.06	-9.85
P3	4.81	4.29	2.54
P4	-2.04	-6.43	-6.45
P5	-7.41	-8.59	-7.16
P6	-6.36	-6.88	-6.47
P7	21.64	21.51	20.1
P8	-6.31	-4.77	-5.14

100mm Slit	Velocity Magnitude (m/sec)		
	-9º	0º	9º
P1	5.25	5.22	4.97
P2	0.94	1.16	1.56
P3	4.13	4.33	3.94
P4	2.53	2.26	3.32
P5	2.71	3.14	2.93
P6	5.26	5.28	5.32
P7	4.26	4.18	4.27
P8	5.76	5.8	5.93

200mm Slit	Static Pressure (Pa)		
	-9º	0º	9º
P1	0.92	3.53	0.27
P2	-9.54	-8.11	-9.12
P3	5	5.18	3.42
P4	-3.43	-4.43	-6.18
P5	-7.35	-7.89	-6.96
P6	-5.56	-6.51	-6.28
P7	21.88	21.94	20.54
P8	-6.4	-5.06	-5.26

200mm Slit	Velocity Magnitude (m/sec)		
	-9º	0º	9º
P1	4.89	4.91	4.94
P2	0.85	0.94	2.07
P3	4.57	4.08	3.79
P4	2.52	2.07	3.11
P5	2.6	3.02	2.92
P6	5.21	5.26	5.3
P7	4.2	4.11	4.18
P8	5.85	5.88	6.01

Optimal Design of a Micro Vertical Axis Wind Turbine for Sustainable Urban Environment
By Kyooseon Park, School of Computing and Engineering, University of Huddersfield, UK (2013)

183

LIST OF PUBLICATIONS

- Park, K. Asim, T. Mishra, R. (2012) Computational Fluid Dynamics based Fault Simulations of a Vertical Axis Wind Turbines, Journal of Physics: Conference Series, vol. 364, pp. 012138

- Park, K. Asim, T. Mishra, R. (2012) Simulation Based Approach to Predict Vertical Axis Wind Turbine Faults using Computational Fluid Dynamics, 1st International Conference on Through-life Engineering Services, Bedfordshire, U.K.

- Park, K. Asim, T. Mishra, R. Shahzad, A. Mirangwanda, G. (2012) Computational Fluid Dynamics based Performance Optimisation of Vertical Axis Marine Current Turbines, 2nd International Workshop and Congress on eMaintenance, Lulea, Sweden

- Park, K. Asim, T. Mishra, R. Pradhan, S. (2012) Condition Based Monitoring of Vertical Axis Wind Turbines using Computational Fluid Dynamics, 39th National Conference on Fluid Mechanics and Fluid Power, Surat, India

- Park, K. Asim, T. and Mishra, R. (2013) Effect of Blade Faults on the Performance Characteristics of a Vertical Axis Wind Turbine, 26th International Congress of Condition Monitoring and Diagnostic Engineering Management, Helsinki, Finland

- Shahzad, A. Asim, T. Park, K. Pradhan, S. Mishra, R. (2012) Numerical Simulations of Effects of Faults in a Vertical Axis Wind Turbine's Performance, 2nd International Workshop and Congress on eMaintenance, Lulea, Sweden
-

Optimal Design of a Micro Vertical Axis Wind Turbine for Sustainable Urban Environment
By Kyooseon Park, School of Computing and Engineering, University of Huddersfield, UK (2013)

184